INFORMATION TO USERS

This manuscript has been reproduced from the microfilm master. UMI films the text directly from the original or copy submitted. Thus, some thesis and dissertation copies are in typewriter face, while others may be from any type of computer printer.

The quality of this reproduction is dependent upon the quality of the copy submitted. Broken or indistinct print, colored or poor quality illustrations and photographs, print bleedthrough, substandard margins, and improper alignment can adversely affect reproduction.

In the unlikely event that the author did not send UMI a complete manuscript and there are missing pages, these will be noted. Also, if unauthorized copyright material had to be removed, a note will indicate the deletion.

Oversize materials (e.g., maps, drawings, charts) are reproduced by sectioning the original, beginning at the upper left-hand corner and continuing from left to right in equal sections with small overlaps.

Photographs included in the original manuscript have been reproduced xerographically in this copy. Higher quality 6" x 9" black and white photographic prints are available for any photographs or illustrations appearing in this copy for an additional charge. Contact UMI directly to order.

Bell & Howell Information and Learning
300 North Zeeb Road, Ann Arbor, MI 48106-1346 USA
800-521-0600

ESL-TH-00/05-01 Development and validation of a computer model for energy - efficient shaded

DEVELOPMENT AND VALIDATION OF A COMPUTER MODEL FOR ENERGY-EFFICIENT SHADED FENESTRATION DESIGN

A Dissertation

by

KIE WHAN OH

Submitted to the Office of Graduate Studies of
Texas A&M University
in partial fulfillment of the requirements for the degree of

DOCTOR OF PHILOSOPHY

May 2000

Major Subject: Architecture

DEVELOPMENT AND VALIDATION OF A COMPUTER MODEL FOR ENERGY-EFFICIENT SHADED FENESTRATION DESIGN

A Dissertation

by

KIE WHAN OH

Submitted to Texas A&M University
in partial fulfillment of the requirements
for the degree of

DOCTOR OF PHILOSOPHY

Approved as to style and content by:

Jeff S. Haberl
(Co-Chair of Committee)

Larry O. Degelman
(Co-Chair of Committee)

David E. Claridge
(Member)

Valerian Miranda
(Member)

Juilus M. Gribou
(Head of Department)

May 2000

Major Subject: Architecture

ABSTRACT

Development and Validation of a Computer Model

for Energy-efficient Shaded Fenestration Design.

(May 2000)

Kie Whan Oh, B. Engr., Pusan National University, Korea;

M. Engr., Pusan National University, Korea;

M. Arch., University of California, Los Angeles

Co-Chairs of Advisory Committee: Dr. Jeff S. Haberl
Prof. Larry O. Degelman

The goal of this study is to develop and validate a computerized model for an energy-efficient fenestration system that can easily be incorporated into the architectural design process. This model is for the thermal analysis of a shaded fenestration system and considers selected effects of the solar shades. Several simulation programs have been developed for the thermal analysis of a shaded window system. However, none of the previous programs has incorporated a validated simulation model into a visually effective display such as a sunpath diagram.

The proposed methodology concentrates on the development of various new graphical aids for effectively displaying a shaded design and develops a thermal model for calculating the heat transfer through an unshaded window at any orientation. A computerized simulation model, called the Shaded Fenestration Design (SFD) model, was developed that is capable of calculating the amount of solar radiation for a clear day as well as calculating the heat transfer through window glazing. The SFD model also provides new computerized displays of the sunpath diagrams that include the equidistant, orthographic, stereographic, gnomonic, and cylindrical projections, as well as the accompanying shading mask protractors.

The program simulates clear sky solar radiation for locations in the U.S. using the methods developed by the *ASHRAE Handbook*, Duffie and Beckman, and Kreider and Rabl. An anisotrophic sky model was applied for the calculation of solar radiation on a tilted surface and the transmitted solar radiation through the single-glazed window.

A highly insulated experimental test box was constructed to measure the total heat gain through the window glazing as well as the amount of solar radiation on the vertical surface. A finite difference model was then developed to provide a comparative validation. The results from the proposed solar simulation model were also compared against the simulated results from the DOE-2 program.

The portions of the work that represent new contributions include: 1) computerization of the four projection methods (i.e., orthographic, stereographic, gnomonic, and cylindrical projections) for the sunpath diagram and the shading mask protractor, 2) display of the hourly intensity of solar data onto the path of the sun for horizontal and vertical orientations at varying off-south azimuths, 3) use of a moveable viewpoint for the sunpath diagram, and 4) development of experimental test sets of the measured heat gain for various shading configurations.

DEDICATION

This dissertation is dedicated to my loving parents, wife and children.
My life has been specially blessed with a woman who was united to me
to become one flesh by God.

ACKNOWLEDGMENTS

There are numerous people who have helped directly or indirectly in the completion of this study. I would like to express my most sincere appreciation to all those who aided as faithful companions whenever I struggled against the fearful enemies of my life including academic, economic, and time constraints.

Without the recommendations and guidance from the advisory committee, this research would have been unachievable. My sincerest thanks to go to Prof. Larry Degelman who brought me to this academic field and continuously guided me with confidence and understanding as my committee co-chair; to Dr. Jeff Haberl for his expert knowledge on the research methodology and his dedicated attention and instructions as my committee co-chair; to Dr. Valerian Miranda for his intuitive suggestions in the development of a computer model, and to Dr. David Claridge for his expertise in the analysis method of the heat transfer in buildings.

I feel greatly in debt to Mr. Frank Scott and Mr. Kelly Milligan in the Energy Systems Laboratory, Texas A&M University Riverside Campus for taking a great deal of their time to help me to create the airflow chamber for the experimental validation. I am also appreciative to Mr. Yong Hoon Sung and Ms. Myungsook Lee for their efforts in arranging the data.

I also express my gratitude to the Department of Architecture, and the Energy Systems Laboratory at Texas A&M University for the financial support for this research, for providing access to the computer network and the equipment for the experiments, and for aiding the development of the computer model. Special thanks to the Texas State Energy Conservation Office (SECO) who partially sponsored the development of the SOLRPATH program. Support from an ASHRAE Grant-in-Aid for Graduate Students is also acknowledged.

Lastly, my heartfelt gratitude to my beloved parents who provided both a foundation and fences through out my life; to my family who became the columns and beams of my life with their unconditional love, endless understanding, and unlimited patience; to friends who had prayed for me as the roof and walls of my life, to the Love of Jesus Christ that was the circulation of my life. All of these have made the architecture of my life purposeful, peaceful, and grateful whatever the outside conditions were.

TABLE OF CONTENTS

CHAPTER Page

CHAPTER Page

CHAPTER Page

LIST OF FIGURES

Page

Page

Page

Page

Page

Page

LIST OF TABLES

NOMENCLATURE

A : Surface area, the area through which heat transfer occurs (ft^2); Apparent solar radiation at air mass $m = 0$ (Btu/hr-ft^2).

A_c : Area of cross section (ft^2).

A_g : Total glazing area of the test chamber (ft^2).

A_i : Anisotropy index (dimensionless).

A_w : Total wall surface area of the test chamber (ft^2).

B : Atmospheric extinction coefficient (dimensionless).

Bi : Biot number (dimensionless).

C : Nozzle discharge coefficient (dimensionless); Clearness number (dimensionless).

$c_{p,\,air}$: Specific heat of air (0.240 Btu/lb_m-°F).

D_t : Throat diameter of the airflow nozzle (ft).

F_d : Sky diffuse factor (dimensionless).

$F_{i\text{-}s}$: View factor from the *i*th surface to the tilted surface (dimensionless).

Fo : Fourier number (dimensionless time).

F_s : Sunlit factor, the sunlit area of a tilted surface divided by the total area of that surface (dimensionless).

$h_{g,in}$: Convection coefficient between the room air and the inside window glazing (Btu/hr-ft^2-°F).

$h_{w,in}$: Convection coefficient between the room air and the inside wall surface (Btu/hr-ft^2-°F).

$h_{w,out}$: Convection coefficient between the ambient air and the outside wall surface (Btu/hr-ft^2-°F).

I_{SC} : Solar constant, the solar radiation on a surface perpendicular to the direction of the sun's rays outside the earth's atmosphere at the mean earth-sun distance (92.9 x 10^6 miles).

I_o : Extraterrestrial radiation, the solar radiation that would be received on a surface perpendicular to the direction of the sun's rays if there were no atmosphere.

I_{BN} : Normal beam radiation (W/m^2).

$I_{BN,c}$: Clear sky normal beam radiation (W/m^2).

I_{BH} : Beam radiation on a horizontal surface (W/m^2).

$I_{BH,c}$: Clear sky beam radiation on a horizontal surface (W/m^2).

I_{BT} : Beam radiation on a tilted surface (W/m^2).

I_{DH} : Diffuse radiation on a horizontal surface (W/m^2).

$I_{DH,c}$: Clear sky diffuse radiation on a horizontal surface (W/m^2).

I_{DT} : Diffuse radiation on a tilted surface (W/m^2).

I_i : Incident solar radiation (W/m^2).

I_r : Reflected solar radiation (W/m^2).

I_{RT} : Reflected radiation on a tilted surface, the sum of the ground reflected solar radiation and reflected solar radiation from shading devices (W/m^2).

$I_{RT,G}$: Ground reflected radiation on a tilted surface (W/m^2).

$I_{RT,S}$: Reflected radiation from the surrounding surfaces (W/m^2).

I_{TH} : Global radiation on a horizontal surface, the sum of the beam and diffuse solar radiation on a horizontal surface for a clear day (W/m^2).

$I_{TH,c}$: Clear sky global radiation on a horizontal surface, the sum of the beam and diffuse solar radiation on a horizontal surface for a clear day (W/m^2).

I_{Trans} : Transmitted solar radiation through a glazing (W/m^2).

I_{TT} : Global radiation on a tilted surface, the sum of the beam, diffuse, and reflected solar radiation on a tilted surface (W/m^2).

K : Extinction coefficient, the value of K varies from approximately 4 m^{-1} for very clear glass to approximately 32 m^{-1} for poor glass (m^{-1}).

k : Thermal conductivity (Btu/hr-ft-°F).

k_T : Hourly clearness index (dimensionless).

L : Thickness of the glazing (ft).

L_t : Throat length of the airflow nozzle (ft).

$\dot{m}$: Mass flow rate (lb_m/hr).

n : Day of the year; $1 \le n \le 365$ (for leap years, $n \le 366$.).

n_1, n_2 : Refractive index.

Q_{fan} : Heat removed by the ventilating fan in the experimental box ($Btu/hr-ft^2$).

$Q_{conv,g,in}$: Inside convection heat transfer through the glazing ($Btu/hr-ft^2$).

$Q_{conv,w,in}$: Inside convection heat transfer through the wall ($Btu/hr-ft^2$).

$Q_{conv,w,out}$: Outside convection heat transfer through the wall ($Btu/hr-ft^2$).

Q_{cond} : Conduction heat transfer through the wall ($Btu/hr-ft^2$).

$Q_{s,abs}$: Solar radiation absorbed by the glazing ($Btu/hr-ft^2$).

$Q_{s,refl}$: Solar radiation reflected by the glazing ($Btu/hr-ft^2$).

$Q_{s,trans}$: Solar radiation transmitted through the glazing ($Btu/hr-ft^2$).

Q_{store} : Heat stored at the discretized wall ($Btu/hr-ft^2$).

P_b : Corrected barometric pressure (in. Hg).

P_e : Saturated vapor pressure at T_w (in. Hg).

P_p : Partial vapor pressure (in. Hg).

R : R-value, unit thermal resistance ($hr-ft^2-°F/Btu$).

R_b : Tilt factor, the ratio of beam radiation on a tilted surface to that on the horizontal surface (dimensionless).

R_g : Gas constant ($ft-lb/lb_m-°R$).

R_α : Static pressure ratio for nozzles (dimensionless).

R_β : Diameter ratio for nozzles (dimensionless).

R_e : Reynolds number (dimensionless).

r : Total reflection of unpolarized radiation (dimensionless).

$r_{||}$: Parallel component of the reflection of unpolarized radiation (dimensionless).

$r_\perp$: Perpendicular component of the reflection of unpolarized radiation (dimensionless).

T_a : Ambient temperature (°F).

T_d : Dry-bulb temperature (°F).

T_{do} : Outside dry-bulb temperature (°F).

T_i : Inside air temperature (°F).

T_{inlet} : Air temperature in inlet tube (°F).

T_o : Inside wall surface temperature (°F).

T_{outlet} : Air temperature in outlet tube (°F).

T_w : Wet-bulb temperature (°F).

T_{wo} : Outside wet-bulb temperature (°F).

U : U-value, unit conductance (Btu/hr-ft^2-°F).

$\dot{V}_x$: Volume flow rate at plane x (cfm).

Y : Nozzle expansion factor (dimensionless).

ΔP : Air pressure difference across the airflow nozzle (in. wg)

Δt : Discretized time interval (s).

Δx : Discretized thickness of material in which conduction occurs (ft).

α : Solar absorptance of a glazing (dimensionless).

α_n : Solar absorptance of normal incidence for a flat black surface (dimensionless).

α_s : Solar altitude angle ($\alpha_s = 90^0 - \theta_z$, when the sun locates above the horizon).

β : Tilt of surface, the angle between the plane of the surface and the horizontal; $0^0 \le \beta \le 180^0$. ($\beta > 90^0$ means that the surface has a downward facing component.)

δ : Declination, north positive; $-23.45^0 \le \delta \le 23.45^0$.

ϕ : Latitude, north positive; ($-90^0 \le \phi \le 90^0$).

γ_s : Solar azimuth angle, displacements east of south are negative and west of south are positive; $-180^0 \le \gamma_s \le 180^0$.

γ_s' : Pseudo solar azimuth angle.

γ : Surface azimuth angle, zero due south, east negative, and west positive; $-180^0 \le \gamma \le 180^0$.

ν : Air velocity (ft/s).

θ : Angle of incidence, the angle between the beam radiation on a surface and the normal to that surface; $0^0 \leq \theta \leq 180^0$. ($\theta < 90^0$ means that the sun locates behind the surface and the amount of the direct beam radiation is zero whether the sun locates above the horizonal or not.)

θ_z : Zenith angle; $0^0 \leq \theta_z \leq 180^0$. ($\theta_z < 90^0$ means that the sun locates below the horizon.)

ρ_d : Reflectance of glazing from the diffuse radiation (dimensionless).

ρ_g : Ground reflectance (dimensionless).

ρ_o : Density of atmospheric air (lb_m/ft^3).

ρ_x : Air density at plane x (lb_m/ft^3).

τ : Transmittance of a window glazing (dimensionless).

τ_b : Atmospheric transmittance for beam radiation (dimensionless).

τ_d : Diffuse radiation to extraterrestrial radiation coefficient (dimensionless).

ω : Hour angle, morning negative, afternoon positive; $-180^0 \leq \omega \leq 180^0$.

CHAPTER I

INTRODUCTION

1.1. Background

The complex heat transfer processes in contemporary buildings are typically outside the scope of conventional architectural problem-solving methodologies. From the earliest application of computer programs in architectural design, the application of the programs in the design of energy-efficient buildings has been one of the primary uses (Radford and Stevens 1987). Currently, there are several widely-used, general purpose, computerized energy simulation programs such as DOE-2 (LBL 1993), BLAST (BSO 1993), ESP-II (Clarke et al. 1993), ENERCALC/ENER-WIN (Degelman 1994, Degelman and Soebarto 1995), and modular programs for the analysis of system components, such as TRNSYS (SEL 1995). Special purpose computerized design tools have also been developed for the thermal analysis of window systems such as Window 4.1 (Arastech et al. 1994), TRNSHD (Hiller 1996), and Solar-5 (Milne et al. 1988), and for solar system analysis such as SOLARSPEC and F-CHART (Beckman et al. 1977). However, despite these efforts to utilize computers in building energy design, the incorporation of computer-aided design into the everyday architectural design process has lagged far behind what is technically possible.

There are several reasons why advanced computerized energy conservation analysis has failed to be incorporated in the actual building design process, including: 1) the complexity of the heat transfer calculations, 2) the lack of suitable easy-to-use tools to visualize the input/output of the energy analysis (Huang et al. 1992) such as the DrawBDL program, 3) the lack of designers' understanding of the value of a proper energy evaluation in their design process (Cockroft 1982), and 4) the requirement of a high level of technical expertise in mastering the operation of the computer programs imposes a heavy burden on the designers who use them.

The availability of more powerful, inexpensive personal computers and improved low-cost monitoring equipment to measure building energy use has brought renewed emphasis toward the measurement and validation of building simulation models. The previous research (Clarke 1982, Cockroft 1982) identified the inconsistency and inaccuracy of simulated results,

---

This dissertation follows the format of *ASHRAE Transactions*.

the importance of program validation, and the importance of the use of measurements from real buildings during the development of the energy simulation models.

To reach the goal of affordable, accurate energy-efficient building design, it is essential to develop computer software that can provide the advanced knowledge of human experts and remain flexible enough to respond to architects' design alternatives. Such a program should meet two distinctive user requirements; ease-of-use without sacrificing accuracy, and proper validation of the program's heat transfer models through comparison and experimentation. Furthermore, since most energy simulation programs require a level of technical knowledge beyond the typical architects' experience, a successful computer simulation program should require only a modest level of knowledge about building energy analysis from the user and should include on-line help to explain the complex calculations that are being performed. The software should also allow the user to clearly visualize the energy impacts with a self-instructional capability.

1.2. Objectives

The objective of this research is to develop and validate improvements in models that will ultimately lead to computer software for energy-efficient fenestration system design. This will allow architectural and engineering designers to calculate and understand the complex heat transfer analysis of shaded building fenestration systems in such a way that it can be easily incorporated into day-to-day design process. To achieve the goal, the specific tasks of this study are defined as follows:

1) To develop accurate and visually effective methods to calculate and view the sun angles, solar radiation, and the thermal performance of the fenestration systems.

2) To develop and test a computerized shaded fenestration system design model which incorporates accurate, complex energy analysis into a window and shading device design tool.

3) To validate portions of the computerized solar simulation model against other models, and against the measured data gathered from a specially constructed experimental model.

4) To develop methods that help the user to clearly visualize the energy impacts with a proper self-guided user interface.

1.3. Organization of the Dissertation

This chapter has discussed the background of the proposed research topic and the purpose and objectives of the research. Chapter II surveys and discusses the previous research in the area relating to this work to provide the basis for the development of this research. The survey area includes general methods for calculating solar geometry and shading analysis, graphical display techniques of sunpath diagrams, calculation of incident solar radiation, methods for calculating the thermal performance of a shaded window, and the validation of a computerized thermal and shading model.

Chapter III discusses the importance of the study and contributions in this research area. The scope and limitations of the research as well as the development of procedures used in this research are also discussed in this chapter.

Cnapter IV discusses the methodology applied in the research. It describes the graphical methods and equations used for solar and shading display, the calculation of heat transfer through a shaded window glazing, the method used for the experimental validation of the new computerized shading and thermal analysis model using measured data, the application of the finite difference model for the dynamic thermal analysis, and comparative validation of the new model against the DOE-2 program.

Chapter V discusses development of the new computer model (i.e., the 'Shaded Fenestration Design Model) for shading and thermal analysis of shaded fenestration systems. The functions of the main program as well as three add-in programs are described in this chapter. The three add-in programs are the 'Solar Data Calculator', the 'Weather Data Converter' and the 'Weather Data Displayer'.

Chapter VI discusses the analysis of the measured and simulated data. A comparison of the results of the simulated data against measured data and the DOE-2 program is also discussed here.

Finally, Chapter VII summarizes this research work and proposes conclusions for the improvement of the research in this area.

CHAPTER II

LITERATURE REVIEW

The categories of the previous literature that are most related to this research include: computerized simulation algorithms for solar geometry and shading analysis; beam and diffuse solar radiation calculations; shading analysis procedures; and the incident angle dependent heat transfer through multi-pane window systems. Widely-used computerized models for fenestration design and the methods for the validation and measurement of solar models will also be reviewed along with previous efforts to analyze shaded fenestration systems.

2.1 Solar Geometry and Shading Analysis

Solar geometry (i.e., the location of the sun and the incident angle of beam radiation on a stationary surface) determines the intensity of solar radiation on a given window. The methods used to calculate the solar altitude and azimuth angles are well developed and described in a number of related textbooks (e.g., Duffie and Beckman 1991, Kreider and Rabl 1994). These methods are used in the newly developed model to calculate the solar geometry for the window aperture.

2.2 Graphical Display Techniques

Analyzing the thermal impact of a shaded fenestration system normally involves an annual analysis in either a tabular or a graphical format. Ultimately, a compact display of the hourly annual solar data such as the sunpath diagram would yield useful results in a familiar visual format that is also compact. The sunpath diagram has been widely used as a graphical presentation of the hourly path of the sun across the sky's hemispherical vault for a given latitude. It is a two-dimensional graphical representation showing the location of the sun in the three-dimensional sky vault at various times. This requires a method for projecting the hemispherical vault of the sky onto a flat plane. The most widely used projection methods are equidistant, orthographic, stereographic, gnomonic, and cylindrical projection. Previous research described displays that used equidistant, orthographic, stereographic, and cylindrical projection techniques. Each of these techniques has advantages and disadvantages over the other techniques. The following sections describe each of the projection techniques. Equation for plotting these displays will be discussed in Section 4.1.1.

2.2.1 Equidistant Projection

The equidistant projection has become the most widely used method for constructing a sunpath diagram and shading mask protractor in the United States. In this method, the 3-D sky dome is flattened onto a 2-D circular display where the sun's path becomes a series of elliptical curves (Figure 2.1). Unlike the case of orthographic or stereographic projection, in the equidistant projection solar altitude lines are not geometrically projected but are equally spaced as concentric circles on a 2-D diagram. This method was developed by Irving F. Hand (1948; ref. in Olgyay and Olgyay 1957) and was used in the 'LOF Sun Calculator' which was created by the Libbey-Owens-Ford Glass Co (LOF 1974). The advantage of this method is that it enables the users to plot both low and high sun altitude angles with the same visual accuracy.

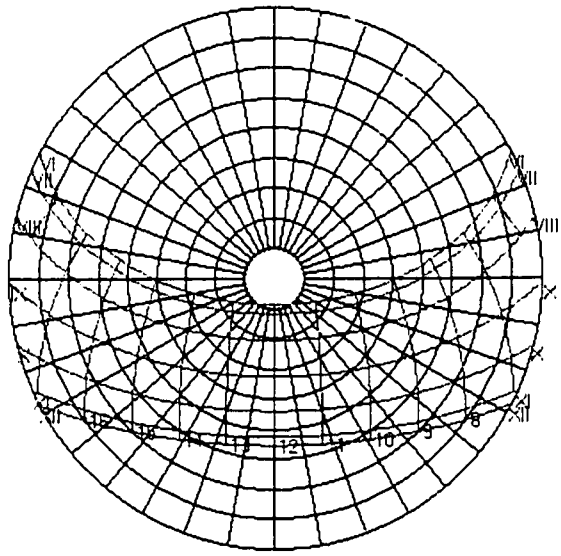

Figure 2.1 Sunpath Diagram Showing an Equidistant Projection. This figure shows a sunpath diagram for 32° N latitude that uses equidistant spacing of the solar altitude lines.

2.2.2 Orthographic Projection

The orthographic sunpath diagram is an exact projection of the sky's hemispherical vault onto a 2-D circular plot (Figure 2.2). This method was first developed by Molesworth (1902; ref. in Olgyay and Olgyay 1957) and later suitably modified by Waldram (1933; ref. in Olgyay and Olgyay 1957). Even though this method is geometrically correct, accurate interpretation of the plots is nearly impossible in the outer rim of the circular plot (i.e., the sunrise or sunset times) because of the severe contraction of the solar altitude angles toward the edges of the diagram. The

advantage of the orthographic plot is that it can be directly compared to 180° globoscope photographs (Olgyay and Olgyay 1957). Hence, it can be helpful in tracing the outline of shading caused by surrounding obstructions (Harkness and Metha 1978) that are optically projected.

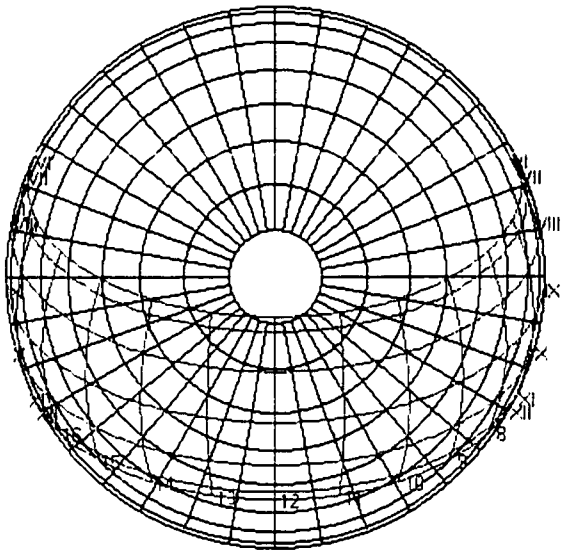

Figure 2.2 Sunpath Diagram Showing an Orthographic Projection. This figure shows a sunpath diagram for 32° N latitude that uses orthographic projection of the solar altitude lines.

2.2.3 Stereographic Projection

In a stereographic projection, any point on the sky vault is first connected to the nadir at the center. Then, the intersection of the lines and the equatorial plane of the sphere are projected down to make solar altitude lines in a 2-D projected plane (Figure 2.3). In this way each sunrise-to-sunset sunpath line is represented as a circle, with the diameter increasing as it approaches winter solstice (i.e., low altitude angles). This method is well researched by noted Swedish architect Gunnar Pleijel (Aronin 1953). It has the advantage of reducing the edge distortion of the sunpath in the diagram. Furthermore, since sunpath lines appear as circles, this projection is the easiest to draw. The diagram does have one drawback, namely, the circles that represent the solar altitude angles become densely packed toward the center of the diagram, thus making it hard to read the solar altitude angles greater than 60 degrees (i.e., summertime values for lower latitudes around noon time).

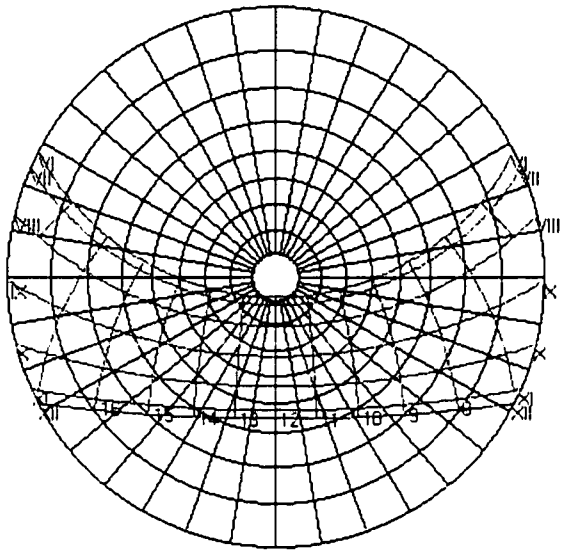

Figure 2.3 Sunpath Diagram Showing a Stereographic Projection. This figure shows a sunpath diagram for 32° N latitude that uses stereographic projection of the solar altitude lines.

2.2.4 Gnomonic Projection

The gnomonic projection is derived from the sundial. The location of the observer is at the center of the celestial sphere facing the vernal equinox sunpath (i.e., the horizon in a celestial sphere). Any point on the sphere is projected on a line that is parallel with the horizon at the center of the zenith (Figure 2.4). The solar lines are, therefore, compressed near the zenith and greatly expanded at low altitudes. The sunrise and sunset cannot be presented on this projection

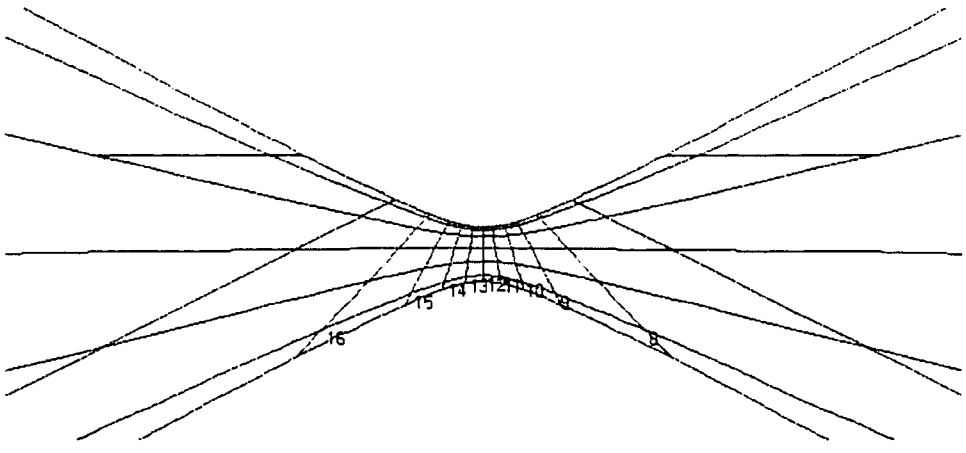

Figure 2.4 Sunpath Diagram Showing a Gnomonic Projection. This figure shows a sunpath diagram for 32° N latitude that uses gnomonic projection of the solar altitude lines.

because the projection line becomes infinite. Because of this inability to display the entire sky vault, this method is rarely used for sunpath diagrams but it is used frequently for building shadow studies and for constructing sundials.

2.2.5 Cylindrical Projection

The cylindrical projection method plots the sun's path onto an equally spaced x-y grid of solar angles where values of the y-axis represent the solar altitude angles and values of the x-axis represent the off-south solar azimuth (Figure 2.5). The x-y grid of sun angles effectively maps the sun's 3-D hemispherical path onto cylindrical coordinates that can be imagined as being unrolled and displayed in a 2-D format. This method has been extensively used in the area of architectural design.

The method was popularized by Edward Mazria (1979) and has been frequently used to visualize the site skyline with solar obstructions that block direct sun from reaching any point on the site. The research of Robert Bennett (1978) gives helpful examples of the cylindrical diagrams for various latitudes with overlay of the shading objects. This method provides very easy reading of solar angles owing to the application of straight lines for the solar altitude and azimuth angles. Unfortunately, the sunpath lines and accompanying shading mask protractor lines lead to some rather obscure shapes with this method.

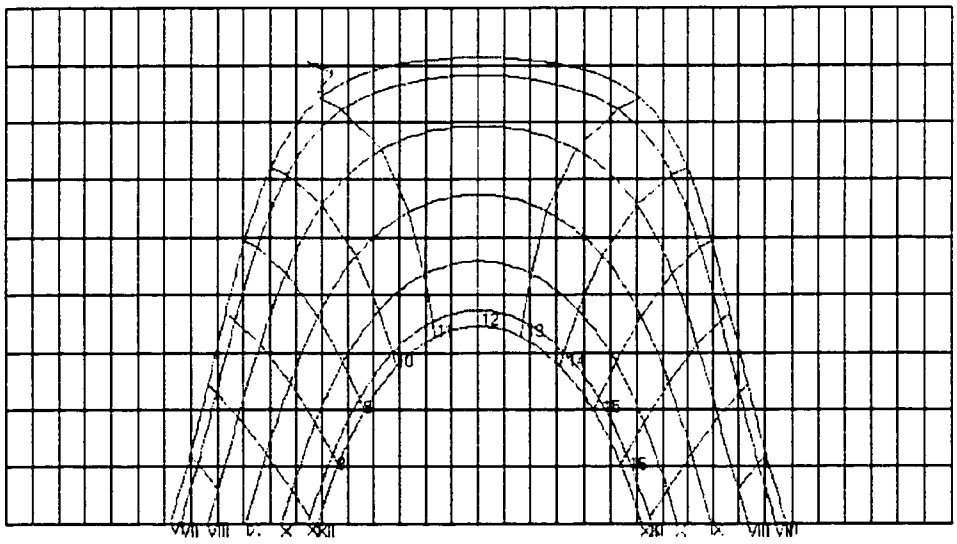

Figure 2.5 Sunpath Diagram Showing a Cylindrical Projection. This figure shows a sunpath diagram for 32° N latitude that uses cylindrical projection of the solar altitude and zenith lines.

2.2.6 Shading Mask Protractor

For an effective solar and shading analysis, a shading mask protractor is usually used along with the sunpath diagram to display the profile of shading objects upon the sunpath. The shading mask protractor is a grid of construction lines that can be used to trace the projected vertical shadow angles and the projected horizontal shadow angles (Figure 2.6). The shading mask protractor was first developed by Olgyay and Olgyay (1957) to overlay the outlines of shaded areas onto the equidistant sunpath diagram. By overlaying the shading mask protractor onto the appropriate sunpath diagram for a given latitude in the proper off-south orientation, a designer can calculate exactly when the beam radiation will be blocked at a point centered at the bottom of the window being analyzed. To accomplish this the x-y-z Cartesian coordinates of the shading device are transcribed onto the shading mask and oriented for the proper off-south azimuth of the window being analyzed. The combined sunpath and shading mask diagrams indicate whether the direct sunlight is blocked by the shading objects at a given time of the year.

The traditional method of using the shading mask protractor with sunpath diagram remains a difficult task because of the troublesome calculations needed to transcribe the x-y-z coordinates of the physical shading devices onto the shading mask protractor. Most published shading mask protractors can only solve a limited number of rectangular shading devices that have edges that are either perpendicular or parallel to the window frames. Furthermore, in the United States, the current application of the shading mask protractor is limited to the equidistant projection.

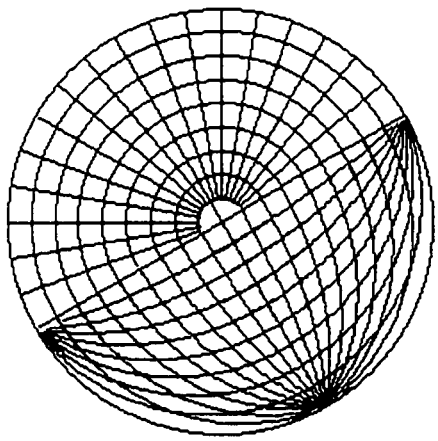

Figure 2.6 Shading Mask Protractor. This figure shows a shading mask protractor for 30° East of due South building azimuth using the equidistant projection.

2.3 Solar Radiation Calculations

A number of previous investigators have derived equations to calculate the solar radiation on a clear day for a given latitude. The most widely accepted clear sky solar radiation models are the ASHRAE clear sky model (ASHRAE 1997), and Hottel's model (Hottel 1976). Hottel's model is applied by both popular textbooks noted earlier (i.e., Duffie and Beckman (1991), and Kreider and Rabl (1994)). Bird and Hulstrom (1981) also proposed a clear sky model for direct and diffuse insolation on horizontal surfaces that uses three 'rigorous radiative transfer codes'.

The *ASHRAE Handbook* provides a table which lists the monthly values of extraterrestrial solar radiation intensity, apparent solar irradiation at air mass m = 0, and atmospheric extinction coefficient of direct normal irradiance. Using values in this table, one can calculate representative solar radiation for each month for conditions on cloudless days for a relatively dry and clear atmosphere. This model has limited use in a computerized simulation model, because it provides only one representative value for each month. Moreover, it does not consider the effects of altitude and visibility at the location.

To develop a more accurate solar simulation model that considers the effects of altitude and visibility of the site, both the Kreider and Rabl (1994) and the Duffie and Beckman (1991) introduced the 'atmospheric transmittance' for beam radiation calculation, which had been developed by H. C. Hottel. Hottel (1976) presented a method for estimating the beam radiation through clear atmospheres which takes into account zenith angle and altitude angle for a standard atmosphere and for four climate types. The application of Hottel's atmospheric transmittance model is more accurate and more flexible than the ASHRAE clear sky model. Unfortunately, a preliminary comparison of the simulation results from these models with solar data measured on the solar test bench at Texas A&M University shows a significant difference on clear days during the winter. Likewise, only on a few clear summer days show an acceptable agreement. Furthermore, there appears to be no clear guidance as to how or when to apply Hottel's climate types.

Bird and Hulstrom (1981) have also proposed a simplified clear sky model for direct and diffuse insolation on horizontal surfaces that uses three 'rigorous radiative transfer codes'. One code is for direct normal irradiance and is called SOLTRAN 4 (Bird and Hulstrom 1980; ref. in Bird and Hulstrom 1981). Two other codes, which include both the beam and the diffuse irradiance, are the BRITE (Bird and Hulstrom 1979; ref. in Bird and Hulstrom 1981) Monte Carlo

code and the Dave (Dave 1978) Spherical Harmonics code. A fairly detailed multi-layered atmosphere is constructed by defining important atmospheric parameters at each layer. Each code then uses its own algorithm to solve the radiative transfer problem. The input parameters required for Bird's model are the solar constant, zenith angle, surface atmospheric pressure, ground albedo, precipitable water vapor, total ozone, turbidity at 0.5 and/or 0.38 /*m* wave-length, and aerosol forward scattering ratio (0.84 recommended). When good weather information is not available, the suggested values are given for some input parameters.

Although Bird's model might be more accurate, it is not readily applicable to an architectural model because it requires very detailed weather information such as hourly values for transmittance of aerosol scattering, transmittance of dry air absorptance, amount of ozone, aerosol optical depth, etc. Therefore, the current work uses measured beam and diffuse solar data to test the experimental model (i.e., Hottel's model).

2.3.1 Calculation of Extraterrestrial Radiation

The extraterrestrial solar radiation (I_o) is the solar radiation that would be received on the earth's surface if there were no atmosphere. In other words, extraterrestrial solar radiation is the intensity of solar radiation outside the earth's atmosphere on a surface perpendicular to the sun's ray. The value of extraterrestrial solar radiation is an important quantity because, in many solar radiation models, the estimated values of the clear day direct and diffuse radiation on the earth are derived from it.

The value of extraterrestrial radiation depends solely on the day of the year (n) and is independent of the latitude of the site and the solar location such as solar hour angle. In other words, any location on the earth would have the same amount of extraterrestrial solar radiation on the same day of the year. Due to the eccentricity of the earth's orbit, the actual value of extraterrestrial solar radiation varies by ±3.3%. The maximum occurs in winter (January 3) and the minimum extraterrestrial radiation is in summer (July 4) in the Northern Hemisphere (ASHRAE, 1997). Thus, the extraterrestrial solar radiation at the average earth-sun distance, that is, the solar constant (I_{SC}) is used to calculate the actual intensity of the extraterrestrial solar radiation with consideration of seasonal variations.

The 1997 *ASHRAE handbook* uses a value of 433.34 Btu/h·ft^2 (1,367 W/m^2) for the solar constant. It varies from a maximum of 448.2 Btu/hr-ft^2 (1,414 W/m^2) on January 3 to a minimum

of 419.2 Btu/hr-ft^2 (1,323 W/m^2) on July 4. The *ASHRAE Handbook* provides a table (Table 2.1) to determine the extraterrestrial and clear day direct normal solar radiation for the 21st day of each month. The values for A, B, and C in Table 2.1 are used to calculate the clear day direct normal radiation and will be described in the next section in more detail.

Duffie and Beckman (1991) used a value of the solar constant rounded to 433 Btu/hr-ft^2 (1,367 W/m^2). The extraterrestrial radiation can be calculated by

$$I_o = \left[1 + 0.033 \times \cos\left(\frac{360^o \times n}{365}\right)\right] \times I_{SC} \qquad (2.1)$$

where n is the day of the year.

Table 2.1 ASHRAE's Extraterrestrial Solar Radiation and Related Data (ASHRAE 1997).

Date	I_o	Declination	A	B	C
	Btu/(hr-ft^2)	Degrees	Btu/(hr-ft^2)	dimensionless	dimensionless
Jan. 21	448.8	-20.0	390	0.142	0.058
Feb. 21	444.2	-10.8	385	0.144	0.060
Mar. 21	437.7	0.0	376	0.156	0.071
Apr. 21	429.9	11.6	260	0.180	0.097
May 21	423.6	20.0	350	0.196	0.121
June 21	420.2	23.45	345	0.205	0.134
July 21	420.3	20.6	344	0.207	0.136
Aug. 21	424.1	12.3	351	0.201	0.122
Sep. 21	430.7	0.0	365	0.177	0.092
Oct. 21	437.3	-10.5	378	0.160	0.073
Nov. 21	445.3	-19.8	387	0.149	0.063
Dec. 21	449.1	-23.45	391	0.142	0.057

Note: Data are for the base year of 1964.

Kreider and Rabl (1994) used a slightly larger value of 435.2 Btu/hr-ft^2 (1,373 W/m^2) for the solar constant and a value of 365.25 for the total days of the year instead of 365 used in the Duffie and Beckman model.

$$I_o = \left[1 + 0.033 \times \cos\left(\frac{360^o \times n}{365.25}\right)\right] \times I_{SC}\,. \qquad (2.2)$$

2.3.2 Calculation of Clear Sky Solar Radiation on a Horizontal Surface

With the ASHRAE method, direct normal radiation at the earth's surface on a clear day ($I_{BN,c}$) can be calculated using the values in Table 2.1. The clear day beam normal solar radiation is

$$I_{BN,c} = \left[\frac{A}{\exp(B / \sin \alpha_s)} \right] \tag{2.3}$$

where, A is apparent solar radiation at air mass $m = 0$ (Table 2.1), B is atmospheric extinction coefficient (Table 2.1) and α_s is the solar altitude angle, in degrees. Values of A and B vary during the year because of seasonal changes in the dust and water vapor content of the atmosphere and because of the variations in the earth-sun distance.

To estimate the solar radiation on a clear sky day, both Kreider and Rabl's and Duffie and Beckman's models used the atmospheric transmittance for beam radiation (τ_b), which had been developed by H. C. Hottel.

Hottel (1976) has presented a method for estimating the normal beam radiation through a clear atmosphere which takes into account altitude, visibility, and climate types as well as zenith angle. He proposed the atmospheric transmittance for beam radiation (τ_b) thatis the factor between clear sky beam normal radiation to extraterrestrial radiation ($\tau_b = I_{BN,c} / I_o$) and is determined by

$$\tau_b = a_o + a_1 \times \left[\exp\left(\frac{-k}{\cos \theta_z} \right) \right] \tag{2.4}$$

where constants a_0, a_1, and k are given by Table 2.2 and Table 2.3. This solar transmittance for a standard atmosphere can be used for any zenith angle and altitude up to 2.5 km.

If one uses atmospheric transmittance for beam radiation, the clear sky beam normal radiation ($I_{BN,c}$) can be calculated by

$$I_{BN,c} = I_o \times \tau_b \cdot \tag{2.5}$$

Table 2.2 Correction Factors for Climate Types in Hottel's (1976) Model.

Climate Type	R_0		r_1	r_k
	23 km visibility	5 km visibility		
Tropical	0.95	0.92	0.98	1.02
Midlatitude summer	0.97	0.96	0.99	1.02
Subarctic summer	0.99	0.98	0.99	1.01
Midlatitude winter	1.03	1.04	1.01	1.00

Table 2.3 Correction Factors for Altitude and Visibility in Hottel's (1976) Model.

	23 km (14.3 mi.) visibility	5 km (3.11 mi.) visibility
a_0	r_0 [0.4237 - 0.00821*(6.0-A)^2]	r_0 [0.2538 - 0.0063*(6.0-A)^2]
a_1	r_1 [0.5055 + 0.00595*(6.5-A)^2]	r_1 [0.7678 + 0.0010*(6.5-A)^2]
k	r_k [0.2711 + 0.01858*(2.5-A)^2]	r_k [0.2490 + 0.0810*(2.5-A)^2]

Note: A is the altitude of the site above sea level in units of km.

When considering solar radiation on a clear day, one may use the value of 23 km for the visibility in Table 2.2 and Table 2.3. The climate type in Table 2.2 is a less critical factor in determining τ_b than the altitude of the site. Table 2.4 shows values of atmospheric transmittance for beam radiation for different altitudes and climate types. These values include a 20% difference between the maximum and minimum values of τ_b among different altitudes, but only about 5% difference among different climate types. As the *ASHRAE Handbook* does not consider the effect of altitude of the site for the clear day beam radiation calculation, there is a considerable discrepancy between the estimate radiation levels from the *ASHRAE Handbook* method and other methods.

Table 2.4 The Atmospheric Transmittance for Beam Radiation (τ_b).

Altitude above sea level	Tropical	Midlatitude summer	Subarctic summer	Midlatitude winter
0 ft (0 km)	.5960	.6034	.6081	.6251
328 ft (0.1 km)	.6054	.6130	.6179	.6352
656 ft (0.2 km)	.6145	.6223	.6273	.6450
1641 ft (0.5 km)	.6399	.6482	.6536	.6722
3281 ft (1.0 km)	.6756	.6847	.6908	.7108
6562 ft (2.0 km)	.7239	.7343	.7415	.7638
8203 ft (2.5 km)	.7374	.7483	.7561	.7792

Note: The calculation is for the case of a non-leap year. The zenith angle is 28° and visibility is 23 km.

Direct solar radiation on a horizontal surface for a clear day ($I_{BH,c}$) is determined by the beam normal radiation, and the angle between the zenith and the sun. It can be calculated by

$$I_{BH,c} = I_{BN,c} \times \cos\theta_z \tag{2.6}$$

where θ_z = zenith angle, in degrees.

Liu & Jordan (1960) developed an empirical relationship between extraterrestrial radiation and diffuse radiation for clear days. The atmospheric transmittance for diffuse radiation (τ_d) is the ratio of clear sky diffuse radiation to extraterrestrial radiation on the horizontal surface and is calculated by

$$\tau_d = \frac{I_{DH,c}}{I_o \times \cos\theta_Z} = 0.271 - 0.294\tau_b \tag{2.7}$$

Diffuse solar radiation on a horizontal surface on a clear day ($I_{DH,c}$) is determined by τ_d, extraterrestrial radiation, and the angle between zenith and the sun and can be calculated by

$$I_{DH,c} = \tau_d \times I_o \times \cos\theta_z \tag{2.8a}$$

and

$$I_{DH,c} = (0.271 \times I_o - 0.294 \times I_{BN,c}) \times \cos\theta_z \tag{2.8b}$$

Thus, total solar radiation on a horizontal surface on a clear day ($I_{GH,c}$) is

$$I_{GH,c} = I_{BH,c} + I_{DH,c} \tag{2.9a}$$

$$= I_o \tau_b \cos\theta_z + I_o \tau_d \cos\theta_z \tag{2.9b}$$

$$= I_o \cos\theta_z (\tau_b + \tau_d) \tag{2.9c}$$

$$= I_o \cos\theta_z (0.271 + 0.706\tau_d) \tag{2.9d}$$

Thus, one can calculate the estimated clear day solar radiation on a horizontal surface if the zenith angle, altitude, and climate type for the location are given. Equation 2.9d shows that the total

clear sky radiation on a horizontal surface is determined by extraterrestrial radiation (I_o), zenith angle (θ_z), and atmospheric transmittance for beam radiation (τ_b).

2.3.3 Calculation of Solar Radiation on a Tilted Surface

Total solar radiation incident on a tilted surface (Figure 2.7) can be calculated from the sum of the various vertical components of solar radiation. These components include beam radiation, diffuse radiation from the sky, and radiation reflected from the various surfaces such as the ground, external shades, and neighboring objects that block the view of the surface.

The beam radiation on a tilted surface (I_{BT}) is calculated by

$$I_{BT} = I_{BH} \cdot R_b \tag{2.10}$$

where R_b is the tilt factor which is the ratio of beam radiation component on a tilted surface to that on the horizontal surface. When the incidence angle of the direct sun is known, R_b can be calculated by

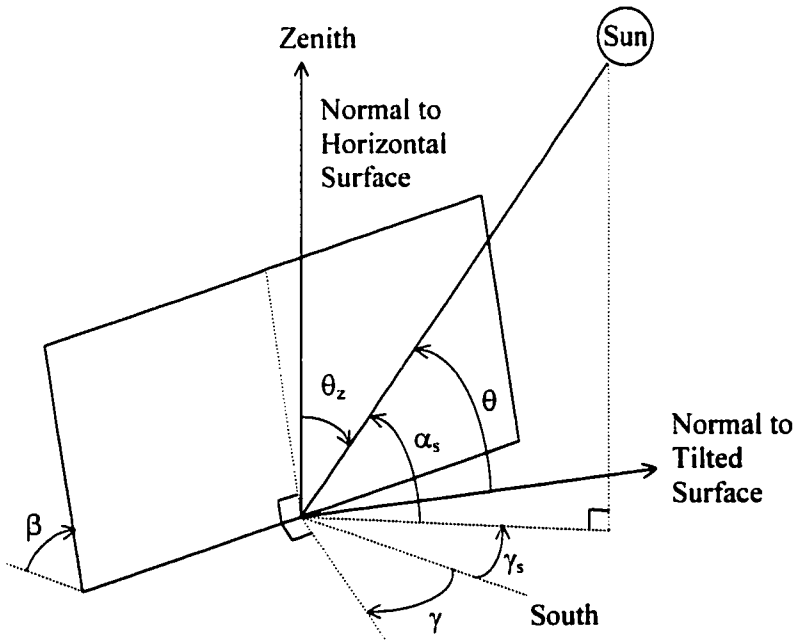

Figure 2.7 Incident Angle (θ), Zenith Angle (θ_z), S*Isometric View* gle (α_s), Solar Azimuth Angle (γ), Surface Tilt Angle (β), and Surface Azimuth Angle (γ_s) for a Tilted Surface.

$$R_b = \frac{I_{BT}}{I_{BH}} = \frac{I_{BN}\cos\theta}{I_{BN}\cos\theta_z} = \frac{\cos\theta}{\cos\theta_z} \tag{2.11a}$$

where θ is the angle of incidence of beam radiation from the normal to the tilted surface and is calculated by

$$\theta = \cos^{-1}\left[\cos\theta_z\cos\beta + \sin\theta_z\sin\beta\cos(\gamma_s - \gamma)\right]. \tag{2.11b}$$

If the view of the surface is blocked from the direct sun, the total incident beam radiation on the tilted surface is

$$I_{BT} = I_{BH}\cdot R_b\cdot F_s \tag{2.12}$$

where F_s is the sunlit factor and is defined by the sunlit area of the tilted surface divided by the total area of that surface.

The calculation of the diffuse radiation component on a tilted surface is a little more complicated. The diffuse radiation consists of three different components: the 'isotropic diffuse' radiation delivered uniformly from the sky hemisphere, the 'circumsolar diffuse' radiation scattered around the direct sun, and the 'horizon brightening' which is concentrated near the horizon (Figure 2.8). In general, there are two kinds of solar radiation models based upon the method to simulate diffuse solar radiation: an anisotropic model and an isotropic model.

In an isotropic sky model, it is assumed that diffuse radiation is isotropic or constant. In other words, the diffuse radiation from the sky is the same regardless of the orientation. The Liu and Jordan (1963) model for the diffuse radiation is the most widely used. In this model, the solar radiation on a tilted surface is composed of beam, isotropic diffuse, and ground reflected solar radiation. Thus, the diffuse radiation on the tilted surface (I_{DT}) is calculated by

$$I_{DT} = I_{DH}\left(\frac{1+\cos\beta}{2}\right) \tag{2.13}$$

where β is the tilt angle of the surface.

Reindl et al. (1990) developed an improved anisotropic model called the 'HDKR model' by adding a horizon brightening component to the model originally developed by Hay and Davies

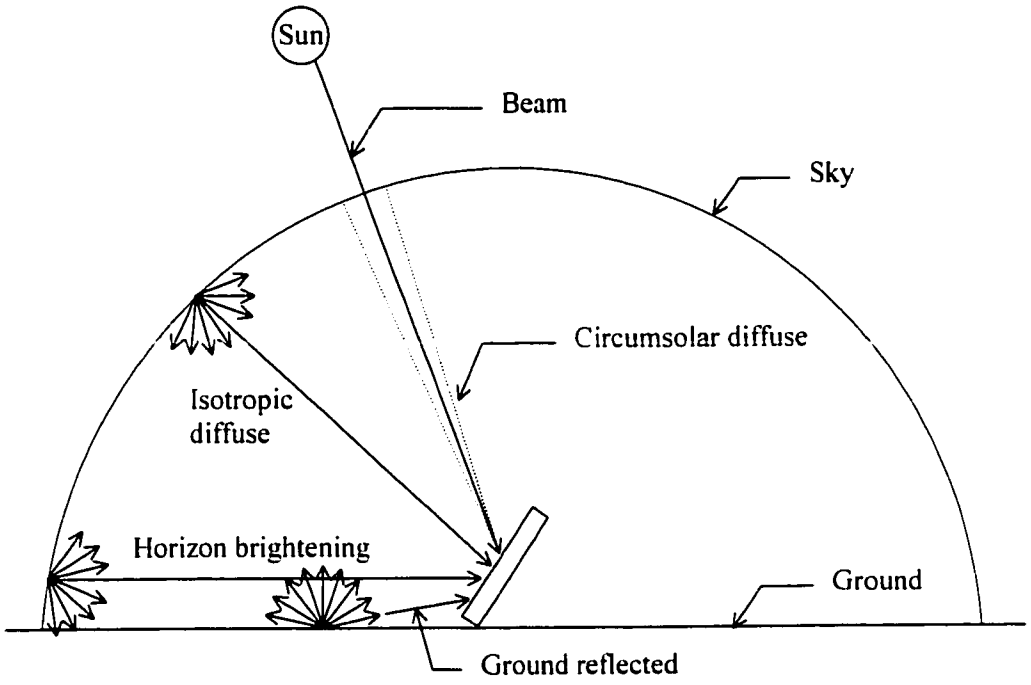

Figure 2.8 Beam, Isotropic Diffuse, Circumsolar Diffuse, Horizon Brightening, and Ground Reflected Radiation on a Tilted Surface.

(1980; ref. in Duffie and Beckman 1991) and modified by Klucher (1979). This model uses an 'anisotropy index' to determine the transmittance of the atmosphere for beam radiation. It is assumed that the isotropic diffuse radiation from the sky has the same angle as the beam radiation. The diffuse radiation on the tilted surface (I_{DT}) using the HDKR model is calculated by

$$I_{DT} = I_{DH}\left(\left(1-A_i\right)\left(\frac{1+\cos\beta}{2}\right)\left[1+f\sin^3\left(\frac{\beta}{2}\right)\right]+A_i R_b\right) \qquad (2.14)$$

where A_i is an anisotropy index and defined by

$$A_i = \frac{I_{BN}}{I_{ON}} = \frac{I_{BH}}{I_{OH}}, \text{ and} \qquad (2.15)$$

$$f = \sqrt{I_{BH}/I_{GH}}\,. \qquad (2.16)$$

Perez et al. (1988; ref. in Duffie and Beckman 1991) also developed another anisotropic sky model which considers the zenith angle of the direct beam, cloud clearness, the air mass, and

brightness coefficient of the sky. The diffuse radiation on the tilted surface (I_{DT}) is again calculated by

$$I_{DT} = I_{DH}\left((1-F_1)\left(\frac{1+\cos\beta}{2}\right) + F_1 R_b + F_2 \sin\beta\right) \tag{2.17}$$

where F_1 and F_2 are circumsolar and horizon brightness coefficients determined by three parameters that describe the sky conditions: the zenith angle, cloud clearness, and brightness. The values of F_1 and F_2 are calculated from the table for brightness coefficients.

The method developed by Liu and Jordan is less accurate than the anisotropic models. The model developed by Perez et al. is difficult to apply to a computer application. Thus, in this research, the anisotropic model developed by Reindl et al. (i.e., HDKR model) was applied to calculate the diffuse component of solar radiation on a vertical surface.

The ground reflected solar radiation on a tilted surface is determined by the total radiation on the horizontal surface (I_{GH}), the view factor of the surface to the ground ($F_{s\text{-}g}$), and the ground reflectance (ρ_g). For a surface directly in the front of a collector extending in all directions, the view factor to the ground is (1-cosβ)/2 and the reflected radiation from the ground on a surface is then calculated by

$$I_{RT,G} = I_{GH}\rho_g\left(\frac{1-\cos\beta}{2}\right). \tag{2.18}$$

Generally, the sky model ignores the reflected radiation from the surrounding objects such as the external walls, because it is much smaller than the reflected radiation from the ground. However, in the case when a large portion of the view from the surface is blocked by external surfaces, the reflected radiation from these surfaces should be considered. The total reflected radiation from the surrounding surfaces ($I_{RT,S}$) can be calculated by

$$I_{RT,S} = \sum I_i \rho_i F_{i-s} \tag{2.19}$$

where I_i is the solar radiation incident on the ith surface, ρ_i is the diffuse reflectance of that surface, and $F_{i\text{-}s}$ is the view factor from the ith surface to the analyzed tilted surface.

Finally, the total solar radiation on a tilted surface (I_{TT}) is calculated as the sum of each

component. From Equations 2.11, 2.14, 2.18, and 2.19, the total solar radiation on a tilted surface is

$$I_{TT} = F_s I_{BH} R_b + I_{DH}\left((1-A_i)\left(\frac{1+\cos\beta}{2}\right)\left[1+f\sin^3\left(\frac{\beta}{2}\right)\right]+A_i R_b\right) + I_{GH}\rho_g\left(\frac{1-\cos\beta}{2}\right)+\sum I_i\rho_i F_{i-s} \qquad (2.20)$$

For the computerized calculation of the total solar radiation on a tilted surface, the proposed model uses Equation 2.20 for calculating the total solar radiation incident on a tilted surface.

2.3.4 Calculation of Transmitted and Absorbed Solar Radiation through Glazing

When the reflection and absorption losses through the glazing are considered, the transmittance (τ) of a single-glazed window can be calculated by applying ray-tracing methods to Fresnel's equation and Snell's law (Duffie and Beckman 1991). Fresnel developed equations for the reflection of unpolarized radiation when it passes from a medium with a refractive index n_1 to

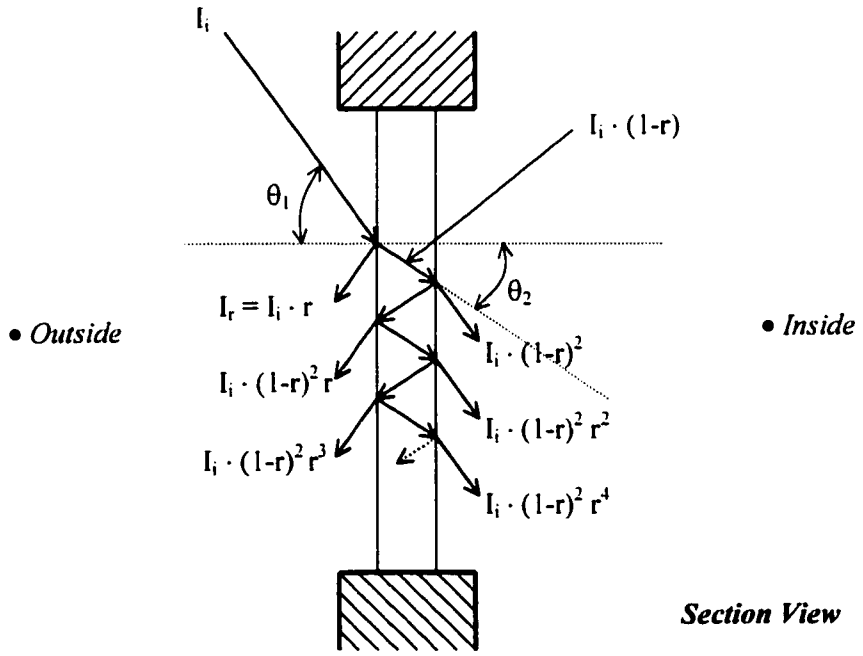

Figure 2.9 Angles of Incidence (θ_1) and Refraction (θ_2) through Single-pane Glazing. This figure also shows the incident, reflected and transmitted solar radiation through the glazing using the ray-tracing method.

another medium with refractive index n_2 (Figure 2.9). The total reflection (r) of unpolarized radiation was calculated using perpendicular ($r_\perp$) and parallel ($r_\parallel$) components of unpolarized radiation as follows

$$r_\perp = \frac{\sin^2(\theta_2 - \theta_1)}{\sin^2(\theta_2 + \theta_1)}, \tag{2.21a}$$

$$r_\parallel = \frac{\tan^2(\theta_2 - \theta_1)}{\tan^2(\theta_2 + \theta_1)}, \text{ and} \tag{2.21b}$$

$$r = \frac{I_r}{I_i} = \frac{1}{2}(r_\perp + r_\parallel) \tag{2.21c}$$

where I_i and I_r are the incident and reflected solar radiation, and θ_1 and θ_2 are incidence and refraction angles. The refraction angle can be calculated using Snell's law as follows

$$\frac{n_1}{n_2} = \frac{\sin\theta_2}{\sin\theta_1} \tag{2.22a}$$

Thus,

$$\theta_2 = \sin^{-1}\left(\frac{n_1}{n_2}\sin\theta_1\right) \tag{2.22b}$$

The total transmittance (τ) of single-pane glazing can be calculated applying the ray-tracing method to Fresnel's equations as follow

$$\tau = \frac{1}{2}(\tau_\perp + \tau_\parallel) \tag{2.23a}$$

where $\tau_\perp$ and $\tau_\parallel$ are the perpendicular and parallel components of transmittance of the glazing and are calculated again by

$$\tau_\perp = \tau_a \frac{1-\tau_\perp}{1+\tau_\perp}\left(\frac{1-\tau_\perp^2}{1+\tau_\perp^2}\right) \text{ and} \tag{2.23b}$$

$$\tau_{\|} = \tau_a \frac{1-\tau_{\|}}{1+\tau_{\|}}\left(\frac{1-\tau_{\|}^{\,2}}{1+\tau_{\|}^{\,2}}\right). \tag{2.23c}$$

where τ_a is the transmittance of glazing when only absorption losses have been considered, and is defined as follows

$$\tau_a = \frac{I_{Trans}}{I_t} = \exp\left(-\frac{KL}{\cos\theta_2}\right) \tag{2.24}$$

where K is the extinction coefficient and L is the thickness of the glazing.

The total amount of the transmitted solar radiation through window glazing can be calculated from Equations 2.23 a, b, c. However, some portion of the transmitted solar radiation is absorbed by the inside surface and some is reflected back to the glazing. Thus, for the calculation of heat gain from the transmitted solar radiation, we need to calculate how much of the transmitted solar radiation is actually absorbed by the inside surfaces. The total solar radiation transmitted through glazing and absorbed by the inside surfaces can be calculated using the transmittance-absorptance product '$(\tau\alpha)$' as follows

$$\begin{aligned} I_{GT,Trans} &= F_s I_{BH} R_b (\tau\alpha)_b \\ &+ I_{DH}\left((1-A_i)\left(\frac{1+\cos\beta}{2}\right)\left[1+f\sin^3\left(\frac{\beta}{2}\right)\right]+A_i R_b\right)(\tau\alpha)_d \\ &+ I_{GH}\rho_g\left(\frac{1-\cos\beta}{2}\right)(\tau\alpha)_g + \sum I_i \rho_i F_{i-s}(\tau\alpha)_s \,. \end{aligned} \tag{2.25}$$

Applying the same ray-tracing method here the $(\tau\alpha)$ can be calculated by

$$(\tau\alpha) = \tau\alpha\sum_{n=0}^{\infty}\left[(1-\alpha)\rho_d\right]^n = \frac{\tau\alpha}{1-\left[(1-\alpha)\rho_d\right]} \tag{2.26}$$

where ρ_d is the reflectance of the glazing for the diffuse radiation from the inside surface and α is the absorptance of the inside surface. This solar absorptance (α) is dependent on the angle of incidence of the radiation striking the surface, and can be calculated as function of the normal incidence for a flat black surface. Thus, solar absorptance (α) is

$$\frac{\alpha}{\alpha_n} = 1 + 2.0345\times10^{-3}\theta - 1.990\times10^{-4}\theta^2 + 5.324\times10^{-6}\theta^3 - 4.799\times10^{-8}\theta^4 \quad (2.27)$$

where α_n is the normal incidence for a flat black surface and θ is incidence angle on the surface.

2.4 Application Methods for the Thermal Analysis of a Shaded Fenestration System

Several general purpose computer-aided energy simulation programs have been developed that calculate the hourly heat gain and loss through fenestration systems. Among whole-building energy performance simulation software, DOE-2, BLAST, TRNSYS, and ESP(Clarke 1993) have been widely used as general purpose computer programs that provide a means to calculate shading effects by carefully selected nearby shading objects.

There are also special purpose computerized shading and fenestration design programs such as Window 4.1 (Arasteh et al. 1994), TRNSHD (Hiller 1996), OPAQUE (Abouella and Milne 1990), SOMBRERO (Schnieders et al. 1997), and AWNSHADE (McCluney 1995). Each of these are described in the following sections.

2.4.1 Methods Used in DOE-2 and BLAST

Both DOE-2 and BLAST have very well-developed algorithms for calculating hourly solar radiation. The DOE-2 program uses the ASHRAE method described in previous sections to calculate solar radiation when none is provided on the weather tape. To calculate beam normal radiation, DOE-2 modifies the solar constant with the atmospheric extinction coefficient often provided on the weather tape. The equations used to calculate the beam normal radiation and diffuse radiation are

$$I_{BN.c} = I_{SC} \times C \times e^{-B/\sin(\alpha_s)} \quad (2.28)$$

and

$$I_{DH} = \left(\frac{F_d}{C^2}\right) \times I_{DN} \quad (2.29)$$

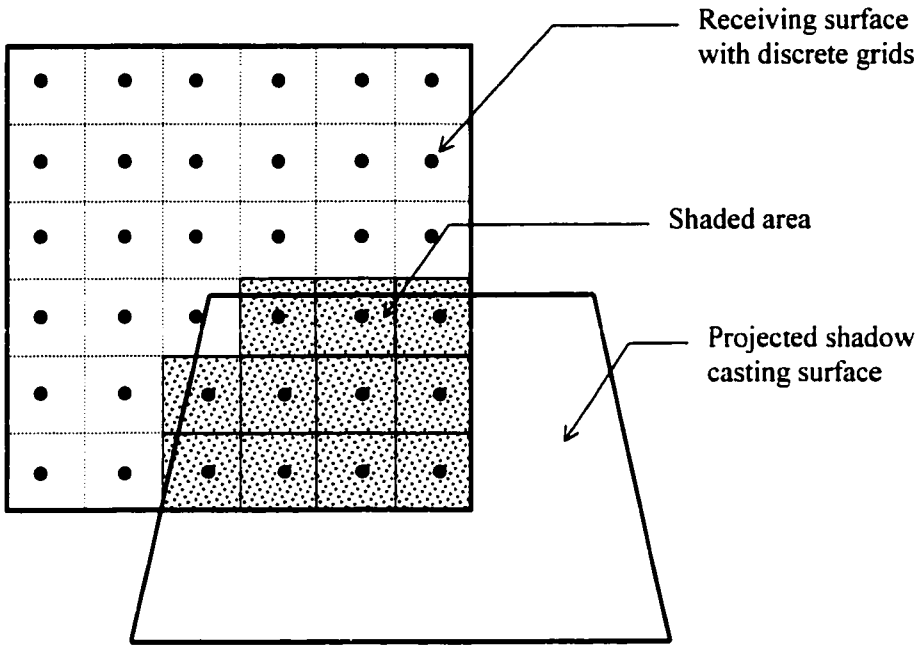

Figure 2.10 Discrete Element Analysis with Grids. This figure shows the method to calculate the shaded area using discrete grid elements.

where C is the clearness number, B is the atmospheric extinction coefficient, and F_d is the sky diffuse factor. By using these modifiers, the DOE-2 program's solar constant is always smaller than the true solar constant to represent average sky conditions (LBL 1982). Thus, the ASHRAE direct normal radiation on a clear day may be as much as 15 percent higher than the values calculated by Equation 2.28.

The method used by the DOE-2 program for a shading analysis is more complicated. Several methods have been developed for the calculation of the sunlit and shaded area of a window. One of the simplest methods is an algorithm with 'discrete element analysis with grids' (Figure 2.10). This method was first developed by Groth and Lokmanheim (1969) and used in the earlier version of DOE-2 (LBL 1982) and BLAST (BSO 1993). In this method, the receiving surface is divided into a two dimensional grid. The center point of each element is then tested by a shading projection algorithm to determine whether it is in sunlit or shaded areas. The sum over the sunlit or shaded grid elements is then used to obtain the sunlit and shaded fraction, respectively. Unfortunately, this method can require excessive processing time for higher resolution. Furthermore, it can only solve rectangular plane surfaces, which means that non-rectangular surfaces must be represented with combinations of rectangular planes.

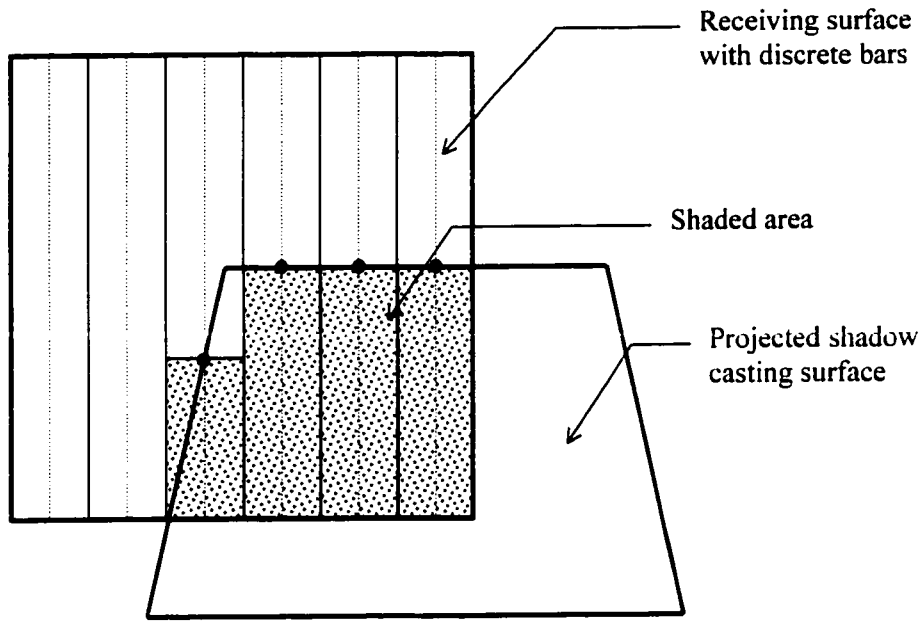

Figure 2.11 Discrete Element Analysis with Bars. This figure shows the method to calculate the shaded area using discrete bar elements.

In the current version of DOE-2 (LBL 1989), an 'improved bar-method' (Figure 2.11) was developed that uses bars instead of grids for a discrete element analysis. This method increased both the speed and accuracy of the calculation. However, the processing speed is still dependent on the desired accuracy and the method still has similar geometrical limitations as the grid method, although not as restrictive.

The most recent version of BLAST uses a 'convex polygon clipping algorithm with homogeneous coordinates' (Figure 2.12) developed by Walton (1979). In Walton's method, the n dimensional Cartesian coordinates are transformed into $n+1$ dimensional homogeneous coordinates. For example, a point given by two dimensional coordinates (x, y) is represented by three dimensional coordinates (hx, hy, h), where h is an arbitrary number. After the coordinate transformation, the algorithm finds the vertices of one polygon within the other and visa versa. Then, the intersecting points of the boundary of both polygons are determined. These overlapped vertices and intersecting points are then transformed again into Cartesian coordinates, ordered clockwise and the area is computed. Though this method is much faster than the discrete element analysis method. However, it is restricted to the use of convex polygons.

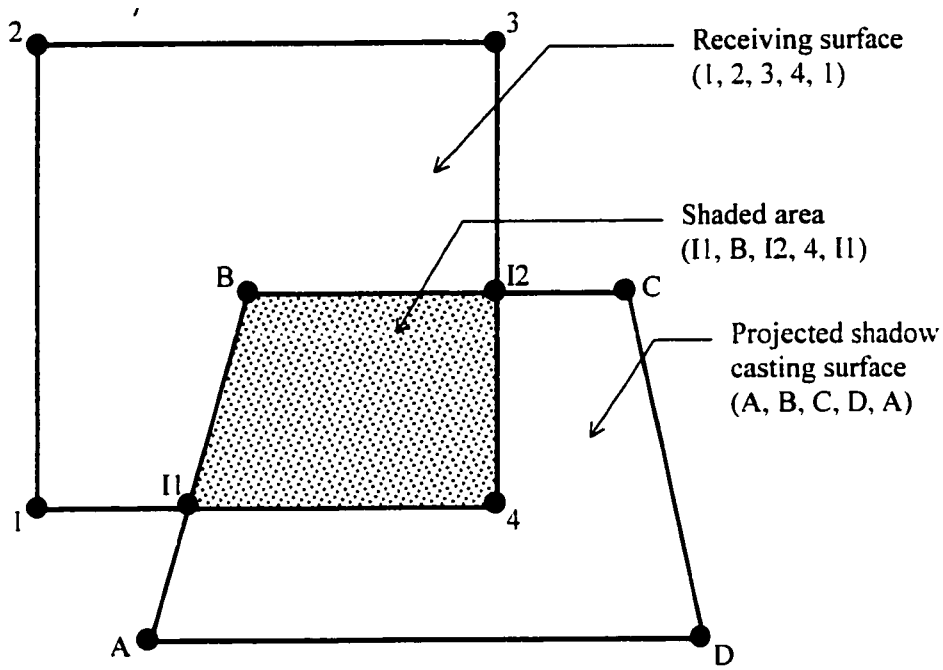

Figure 2.12 Convex Polygon Clipping with Homogeneous Coordinates. This figure shows the method to calculate the shaded area using the convex polygon clipping method.

Another accurate method is the 'boundary evaluation using 2D concave polygon clipping' (Hiller 1996). This technique was developed as a hidden line removal algorithm in computer graphics by Weiler and Atherton (1977). The method is used in some solar analysis programs such as XSUN (Grau and Johnsen 1995) and SOLAR GRAPHICS (Johnson 1985). This complex, powerful method allows accurate calculations for all kinds of overlapping planar polygons in two dimensions. An advantage of this method over discrete element methods is that the remaining sunlit and shaded polygons are represented the same way as the original receiving polygon. For the more detailed description on shading area calculation algorithms, refer to the research of Hiller (1996), Grau and Johnsen (1995), Walton (1979), and the DOE-2 Engineers Manual (LBL 1982b).

2.4.2 Methods Used in TRNSHD

The University of Wisconsin (Hiller 1996) developed a computerized program called TRNSHD that performs external shading and internal insolation calculations for a given geometric configuration of shading objects. In this program, surfaces are considered as a series of polygons projected onto a plane. The function 'polygon clipper' determines the boundary of polygons when they overlap each other. Using this method TRNSHD calculates the sunlit

fractions by calculating the ratio of solar radiation on the shaded area to that on the unshaded area. Using these fractions, the program calculates the transmitted beam radiation through the glazing. For the boundary test, each exterior window and each internal wall is divided into 288 patches, and the results of the 288 sunlit fractions for beam radiation for each internal wall and window are saved in the output file.

For the validation of the program, the results of the TRNSHD program were compared against the algorithms called TYPE 34 (overhang and wingwall shading) used in the TRNSYS (SEL 1988), and against Xsun, a proposed European Standard (CEN 1995) procedure. For the validation of the internal solar distribution, the results from the TRNSHD program were compared against the experimental measurements. There was a good agreement between results from TRNSHD and TRNSYS. The results showed that 72 sky patches provided an acceptable accuracy for diffuse radiation shading. This program will also calculate sunlit fractions and view factors for a complicated shading configuration. However, the program calculates only sunlit fractions for the external walls and the external windows.

2.4.3 Methods Used in WINDOW 4.1

Window 4.1 (LBL 1994), developed by the Windows and Daylighting Group at Lawrence Berkeley Laboratory (Arastech et al. 1994), is a computerized program for analyzing the thermal performance of fenestration products in accordance with the standard National Fenestration Rating Council (NFRC 1991) procedures. The program calculates total window thermal performance indices (i.e., U-values, solar heat gain coefficients, shading coefficients, and visible transmittances). The program treats a fenestration product as an assembly of one or more glazing systems, including the window, the window frame/edge, and any divider elements such as grilles, muntin bars, etc. The glazing system is composed of one or more glazing layers separated by gas layers. The glazing area is divided by its thermal performance such as the center of glass, the edge of glass, and the divider edge.

The Window 4.1 program also provides direct access to the various kinds of libraries for window system components including the glass library, the gas library, the frame and divider libraries, and environmental conditions library. The elements in these libraries include assembled system libraries such as the window library and the glazing system library. The glass library contains the various thermal and optical properties for more than 600 glass products.

When presented with a well-configured fenestration system, the Window 4.1 program may provide very accurate heat transfer calculations. Libraries in this program have useful information and are well organized. The proposed SFD program is designed to use a Window 4.1 glass library file for the user input of the glass description.

2.4.4 Previous Work on the SOLRPATH Program

A series of efforts by Texas A&M University (TAMU) have led to the development of a computerized program for plotting the sunpath diagram and shading effects drawn with a shading mask protractor. The previous research at TAMU began as class project in the Spring 1992 Mechanical Engineering HVAC class by Mr. Jay Mattern who developed the basic shading mask protractor line equations. Ken McWatters then proceeded to refine the shading mask protractor to include rotations for various azimuths, clipping functions and a complete FORTRAN SOLRPATH code for the sunpath diagram (McWatters and Haberl, 1994a; 1994b; 1995). Oh and Haberl (1996; 1997) then developed an improved MS-Windows version of SOLRPATH (ver 0.91B) that displayed equidistant charts with projection of global horizontal solar radiation in the sun's path The current work extends the previous SOLRPATH program to include McWatters and Haberl (1994a; 1994b; 1995) and Oh and Haberl (1996; 1997).

2.4.5 Other Thermal Analysis Programs for a Shaded Fenestration System

There are several other thermal analysis programs that are indirectly related to this work including: the OPAQUE (Abouella and Milne 1990), SOMBRERO (Schnieders et al. 1997), AWNSHADE (McCluney 1995), SOLAR-2 (Sheu 1986), SUNPATH (McCluney 1995), and SUNSPEC (McCluney 1995) programs.

OPAQUE (Abouella and Milne 1990), developed by the Department of Architecture at UCLA, draws a detailed wall or roof section, calculates the U-value, time-lag, and decrement factor. It also plots daily and annual outdoor and sol-air temperatures, normal and total surface radiation, and the heat flow through an opaque envelope (i.e., a building wall section which excludes the window).

The computerized shadow calculation program SOMBRERO (Schnieders et al. 1997) was developed by the University of Siegen, Germany for calculating the GSC (geometrical shading coefficient), that is the proportion of shaded area of an arbitrarily oriented surface

surrounded by shading elements as a function of time and location. In SOMBRERO the reduction of isotropic diffuse radiation due to different kinds of obstacles is calculated by means of view factors. SOMBRERO contains a geometry file generator that facilitates the input of 3 dimensional external objects such as a standardized house and trees.

Finally, McCluney (1995) developed a shading device design program called AWNSHADE that calculates the sunlit fraction of a vertical window that is irradiated by direct beam solar radiation as well as the approximate effective sunlit fraction by isotropic radiation from the sky and from the ground. AWNSHADE can simulate awnings with horizontal or inclined side-walls, overhangs, and vertical side-fins with horizontal or inclined top edges, and combinations of these.

Several shading and window design programs that provide graphical methods to display the solar analysis, including SOLAR-2 (Sheu 1986), SUNPATCH (Taylor 1987), SUNPATH (McCluney 1995), SUNSPEC (McCluney 1995), and SOLRPATH (McWatters and Haberl 1994a; 1994b; 1995; Oh and Haberl 1996; 1997).

SOLAR-2 (Sheu 1986), developed by the Department of Architecture at UCLA, displays sunlight penetrating through a window with any combination of rectangular fins and overhangs. It also plots on an hourly-basis, an animated, 3-D sun's-eye-view of the building, and provides annual tables of the percent of the window in full sun, and radiation on the glass.

SUNPATH, developed by McCluney (1995), calculates the position of the sun in the sky at any given time and location on earth as well as sequences of positions to display the sun's path. It also calculates the dates and times that the sun will be within a specified range of directions in the sky, and the times of sunrise and sunset for any location and date. The linked program PATHPLOT is used to plot a sunpath chart for any location.

McCluney (1995) also developed a solar radiation calculation program called SUNSPEC that calculates the direct beam and diffuse sky spectral and broadband solar irradiance incident on a vertical surface for a cloudless sky. It allows the user to specify the concentrations of various atmospheric gases and particles. SUNSPEC was developed based on Gueymard's SMARTS solar spectral irradiation algorithm (1993). It also integrates these spectra to determine the total irradiance and illuminance from the sun, sky, and ground incident upon a window aperture. The

linked program SPECPLOT can be used to plot solar spectral irradiance distributions calculated by SUNSPEC.

2.5 Review of Validation Methods for Computerized Simulation Models

The validation process is essential in the development of computer software. In general, validation of the program can be conducted at two levels: the model validation (i.e., the verification of the accuracy in the model's equations and the simulated results), and software usability validation (i.e., evaluation of effectiveness of the user interface and program itself). In the development of general-purpose computer applications that can be used in various fields of research, the usability test is an essential part that can help avoid an awkward user interface.

ASHRAE (ASHRAE SPC-140 SMOT) is developing a standard for accuracy tests for building energy simulation programs (Judkoff 1997). The proposed standard includes several different levels of accuracy tests as follows: 1) comparing the results of the simulation from the tested computer model with that from widely approved building energy simulation software such as DOE-2 or BLAST for the same given condition (comparative test), 2) comparing the simulated data with measured data collected from real building projects or well designed physical test models (empirical validation test), and 3) testing the accuracy of simulated results by traditional methods such as hand calculations using the dynamic heat transfer equations or psychrometric analysis of HVAC system (analytical verification test).

For the validation process in the development of the program in this research, two different types of accuracy tests were conducted (i.e., the comparative test and the empirical validation test). The comparative test was conducted by comparing the simulated results against the results of the DOE-2 program. For the empirical validation test a specially designed physical test box was constructed and tested under various conditions.

With the application of hourly monitoring in large-scale building energy conservation projects since the late 1980s, there has been an increased need for improved accuracy of the measurements of energy and likewise the calibration of sensors (Haberl et al. 1992). However, the accuracy of computerized models for the calibrated simulation of an existing building has significant room for improvement. Previous research concerning the comparison of computerized building simulations against measured data has been carried out by the International Energy Agency (IEA). The test results of the IEA project showed that there is a large degree of

uncertainty in the prediction of building energy flows, especially in the prediction of infiltration rates (Irving 1982). This research demonstrated the importance of empirical validation tests and the difficulty of testing for a specific measurement by controlling unknown factors. For an accurate validation, it was concluded that it is important to first determine what parameters are important and how to measure and then design very carefully to exclude all other factors that can cause errors in a test. This procedure will be used in the current research.

Previous research in Canada introduced empirical validation tests using an uninhabited test facility to test the energy performance of window glazing and the effectiveness of shading devices on passive solar test cells. Work performed at the University of Alberta (Dale 1985) used near full size uninhabited models to simulate the effective utilization of passive solar heating in a northern climate. Dale constructed a facility that consisted of six, single-story modules each 6.7 meters by 7.3 meters to evaluate the various levels of insulation with effects of passive and active solar heating systems. Then, different solar heating systems (e.g. exterior insulating shutters, shutters controlled by a light sensing cell, interior insulating shutters, etc.) were evaluated under varying operation. Dale's research showed that high insulation with a carefully designed air/vapor barrier is more important than the addition of thermal mass for the effective utilization of solar gains in extreme weather conditions such as those in Canada where the tests were carried out. This empirical test demonstrates that the same shading design can operate differently according to the site conditions and that careful control of the tested items with a well designed test schedules is very important.

Previous work was also performed at the Los Alamos Scientific Laboratory (Kerrisk et al. 1980) to improve the passive solar modeling capabilities in the DOE-2 computer program by introducing specialized custom weighting factors which generally follow the recommendations of ASHRAE (1977). For more accurate simulation of the thermal behavior of direct-gain passive-solar buildings, the calculated results of the improved DOE-2 program were compared with the measured heat-extraction rates and air temperatures for a number of test buildings. These comparisons showed that DOE-2 could accurately simulate direct-gain, passive-solar buildings and could account for night ventilation cooling and water walls in an approximate manner. This research demonstrated that a general purpose building energy simulation program such as DOE-2 could be tested against data from actual buildings for validation purposes.

Hiller (1996) validated her shading and insolation computer program TRNSHD using different levels of accuracy tests. For the validation of the sunlit fraction calculation, TRNSHD was tested by comparing with other computer algorithms such as TYPE 34 (overhang and side-fin shading) of TRNSYS and Xsun. To calculate the sunlit and shaded window areas, TYPE 34 of TRNSYS uses an ASHRAE algorithm (ASHRAE 1975), whereas Xsun and TRNSHD employ a boundary evaluation method developed by Weiler and Atherton (1977). Hiller also tested the accuracy by comparing the simulated results with the proposed European standard (CEN 1995) under six different test conditions. For the validation of internal insolation calculation, she compared the simulated results with previously measured data from an experimental test room constructed by Messadi (1990) at the University of Michigan, Ann Arbor. Though Hiller's accuracy tests include two types of ASHRAE accuracy tests (i.e., comparative test, empirical validation test), the comparative test is limited to one test on a single function of her program. Furthermore, since Hiller's model only includes very simple geometrical shapes without shading objects, she was only able to validate it with hand calculations.

Previous research on the experimental measurement of low-volume airflow was also reviewed. One study by Baltrip (1997) used an airflow chamber to evaluate the heat removal performance of cooling fans in personal computers. The airflow chamber was constructed of 0.5 inch plexiglass and consisted of a variable speed DC blower, air diffusers, AMCA airflow nozzles, and pressure taps. The chamber was designed to carefully match the American National Standards Institute (ANSI)/ Air Movement and Control Association (AMCA) Standard 210-285 and ANSI/American Society of Heating, Refrigerating, and Air-Conditioning Engineers (ASHRAE) Standard 51-1985 (ANSI/AMCA 1985). The pressure taps were installed to measure the differential pressure across the nozzle board and the static pressure at the outlet of the chamber. Baltrip also used a thermometer to measure the temperature of the air at the nozzle board and a strobe light to measure the rotational speed of the fan. The carefully-designed airflow chamber was first used to measure the effect of the fan on the heat removal in a PC. A similar airflow chamber will be constructed to measure the amount of heat removal in the proposed test box.

For the validation of the computer model, an experimental test box was designed, built, and used to validate the computer simulation. The environment of the physical model was restricted to focus on the effects of solar gain through window glazing. A modified version of Baltrip's airflow chamber was used for the accurate measurement of the low volume airflow

through the test model. This device makes it possible to measure the low volume airflow that is needed to calculate the total heat gain/loss through the fenestration system of the proposed test box.

2.6 Summary of Literature Review

Though most computer programs can provide very useful simulation results for window system analysis, none of the previous work provided a combined tool for the thermal analysis and shading device design that was validated with experimental data and that used the sunpath diagram to display the results. The research will introduce a combined tool that can simulate the thermal analysis of a fenestration system and provide a shading analysis. The well-designed sunpath plots will be very helpful to provide the users with visual descriptions of thermal impacts. The validation process includes comparative tests, empirical validation tests, and analytical verification tests.

CHAPTER III

SIGNIFICANCE OF THE STUDY

3.1 Expected Contributions from This Research

This research will contribute to the development of a methodology that can be applied to a computerized thermal and shading analysis model. Any new thermal and shading analysis model can only be deemed reliable after it is fully tested through a validation process such as an experimental validation using measured data and/or a comparative validation against another previously validated computer model. For this reason, this research will provide the following contributions toward the development of an energy-efficient architectural design model:

1) The development of a new computer program for displaying several versions of the sunpath diagram including orthographic, stereographic, gnomonic, and cylindrical projection techniques as well as overlaying shading and solar data onto the sunpath diagram.

2) The development of a combined analysis model that can evaluate both a thermal analysis and a shading design for fenestration systems.

3) The development of measured test data sets from a carefully calibrated window test facility and the application of a finite difference model to simulate the dynamic transfer of the experimental test box.

4) The validation of the model against the simulated results from the DOE-2 program.

5) The development of a self-instructed user interface for an improved fenestration system design that can be easily used in the architectural design process.

3.2 Scope and Limitations of the Research

This research focuses on the thermal and shading analysis of a single-glazed window. It does not investigate the heat transfer through multi-pane glazing although the analysis methods for treating multiple panes are described. The thermal effects of the window frame and divider are also not included in this study. This study primarily focuses on the accuracy of solar radiation

calculations and the proper techniques to display them.

In the experimental tests, vertical and horizontal solar radiation were measured and the transmitted solar radiation was measured for the experimental case of non-shaded fenestration. The result of a glazing transmittance test showed that the model's Fresnel equations created reliable results when compared with measured data. Thus, the model's equations for the calculation of the transmitted solar radiation from the measured vertical solar radiation may be used with confidence for an unshaded fenestration.

In the future, it is recommended to install pyranometers inside the glazing at various locations to improve the results for shading and thermal analysis of a shaded window.

The site location where the experiments were conducted is in a hot and humid area. Therefore, the haziness caused an increase in the diffuse solar radiation. Thus, for this model to be widely accepted, it needs to be further validated against measured data collected for other climates.

3.3 Procedure of the Research

This research was conducted using the following procedures. First, previous research on graphical display techniques for sunpath diagrams and the application of solar radiation calculations and shading analysis were investigated. This review provided the basis for the development of an improved model for fenestration system design. Second, a new computer simulation model was developed for displaying a shading and a thermal analysis of a fenestration system. Third, an experimental test box was constructed and used with various shading designs. The data collected from the experimental box was then used to test the accuracy of the finite difference simulation model. Finally, the results from the DOE-2 simulation program were compared with the simulation model as well as the measured data.

New computerized techniques for displaying sunpath diagram were developed to be used in the shading design and in the display of solar data. A linear time-stamp interpolation method was also developed and applied in the development of the data conversion program. This interpolation was needed in various phases such as creation of a data file for the finite difference model and in converting hourly result files of the DOE-2 simulation into 15-minutes data files to be compared with the 15-minute measured data.

CHAPTER IV

METHODOLOGY

4.1 Graphical Display of Solar and Shading Information

The sunpath diagram can be used to display various kinds of information that can be represented as function of solar angle such as the location of the sun, the projected shading area, the amount of solar radiation either on the horizon or on a vertical surface, and so on. In the previous research (McWatters and Haberl 1994a, 1994b, 1995; Oh and Haberl 1996, 1997) the development of a computerized display of the sunpath and shading mask protractor using an equidistant projection method was presented. Detailed descriptions and equations of each type of line used in the equidistant method have been well described in the research of McWatters and Haberl (1994).

Though the previous research in the development of a computerized shading analysis program increased its effectiveness by overlaying the shading mask protractor onto the sunpath diagram, the program has a limitation that it can be used only in the equidistant sunpath diagram. No previous research described how the shading mask protractor was applied to a different projection types (i.e., orthographic, cylindrical, etc). Furthermore, although the other display types have been graphically presented in various texts, none of the previous works described the exact equations for plotting the diagrams. Therefore, the new proposed model provides the equations and a computerized method for plotting various sunpath diagrams including orthographic, stereographic, gnomonic, and cylindrical projections to display the shading.

The following sections will describe the mathematical methods to calculate the coordinates of the solar azimuth and altitude angles using the various projection methods, and will present methods for displaying various kinds of solar and shading information.

4.1.1 Display of the Solar Altitude and Azimuth Angles

The sunpath diagram consists of various types of lines, circles, and ellipses that represent different kinds of information. The equidistant sunpath diagram (Figure 4.1.a) has a series of equally-spaced concentric circles (Figure 4.1.b) and radial lines (Figure 4.1.c)

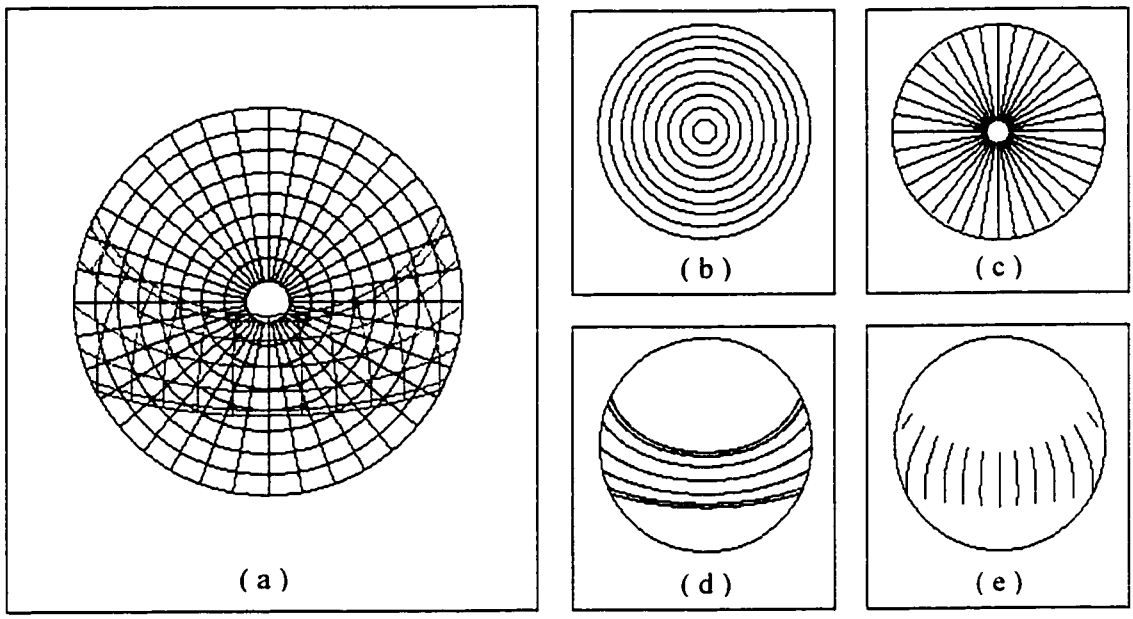

Figure 4.1 Sunpath Diagram with the Solar Altitude and Azimuth Lines Plotted Using the Equidistant Projection Method. This figure shows the four sets of lines and curves including the concentric circles of the solar altitude angles (Figure 4.1.b), radial lines of the off-south solar azimuth angles (Figure 4.1.c), sunpath lines for the months (Figure 4.1.d) and hours (Figure 4.1.e).

representing solar altitude and off-south azimuth angles respectively. It also includes the sunpath lines that are composed of a series of monthly lines (Figure 4.1.d) and hourly lines (Figure 4.1.e) to display the projected locations of the sun.

When we use the sunpath diagram for a shading analysis, the diagram is usually used along with a superimposed shading mask protractor (Figure 4.2.a). The shading mask protractor also consists of four sets of circles and lines. The concentric circles (Figure 4.2.b) and radial lines (Figure 4.2.c) displayed in the upper half of the protractor can be plotted the same way as the previously described sunpath diagram (Figure 4.1.b, c) except that they are rotated to correspond to the surface azimuth angle. The horizontal and vertical sets of ellipses (Figures 4.2.d and 4.2.e) are used to trace the horizontal (i.e., line *CE* on Figure 4.11) and vertical outlines (i.e., line *AC* on Figure 4.11) of the shading area projected from horizontal and vertical edges of shading devices.

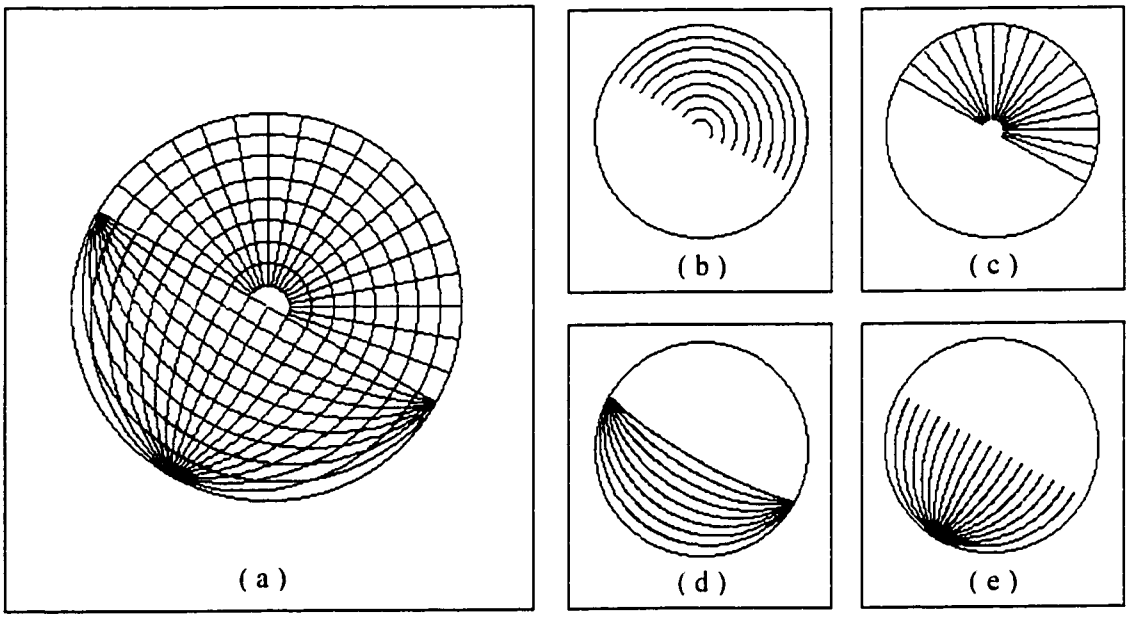

Figure 4.2 Shading Mask Protractor Plotted Using the Equidistant Projection Method. This figure shows the four sets of lines and curves including the concentric semicircles of solar altitude angles (Figure 4.2.b), radial lines of the off-south solar azimuth angles (Figure 4.2.c), horizontal ellipses for the forward edge of horizontal shade (Figure 4.2.d) and vertical ellipses for describing the upper edge of a side fin (Figure 4.2.e).

4.1.1.1 Equations for the Equidistant Projection

The previously described sunpath projection methods, including equidistant, orthographic, stereographic, and gnomonic projection use concentric circles to display solar altitude and straight radial lines to display solar azimuth. However, because of the difference in the projection method of the 3-D solar altitude onto 2-D Cartesian X-Y coordinates, the radii of circles displaying solar altitude are determined differently. Thus, if we know the equations that calculate the different radius of solar altitude circle, then the location of the sun can be easily calculated as an X and Y coordinate pair on a sunpath diagram regardless of the projection method.

In the equidistant projection method, solar altitude lines are equally spaced as concentric circles on a two-dimensional *X-Y* coordinate as described in Chapter II. Thus, the radius of the solar altitude circle decreases in direct proportion to an increase in the solar

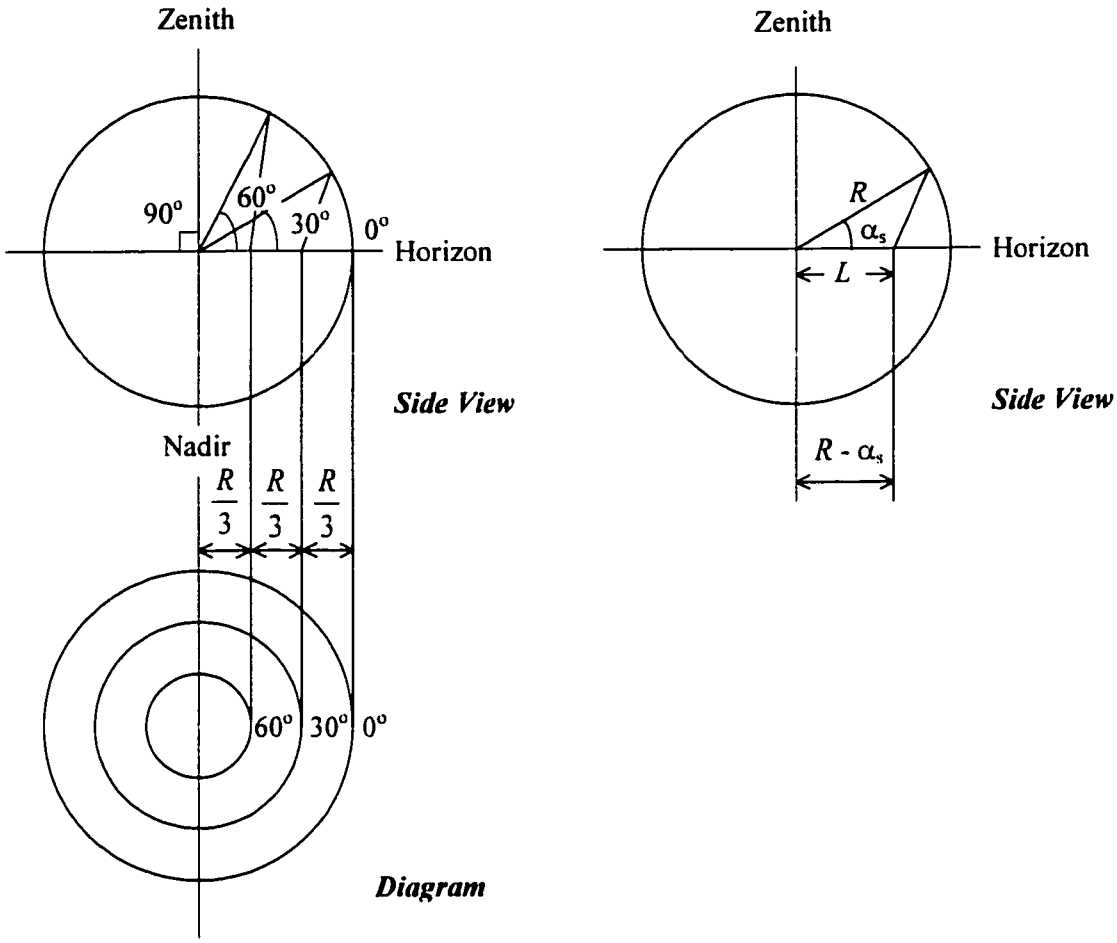

Figure 4.3 Calculation of Solar Altitude Angle Using the Equidistant Projection Method.

altitude angle (Figure 4.3). The radius 'L' of a given altitude angle (α_s) is equal to the difference between the altitude angle and the radius (R) of the solar altitude circle when the angle is 0°. Thus, the radius of the solar altitude angle can be calculated by

$$L = R - \alpha_s . \qquad (4.1)$$

Then, X and Y coordinates of the sun's location are determined as the product of the radius L and the sine and cosine values of solar azimuth angle (γ_s). To begin, one calculates the X-Y coordinate when the sun is located in the third quadrant of sunpath diagram (Figure 4.4). The sun is west of due south and the solar azimuth angle should be a positive number between 0° and 90°. The X and Y coordinates are then

$$x = -\Delta x = -L\sin(\gamma_s) \tag{4.2a}$$

$$y = -\Delta y = -L\cos(\gamma_s) \tag{4.2b}$$

where $0° \le \gamma_s \le 90°$.

When the sun's location is west of due south and the solar azimuth angle has a positive value between 90° and 180°, the sun may be located in the second quadrant of sunpath diagram (Figure 4.4). Using the fact that $0° \le (180°-\gamma_s) \le 90°$, the X and Y coordinates can be calculated by

$$x = -\Delta x = -L\sin(\gamma_s) \tag{4.3a}$$

$$y = \Delta y = -L\cos(\gamma_s) \tag{4.3b}$$

where $90° \le \gamma_s \le 180°$.

In the same way, we can calculate the X and Y coordinates when the sun is located east of due south which yields

$$x = -L\sin(\gamma_s) \tag{4.4a}$$

$$y = -L\cos(\gamma_s). \tag{4.4b}$$

Finally, if we replace radius (L) of the solar altitude circle with Equation 4.1, we can calculate the coordinates of the sunpath diagram directly from solar altitude and azimuth angles as follows

$$x = -(R-\alpha_s)\times\sin(\gamma_s) \tag{4.5a}$$

$$y = -(R-\alpha_s)\times\cos(\gamma_s). \tag{4.5b}$$

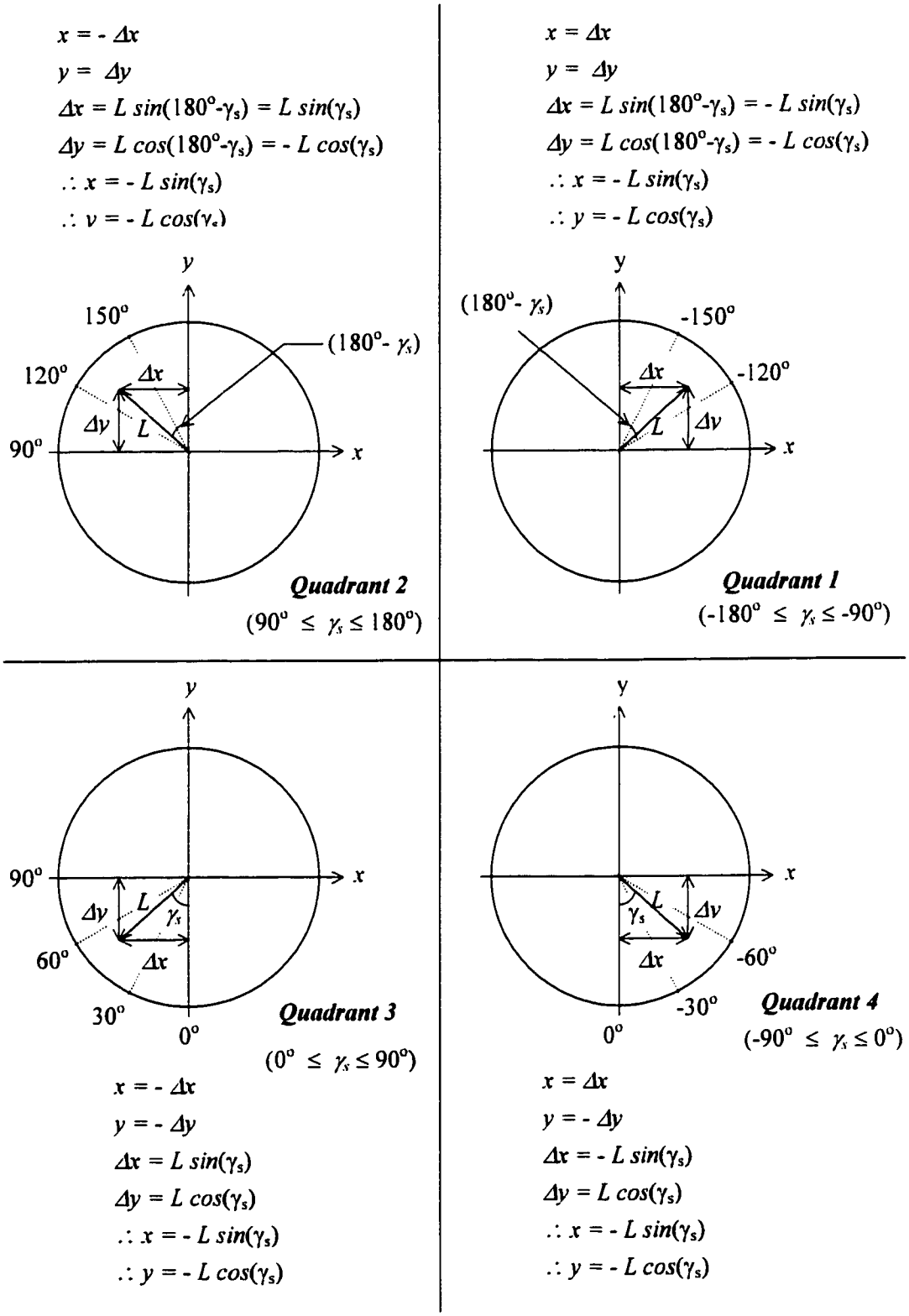

Figure 4.4 *X-Y* Coordinate Calculation in Different Quadrants for the Equidistant Projection.

4.1.1.2 Equations for the Orthographic Projection

The calculation of the radius (L) of solar azimuth circles in orthographic projection (Figure 4.5) is slightly more complicated than the equidistant projection. In the orthographic projection method, the location of the sun is vertically projected from a point on a celestial sphere onto a two dimensional circular diagram which represents the exact geometric projection. In the orthographic method the length of L for a given solar altitude angle (α_s) is calculated by

$$L = R\cos(\alpha_s). \tag{4.6}$$

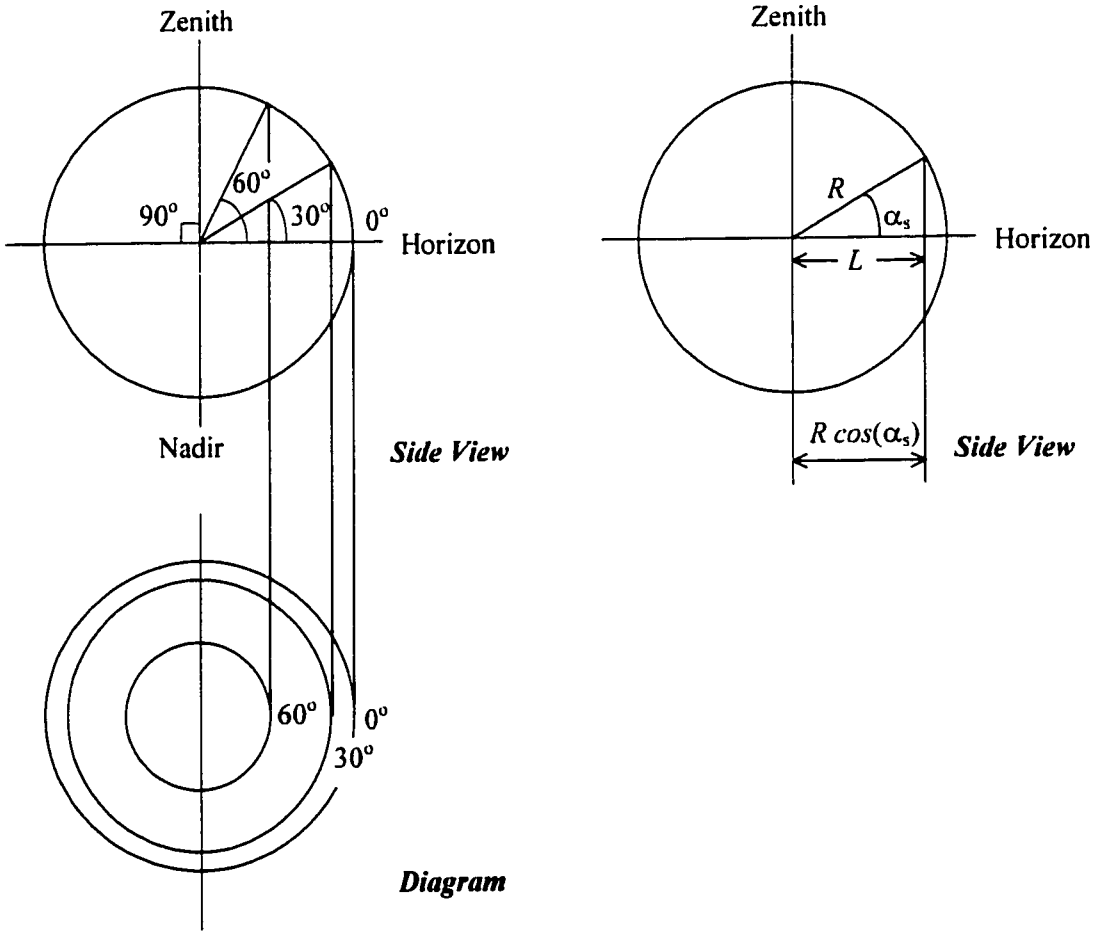

Figure 4.5 Calculation of Solar Altitude Angle Using the Orthographic Projection Method.

The remaining calculations then proceed the same as for equidistant projection, with the radius 'L' in Equations 4.4a and 4.4b replaced with '$R\cos(\alpha_s)$'. We can calculate the X and Y coordinates in an orthographic sunpath diagram as follows

$$x = -R\cos(\alpha_s)\cdot\sin(\gamma_s) \tag{4.7a}$$

$$y = -R\cos(\alpha_s)\cdot\cos(\gamma_s). \tag{4.7b}$$

4.1.1.3 Equations for the Stereographic Projection

In the stereographic sunpath diagram (Figure 4.6), the intersection of the equatorial plane of a celestial sphere is used as the projection line. In this method, a line is first drawn from the sun's location (S') on the celestial sphere to the Nadir (N'). The intersection point (P') of this line ($S'N'$) and the horizon line ($O'H'$) is vertically projected down to determine the radius (L) of the solar altitude circle.

As we can see in Figure 4.6, the angle ($\angle O'S'N'$) between the celestial sphere center and Nadir at the sun's location (symbol 'β') is the same as the angle ($\angle O'N'S'$) between the Zenith and the sun's location on the celestial sphere at Nadir. In other words,

$$(\alpha_s + 90^o) + 2\beta = 180^o. \tag{4.8}$$

Thus,

$$\beta = (90^o - \alpha_s)/2. \tag{4.9}$$

From the triangle $\Delta O'P'N'$, the radius L can be calculated as follows

$$L = R\tan(\beta). \tag{4.10}$$

Using the Equations 4.9 and 4.10, the radius L is

$$L = R\tan\left[\frac{(90^o - \alpha_s)}{2}\right]. \tag{4.11}$$

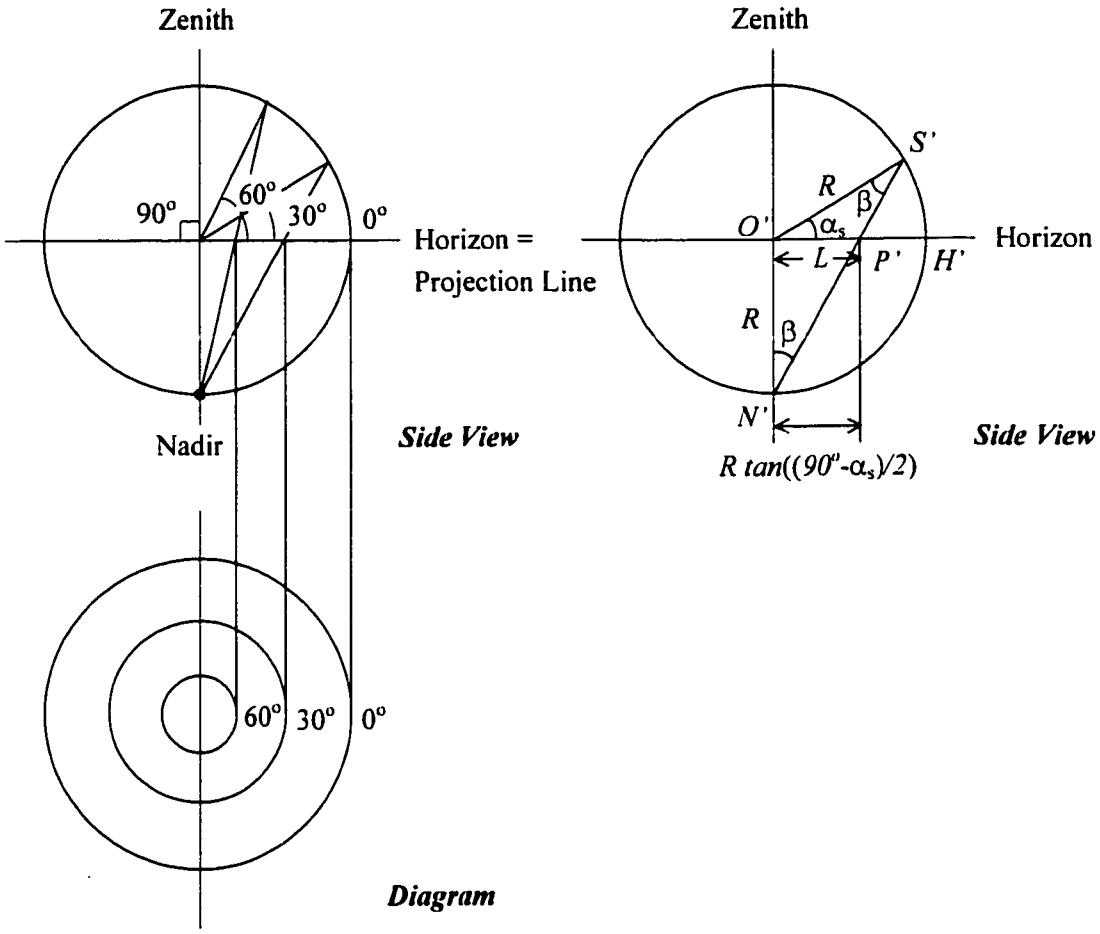

Figure 4.6 Calculation of Solar Altitude Angle Using the Stereographic Projection Method.

Therefore, using Equations 4.4a, 4.4b, and 4.11, the coordinates of solar altitude and azimuth angles in the stereographic sunpath diagram are calculated by

$$x = -R\tan\left[\frac{(90^o - \alpha_s)}{2}\right]\cdot\sin(\gamma_s) \qquad (4.12a)$$

and

$$y = -R\tan\left[\frac{(90^o - \alpha_s)}{2}\right]\cdot\cos(\gamma_s). \qquad (4.12b)$$

4.1.1.4 Equations for the Gnomonic Projection

In the gnomonic projection (Figure 4.7), the projection line is a horizontally extended line from the Zenith of the celestial sphere instead of the horizon line in a stereographic projection. From the triangle $\Delta O'Z'P'$, the length L can be calculated by

$$L = R\tan\left(90^o - \alpha_s\right) \tag{4.13}$$

or, it can be given from the triangle $\Delta O'P'H'$ as follow

$$L = \frac{R}{\tan(\alpha_s)}. \tag{4.14}$$

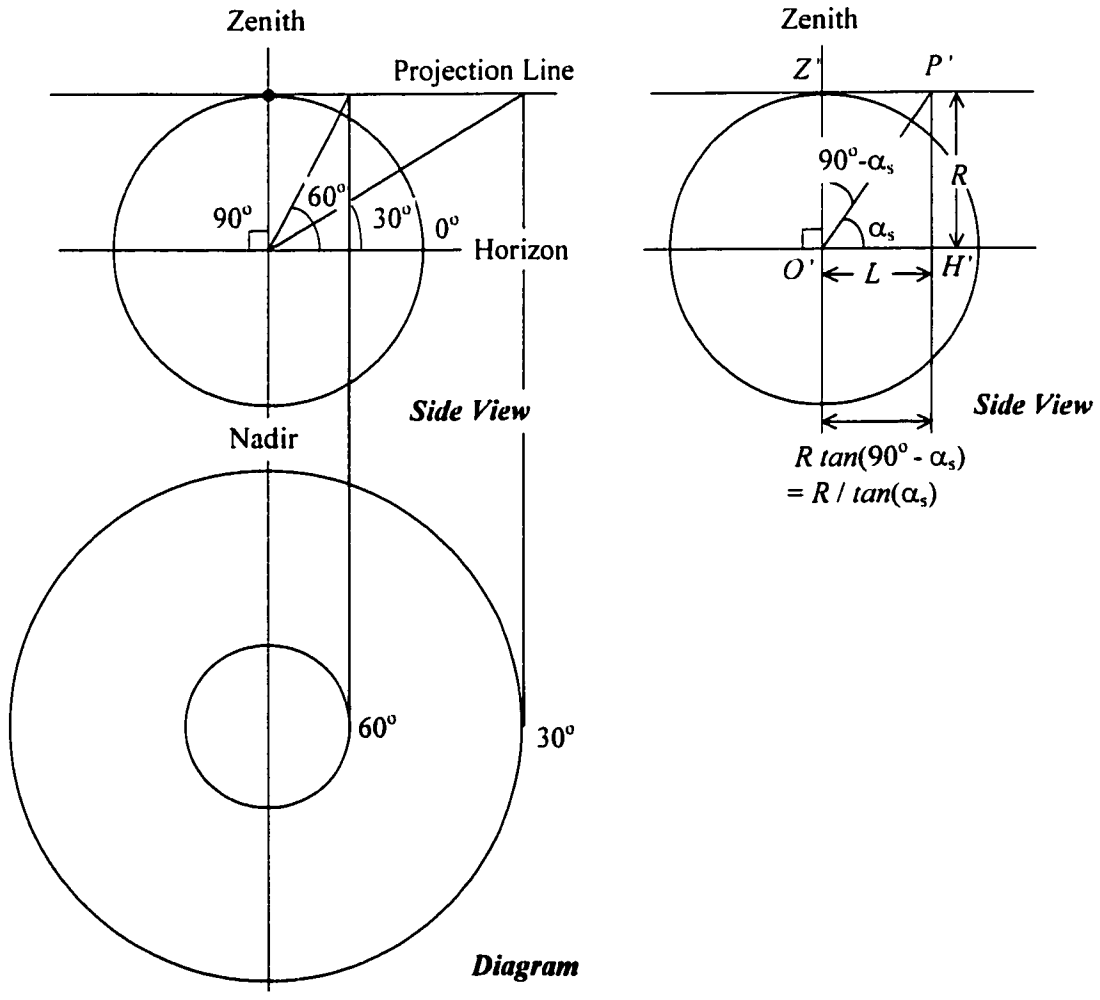

Figure 4.7 Calculation of Solar Altitude Angle Using the Gnomonic Projection Method.

Finally, using Equations 4.4a, 4.4b, and 4.13, the X and Y coordinates are calculated by

$$x = -R\tan(90^o - \alpha_s)\cdot\sin(\gamma_s) \tag{4.15a}$$

$$y = -R\tan(90^o - \alpha_s)\cdot\cos(\gamma_s). \tag{4.15b}$$

4.1.1.5 Equations for the Cylindrical Projection

In the cylindrical projection method, we don't need a function to calculate the X and Y coordinates because the X and Y-axes represent the solar azimuth and solar altitude angles respectively. However, we do need to define the maximum and minimum ranges of the X and Y coordinates differently from the other projection methods. For most of the displays of the sunpath, the cylindrical sunpath diagram usually does not use the maximum range (–180° to 180°) of solar azimuth angle for the X-axis. For example, Bennett (1979) used ranges from –120° to 120° for the solar azimuth angle (X-axis) in his research. However, the maximum solar azimuth range will be used in this research because the software can zoom into any portion of the diagram whenever it is needed.

4.1.1.6 Plotting Solar Altitude and Azimuth Angles

When we apply the previously described projection methods in a computer application to plot the sunpath diagram, we don't need to develop individual subroutines for each projection method. By using a function to calculate the X and Y coordinates for a given solar angle in a requested projection method, we can display any information that is related with solar angles. Figure 4.8 shows an example of the Visual Basic source code that calculates the X and Y coordinates in a given projection method.

In these functions, the 'Dsin', 'Dcos' and 'Dtan' are the trigonometric functions that calculate the sine, cosine, and tangent values respectively with degree angles instead of radians as input arguments. The constant variable 'R' is for the radius of the solar azimuth circle when the solar altitude angle is equal to 0 degree. For a given projection type, solar altitude, and solar azimuth, these functions return the values for the X and Y coordinates in the sunpath diagram.

```
Function Get_X_Coord (ProjectionType As Integer, SolarAltitude As Single, SolarAzimuth As
Single) As Single

        Select Case (ProjectionType)
        Case 1: 'Equidistant Projection
                Get_X_Coord = - (R - SolarAltitude) * DSin(SolarAzimuth)
        Case 2: 'Orthographic Projection
                Get_X_Coord = - R * DCos(SolarAltitude) * DSin(SolarAzimuth)
        Case 3: 'Stereographic Projection
                Get_X_Coord = - R * DTan((90 - SolarAltitude) / 2) * DSin(SolarAzimuth)
        Case 4: 'Gnomonic Projection
                Get_X_Coord = - R * DTan(90 - SolarAltitude) * DSin(SolarAzimuth)
        Case 5: 'Cylindrical Projection
                Get_X_Coord = SolarAzimuth
        End Select
End Function


Function Get_Y_Coord (ProjectionType As Integer, SolarAltitude As Single, SolarAzimuth As
Single) As Single

        Select Case (ProjectionType)
        Case 1: 'Equidistant Projection
                Get_Y_Coord = - (R - SolarAltitude) * DCos(SolarAzimuth)
        Case 2: 'Orthographic Projection
                Get_Y_Coord = - R * DCos(SolarAltitude) * DCos(SolarAzimuth)
        Case 3: 'Stereographic Projection
                Get_Y_Coord = - R * DTan((90 - SolarAltitude) / 2) * DCos(SolarAzimuth)
        Case 4: 'Gnomonic Projection
                Get_Y_Coord = - R * DTan(90 - SolarAltitude) * DCos(SolarAzimuth)
        Case 5: 'Cylindrical Projection
                Get_Y_Coord = SolarAltitude
        End Select
End Function
```

Figure 4.8 Functions Get_X_Coord( ) and Get_Y_Coord( ). Visual Basic source code for calculating X and Y coordinates for a given solar altitude and azimuth angle in the various projection methods.

Using functions Get_X_Coord( ) and Get_Y_Coord( ), we can easily draw the solar altitude and solar azimuth lines with a given increment in various projection methods. Figure 4.9 shows the Visual Basic source code used to display the solar altitude and azimuth lines. Figure 4.10 shows examples of the sunpath diagrams plotted using the five different projection methods including equidistant (Figure 4.10.a), orthographic (Figure 4.10.b), stereographic (Figure 4.10.c), gnomonic (Figure 4.10.d) and cylindrical (Figure 4.10.e) projection. The methods used to draw sunpath lines included in these diagrams will be explained in the following section.

```
Sub DiagramSolarAltitude (ControlName As Control, ProjectionType As Integer)

        Dim I As Single

        If (Projection_Type<= 4) Then
                For I = 0 To 80 Step 10
                        Select Case (ProjectionType)
                        Case 1: 'Equidistant Projection
                                ControlName.Circle (0, 0), (R – I)
                        Case 2: 'Orthographic Projection
                                ControlName.Circle (0, 0), R * DCos(I)
                        Case 3: 'Sereographic Projection
                                ControlName.Circle (0, 0), R * DTan((90 - I) / 2)
                        Case 4: 'Gnomonic Projection
                                ControlName.Circle (0, 0), R * DTan(90 - I)
                        End Select
                Next I
        Else            'Cylindrical Projection
                For I = 0 To R Step 10
                        ControlName.Line (-180, I) - (180, I)
                Next I
        End If
End Sub


Sub DiagramSolarAzimuth (ControlName As Control, ProjectionType As Integer)

        Dim X1 As Single, Y1 As Single, X2 As Single, Y2 As Single
        Dim I As Single

        If (Projection_Type <= 4) Then
                For I = -180 To 180 Step 10
                        X1 = Get_X_Coord (ProjectionType, 80, I)
                        Y1 = Get_Y_Coord (ProjectionType, 80, I)
                        X2 = Get_X_Coord (ProjectionType, 0, I)
                        Y2 = Get_Y_Coord (ProjectionType, 0, I)
                        ControlName.Line (X1, Y1) - (X2, Y2)
                Next I
        Else            'Cylindrical Projection
                For I = -180 To 180 Step 10
                        ControlName.Line (I, 0) - (I, R)
                Next I
        End If
End Sub
```

Figure 4.9 Visual Basic Subroutines DiagramSolarAltitude ( ) and DiagramSolarAzimuth ( ). Visual Basic source code for plotting the solar altitude and azimuth angle lines in various projection methods.

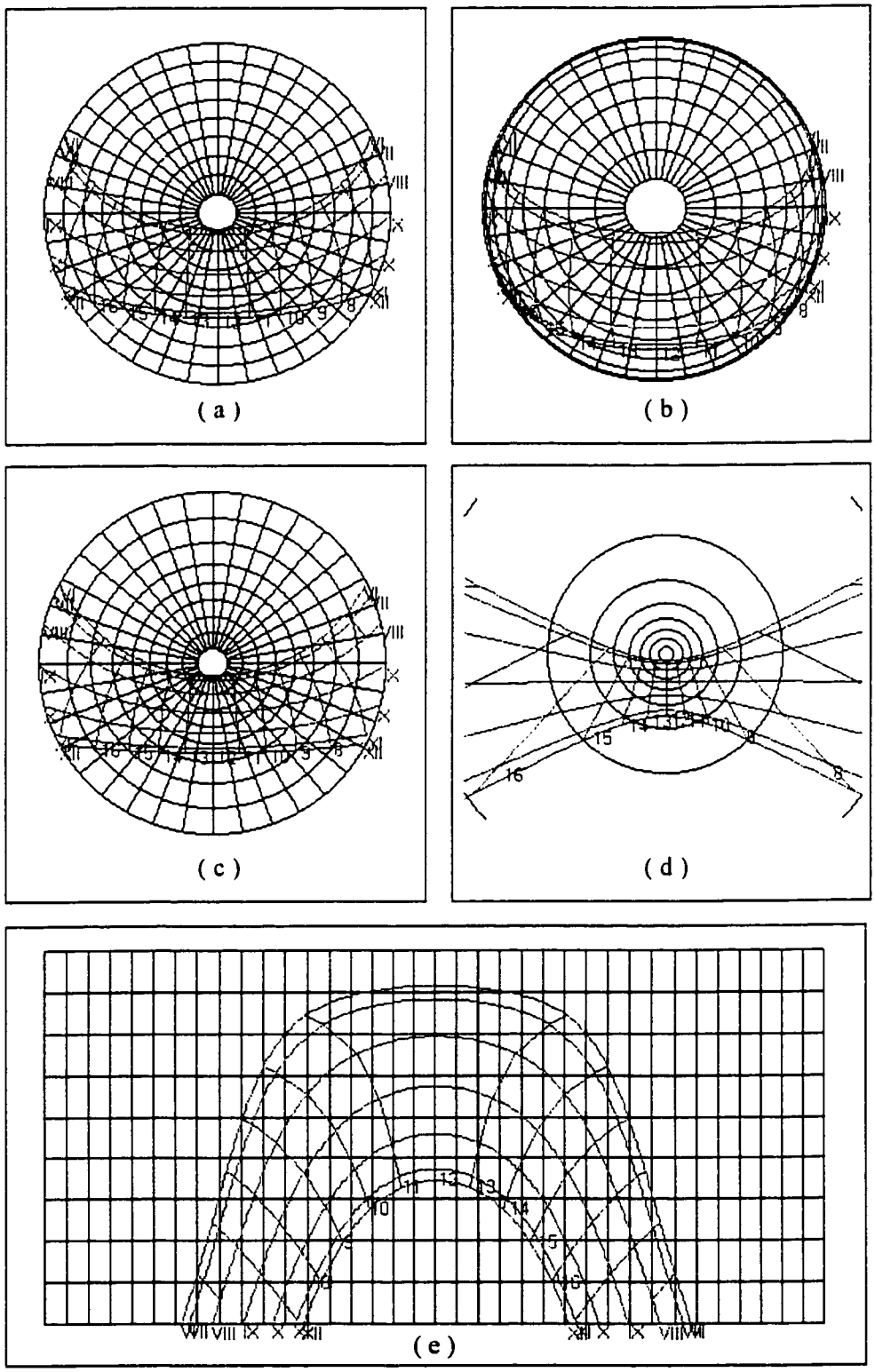

Figure 4.10 Sunpath Diagrams Plotted with Various Projection Methods. This figure shows sunpath diagrams plotted using five different projection methods including: equidistant (a), orthographic (b), stereographic (c), gnomonic (d) and cylindrical (e) projections.

4.1.2 Display of the Path of the Sun

Displaying the path of the sun uses two sets of curves: horizontal curves (Figure 4.1.d) representing sun's path through the 21st day of every month and vertical curves (Figure 4.1.e) connecting the same hour each month. Four Visual Basic functions are developed and used to determine the location of the sun (i.e., the solar altitude and azimuth angles) in the user-defined interval on the 21st day of each month. The functions are

GetDOY (Year, Month, Date),

GetDeclination (DOY, SolarModel),

GetSolarAltitude (Latitude, Declination, SolarHourAngle, SolarModel), and

GetSolarAzimuth (Latitude, Declination, SolarHourAngle, SolarAltitude, SolarModel).

The first function 'GetDOY' is used to calculate the day of the year (DOY), including a consideration of the leap year. The function 'GetDeclination' returns the solar declination angle on the day of the year given by the function GetDOY. Using the latitude from the user input, the solar hour angle, and the previously calculated declination, the functions 'GetSolarAltitude' and 'GetSolarAzimuth' calculate the solar altitude and azimuth angles respectively. The input argument 'SolarModel' indicates the simulation model used for the solar angle calculation. The three different solar models used in the program are: the *ASHRAE Handbook* method(1993), a method from Duffie and Beckman (1991), and the method described in Kreider and Rabl (1994).

The *ASHRAE Handbook* provides a table (the first column in Figure 4.1) for the declination angle (δ) of each month for the given solar time, but it does not provide the equation. Thus, to apply this model in a computer application, interpolation of the values is needed to determine the declination on days except for the 21st day of each month, or the declination value need to be calculated.

Duffie and Beckman (1991) used the equation developed by Cooper (1969), which is given by

$$\delta = 23.45 \times \sin\left[\frac{360 \times (284 + n)}{365}\right]. \tag{4.16}$$

Kreider & Rabl (1994) use an equation that uses 365.25 days for a year instead of 365 with the declination angle given by

$$\delta = \sin^{-1}\left[-\sin 23.45 \times \cos\frac{360 \times (n + 10)}{365.25}\right]. \tag{4.17}$$

Table 4.1 shows the small differences in declination angles in these three models. The values for the *ASHRAE Handbook* method are from the table in the *ASHRAE Handbook* (1993), the other values are results of the computer application using Cooper's (1969) and Kreider & Rabl's (1994) model respectively. There are no significant differences among calculation results of these models. In general, Cooper's model provides closer results to the values in the *ASHRAE Handbook* when the declination angles are high, whereas Kreider & Rabl's model shows closer matching when the declination angles are low.

Table 4.1 Declination Angles Calculated Using Various Solar Models and Compared against the *ASHRAE Handbook* (in Degrees).

Date	ASHRAE Handbook (1997)	Cooper (1969)	(Δ)	Kreider & Rabl (1994)	(Δ)
Jan. 21	-20.0	-20.1	(-.1)	-20.0	(0)
Feb. 21	-10.8	-11.2	(-.4)	-11.1	(-.3)
Mar. 21	0.0	-0.4	(-.4)	-0.5	(-.5)
Apr. 21	11.6	11.6	(0)	11.2	(-.4)
May 21	20.0	20.1	(.1)	19.9	(-.1)
June 21	23.45	23.4	(-.05)	23.4	(-.05)
July 21	20.6	20.4	(-.2)	20.4	(-.2)
Aug. 21	12.3	11.8	(-.5)	11.6	(-.7)
Sep. 21	0.0	-0.2	(-.2)	0.0	(0)
Oct. 21	-10.5	-11.8	(-1.3)	-11.3	(-.8)
Nov. 21	-19.8	-20.4	(-.6)	-20.2	(-.4)
Dec. 21	-23.45	-23.4	(.05)	-23.4	(.05)

Note: The calculation is for the case of a non-leap year.

All three methods use the same equation to calculate solar altitude angles (α). The solar altitude angle is given by

$$\alpha_s = \sin^{-1}(\cos\phi\cos\delta\cos\omega + \sin\phi\sin\delta). \tag{4.18}$$

The calculation of solar azimuth angles (γ_s) is a little more complicated. The *ASHRAE Handbook* calculates solar azimuth angles by

$$\gamma_s = \cos^{-1}\left(\frac{\sin\alpha_s \times \sin\phi - \sin\delta}{\cos\alpha_s \times \cos\phi}\right) \tag{4.19}$$

Since the program uses positive values when the sun is west of due south, the values of solar azimuth angle must be positive in the afternoon and negative in the morning. Unfortunately, Equation 4.19 provides positive numbers only. Therefore, to use the ASHRAE equation, the solar time should be checked to determine if it is before noon or not. If it is, then the sign of the solar azimuth should be changed as follows

$$If\ (\omega < 12)\ then,\ \gamma_s = -\gamma_s \cdot \tag{4.20}$$

For the solar azimuth angle calculation, Duffie and Beckman (1991) applied the equation developed by Braun and Mitchell (1983). Braun and Mitchell's equation is written in terms of a pseudo solar azimuth angle (γ_s'). As the solar azimuth is determined by the relationship of the solar hour angle (ω) to the hour angle (ω_{ew}) when the sun is due east (or west), the coefficient C1, C2, C3 determines in which quadrant the sun will be. The pseudo solar azimuth angle (γ_s'), due east (or west) hour angle (ω_{ew}), and the solar azimuth angle (γ_s) are calculated by

$$\gamma_s' = \frac{\sin\omega\cos\delta}{\sin\theta_z} \tag{4.21a}$$

$$\omega_{ew} = \cos^{-1}\left(\frac{\tan\delta}{\tan\theta}\right) \tag{4.21b}$$

$$\gamma_s = C_1 C_2 \gamma_s' + C_3\left(\frac{1 - C_1 C_2}{2}\right)180 \tag{4.21c}$$

where

$$C_1 = \begin{cases} 1 \text{ if } |\omega| < \omega_{ew} \\ -1 \text{ otherwise} \end{cases} \tag{4.21d}$$

$$C_2 = \begin{cases} 1 \text{ if } \phi(\phi - \delta) \geq \omega_{ew} \\ -1 \text{ otherwise} \end{cases} \tag{4.21e}$$

$$C_3 = \begin{cases} 1 \text{ if } \omega \geq 0 \\ -1 \text{ otherwise} \end{cases}. \tag{4.21f}$$

To calculate the solar azimuth angle, Kreider & Rabl (1994) used the solar hour angle and zenith instead of latitude and solar angles, resulting in

$$\gamma_s = \frac{\cos\delta \cos\omega}{\sin\theta_s}. \tag{4.22}$$

Table 4.2 shows the values of solar azimuth angles on the 21st day of each month at 10:00 AM in solar time at the location of 32° N latitude calculated using three different models. The table shows that the calculation of Braun and Mitchell's model is exactly the same to three significant figures as that of the *ASHRAE Handbook's* model except for slight differences in January 21 and May 21. Figure 4.10 shows a series of sunpath lines calculated by Duffie and Beckman's model and plotted in different projection methods.

Table 4.2 Solar Azimuth Calculated Using Various Solar Models (in Degrees).

Date	ASHRAE Handbook (1997)	Diffie & Beckman (1969)	(Δ)	Kreider & Rabl (1994)	(Δ)
Jan. 21	-30.0	-30.2	(-.2)	-30.2	(-.2)
Feb. 21	-34.1	-34.1	(0)	-34.2	(-.1)
Mar. 21	-40.1	-40.1	(0)	-40.0	(.1)
Apr. 21	-48.6	-48.6	(0)	-48.3	(.3)
May 21	-55.7	-55.6	(.1)	-55.8	(-.1)
June 21	-61.2	-61.2	(0)	-61.2	(0)
July 21	-57.4	-57.4	(0)	-57.2	(.2)
Aug. 21	-48.7	-48.7	(0)	-48.7	(0)
Sep. 21	-40.0	-40.0	(0)	-40.1	(-.1)
Oct. 21	-33.9	-33.9	(0)	-34.0	(-.1)
Nov. 21	-30.0	-30.0	(0)	-30.2	(-.2)
Dec. 21	-28.9	-28.9	(0)	-28.7	(.2)

Note: The calculation is for the case of a non-leap year. The time for solar hour angle is 10:00 a.m. in solar time, and the location is 32° north latitude.

4.1.3 Display of Shading Mask Protractor

Traditionally, the shading mask protractor has been used to trace the image of an actual shading device onto the sunpath diagram to determine those periods of the day when a point at the middle of the bottom of the window is shaded. The shading mask protractor consists of a series of construction lines that are used to represent the edge of rectangular shades. The equations used to produce the shading mask protractor lines in the equidistant projection method were first described in McWatters and Haberl (1994).

Figure 4.2 shows that the shading mask protractor is composed of four different sets of curves and lines. The first set of curves is a series of semicircles (Figure 4.2.b) in the semicircular region of shading mask protractor. The orientation of the semicircular region is determined by the given azimuth angle (γ) of the surface being analyzed. To generate the concentric circles, we apply the same equations (Equations 4.2a and 4.2b) used to calculate the X and Y coordinates of the solar altitude curves. However, the start and end angles of each semicircle should be defined such as

$$A_{start} = \gamma + 90^o \tag{4.23a}$$

$$A_{end} = \gamma - 90^o . \tag{4.23b}$$

The radius of each semicircular line is then increased by 10° at a time from 10° to 90° for each FOR loop statement.

The second group of lines in the shading mask protractor is a series of radial lines (Figure 4.2.c). These lines can be plotted by slightly modifying the subroutine 'DiagramSolarAzimuth' (Figure 4.9) that was used to display solar azimuth lines. The only modification needed in this subroutine is applied to define the start and end values of the half circle in the FOR loop statement instead of −180 to 180. The start and end angles to plot the radial lines in the semicircular region are given by the Equations 4.16a and 4.16b.

The third group of lines in the shading mask protractor is a set of horizontal ellipses (Figure 4.2.d) that are used to determine the projected line of the horizontal edge of an overhanging shade. Given that surface azimuth angle of the wall is γ, the window width is $2W$,

the window height is H, and the projected length of overhang is D (Figure 4.11), the azimuth angle (γ') of the Point C against the surface outward normal is

$$\gamma' = \tan^{-1}\left(\frac{D}{W}\right) = \tan^{-1}\left(\frac{H\tan\beta}{H\tan\alpha}\right) = \tan^{-1}\left(\frac{\tan\beta}{\tan\alpha}\right). \tag{4.24}$$

Thus, the solar azimuth angle (γ_s) is

$$\gamma_s = \gamma + \tan^{-1}\left(\frac{\tan\beta}{\tan\alpha}\right). \tag{4.25}$$

Again, from the triangle ΔOCB,

$$90^o - \alpha_s = \tan^{-1}\left(\frac{L}{H}\right) = \tan^{-1}\left(\frac{\sqrt{W^2 + D^2}}{H}\right) \tag{4.26a}$$

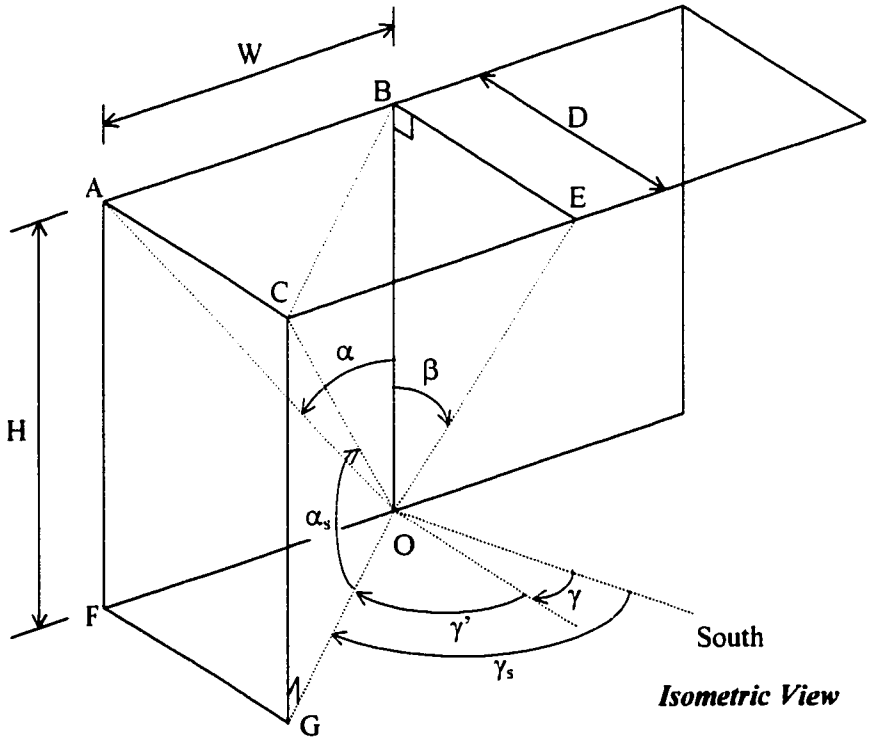

Figure 4.11 Calculation of the Angles of Shading Mask Protractor. This figure shows the calculation of solar azimuth (γ_s) and solar altitude angles (α_s) when the horizontal (α) and vertical (β) angles for the shading mask ellipses are given.

$$90^o - \alpha_s = \tan^{-1}\left(\frac{\sqrt{H^2 \tan\alpha^2 + H^2 \tan\beta^2}}{H}\right) = \tan^{-1}\sqrt{\tan\alpha^2 + \tan\beta^2} \quad . \quad (4.26b)$$

Thus, the solar altitude angle (α_s) is

$$\alpha_s = 90^0 - \tan^{-1}\sqrt{\tan\alpha^2 + \tan\beta^2} \quad . \quad (4.27)$$

Finally, to plot the horizontal ellipses of the shading mask protractor onto a sunpath diagram, the *X* and *Y* coordinates can be calculated using the functions Get_X_Coord ( ) and Get_Y_Coord in Figure 4.8 which can be adjusted for equidistant, orthographic, stereographic, gnomonic, or cylindrical coordinates.

The fourth group of lines in the shading mask protractor is a set of vertical ellipses (Figure 4.2.e) that are used to determine the projected line of the vertical edge of a side fin. To plot the vertical ellipses of the shading mask protractor onto a sunpath diagram, the equations and functions used for plotting horizontal ellipses can be used. In this case, the FOR loop statement of horizontal angles (α) of ellipses should be nested within the vertical angles (β).

Figure 4.12 shows examples of shading mask protractor plotted using various projection methods. The projected lines of shading devices (lines CD, AC, BD, and CG in Figure 4.11) are highlighted on the different sunpath diagrams. In the cylindrical sunpath diagram, left side-fins are displayed in the right hand side of the diagram because the right hand side is west.

4.1.4 Display of Shading

To plot the shading area onto the sunpath diagram, first, one needs to understand the coordinate system used in the traditional shading device design. After calculating the angular relationship between the viewpoint (usually centered at the bottom of the window) and each corner of the shading device, the projection of the shading onto a sunpath diagram can be calculated. Thus, in this section, first, the coordinate system of the program Shaded Fenestration Design (SFD) model will be explained, then the methods to calculate the *X* and *Y* coordinates of projected shading in a sunpath diagram will be explained.

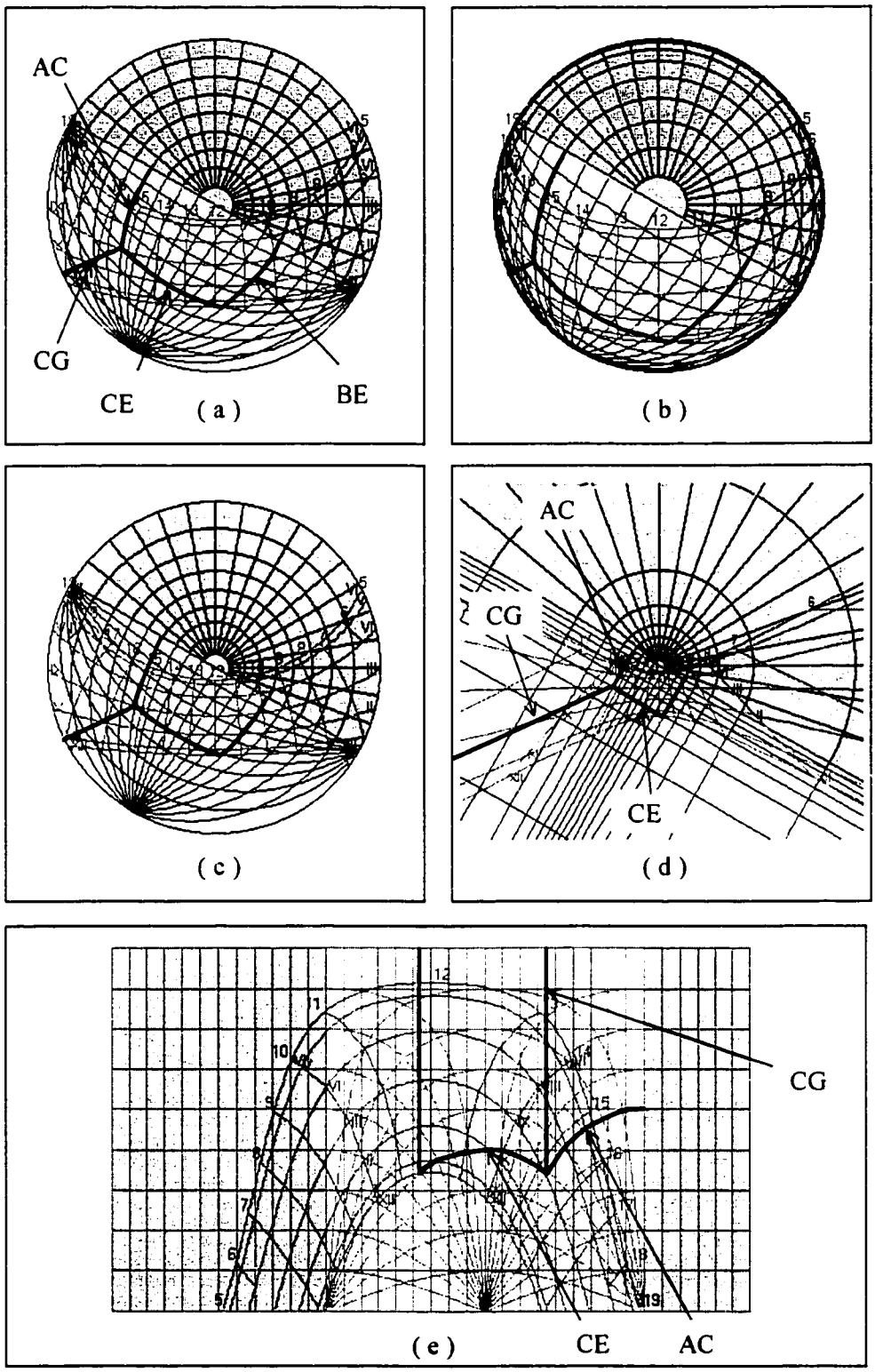

Figure 4.12 Shading Mask Protractor Plotted Using Various Projection Methods. This figure shows the shading mask protractor for a surface 30° west of due south for equidistant (a), orthographic (b), stereographic (c), gnomonic (d) and cylindrical (e) projections.

4.1.4.1 Coordinate System of the Shaded Fenestration Design (SFD) Model

The SFD program uses a hierarchy of three nested 'right hand Cartesian' coordinate systems: the 'surface coordinate system' (Figure 4.13), the 'window coordinate system' (Figure 4.14), and the 'shading coordinate system' (Figure 4.15). The wall is defined relative to the origin of the surface coordinate system, the window is defined relative to the origin of the window coordinate system, and a shading device is defined relative to the origin of the shading coordinate system. Hence, the reference point of each object becomes the origin of the next level coordinate system. In other words, the reference point of the wall surface becomes the origin of the window coordinate system, and the window reference point becomes the origin to determine the coordinates of shading devices.

The reference point of the wall surface is the bottom of the right-hand corner of the wall (Figure 4.13). The surface azimuth angle is the angle between the surface outward normal and the angle west of due south as positive and east of due south as negative. The range is -180° to 180°. The tilt angle of the surface is the angle between the surface and the horizon. For an example, a vertical wall has a 90° tilt angle. If the tilt angle is smaller than 90° the surface normal is tilted upward; if the angle is greater than 90° it is tilted downward. The range of the tilt angle is 0° to 180°.

The reference point of the window is at the center of the bottom edge of the window (Figure 4.14). The window reference point does not use the Z coordinate (i.e., the window cannot be projected or recessed from the wall surface).

The origin of the shading coordinate system is at center of the bottom edge of the window. All the reference points are measured from this point (Figure 15). For example, if the overhang is aligned at the top edge of the window, the X and Z coordinates are equal to 0 and Y coordinate is equal to the height of the window. If the left-fin is aligned with the left side of the window, the X and Y coordinates of the reference point are equal to half of the window width and half of the window height respectively. When there is a gap between the wall surface and shading devices, the Z coordinate indicates the distance (i.e., the shade is "floating" in the front of the window).

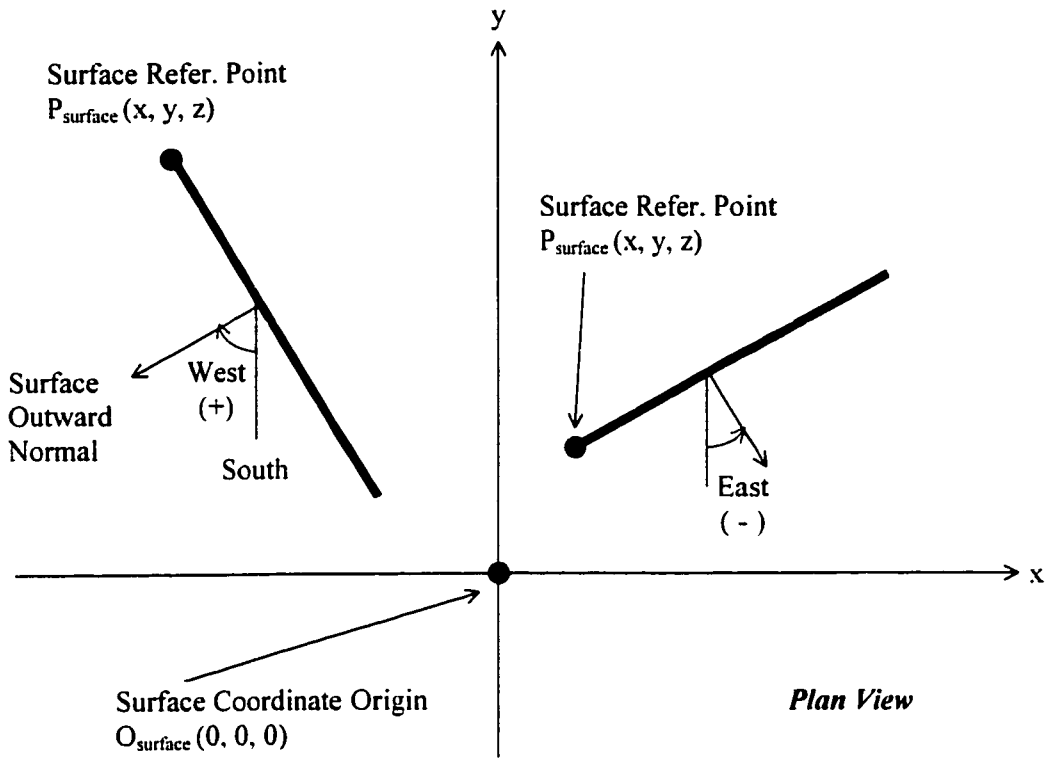

Figure 4.13 Example of Surface Coordinate System. All the surfaces are defined relative to the origin of the surface coordinate system. The reference point of a surface is the bottom of the right-hand corner of the wall. The azimuth angle is measured west of due south as positive and east of due south as negative.

The tilt angle of the shading device is the angle between the shading device and the wall surface. The perpendicular shading device has a 90° tilt angle. If the tilt angle is smaller than 90° the shading device is tilted outward. Likely, if the angle is greater than 90° it is tilted inward. The tilt angle range is 0° to 180°.

The shading device also has two additional angles (Angle1 and Angle2). These two angles are used to solve the problem caused when two shading devices are tilted and overlap each other. With these angles, we may be able to analyze various configurations of shading devices. When the value of the Angle1 or Angle2 of an overhang is set to positive, it will slope toward the left side. If the value of the Angle1 or Angle2 of a side fin is set to positive, it will slope upward. The range of Angle1 and Angle2 is -90° to 90°.

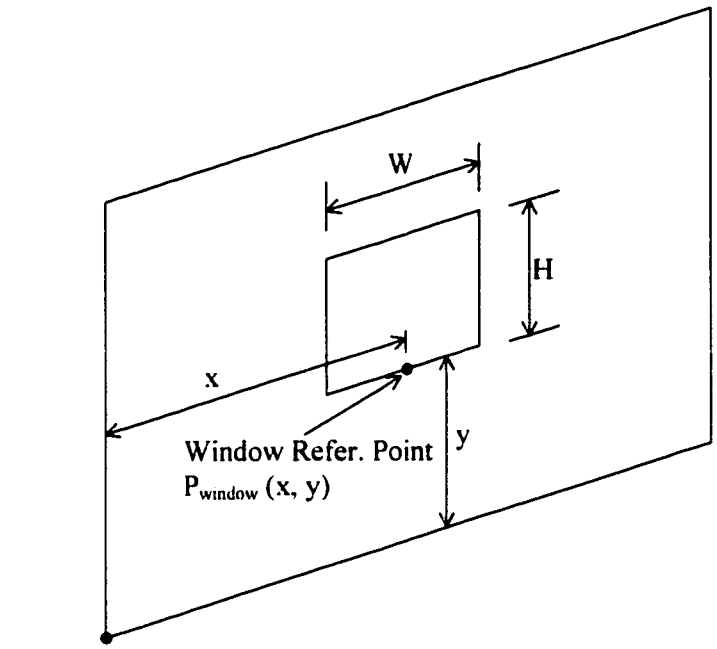

Figure 4.14 Example of the Window Coordinate System. The location of the window is defined relative to the origin of the window coordinate system. The reference point of the window is at the center of the bottom edge of the window.

4.1.4.2 User-defined Viewpoint

In all the previously described cases of shading design using the sunpath diagram, the viewpoint was always a point at the bottom center of the window. Unfortunately, this limits the analysis to a single point and does not allow the user to evaluate other viewpoints on the window without redimensioning and recalculating the shading mask protractor.

To solve this problem, the SFD program was modified to permit the user to set the viewpoint as any point within the window. This movable viewpoint has *X*, *Y* and *Z* coordinates measured from the origin of the shading coordinate system (i.e., the center of the bottom edge of a window). Using the movable viewpoint, the projection of shading area is recalculated by shifting the coordinates from the reference point of shading devices.

The following sections describe the equations to calculate the projected coordinates of shading devices in order to superimpose the shading area onto a sunpath diagram. To

accomplish this, the projected coordinates of shading devices are first calculated against the origin of shading coordinate system (O_{shade}). Then, the coordinates are recalculated using the viewpoint (P_{view}).

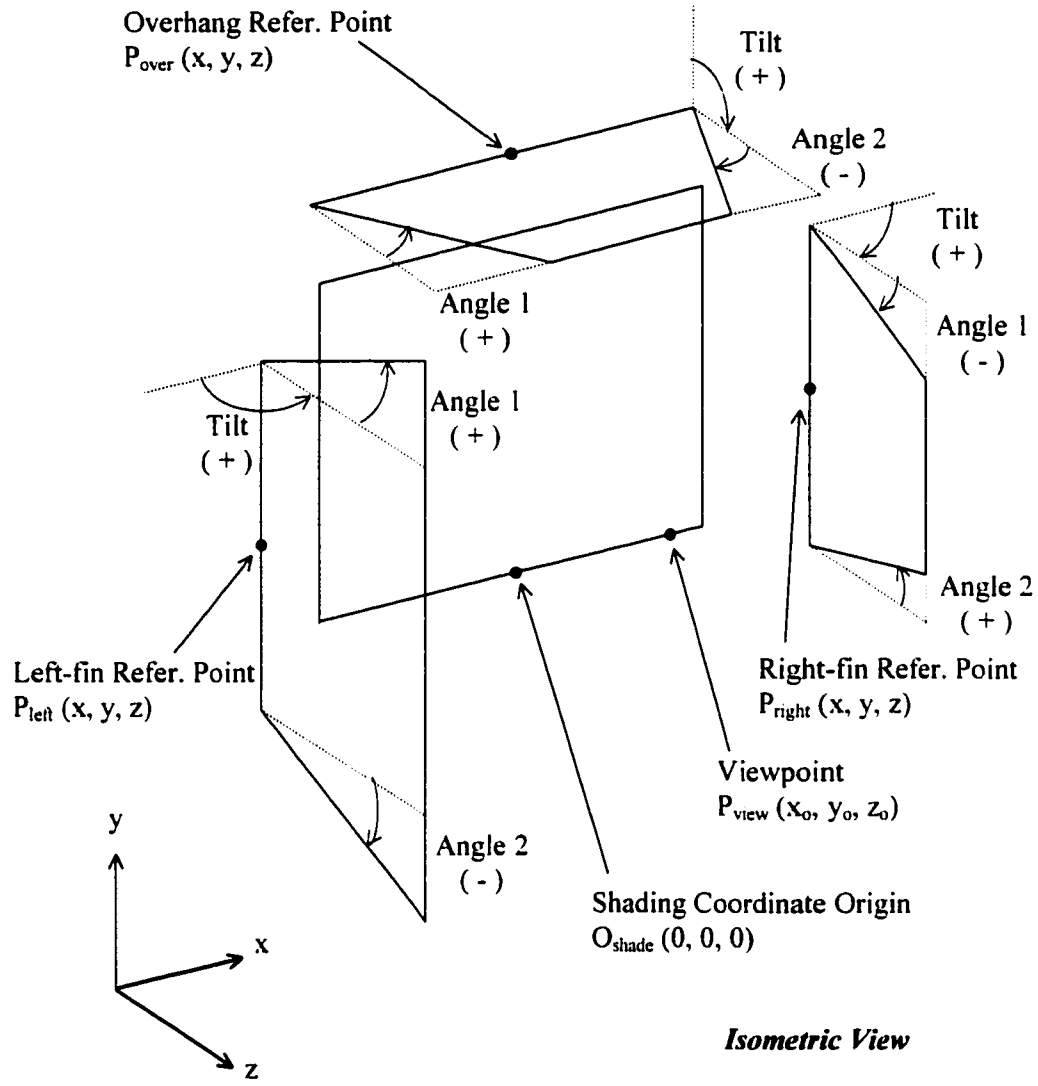

Figure 4.15 Example of the Shading Coordinate System. The location of a shading device is defined relative to the origin of the shading coordinate system. This figure shows the reference points of overhang and side-fins and viewpoint measured from the origin of the shading coordinate system.

4.1.4.3 Plotting the Shading of an Overhang

To plot the shading area projected from an overhang, one needs to calculate the angles (α and β in Figure 4.11) of the four corner points of a shading device measured from the viewpoint (P_{view}). With these angles, one can transfer the coordinates onto the sunpath diagram using the same method used for plotting the shading mask protractor.

Figure 4.16 shows an example of the calculation of the angles for an overhang. The coordinates of the four corner points (A, B, C', E') of the imaginary rectangular shape measured from the origin of the shading coordinate system (O_{shade}) are

$$A = \left(x - \frac{W}{2}, y, z \right), \tag{4.28a}$$

$$B = \left(x + \frac{W}{2}, y, z \right), \tag{4.28b}$$

$$C' = \left(x - \frac{W}{2}, y + D\cos T, z + D\sin T \right), \text{ and} \tag{4.28c}$$

$$E' = \left(x + \frac{W}{2}, y + D\cos T, z + D\sin T \right). \tag{4.28d}$$

Thus, the coordinates of the two outer corner points C and E measured from the origin of the shading coordinate system are

$$C = \left(x - \frac{W}{2} + D\tan A1, y + D\cos T, z + D\sin T \right), \text{ and} \tag{4.28e}$$

$$E = \left(x + \frac{W}{2} + D\tan A2, y + D\cos T, z + D\sin T \right). \tag{4.28f}$$

Finally, the coordinates of the four corner points (A, B, C, E) of the overhang measured from the viewpoint (P_{view}) instead of the shading coordinate origin (O_{shade}) are

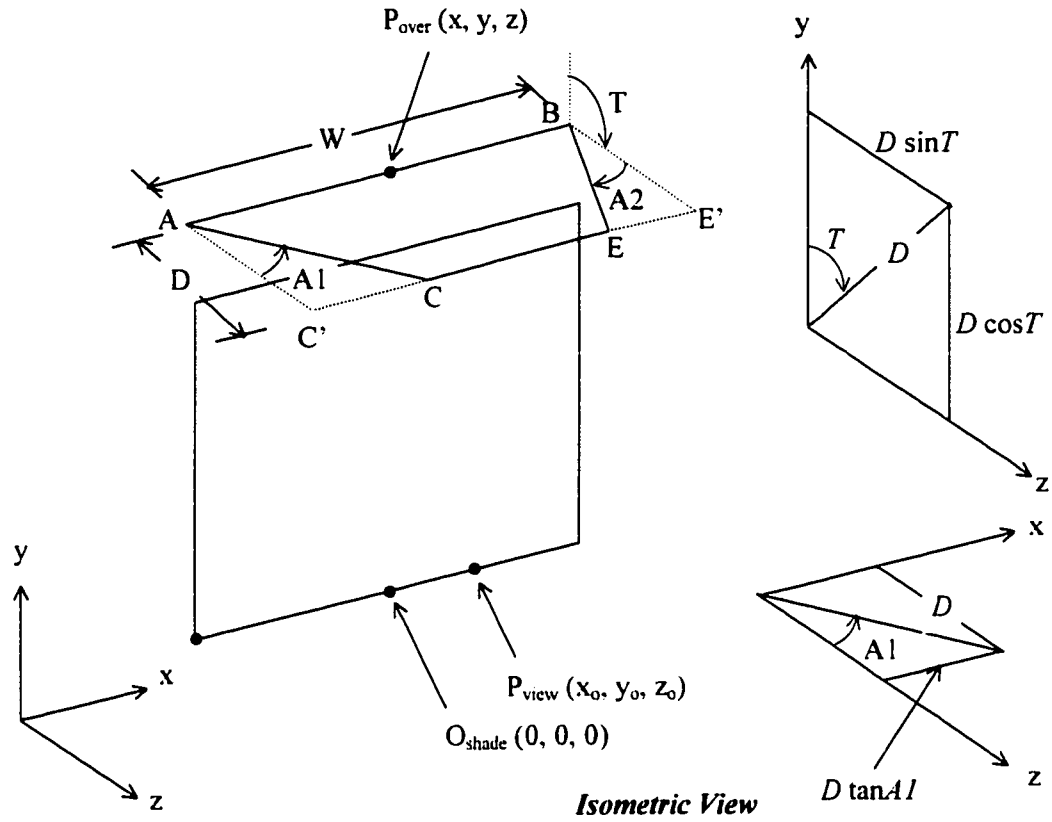

Figure 4.16 Calculation of the Shading of an Overhang.

$$A = \left(x - \frac{W}{2} - x_o, y - y_o, z - z_o \right), \tag{4.28g}$$

$$B = \left(x + \frac{W}{2} - x_o, y - y_o, z - z_o \right), \tag{4.28h}$$

$$C = \left(x - \frac{W}{2} + D\tan A1 - x_o, y + D\cos T - y_o, z + D\sin T - z_o \right), \text{ and} \tag{4.28i}$$

$$E = \left(x + \frac{W}{2} + D\tan A2 - x_o, y + D\cos T - y_o, z + D\sin T - z_o \right). \tag{4.28j}$$

The solar altitude angle and solar azimuth angle in the sunpath diagram for these four corner points are then calculated using Equations 4.18 and 4.19 respectively.

4.1.4.4 Plotting the Shading of a Right-fin

The method for plotting the shading area projected from the right-fin is quite similar to the way of plotting the shading by an overhang. In this case, however, the shading device is vertical instead of horizontal. Hence, the coordinates can be given by replacing the factors in X and Y coordinates.

Figure 4.17 shows an example of the calculation of the angles for a right-fin. The coordinates of the four corner points (A, B, C', E') of the imaginary rectangular shape measured from the origin of the shading coordinate system (O_{shade}) are

$$A = \left(x, y + \frac{H}{2}, z \right), \tag{4.29a}$$

$$B = \left(x, y - \frac{H}{2}, z \right), \tag{4.29b}$$

$$C' = \left(x + D\cos T, y + \frac{H}{2}, z + D\sin T \right), \text{ and} \tag{4.29c}$$

$$E' = \left(x + D\cos T, y - \frac{H}{2}, z + D\sin T \right). \tag{4.29d}$$

Thus, the coordinates of the point C and E measured from the origin of the shading coordinate system are

$$C = \left(x + D\cos T, y + \frac{H}{2} + D\tan A1, z + D\sin T \right), \text{ and} \tag{4.29e}$$

$$E = \left(x + D\cos T, y - \frac{H}{2} + D\tan A2, z + D\sin T \right). \tag{4.29f}$$

Finally, coordinates of four corner points (A, B, C, E) measured from the viewpoint (P_{view}) instead of the shading coordinate origin (O_{shade}) are

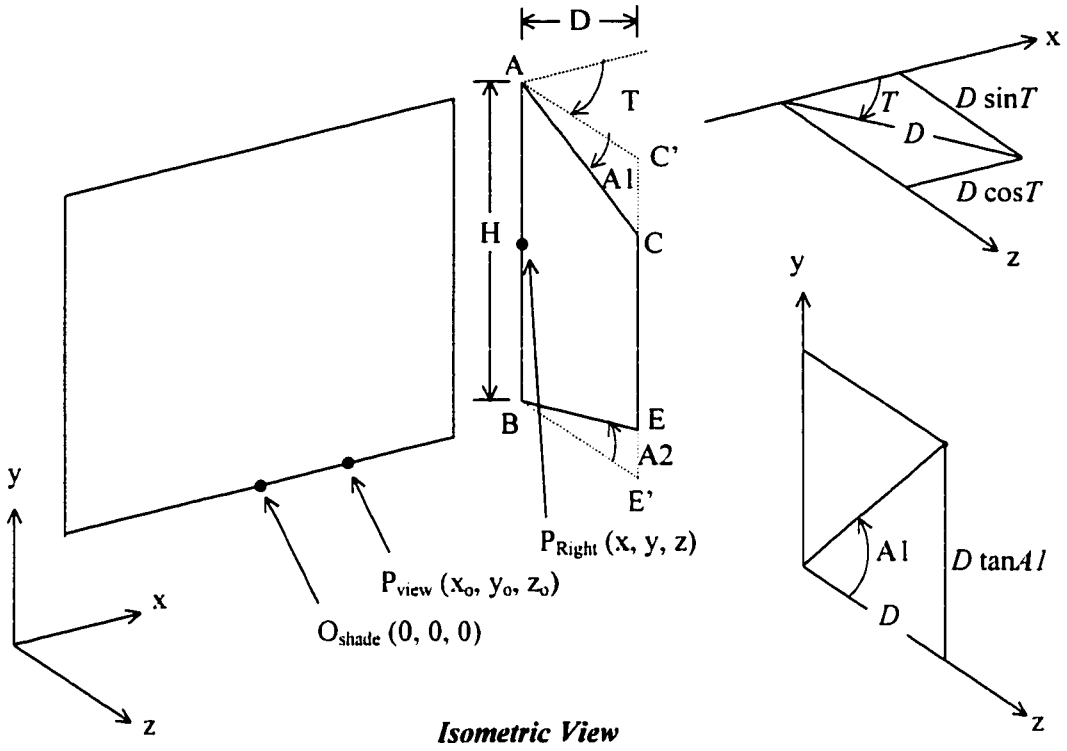

Figure 4.17 Calculation of the Shading of a Right-fin.

$$A = \left(x - x_o, y + \frac{H}{2} - y_o, z - z_o \right), \tag{4.29g}$$

$$B = \left(x - x_o, y - \frac{H}{2} - y_o, z - z_o \right), \tag{4.29h}$$

$$C = \left(x + D\cos T - x_o, y + \frac{H}{2} + D\tan A1 - y_o, z + D\sin T - z_o \right), \text{ and} \tag{4.29i}$$

$$E = \left(x + D\cos T - x_o, y - \frac{H}{2} + D\tan A2 - y_o, z + D\sin T - z_o \right). \tag{4.29j}$$

4.1.4.5 Plotting the Shading of a Left-fin

The method used to plot the shading area projected from a left-fin is almost the same as that for a right-fin except that the value of $D\cos(T)$ in the X coordinate is positive instead of negative. Figure 4.18 shows an example of calculation of the angles for a left-fin. The coordinates of the four corner points (A, B, C, E) of the right-fin measured from the viewpoint (P_{view}) are

$$A = \left(x - x_o, y + \frac{H}{2} - y_o, z - z_o \right), \tag{4.30a}$$

$$B = \left(x - x_o, y - \frac{H}{2} - y_o, z - z_o \right), \tag{4.30b}$$

$$C = \left(x - D\cos T - x_o, y + \frac{H}{2} + D\tan Al - y_o, z + D\sin T - z_o \right), \text{ and} \tag{4.30c}$$

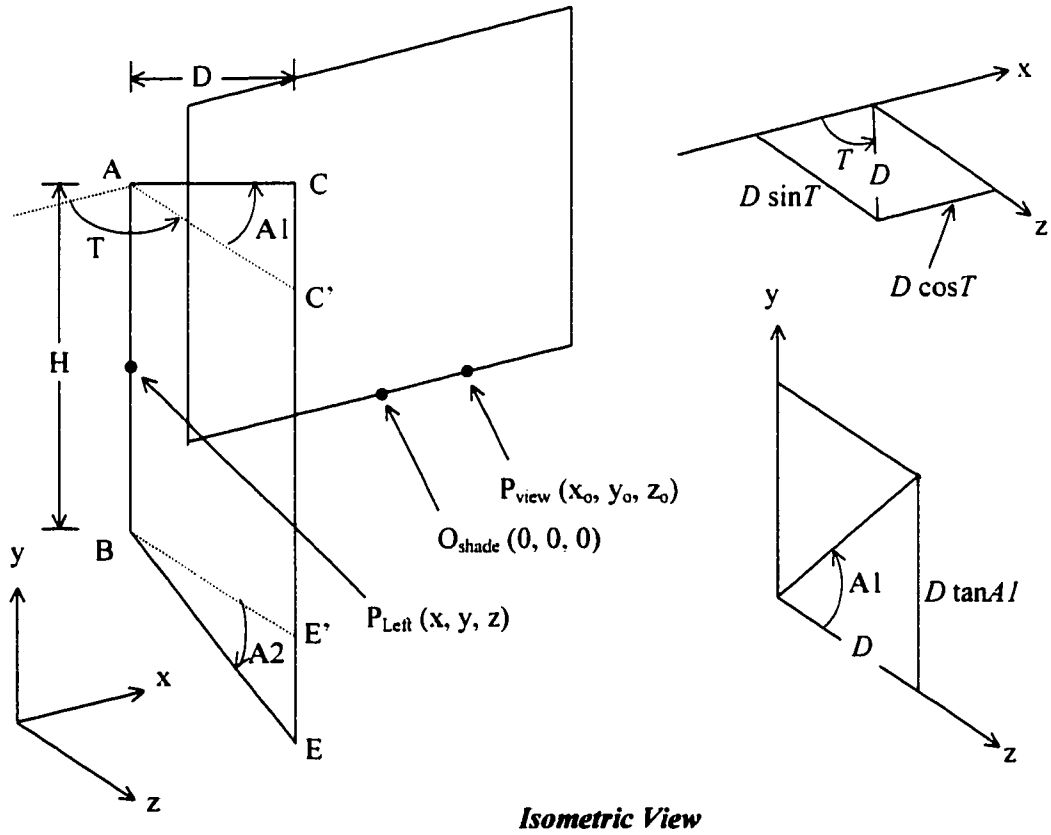

Figure 4.18 Calculation of the Shading of a Left-fin.

$$E = \left(x - D\cos T - x_o, y - \frac{H}{2} + D\tan A2 - y_o, z + D\sin T - z_o \right). \qquad (4.30d)$$

4.1.4.6 Example Plotting of Shading

Figure 4.19 shows the graphical description of an example of the combined shading devices. The example consists of an overhang, a left-fin, and a right-fin. All of the shades have the same length. The depths of the side-fins are both 1 in. The overhang is tilted downward about 120° from the wall surface, and the depth of it is set to 1.1547 in. to have the same projection with side fins. To remove the overlapped areas to improve the shading analysis, the values of Angle1 of each side-fin are given as 30°. The viewpoint is at the middle point between the shading coordinate origin and the bottom of the right-hand corner of the window. The coordinates and sizes of shading devices and the coordinates of the viewpoint are given in Table 4.3.

The coordinates of the viewpoint are $P_{view}(x_o, y_o, z_o) = (1, 0, 0)$. From Equations 4.28g to 4.28j, the coordinates of the four corner points (A, B, C, E in Figure 4.16) of the overhang are calculated as follows

$$A_1 = \left(0 - \frac{4}{2} - 1, 3 - 0, 0 - 0 \right) = (-3, 3, 0), \qquad (4.31a)$$

Table 4.3 User Input for Shading Devices in Figure 4.19.

Object	Surface	Window	P_{view}	Overhang	Right-fin	Left-fin
X	0 ft.	6 ft.	1 ft.	0 ft.	2 ft.	-2 ft.
Y	0 ft.	3 ft.	0 ft.	3 ft.	1 ft. 6 in.	1 ft. 6 in.
Z	0 ft.	-	0 ft.	0 ft.	0 ft.	0 ft.
Length	12 ft.	4 ft.	-	4 ft.	3 ft.	3 ft.
Height/Depth	9 ft.	3 ft.	-	1.15 ft.	1 ft.	1 ft.
Tilt	90°	-	-	120°	90°	90°
Azimuth	30°	-	-	-	-	-
Angle1	-	-	-	0°	-30°	-30°
Angle2	-	-	-	0°	0°	0°

Note: The site location is 32° N latitude.

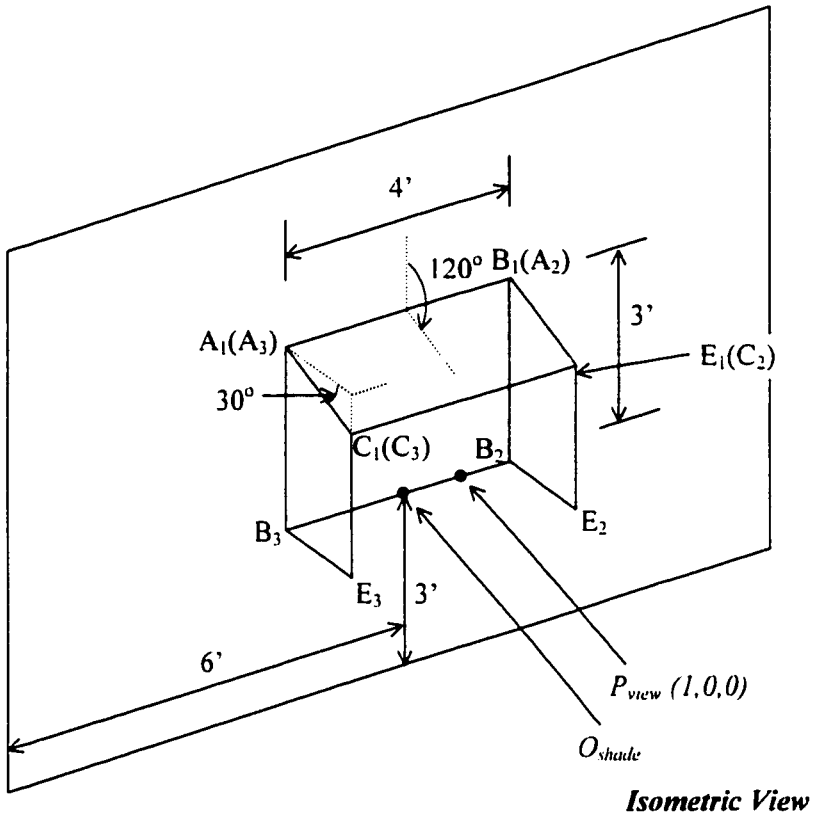

Figure 4.19 An Example of a Shading Device Design.

$$B_1 = \left(0 + \frac{4}{2} - 1, 3 - 0, 0 - 0\right) = (1, 3, 0), \tag{4.31b}$$

$$C_1 = \left(-\frac{4}{2} - 1, 3 + 1.15 \times \cos 120, 1.15 \times \sin 120\right) = (-3, 2.43, 1), \tag{4.31c}$$

$$E_1 = \left(\frac{4}{2} - 1, 3 + 1.15 \times \cos 120, 1.15 \times \sin 120\right) = (1, 2.43, 1). \tag{4.31d}$$

In the same way, from Equations 4.29g to 4.29j, the coordinates of four corner points of the right-fin are calculated: $A_2 = (1, 3, 0)$, $B_2 = (1, 0, 0)$, $C_2 = (1, 2.43, 1)$, and $E_2 = (1, 0, 1)$. Using Equations 4.30a to 4.30d, the coordinates of the left-fin are calculated as $A_3 = (-3, 3, 0)$, $B_3 = (-3, 0, 0)$, $C_3 = (-3, 2.43, 1)$, and $E_3 = (-3, 0, 1)$. Figure 4.20 shows the shading areas of overhang, left-fin, and light-fin in the example of displayed in the various sunpath diagrams.

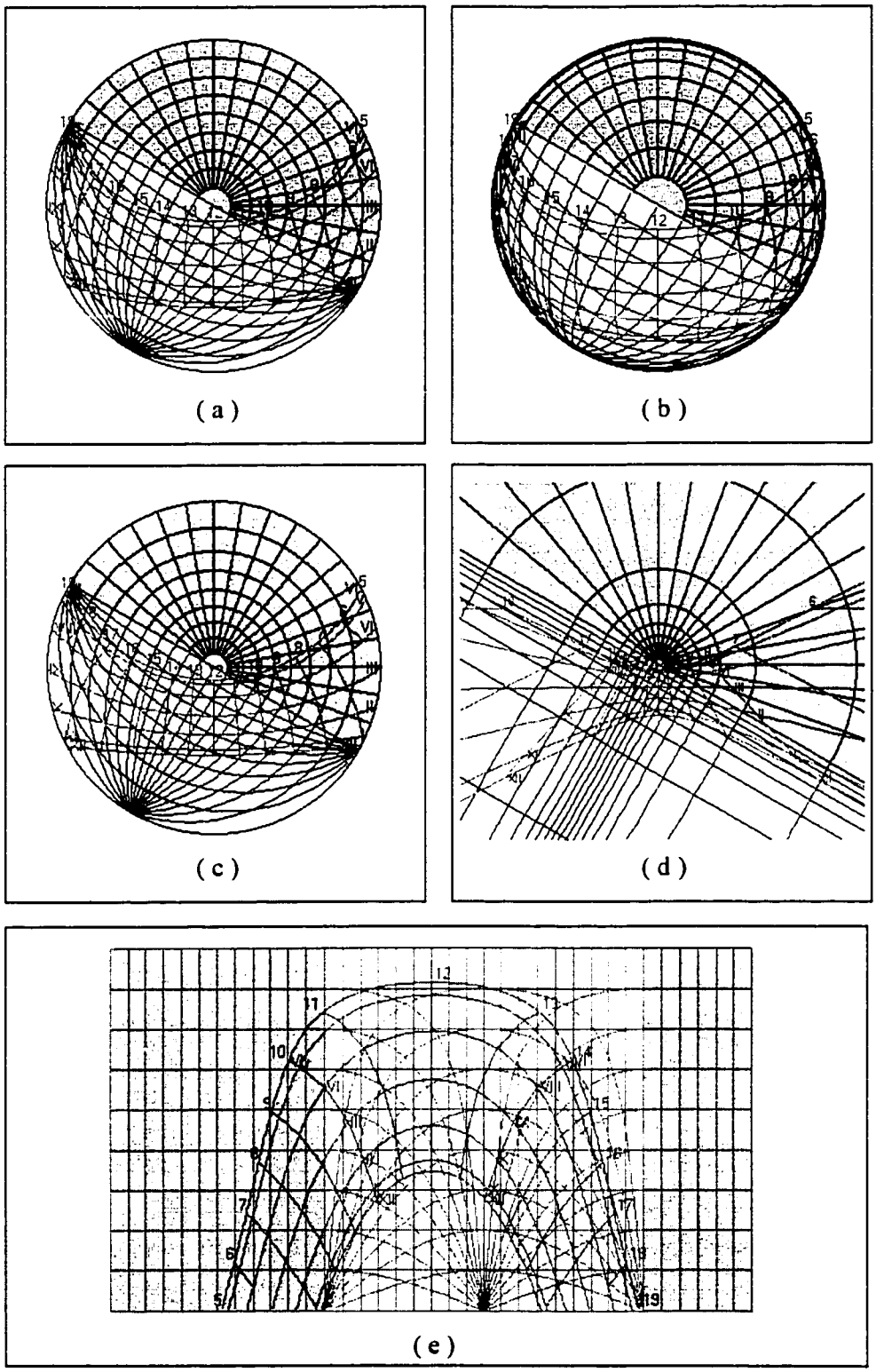

Figure 4.20 Sunpath Diagrams with Shading Area Plotted with Various Projection Methods. This figure shows sunpath diagrams for equidistant (a), orthographic (b), stereographic (c), gnomonic (d) and cylindrical (e) projections.

4.1.5 Display of Solar Radiation on a Sunpath Diagram

One of the additional benefits of a computerized sunpath diagram is its use in displaying any hourly weather data including solar radiation. The amount of solar radiation at a given solar angle is one of best examples of data that can be overlapped onto sunpath diagram. Solar incident angles can be calculated from the solar or local standard time. As the coordinate of sunpath diagram indicates the solar angles, we need a third indicator to represent the intensity of solar radiation. The program SFD uses a color scale indicator to represent the intensity of solar radiation.

Figures 4.21, 4.22, and 4.23 show the equidistant sunpath diagrams displaying the intensities of global solar radiation on a horizontal surface, total solar radiation on a vertical surface facing 30° west of due south and transmitted solar radiation through a window glazing respectively. The color scale has thirteen different colors to display the intensity of solar radiation in increments of 100 W/m^2. Ramsey and Sleeper (1970) also provided a graphical solar radiation calculator to determine the intensity of solar radiation falling on either horizontal or vertical surfaces using equi-intensity solar radiation lines. However, the SFD program provides a more convenient graphical method by displaying nicely trimmed solar radiation lines to fit the sunpath diagram for solar radiation incident or the exterior of the window

Figures 4.24, 4.25, and 4.26 show the cylindrical sunpath diagrams displaying the same solar information as the equidistant display. Mazria (1979) also developed the solar intensity masks to calculate the solar radiation incident on a surface. He provided a series of transparent masks for vertical surfaces, for titled surfaces of 60° and 30°, and for horizontal surfaces. By overlaying a solar intensity mask onto the proper cylindrical sunpath diagram for the latitude of the location, the hourly solar radiation on a surface having the selected title angle can be determined. However, the SFD program easily provides a graphical display of solar radiation on a tilted surface at any off-south azimuth angle for any latitude. Moreover, it also provides the transmitted solar radiation through a window glazing (Figure 4.26) as well as the incident solar radiation on a titled or horizontal surface (Figure 4.25).

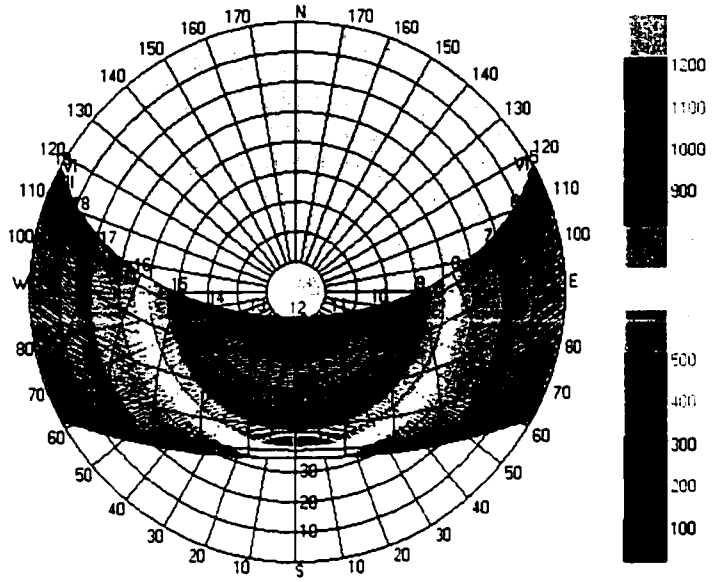

Figure 4.21 Equidistant Sunpath Diagrams Displaying the Total Solar Radiation on a Horizontal Surface. This figure shows the intensity of global solar radiation on a horizontal surface at 32° N latitude.

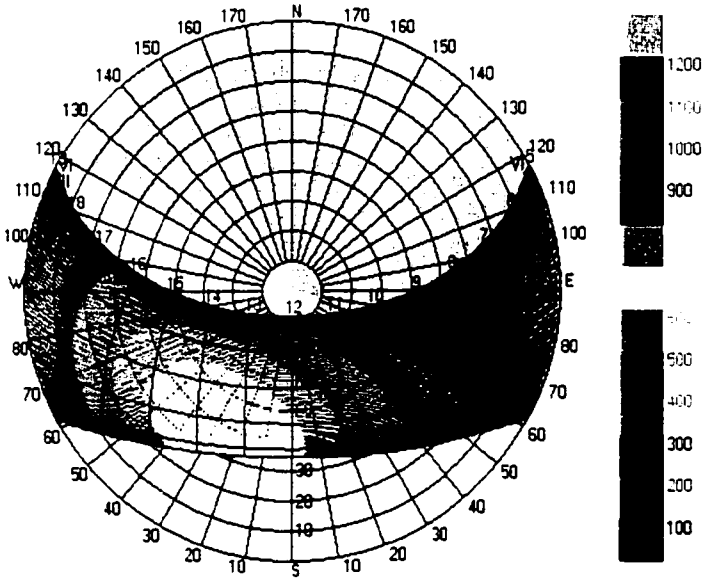

Figure 4.22 Equidistant Sunpath Diagrams Displaying the Total Solar Radiation on a Vertical Surface. This figure shows the intensity of global solar radiation on a vertical surface facing 30° west of due south at 32° N latitude.

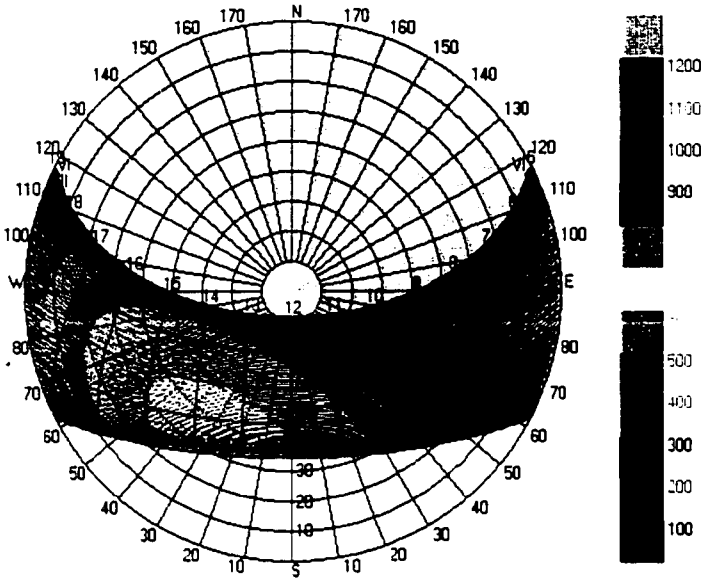

Figure 4.23 Equidistant Sunpath Diagrams Displaying the Transmitted Radiation through a Vertical Glazing. This figure shows the intensity of transmitted solar radiation through a vertical window glazing facing 30° west of due south at 32° N latitude.

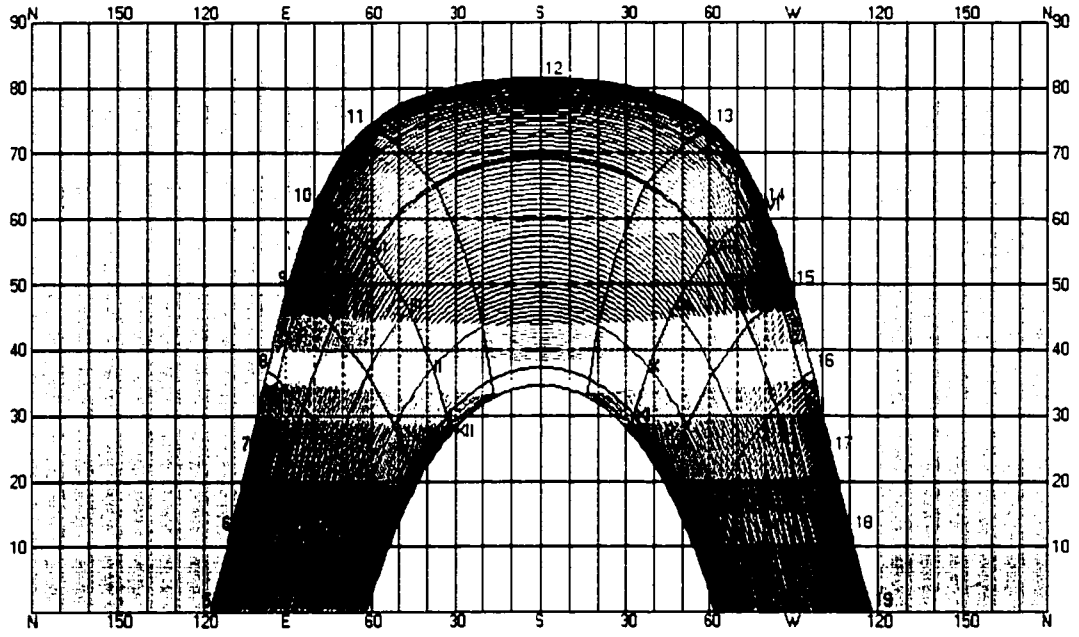

Figure 4.24 Cylindrical Sunpath Diagrams Displaying the Total Solar Radiation on a Horizontal Surface. This figure shows the intensity of global solar radiation on a horizontal surface at 32° N latitude.

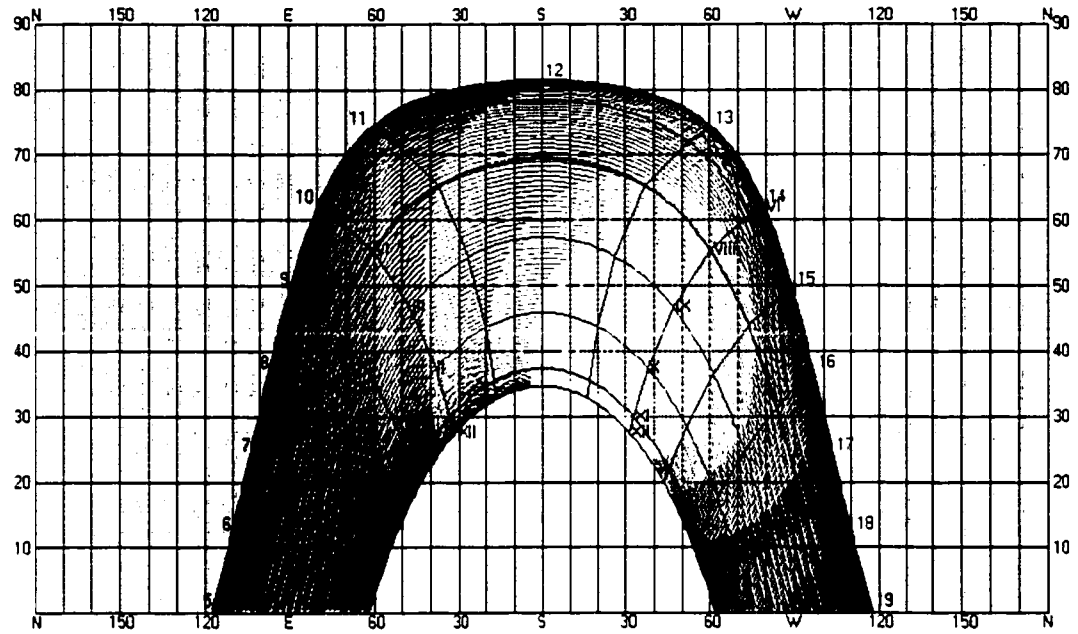

Figure 4.25 Cylindrical Sunpath Diagrams Displaying the Total Solar Radiation on a Vertical Surface. This figure shows the intensity of global solar radiation on a vertical surface facing 30° west of due south at 32° N latitude.

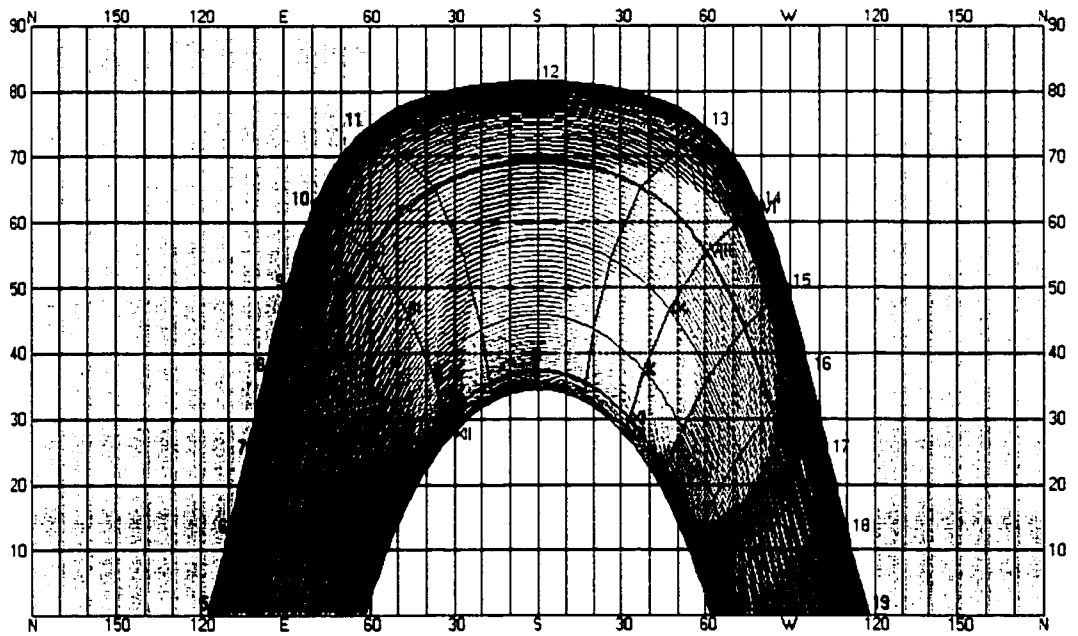

Figure 4.26 Cylindrical Sunpath Diagrams Displaying the Transmitted Radiation through a Vertical Glazing. This figure shows the intensity of transmitted solar radiation through a vertical window glazing facing 30° west of due south at 32° N latitude.

4.2 Calculating Solar Heat Gain through Window Glazing

The solar heat gain through a window system is determined by calculating the incident angle dependent heat gains from the direct, diffuse, and reflected solar radiation. The net heat gain or loss through a window includes this solar heat gain and the corresponding heat transfer due to conduction, convection, and thermal radiation which are driven by the indoor-outdoor temperature difference and the temperature of the surfaces adjacent to the window.

The total solar radiation gain through a specific window system on a tilted wall contains three components: direct radiation, diffuse sky radiation, and radiation reflected from the ground and/or shading devices. When the window is not shaded, the direct component of the incident solar radiation is determined by the beam normal radiation times the tilt factor using Equation 2.10. When the weather file provides only the global horizontal radiation, the direct and diffuse components can be calculated using the equation developed by Erbs et al. (1982) as follows

$$\frac{I_{DH}}{I_{GH}} = \begin{cases} 1.0 - 0.09k_T & \text{for } k_T \le 0.22 \\ 0.9511 - 0.1604k_T + 4.388k_T^2 & \\ \quad -16.638k_T^3 + 12.336k_T^4 & \text{for } 0.22 < k_T \le 0.80 \\ 0.165 & \text{for } k_T > 0.80 \end{cases} \tag{4.32}$$

where k_T is hourly clearness index and defined as

$$k_T = \frac{I_{GH}}{I_{OH}}. \tag{4.33}$$

To use Erbs' equation to calculate the diffuse solar radiation, the hourly clearness index is first determined by dividing the hourly global horizontal radiation by the calculated hourly extraterrestrial solar radiation on the horizontal surface. The extraterrestrial radiation can then be calculated by either Equation 2.1 or Equation 2.2. Next, the beam and diffuse components of the horizontal radiation are calculated using Equations 4.32 and 4.33. Finally, the beam component the global solar radiation on the tilted surface is calculated using Equation 2.10.

When the window is shaded, the ratio of the unshaded area to the total surface area needs to be calculated. This factor can be calculated using the boundary evaluation of the 2D

concave polygon clipping as described in Section 2.4.1. The current version of the SFD program only calculates solar radiation on an unshaded surface.

The diffuse component of the total radiation on a tilted surface can be calculated using either an isotropic or anisotropic diffuse sky model. In the isotropic sky model, the uniform diffuse radiation from the sky is determined by the diffuse radiation on the horizontal surface and the shape factor from the surface to the sky using Equation 4.12. Though an isotropic model is more widely used for building simulation (Hay 1979), an anisotropic model, the HDKR model is used in the proposed model because of its improved accuracy. The diffuse component of the global radiation on a tilted surface is therefore calculated by Equation 2.14.

The calculation of the reflected solar radiation is composed of the reflected radiation from the ground and the reflected radiation from external surfaces. The reflected solar radiation from the ground immediately in front of the window is calculated by Equation 2.18 with a user-input ground reflectance. The total reflected radiation from all external surfaces is calculated by Equation 2.19.

The total solar radiation on a vertical surface is calculated using Equation 2.10. The transmitted solar radiation through a shaded window glazing is calculated using Equation 2.25. For this calculation, the values for the transmittance-absorptance product for the beam, diffuse, and reflected components need to be calculated in advance.

4.3 Experimental Validation Using a Physical Model

The experimental model validation is one of the main contributions of this research since very few well-documented data sets have been published for a shaded fenestration. Furthermore, since the objective of this research is to develop a computerized design tool that can provide an accurate thermal simulation of a shaded window, these tests provide evidence that the complex set of equations can be used to calculate the solar heat gain through a window. For the empirical validation test, a specially designed test box was constructed and used to collect 15-minute data over a series of tests. The data from the test box and the nearby solar test bench were downloaded and analyzed weekly. The measured data from this experimental box were compared against the SFD's finite difference model and the DOE-2 program. The experiment was conducted under various shading arrangements for selected periods.

4.3.1 Experimental Box

An approximately 4 ft. x 2 ft. x 3 ft. test box (Figure 4.27) was constructed to measure the effects of various shading devices on the thermal performance of a window. The experimental model box consists of three rooms: the test chamber, an instrument room having various instruments to measure the thermal performance of the test chamber, and a room for the storage of equipment. The window aperture of the test box was located facing the due south.

The test chamber (Figure 4.28) has a width of 2 ft., a depth of 1 ft, and a height of 2 ft. Two tubes (i.e., the inlet tube and the outlet tube) are installed between the test chamber and the instrument room. Air is continuously circulated by a variable speed DC fan through these tubes. Instrument room air is exchanged with the outside air using an exhaust fan. Thus, the inlet air temperature was kept as close as possible to the ambient air temperature to avoid unwanted heat gain to the camber.

The window aperture is a 1 ft. by 1 ft. opening installed in the center of the front wall and penetrates into the test chamber. The walls, roof, and floor of the test chamber are highly insulated (i.e., about 6 in. of layered Styrofoam). The window area and the thickness of insulation in the experimental test box were deliberately designed so that the heat conducted through the envelope is less than 10% of the expected heat gain through the window glazing.

The air temperatures in the inlet and the outlet tubes were measured using 1.000 ohm Platinum RTD temperature sensors installed in the inlet and outlet tubes to the airflow chamber in the instrument room close to the interior wall. The RTD sensors were calibrated against NIST-traceable thermometers. A carefully designed airflow measurement chamber was installed in the inlet tube. This airflow chamber is composed of an AMCA airflow nozzle (1.250" w/o taps), a filter, and a ½-inch Plexiglass tube having holes for the equivalent air pressure measurement. The air pressure difference between both sides of the airflow nozzle was measured and collected using a Setra Low Pressure Transducer (Model 264) to measure the low air pressure less 1.0 in. w.g. The transducer was calibrated periodically against a Dwyer U-inclined Manometer (Dual Range Flex-Tube; Model 1127). A complete list of instruments is provided in the Appendix A.2.

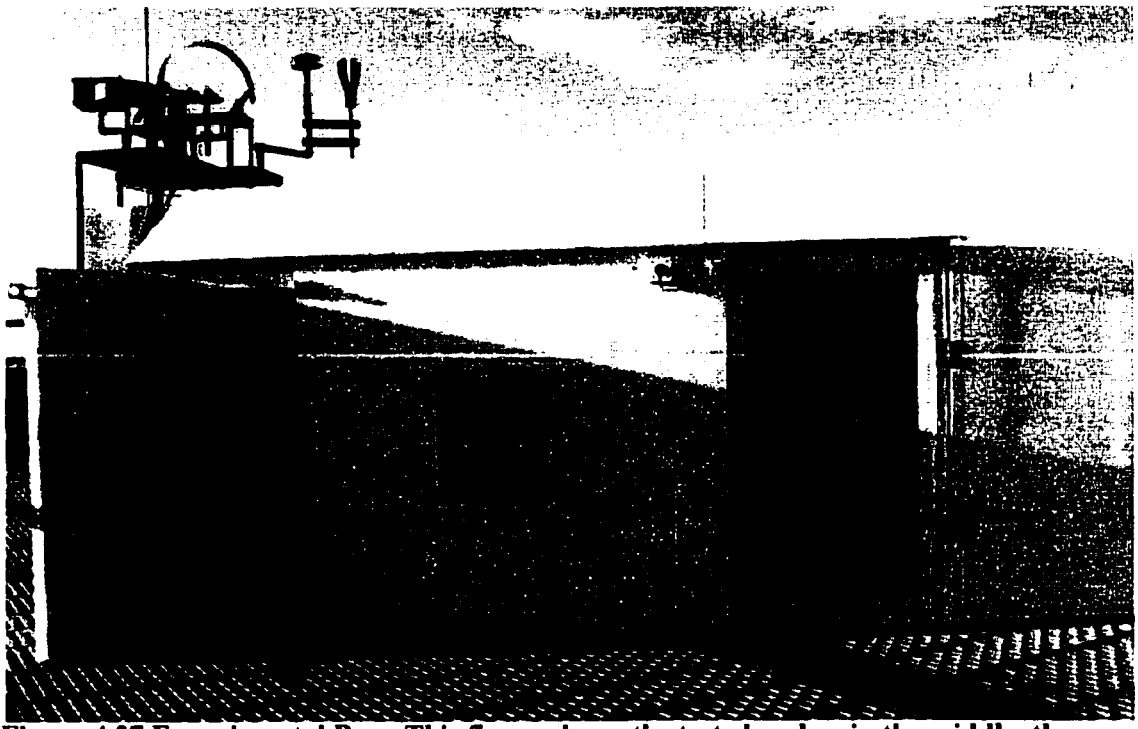

Figure 4.27 Experimental Box. This figure shows the test chamber in the middle, the instrument room on the right and the storage room on the left. The solar test bench is located behind the model box.

A Li-Cor Pyranometer (Model LI-200SA) was installed in the front wall to measure the incident solar radiation on the vertical wall facing the south. A 2-wire Millivolt Transmitter (Moore Industries) was used to convert the signal from the solar sensor and send the data to the logger. For the glazing transmittance test, two solar sensors were installed near the center of the window glazing one inside and one outside. All of the instruments were connected to a Synergistic data logger (Figure A.6 in Appendix A) that recorded 15-minute data. Using this data logger, the measured data were remotely downloaded using a modem into the Energy Systems Laboratory (ESL)'s database.

To measure the temperature of the window glazing, two Hobo Temperature Data Loggers were installed behind insulated caps up against the glazing at the center of the left half and the right half of the glazing (NOTE: These appear in Figure 4.1 as the two white dots on the window). The data from these loggers were manually downloaded every week and merged with the data from the Synergistic data logger. The data collection procedure is described in Section 4.3.3. All the instruments were calibrated prior to performing the experiments. The procedures for the calibration of the instruments used in the experimental test are described in the Section 4.3.2.

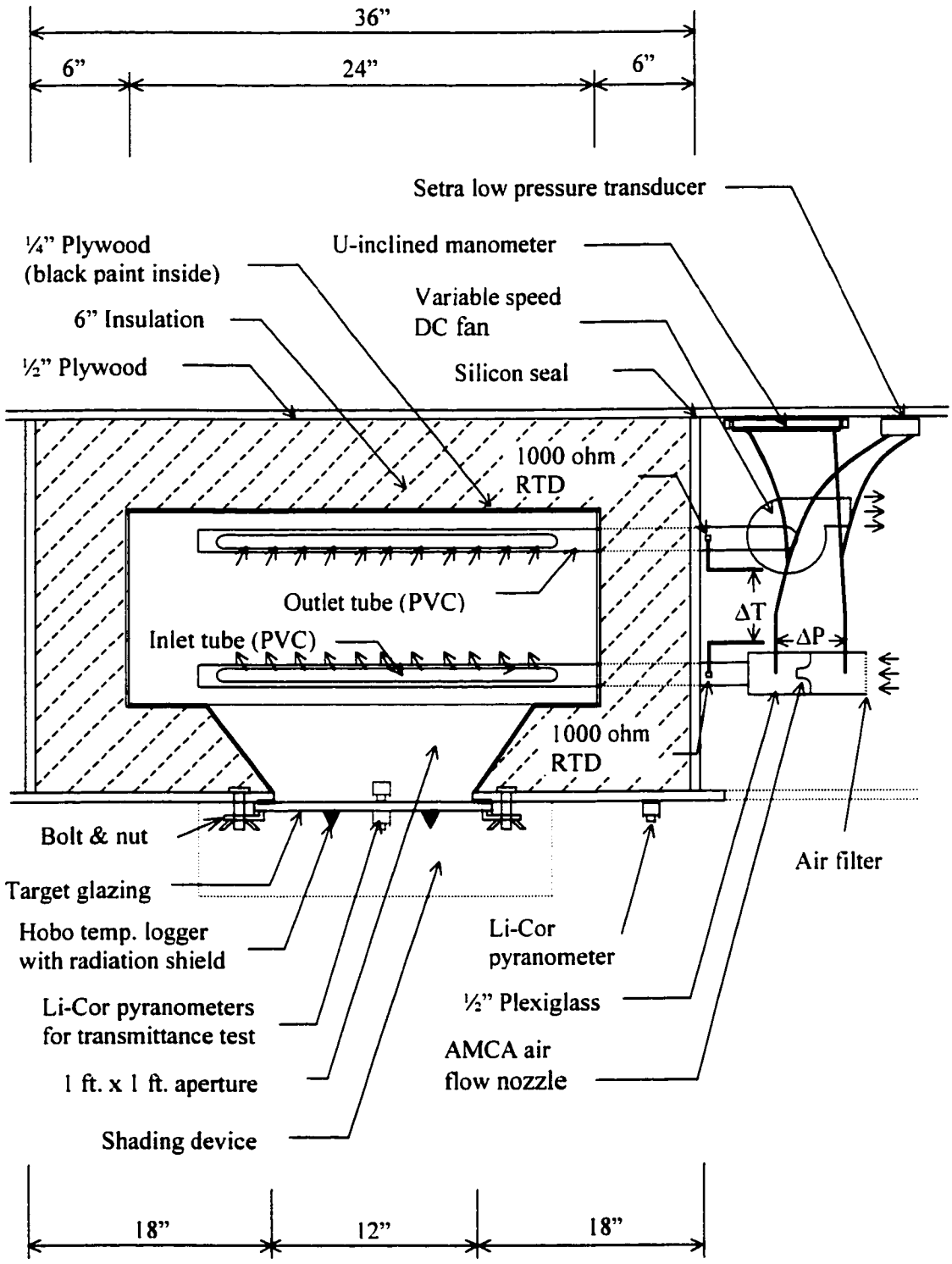

Figure 4.28 Plan View (Cross Section) of the Test Chamber of the Experimental Box.

The total heat gain or loss through the window was calculated by measuring the airflow rate and the air temperature difference between inlet and outlet tubes. To validate the effects of the shading, various geometrical shapes were tested.

4.3.2 Instrument Calibration

Vertical solar radiation is measured with a Li-Cor LI-200SA pyranometer. Signal conversion is conducted by Li-Cor 147ohm Resistor (model 2220) and Moore Industries millivolt transmitter(MVX/10-20MVFS/4-20MA/12-42DCFL). The Li-Cor 147 ohm resistor outputs 0.0-20.0 millivolts, and Moore millivolt transmitter is used to convert 0.0-20.0 millivolts input to 4.0-20.0 milliamps output.

The calibration of the transmitter was required before the solar sensor itself could be calibrated. The procedure to calibrate millivolt transmitters and solar sensors is well documented in an ESL memorandum, i.e., 'Calibration Procedure for Solar Sensors' prepared by Curtis Boecker (1997). For the calibration of millivolt transmitters, Beta Voltage Analyzer (model 435) and BETA 20 milliamps Signal Analyzer (model 434) were used.

A millivolt source provided by a Beta voltage analyzer is used to simulate the voltage drop created by Li-Cor pyranometer 147ohm dropping resistor. A BETA 20 milliamps signal analyzer is used to provide power to the millivolt transmitter, and display the output signal of the transmitter.

After the combination of solar sensors were connected to the Synergistic data logger, the recorded output signal from the calibrated Li-Cor sensor was linearly calibrated against the Epply pyranometer installed along with a nearby Li-Cor sensor in the Langford Architecture Solar Test Bench. The linear calibration result is attached in the Appendix A.3.

To measure the air pressure difference across the AMCA flow nozzle in the main chamber, a Setra pressure transducer (1-0" w.g. range; 0-5 volt output) was used. A Dwyer U-inclined manometer is installed in parallel with the pressure transducer, which was used for a spot reading of the air pressure difference to control the speed of the circulation fan. Thus, the pressure transducer and the manometer needed to be calibrated in order to provide the same readings through the measuring range. The calibration method recommended by the AMCA/ASHRAE Standard (1985) suggests at least 11 points of calibration for pressure

indicating instruments, i.e., 'at both ends of the scale and at least nine equally spaced intermediate points.'

The pressure transducer and manometer were calibrated against a one-thousandth scale Merian Micro-manometer (model 34FB2TM, S/N M-55942, 20" w.g. range) installed in the ESL at the Riverside campus of Texas A&M University using the previously described calibration procedure. As the difference between the minimum and the maximum values of measuring range is 1" w.g., air pressure difference was inspected at intervals of every 0.1" w.g. of air pressure. The result of the calibration provided very close agreement within the allowable air pressure error (less than 1/100 of the range) for both the pressure transducer and the manometer.

Three Taylor laboratory glass thermometers (model 6321, 0-230^{0}F range, 12" length) were calibrated against a series of calibrated ASTM partial-immersion thermometers in the Thermometer Calibration Lab., ESL Riverside Laboratory, using the temperature calibration procedures of Wise and Soulen (1986 National Bureau of Standards).

An appropriate ASTM thermometer was placed in a thermometer rack along with the Taylor thermometers being calibrated, then properly placed in a variable constant-temperature oil bath. Partial-immersion thermometers should be immersed only to the immersion lines or specified depth. Because the NBS Thermometer Calibration Procedure recommends that 'thermometers should be calibrated at the temperatures specified by the customer or at intervals of approximately every 100 scale divisions', the thermometers were calibrated at intervals of every 2 °F of temperature from the minimum 32 °F to the maximum 170 °F. Two of the thermometers provided close agreement within allowable air pressure error (less than 0.5 °F of the range). The third thermometer made about 0.5 °F difference in temperature reading at temperatures lower than 100 °F, even though the temperature difference became smaller as the inspected temperature increased above 100 °F. Thus, the first two thermometers were used for the air temperature measurement of inlet and outlet tubes in the physical experiment box.

An RTD cannot be calibrated by itself. Instead, it is calibrated when it is connected to the Synergistic data logger, because every data logger can provide different output signals. In the Synergistic data logger, there is a button called 'i-cal' that is used only to calibrate the input from RTD sensors. The RTDs used for the test box were calibrated against the calibrated thermometers installed adjacent to the RTDs.

4.3.3. Test Procedures and Data Collection

For the experimental tests, 21 data points were collected every 15 minutes from the Langford Architecture Center solar test bench, the experimental box, the College Station National Weather Service (CLL), and the weather station on the roof of the Zachry Engineering Center (Figure 4.29). Table B.1 in the Appendix B shows the list of data elements used for the experiment validation.

Eight analog channels were used to record the various solar radiation measurements from the solar test bench. The other four analog data channels are used to record data from the experimental box including solar radiation on the south facing vertical wall, air pressure difference across the AMCA airflow nozzle, air temperature at the inlet tube, and air temperature at the outlet tube. Each channel recorded data in 15-minute intervals. The Parset computer program was then used to remotely setup the configuration of the Synergistic data logger and download TSR data into a text file with the RAW file format.

The 'R2A930' AWK subroutine (Haberl et al. 1992) converts RAW data files into ACS file format (Loan STAR database format). Every Tuesday the measured data were downloaded from the data logger and stored into the LoanSTAR database along with other data measured in other sites. Using the 'GETDATC' Unix subroutine, the selected data elements that were measured in the College Station National Weather Service (CLL) and in the weather station on the roof of the Zachry Engineering Center were retrieved from the Loan STAR database. These data were then merged with the data from the solar bench and the experimental box using a MS Excel program.

Total of eight different experimental cases tested to validate the proposed computer model. Appendix B shows the graphical and tabular results of measured data from these experiments. The analysis of the data and comparison against the simulated data will be described in Chapter VI. Table B.2 shows the summary of data analysis.

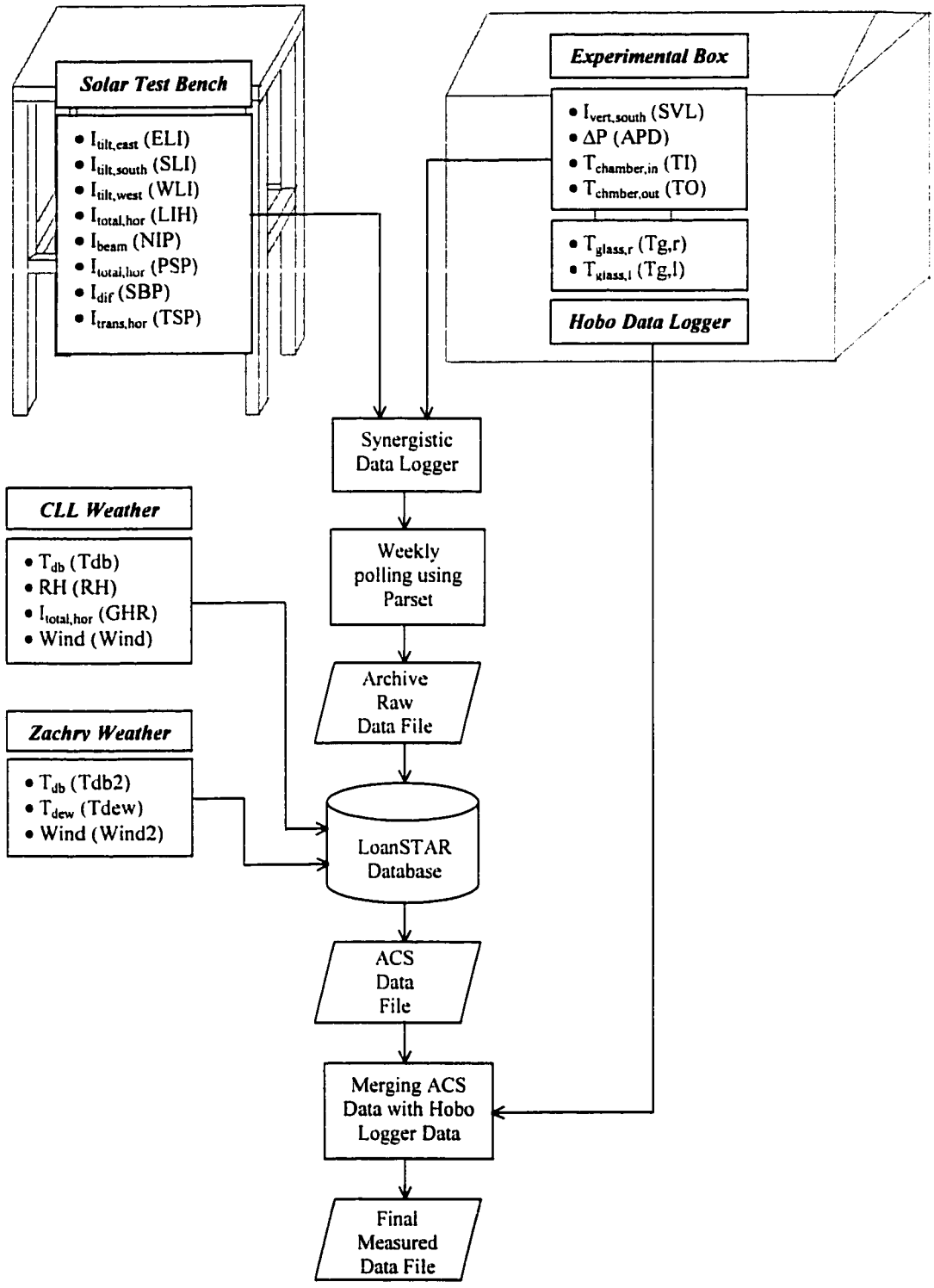

Figure 4.29 Flow Chart for Data Collection and Creating Data File.

4.4 Finite Difference (F.D.) Model of the Experimental Box

In general, manual thermal performance analysis of a building is conducted under steady-state conditions where the temperature is linearly distributed through each material. This assumption does not cause problems in most building heat transfer simulations because the boundary condition (i.e., the outside weather condition) does not rapidly change with the simulation period of one hour. However, for a special condition such as a building that has extremely high insulation or under extreme outside weather conditions, the thermal analysis should be conducted with consideration of change in boundary conditions over time.

To solve the time varying temperature distributions through a highly insulated wall, the 'Finite Difference (F.D.) Method' is widely used as a solution for transient heat transfer problems. There are two different F.D. methods, the explicit method and the implicit method. In the explicit method, the temperature of any node at a new time $t + \Delta t$ is calculated from the temperature at the same node and neighboring nodes for the previous time t. In the implicit method, the future nodal temperature is solved using matrix inversion. For a more detailed description of the finite difference methods, the reader is referred to the heat transfer textbook by Incropera and DeWitt (1996).

Figure B.2 in Appendix B shows that the chamber outlet temperature is about two or three degrees Fahrenheit higher than the chamber inlet temperature during the night because of the storage effect of the highly insulated walls. To calculate the exact amount of the heat transfer through window glazing, we need to figure out the dynamic heat transfer through the walls first. For this research, an 'explicit finite difference model' was applied in order to solve the dynamic heat storage and transfer effects of the highly insulated walls of the experimental box.

Though the explicit F.D. method provides computational convenience, it can provide difficulty caused by the limitations of the selection of Δt. In other words, extremely small values of Δt can be needed for a solution. In the measured data used in this research a 15-minute data interval was used. Unfortunately, the calculation of the conditions to satisfy the stability criterion showed that the required values of Δt should be less than two or three minutes. Therefore, before the finite difference method could be applied, the measured data were converted into one-minute data using the 'Weather Data Converter' program. In this research,

two different cases of finite difference calculations were applied to a series of experiments in order to characterize the test box: 1) A F.D. model of the box alone (i.e., the window was covered over with insulation. This case included one with existing ambient conditions and one with a periodic forced heat input.) 2) A case which includes an unshaded window on a clear day.

4.4.1 Application of a Finite Difference Model for Thermal Analysis of the Experimental Box

Figure 4.30 shows a diagram of the experimental model box with the window glazing in the south wall. Solar radiation incident on the window glazing is transmitted, absorbed, or reflected. The solar radiation absorbed by the window glazing drives the convection heat transfer between the glazing and the room air. The transmitted solar radiation is absorbed by the inside surface of the blackened cavity. In this research, the roof, walls, and floor are considered to be exterior surfaces because the experimental box is supported by the metal grate platform which is raised about three feet above the roof of the Langford Architecture Center (Figure A.2 in Appendix A). To simplify the analysis, it was assumed that all the walls consist of equivalent

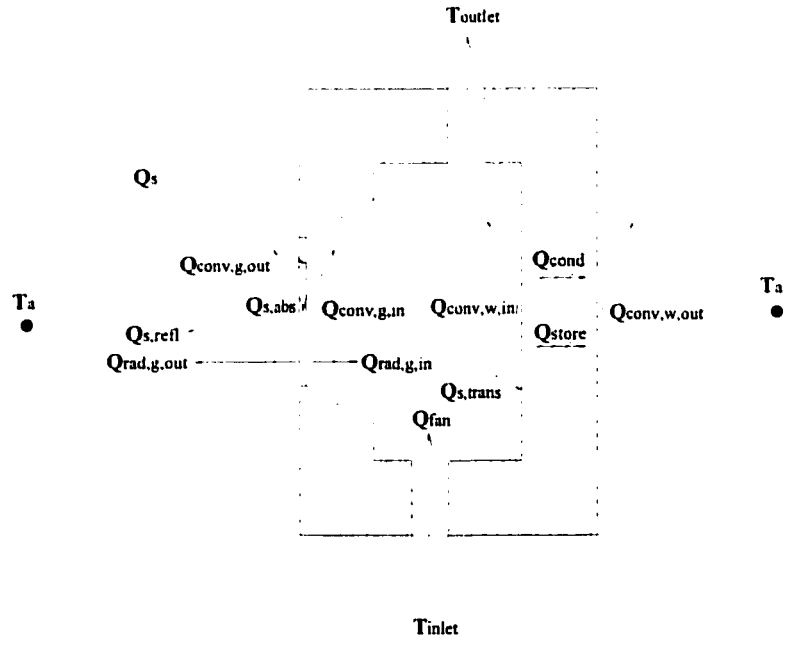

Figure 4.30 Diagram of the Experimental Box with Window Glazing in the South Wall.

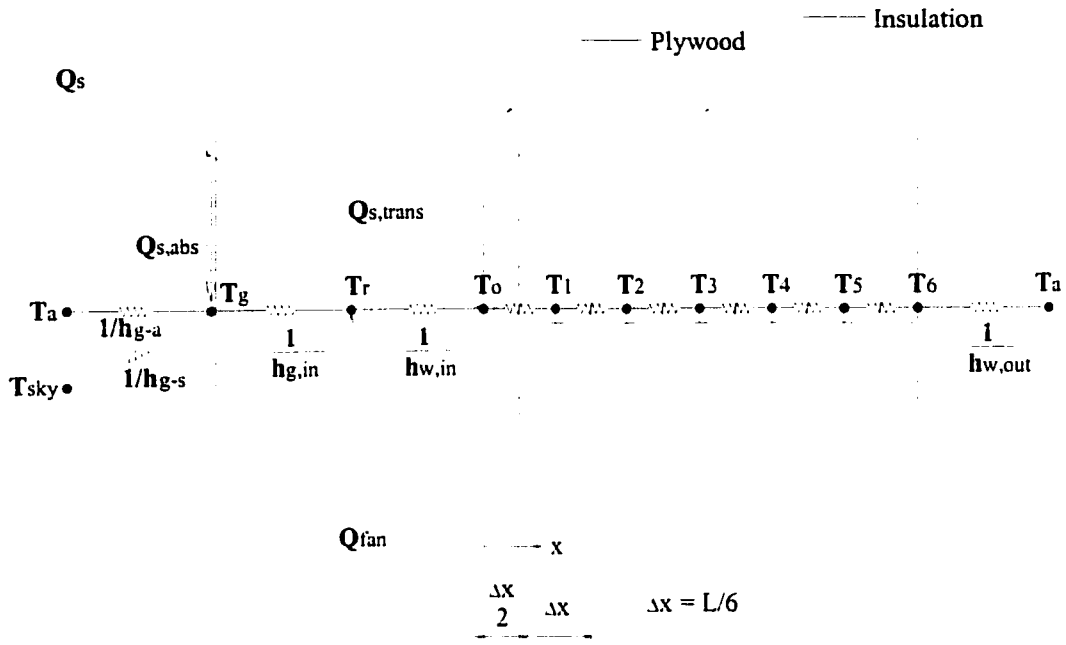

Figure 4.31 Equivalent Thermal Circuit for the Experimental Box with Window Glazing in the South Wall.

material. The room air was continuously circulated by a fan that was used to calculate the heat gain.

Figure 4.31 shows the F.D. equivalent thermal circuit for the experimental box with the window glazing. A one-dimensional thermal mass wall was used to simplify the analysis and regression was used to solve for the equivalent thermal parameters (i.e., $h_{g,in}$, $h_{w,in}$, and $h_{w,out}$). The total equivalent thickness of the test box wall is equally divided into six nodes. A nodal thickness, Δx of 1 inch was chosen and discrete nodal points labeled 0 to 6 from the inside wall surface toward the outside wall surface as indicated. The variable T_m stands for the temperature at a discrete nodal point m. Using energy balance equations, the temperature of each nodal point was calculated from the inside outward.

From the energy balance at the room air node, the total convection heat transfer between the room air and the glazing as well as the walls is equal to the amount of heat removed by the circulation fan. Thus, the equation for the energy balance at the room air node can be given by

$$Q^p_{fan} = Q^p_{conv,g,in} + Q^p_{conv,w,in} \cdot \qquad (4.34)$$

In the finite difference method of dynamic heat transfer calculation time t (hr) is given by

$$t = p\Delta t \tag{4.35}$$

where t is the hourly interval time for the heat conduction, p is an integer introduced to discretize or approximate the hourly time t into Δt time steps for the finite difference approximations of the dynamic heat transfer equation.

The amount of heat removed by the circulation fan can be calculated from the outlet-inlet temperature difference ($T_{outlet} - T_{inlet}$), the mass airflow rate ($\dot{m}_{fan}$), and the specific heat of air ($c_{p,air}$). Thus, the explicit finite difference expression for this heat transfer is

$$\dot{m}_{fan}^{p} \cdot c_{p,air} \cdot \left(T_{outlet}^{p} - T_{inlet}^{p}\right) = h_{g,in} A_g \left(T_g^p - T_r^p\right) + h_{w,in} A_w \left(T_o^p - T_r^p\right) \tag{4.36}$$

where T_r^p is the air temperature in the experiment chamber at time p, T_g^p is the surface temperature of the window glazing, and T_o^p is the averaged interior surface temperature of the surrounding walls including the roof and floor areas. The value of $h_{w,in}$ is the constant convection coefficient between the room and the interior wall, and $h_{g,in}$ is the constant convection coefficient between the window glazing and the room air node.

Solving this expression for the room temperature T_r^p yields

$$\begin{aligned} T_r^p = & \frac{h_{g,in} A_g}{h_{w,in} A_w + h_{g,in} A_g} \cdot T_g^p + \frac{h_{w,in} A_w}{h_{w,in} A_w + h_{g,in} A_g} \cdot T_o^p \\ & - \frac{\dot{m}_{fan}^{p} \cdot c_{p,air}}{h_{w,in} A_w + h_{in,g} A_g} \cdot \left(T_{outlet}^{p} - T_{inlet}^{p}\right). \end{aligned} \tag{4.37}$$

Finally, substituting $60 \dot{V}_{fan}^{p} \cdot \rho_{air}$ for $\dot{m}_{fan}^{p}$ yields

$$\begin{aligned} T_r^p = & \frac{h_{g,in} A_g}{h_{w,in} A_w + h_{g,in} A_g} \cdot T_g^p + \frac{h_{w,in} A_w}{h_{w,in} A_w + h_{g,in} A_g} \cdot T_o^p \\ & - \frac{60 \dot{V}_{fan}^{p} \cdot \rho_{air} \cdot c_{p,air}}{h_{w,in} A_w + h_{g,in} A_g} \cdot \left(T_{outlet}^{p} - T_{inlet}^{p}\right) \end{aligned} \tag{4.38}$$

where $\dot{m}^{p}_{fan}$ and $\dot{V}^{p}_{fan}$ are the mass flow rate (lb/hr) and volume flow rate (cfm) of the circulated air respectively. The variables ρ_{air} and $c_{p,air}$ are the density (lb/ft^3) and specific heat (Btu/lb-°F) of the air respectively.

Next, the temperature at the inside wall surface node, T_o can be calculated. As the solar radiation transmitted through the window glazing heats up the inside surface of the experimental model box, the effects of the transmitted solar radiation ($Q_{s,trans}$) should be considered for the energy balance calculation at the inside wall surface node T_o. The equation of the energy balance at this node is given by

$$Q^{p}_{conv,w,in} + Q^{p}_{cond} + Q^{p}_{s,trans} = Q^{p}_{store}. \tag{4.39}$$

The explicit finite difference expression for this heat transfer is

$$\begin{aligned} &h_{w,in} A_w \left(T_r^p - T_o^p\right) + \frac{k_{avg} A_w}{\Delta x}\left(T_1^p - T_o^p\right) + Q^p_{s,trans} \\ &\quad = \rho_{ply} c_{p,ply} A_w \frac{\Delta x}{2} \frac{\left(T_o^{p+1} - T_o^p\right)}{\Delta t} \end{aligned} \tag{4.40}$$

where k_{avg} is the weighted average value of the thermal conductivity of the plywood and the insulation. In other words, $k_{avg} = \dfrac{1}{\dfrac{1}{k_{ply}} + \dfrac{1}{k_{ins}}} = \dfrac{1}{\dfrac{k_{ply} + k_{ins}}{k_{ply} \cdot k_{ins}}} = \dfrac{k_{ply} \cdot k_{ins}}{k_{ply} + k_{ins}}$. The variables ρ_{ply} and $c_{p,ply}$ are the density (lb/ft^3) and specific heat (Btu/lb-°F) of the inside plywood respectively.

Using the explicit method this is solved for T_o^{p+1}, which is the future temperature of the inside wall surface at the *new* time step (p+1)

$$\begin{aligned} T_o^{p+1} = T_o^p &+ \frac{2h_{w,in}\Delta t}{\rho_{ply} c_{p,ply} \Delta x}\left(T_r^p - T_o^p\right) + \frac{2k_{avg}\Delta t}{\rho_{ply} c_{p,pky} \Delta x^2}\left(T_1^p - T_o^p\right) \\ &+ \frac{2\Delta t}{\rho_{ply} c_{p,ply} A_w \Delta x} Q^p_{s,trans} \end{aligned} \tag{4.41}$$

By using the Biot number $Bi_{in} = \frac{h_{w,in}\Delta x}{k_{avg}}$, and the Fourier number $Fo_o = \frac{k_{avg}\Delta t}{\rho_{ply} c_{p,ply} \Delta x^2}$ to simplify the expression, we get

$$T_o^{p+1} = T_o^p + 2Bi_{in}Fo_o\left(T_r^p - T_o^p\right) + 2Fo_o\left(T_1^p - T_o^p\right) + \frac{2\Delta t}{\rho_{ply} c_{p,ply} A_w \Delta x} Q_{s,trans}^p \quad (4.42)$$

The Biot Number (Bi) is a dimensionless measurement of the temperature change in the solid relative to the temperature difference between the surface and fluid. The definition of the Bi is given by

$$Bi = \frac{T_{s,1}{}^p - T_{s,2}{}^p}{T_{s,2}{}^p - T_\infty{}^p} = \frac{R_{cond}}{R_{conv}} = \frac{(L/kA)}{(1/hA)} = \frac{hL}{k} \quad (4.43)$$

where $T_{s,1}$ and $T_{s,2}$ are the temperatures of two surfaces of the solid where the conductive heat transfer occurs, T_∞ is the temperature of the fluid that invokes the convective heat transfer at the solid-liquid interface, and L is the length of the surface in the direction of the fluid flow. The Biot number in a finite-difference form of the heat equation is calculated from

$$Bi = \frac{h\Delta x}{k} \quad (4.44)$$

where Δx is a space increment, in the direction of conduction, that is used to discretize the location of the solid.

The Fourier number (Fo) is a dimensionless time parameter that characterizes transient conduction heat transfer and is defined as

$$Fo = \frac{\alpha \cdot t}{L_c{}^2} \quad (4.45)$$

where, $\alpha = k/\rho c$ and the characteristic length (L_c) is the ratio of the solid's volume to surface area, $L_c \equiv V/A$. The Fourier number (Fo) in a finite difference heat equation is calculated from

$$Fo = \frac{\alpha \Delta t}{(\Delta x)^2} = \frac{k \Delta t}{\Delta x^2 \rho c}. \tag{4.46}$$

To prevent unstable results, Δt must remain within the stability limit. To satisfy the stability criterion in a case of one-dimensional transient conduction, the value of Δt should be determined as the minimum number that satisfies the following two conditions;

$$Fo \le \frac{1}{2}, \tag{4.47a}$$

and for conduction and convection

$$Fo(1 + Bi) \le \frac{1}{2}. \tag{4.47b}$$

Arranging by temperature yields

$$T_o^{p+1} = 2Fo_o T_1^p + 2Bi_{in} Fo_o T_r^p + \frac{2\Delta t}{\rho_{ply} c_{p,ply} A_w \Delta x} Q_{s,trans}^p + [1 - 2Bi_{in} Fo_o - 2Fo_o] T_o^p. \tag{4.48}$$

Thus,

$$T_o^{p+1} = 2Fo_o T_1^p + 2Bi_{in} Fo_o T_r^p + 2Fo_o \frac{\Delta x}{k_{avg} A_w} Q_{s,trans}^p + [1 - 2Bi_{in} Fo_o - 2Fo_o] T_o^p \tag{4.49}$$

where $Q_{s,trans}^p$ is the solar radiation transmitted through window glazing during the previous time step. The values of T_o^{p+1} and T_o^p are the future and the previous temperatures of the inside wall surface respectively, and T_1^p is the previous temperature at the first node among the interior wall nodes, which are numbered from the inside to the outside. The value of Bi_{in} is the Biot number for the heat transfer between the room air T_r and the inside wall surface T_o. The value of Fo_o is the Fourier number used at the inside wall surface node T_o.

The stability criterion is determined by requiring that the coefficients are greater than or equal to zero. Thus, in this case, the value of Δt needs to be determined as the minimum number that satisfies the following two conditions

$$\left[1 - 2Bi_{in}Fo_o - 2Fo_o\right] \geq 0\,, \tag{4.50a}$$

and

$$Fo_o\left[Bi_{in} + 1\right] \leq \frac{1}{2}. \tag{4.50b}$$

Next, let's consider the energy balance at the interior wall node m. Because of the thick insulation installed in the envelope of the experimental box, a significant time lag exists in the heat transfer from a surface to the opposite surface of the wall. The heat temporarily stored inside the wall interior node m can be calculated from the energy difference between the heat transfer toward the left hand side (i.e., the inside) and that toward the right hand side (i.e., the outside). Thus, the heat balance at the wall interior node m is

$$Q^p_{cond,left} + Q^p_{cond,right} = Q^p_{store}\,. \tag{4.51}$$

The explicit finite difference expression for this heat transfer is

$$\frac{k_{ins}A_w}{\Delta x}\left(T^p_{m-1} - T^p_m\right) + \frac{k_{ins}A_w}{\Delta x}\left(T^p_{m+1} - T^p_m\right) = \rho_{ins}c_{p,ins}A_w\Delta x\frac{\left(T^{p+1}_m - T^p_m\right)}{\Delta t}. \tag{4.52}$$

Solving for $T_m{}^{p+1}$, the future temperature of the interior wall node m yields

$$T^{p+1}_m = T^p_m + \frac{k_{ins}\Delta t}{\rho_{ins}c_{p,ins}\Delta x^2}\left(T^p_{m-1} - T^p_m\right) + \frac{k_{ins}\Delta t}{\rho_{ins}c_{p,ins}\Delta x^2}\left(T^p_{m+1} - T^p_m\right). \tag{4.53}$$

Using the Fourier substitution $Fo_m = \frac{\alpha_{ins}\Delta t}{\Delta x^2} = \frac{k_{ins}\Delta t}{\rho_{ins}c_{p,ins}\Delta x^2}$, yields

$$T^{p+1}_m = T^p_m + Fo_m\left(T^p_{m-1} - T^p_m\right) + Fo_m\left(T^p_{m+1} - T^p_m\right). \tag{4.54}$$

Arranging the equation by temperature, $T_m{}^{p+1}$ results in

$$T_m^{p+1} = Fo_m T_{m-1}^p + Fo_m T_{m+1}^p + [1 - 2Fo_m] T_m^p \tag{4.55}$$

where T_m^{p+1} and T_m^p are the future and the previous temperatures respectively of the given interior wall node T_m. The values of T_{m-1}^p and T_{m+1}^p are the previous temperatures measured at the next interior wall nodes on both side of the current node. The Fourier number Fo_m is the Fourier number at the given interior wall node m. The stability criterion is determined by requiring that the coefficients are greater than or equal to zero. Thus, the two stability conditions to determine the discrete time Δt are

$$[1 - 2Fo_m] \geq 0 \tag{4.56a}$$

and

$$Fo_m \leq \frac{1}{2}. \tag{4.56b}$$

Finally, the outside surface wall node, T_6. The energy balance at the outside wall surface node is

$$Q_{conv,w,out}^p + Q_{cond}^p = Q_{store}^p. \tag{4.57}$$

The explicit finite difference expression is

$$h_{w,out} A_T \left(T_a^p - T_6^p\right) + \frac{k_{avg} A_T}{\Delta x}\left(T_5^p - T_6^p\right) = \rho_{plyg} c_{p,ply} A_T \frac{\Delta x}{2} \frac{\left(T_6^{p+1} - T_6^p\right)}{\Delta t}. \tag{4.58}$$

where $k_{avg} = \frac{k_{ply} \cdot k_{ins}}{k_{ply} + k_{ins}}$. The variables ρ_{ply} and $c_{p,ply}$ are the density (lb/ft^3) and specific heat (Btu/lb-°F) of the outside plywood respectively. Solving for the future temperature T_6^{p+1}, yields

$$T_6^{p+1} = T_6^p + \frac{2h_{w,out}\Delta t}{\rho_{ply} c_{p,ply} \Delta x}\left(T_a^p - T_6^p\right) + \frac{2k_{avg}\Delta t}{\rho_{ply} c_{p,ply} \Delta x^2}\left(T_5^p - T_6^p\right). \tag{4.59}$$

Using $Bi_{out} = \frac{h_{w,out}\Delta x}{k_{avg}}$, and $Fo_6 = \frac{\alpha_{avg}\Delta t}{\Delta x^2} = \frac{k_{avg}\Delta t}{\rho_{ply} c_{p,ply} \Delta x^2}$, we can further simplify it as follows

$$T_6^{p+1} = T_6^p + 2Bi_{out}Fo_6\left(T_a^p - T_6^p\right) + 2Fo_6\left(T_5^p - T_6^p\right). \tag{4.60}$$

Arranging by temperature yields

$$T_6^{p+1} = 2Fo_6T_5^p + 2Bi_{out}Fo_6T_a^p + \left[1 - 2Bi_{out}Fo_6 - 2Fo_6\right]T_6^p \tag{4.61}$$

where T_6^{p+1} and T_6^p are the new and the previous temperatures of the outside wall surface, and T_a^p is the previous ambient temperature. The value of T_5^p is the previous temperature at the last interior wall node. The value of Bi_{out} is the Biot number considering the heat transfer between the outside wall surface temperature T_6 and the ambient air temperature T_a where convection is assumed to be the dominant heat transfer mechanism. The value of the Fo_6 is for the Fourier number at the outside wall surface node T_6. The equations for the stability criterion are given by

$$\left[1 - 2Bi_{out}Fo_6 - 2Fo_6\right] \geq 0 \tag{4.62a}$$

and

$$Fo_6\left[Bi_{out} + 1\right] \leq \frac{1}{2}. \tag{4.62b}$$

So far, we calculated the temperatures at the discrete wall interior nodes as well as at the room node and inside and outside surface nodes. The new discrete temperature of any node point can be calculated from the temperatures of the same node and neighboring nodes at previous discrete time using the Equations 4.38, 4.49, 4.55, or 4.61. The discrete time Δt can be set with a value that satisfies the conditions for the stability criterion. The amount of the transmitted solar energy ($Q_{s,tans}$) can be estimated from the measured solar radiation on the vertical surface. However, we still need to know the convection coefficients of the glazing and of the inside and outside wall surfaces, and the effective thermal conductivity of plywood and insulation. The Fourier number and Biot number are derived from these values. The next experiment was conducted to reduce the number of unknown values by removing the effects of the convection coefficient of the glazing.

4.4.2 Application of Finite Difference Model for Thermal Analysis of Walls Only

To estimate the heat transfer only through the walls of the experimental model box, the south window was blocked with the same thickness of wall insulation material (i.e., 6 in. layers of Styrofoam insulation). Figure 4.32 shows the diagram of the experiment model box with an insulation block in the window aperture. As shown in Figure 4.33, the walls, roof, and floor of the box are represented with one-dimensional equivalent thermal properties. Hence, there is no heat gain through the window glazing. Therefore, the amount of convection heat transfer between the room air and the inside wall surface is the same as the amount of sensible heat transfer removed by the circulation fan. Thus, the equation for the energy balance at the room air node is given by

$$Q^{p}_{fan} = Q^{p}_{conv,in} \cdot \tag{4.63}$$

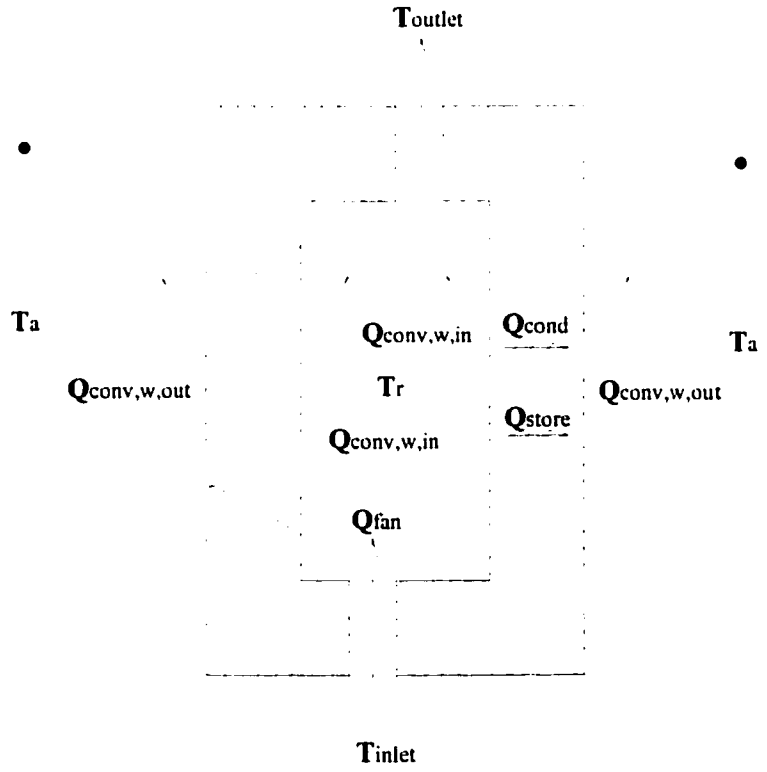

Figure 4.32 Diagram of the Experimental Test Box with an Insulation Block in the Window Aperture.

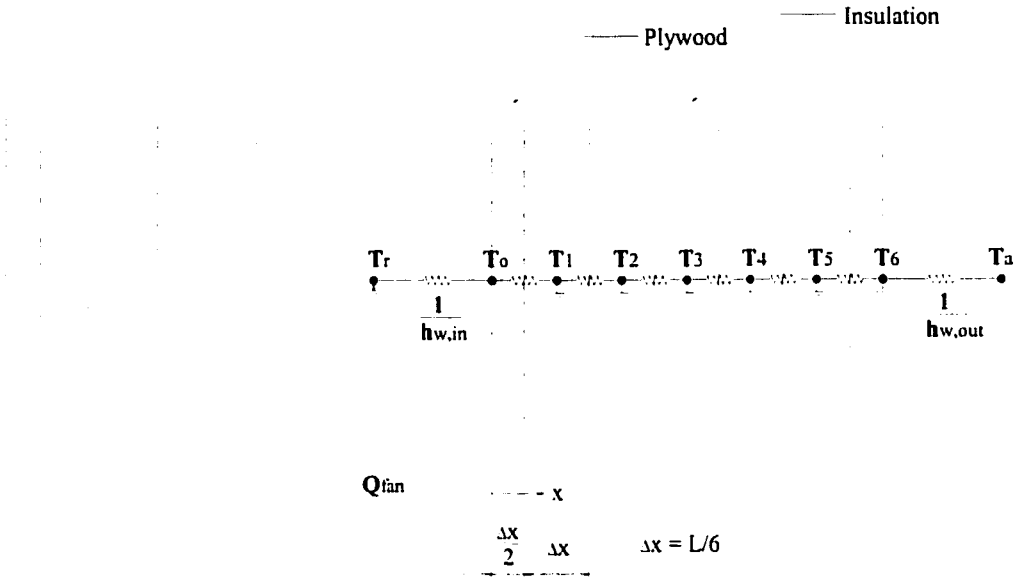

Figure 4.33 Equivalent Thermal Circuit for the Experimental Test Box with an Insulation Block in the Window Aperture

The explicit finite difference expression for this heat transfer is

$$\dot{m}^{p}_{fan} \cdot c_{p,air} \cdot \left(T^{p}_{outlet} - T^{p}_{inlet}\right) = h_{w,in} A_T \left(T^{p}_{o} - T^{p}_{r}\right). \tag{4.64}$$

Solving for the room temperature T_r^p, yields

$$T^{p}_{r} = T^{p}_{o} - \frac{\dot{m}^{p}_{fan} \cdot c_{p,air}}{h_{w,in} A_T} \times \left(T^{p}_{outlet} - T^{p}_{inlet}\right). \tag{4.65}$$

Substituting $60\dot{V}^{p}_{fan} \cdot \rho_{air}$ for $\dot{m}^{p}_{fan}$ yields

$$T^{p}_{r} = T^{p}_{o} - \frac{60\dot{V}^{p}_{fan} \cdot \rho_{air} \cdot c_{p,air}}{h_{w,in} A_T} \times \left(T^{p}_{outlet} - T^{p}_{inlet}\right) \tag{4.66}$$

where T_r^p is the room air temperature, and T_o^p represents the averaged interior surface temperature of all the surrounding walls including the roof and floors. The value of $h_{w,in}$ is the effective convection coefficient between the room air and the inside wall surface of the box.

Next, from the energy balance at the inside wall surface node using the equation of energy balance given by

$$Q^{p}_{conv,in} + Q^{p}_{cond} = Q^{p}_{store}. \tag{4.67}$$

The explicit finite difference expression for this is

$$h_{w,in} A_T \left(T_r^p - T_o^p\right) + \frac{k_{avg} A_T}{\Delta x}\left(T_1^p - T_o^p\right) = \rho_{ply} c_{p,ply} A_T \frac{\Delta x}{2} \frac{\left(T_o^{p+1} - T_o^p\right)}{\Delta t}. \tag{4.68}$$

We solve this for the T_o^{p+1}, which is the future temperature of the inside wall surface at the *new* time step $(p+1)$:

$$T_o^{p+1} = T_o^p + \frac{2h_{w,in}\Delta t}{\rho_{ply} c_{p,ply} \Delta x}\left(T_r^p - T_o^p\right) + \frac{2k_{avg}\Delta t}{\rho_{ply} c_{p,ply} \Delta x^2}\left(T_1^p - T_o^p\right). \tag{4.69}$$

By using the Biot number $Bi_{in} = \frac{h_{w,in}\Delta x}{k_{avg}}$, and the Fourier number $Fo_o = \frac{k_{avg}\Delta t}{\rho_{ply} c_{p,ply} \Delta x^2}$ to simplify the expression, we get

$$T_o^{p+1} = T_o^p + 2Bi_{in} Fo_o \left(T_r^p - T_o^p\right) + 2Fo_o \left(T_1^p - T_o^p\right). \tag{4.70}$$

Arranging by temperature yields

$$T_o^{p+1} = 2Fo_o T_1^p + 2Bi_{in} Fo_o T_r^p + \left[1 - 2Bi_{in} Fo_o - 2Fo_o\right] T_o^p \tag{4.71}$$

where T_o^{p+1} and T_o^p are the future and the previous temperatures of the inside wall surfaces respectively, and T_1^p is the previous temperature of the first node among the interior wall nodes. The value of Bi_{in} is the Biot number considering the heat transfer between the room air T_r and the inside wall surface T_o. The value of the Fo_o is the Fourier number at the inside wall surface node. The conditions for stability criterion are

$$\left[1 - 2Bi_{in} Fo_o - 2Fo_o\right] \geq 0, \tag{4.72a}$$

and

$$Fo_o[Bi_{in}+1] \le \frac{1}{2}. \qquad (4.72b)$$

The temperature calculations at the remaining interior wall nodes and at the outside wall surface node are exactly same as the other experimental cases described in previous section. Thus, the new temperature of any interior node, T_m^{p+1} is calculated by the Equation 4.55, and the new outside wall surface temperature, T_6^{p+1} is calculated by the Equation 4.61.

In this experimental case, we still need to know the convection coefficient of the inside and outside wall surfaces, and the thermal conductivity of the plywood and insulation. After determining these values, the convection coefficient of the glazing can be calculated. These unknown values were determined using a sensitivity analysis when the test box had the insulated block in the window aperture.

4.4.3 Calculation of Finite Difference Model Using a Spreadsheet

The calculation of the finite difference model was conducted with the following procedure using a computer spreadsheet program.

First, the data need to be converted to have less than the required time interval. In this research, the original 15-minute data were linearly interpolated into one-minute data using the 'Weather Data Converter' program.

In the spreadsheet, a set of reasonable values for the inside and outside convection coefficients and thermal conductance of the wall materials were input. The final values for these variables were calculated by performing a sensitivity analysis on each parameter. From these numbers, the Biot numbers and Fourier numbers were then calculated.

Next, we need to estimate the initial temperature of each node in the first row of the spreadsheet to begin the first calculation. As we don't know the initial temperatures yet, it can be assumed that the initial condition is the steady-state condition. Thus, linearly interpolated temperatures are given between the room temperature and the ambient temperature. Later, the acceptable initial temperatures will be determined from previously run regression results calculated.

Then, the finite difference equations need to be typed in the next row of spreadsheet to calculate the node temperatures at the first new time. These equations in this row are then copied through the whole simulation period.

However, we don't know the inside and outside convection coefficients and thermal conductance of the wall materials. These values were estimated by selecting the numbers that provide the maximum R-square value after the linear regression analysis between the measured room temperature and the simulated temperature. From these results, the transient heat transfer through walls was then solved.

4.5 Comparative Validation Using the DOE-2 Program

4.5.1 DOE-2 Analysis of Solar Heat Gain through Window Glazing

In the DOE-2 program, the heating and cooling loads are calculated based on the ASHRAE algorithms (ASHRAE 1997). In each space that is conditioned the room air remains at pre-determined constant temperature (LBL 1982b). Therefore, the hourly load is calculated without considering the effects of ventilation air. In the cooling and heating load calculations, the DOE-2 program permits the user to use either the weather file or 'DESIGN-DAY' instructions for the outside weather condition input. The DESIGN-DAY instruction is used when either the data in the weather file is not typical or the user wants to design the building under the special weather conditions at its location. When the DESIGN-DAY instructions are given, these instructions override the weather file. In this research, both methods were used to validate the accuracy of the SFD program.

When the user wants to use a specific weather file for the LOADS calculation, a weather file for the given site should be packed into a binary format from one of the weather files stored in an acceptable format. The weather file format to be used with the DOE-2 weather input file should be either in the Test Reference Year (TRY), the Typical Meteorological Year (TMY), National Climate Center (TD1440, or CD144), the California Typical Climate Zone (CTZ), or the Weather Year for Energy Computation (WYEC) format. The TRY and TMY weather files are the most widely used among these weather files. The method to pack a weather file from a TRY weather file is well documented in the report by Bronson (1992). The process to pack the DOE-2 weather input file from a TMY weather file will be described in detail in the

Section 4.5.3. In this research, the weather file was packed from a TMY weather file that was created by overwriting the measured data onto an original TMY file.

When the DESIGN-DAY instruction is used, the building's external loads are calculated by the given DESIGN-DAY data plus solar data calculated by the program itself. The building internal loads are determined by the schedules in the SPACE-CONDITION instruction. The calculations of solar radiation in the DOE-2 program follow the ASHRAE algorithms (ASHRAE 1997). The methods to calculate the solar radiation and methods to analyze the shading are described in detail in Chapter II.

4.5.2 Creating a DOE-2 Input File to Simulate the Experimental Box

To create a DOE-2 input file for the simulation of the experimental model box, the shape of the model box was geometrically simplified. Two categories of input files were created: files using design-day instructions and files using the packed weather data. The design-day instruction for the outside weather condition was derived from the measured data on the simulated day such as the minimum and maximum ambient dry-bulb temperatures and dew point temperatures, average wind speed, etc. The weather file was created by the methods described in the following section using the DOE-2 weather processor developed by LBL (1981). An example of the DOE-2 input file is included in Appendix C.1.

The main box was assumed to be a rectangular space surrounded by walls and a roof having equivalent average thermal properties. Thus, the average thermal properties of walls and roof were given in the material and layer instructions instead of a list of the real materials. The inside-film resistance specifies the combined convective and radiative air film resistance for the inside surface of an exterior wall. This value was given from the result of the finite difference model for the experimental model box. Uncoated single pane glazing, which has 79 percent transmittance, 7 percent reflectance 1.47 (Btu/hr-ft^2-^{o}F) default conductance, was chosen from the table of the glass type code in the DOE-2 Reference Manual (i.e., CLASS-TYPE = 3).

As we see from the southeast view in Figure A.3 in Appendix A, the experimental box is blocked from receiving direct solar radiation in the early morning by the penthouse of the Langford Architecture Center and a neighboring high rise building (O&M building). The building shade instructions were used to specify the external surfaces that shade the

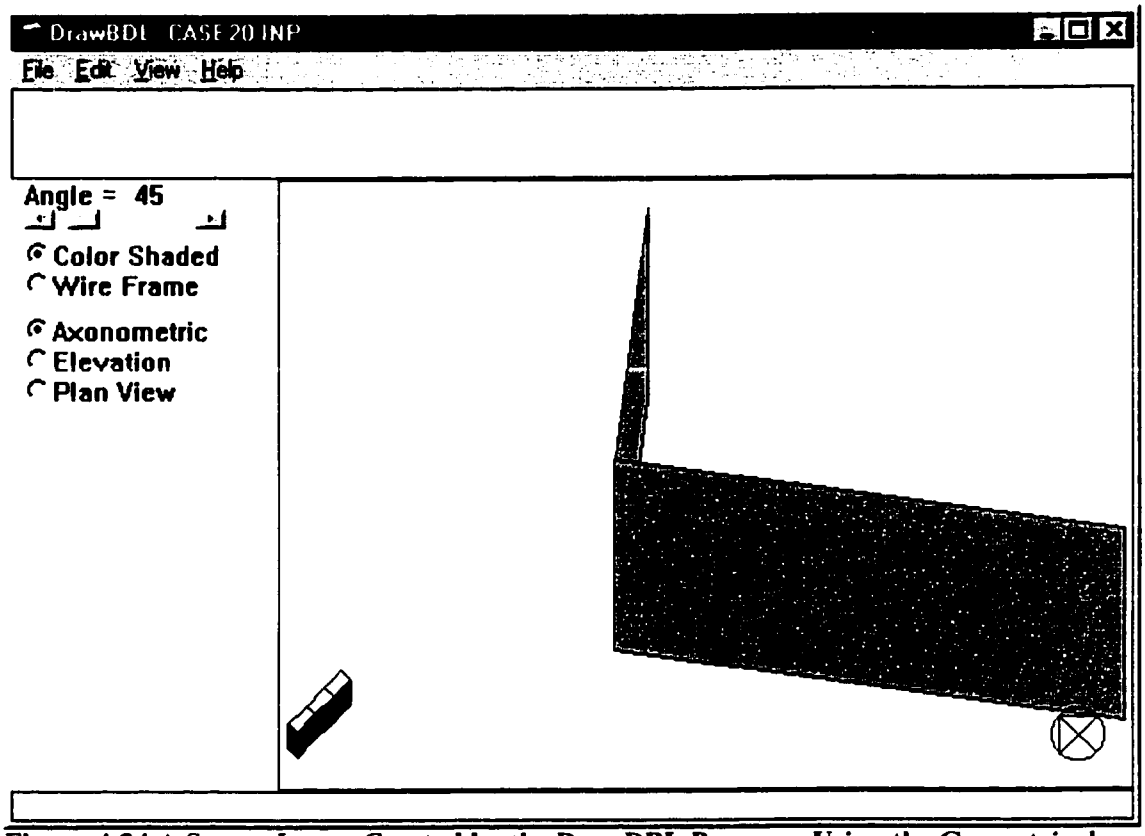

Figure 4.34 A Screen Image Created by the DrawDBL Program Using the Geometrical Information on a DOE-2 Input File.

experimental box. Figure 4.34 shows the experimental box and the external surfaces created by the 'DrawDBL' program, version 2.02 (Huang 1994) using the geometrical instructions in the input file.

Two different day schedule instructions (i.e., one with the schedule ON and one with schedule OFF) were used to set the 100 percent on or off for 24 hours. These schedule instructions were used to define the people, lighting and equipment schedules in the space condition instruction. As the zone type was set to unconditioned zone, an average temperature of the inside room air was given. To estimate the effect of the circulation fan, the average value of the infiltration rate was given, and the air change method was chosen as the infiltration method.

When the simulation process is completed, the DOE-2 program creates not only the loads-report for the space and building monthly and peak loads calculations but also the hourly-report that contains the hourly values of the specified variables. In this research, four different levels of hourly-report instructions were used in the input file. The first hourly-report instruction

is for global variables including diffuse horizontal radiation, direct normal solar radiation, total horizontal solar radiation, sunrise hour angle, current hour angle, tangent of declination, and cosine of zenith angle. The next level is for the variables of the space including window conduction load, delayed wall and roof loads, interior wall load, and sensible and latent infiltration loads. The third level of hourly-report instruction is for the variables relating to the exterior wall. This hourly-report contains the hourly calculation of solar radiation on the wall after shading, shaded fraction of the wall, total heat transfer from wall to the zone, cosine angle between the direction of the sun and the surface outward normal, solar radiation on the wall reflected from the ground, diffuse and direct solar radiation on the surface, and total solar radiation on the wall with neglect of shading. The final level of hourly report is for the window including shaded fraction of window area, direct solar radiation on unshaded part of window divided by total window area, diffuse solar radiation incident on window, transmitted and absorbed solar energy, shading coefficient, and conductive heat transfer through window. An example of DOE-2 hourly report is included in the Appendix C.2. The result and its analysis of the DOE-2 simulation will be described in the Chapter VI.

4.5.3 Packing a DOE-2 Weather Input File

To create the weather file that can be used by the DOE-2 program, it must be in a specific binary file format that the program can read. LBL developed a computer program to accomplish this called the 'DOE-2 weather processor' that converts an ASCII format weather file into a DOE-2 readable binary weather file (LBL 1982a). The processor consists of a batch file managing the weather packing program 'WTHPACK.BAT', a MS-DOS based weather packing program 'DOEWTH.EXE', and a file that contains an error checking subroutine 'F33L3.ERR'. For the actual weather packing, two more files are needed: the weather file to be converted and an instruction file. Table 4.4 shows the list of files needed to pack the weather file for the DOE-2 program.

The file types that the DOE-2 weather processor can pack are the Test Reference Year (TRY), Typical Meteorological Year (TMY), California Climate Zone (CTZ), CD1440, TD1440, and Weather Year for Energy Consumption (WYEC) files. The TRY file is stored in standard time. However, it contains only global horizontal solar radiation for solar radiation data. Though a TRY file also contains weather items such as the amount and type of cloud layers, these values are useless to the DOE-2 program when the measured solar radiation is

Table 4.4 Files Needed to Pack a DOE-2 Weather Input File.

File Name	Description
WTHPACK.BAT	Batch file activating the weather packing program DOEWTH.EXE
DOEWTH.EXE	Weather packing program running in the MS-DOS operating system.
F33L3.ERR	Subordinate file checking errors while a weather file is being packed.
Weather File	The ASCII format weather file that needs to be converted that contains weather data for the simulated city in the format of either the Test Reference Year (TRY), the Typical Meteorological Year (TMY), National Climate Center (TD1440, or CD144), the California Typical Climate Zone (CTZ), or the Weather Year for Energy Computation (WYEC).
Filename.INS	Instruction file that contains the weather packing instructions such as the type of weather data, the location of the city, time zone, soil diffusivity, monthly clearness numbers, etc.

available (Bronson 1992). The CTZ weather file contains no measured solar radiation data, therefore the DOE-2 program uses a cloud cover modifier to estimate solar radiation from cloud cover data.

The TMY file contains various solar radiation data, including extraterrestrial, direct normal, diffuse, net, tilt, (observed, engineering corrected), and standard year corrected radiation (NREL 1995). Though a TMY file is stored in solar time, it also contains local standard time corresponding to the given solar time. When a TMY file is packed, the DOE-2 weather processor converts the data from solar time to standard time and linearly interpolates between solar time and standard time.

Whatever weather type file is used for packing a weather file, the weather data processing program cannot convert every type of solar information. The process can convert only extraterrestrial, direct normal and global horizontal solar radiation to create a packed binary DOE-2 weather file. The standard year corrected radiation in the TMY file is used as the global horizontal solar radiation in the DOE-2 program. Though the TMY file contains diffuse solar radiation data, the process can convert it. Thus, the DOE-2 program itself calculates the diffuse solar radiation when a weather file is used for the loads calculation. Table 4.5 shows the list of fields actually used by the DOE-2 weather processor (LBL 1981).

Though the TMY file has the inconvenience of a time conversion and a unit conversion, the TMY file was used as the base weather file in this research because the various measured solar data could be directly packed into a TMY weather file.

Table 4.5 Fields of a TMY Weather File Used by the DOE-2 Weather Processor.

Column	Contents
1-5	WBAN station number.
6-15	Solar time at the end of hourly solar observation (YYMMDDHH).
16-19	Local standard time in hours and minutes corresponding to the solar time given above.
20-24	Extraterrestrial radiation (kJ/m^2) based on solar constant = 1377 J/m^2s.
25-29	Direct normal radiation (kJ/m^2).
54-58	Standard year corrected radiation (kJ/m^2). This is used by DOE-2 as the total horizontal radiation. Column 54 is a model flag.
71-72	Time of surface observation in hour (00-23).
99-103	Station atmospheric pressure (tenths of millibars).
104-107	Dry-bulb temperature in tenths of ^0C (-700 - 600)
108-111	Dew point temperature in tenths of ^0C
112-114	Wind direction (degrees)
115-118	Wind speed in tenth of m/s (0000-1500)
119-120	Total sky cover (tenths) (00-10)
121-122	Total opaque sky cover (tenths)

As we can see in Figure 4.35, a TMY file has hourly data in a fixed column data format. When users want to create a weather file using their own measured data, the measured data can be overwritten onto an original TMY file using a text editor such as the MS Notepad.

The TMY file uses SI units, whereas a LoanSTAR data file is measured using mixed units such as W/m^2 for solar radiation, °F for temperature, and mph for wind speed. Thus, when

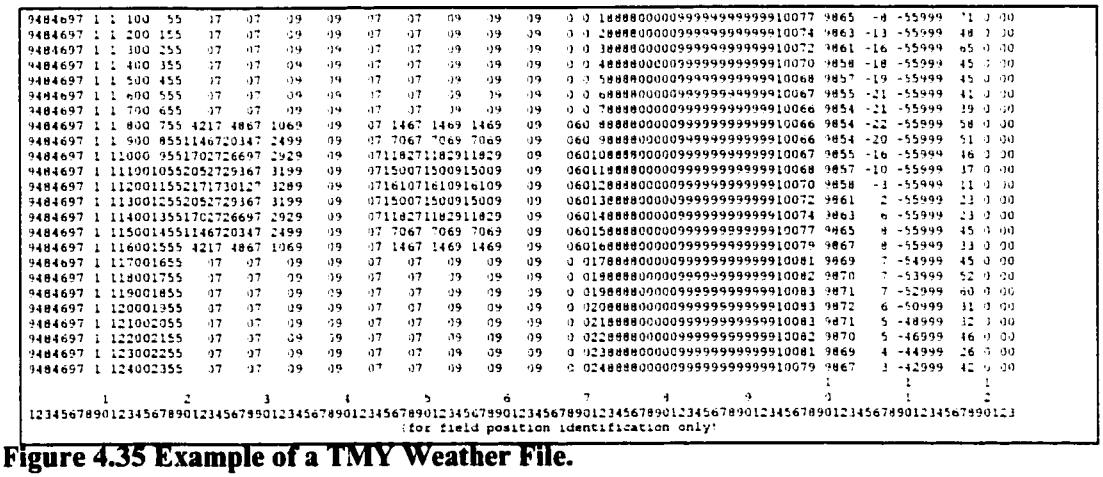

Figure 4.35 Example of a TMY Weather File.

users want to apply a weather data from an existing database such as LoanSTAR database, unit conversion is needed. The following table shows the units used in the LoanSTAR ASCII file and the TMY file as well as their conversion factors from ASCII units to TMY units.

Table 4.6 Units Used in ASCII Files and TMY Files and Conversion Factor from ASCII Units to TMY Units.

Items	ACS file Units	Conversion Factor	TMY Units
Solar Radiation	W/m^2	36	tenths of $kJ/hr\text{-}m^2$
Temperature	°F	(°F - 32) x 5/9 x 10	tenths of °C
Wind Speed	mph	3.048	tenths of m/s
Atmospheric pressure	"Hg	338.753	tenths of millibars

To pack a DOE-2 weather input file from a TMY file, the user needs to prepare two input files: a TMY weather file and an instruction file. TMY file contains one-year of weather data. The instruction file has to be made in the exact format that contains the weather packing instructions including: the type of weather data, the location of city, time zone, soil diffusivity, monthly clearness numbers, etc. The example of an instruction file and their description are given in Figures 4.36 and 4.37 respectively.

The DOE-2 weather processor consists of four functions including PACK, LIST, EDIT, and STAT. The command 'PACK' in the first line of a DOE-2 weather processor instruction file activates the function PACK to begin the weather packing. The station name is given in the second line. The first item in the third line is a code-word specifying the unpacked tape type. The station number, the number for missing data, the time zone, the latitude and the longitude of the station follow. The next item is for a code-word specifying the number of bits per word to be used in packing the output file. The options are 60-BIT (for CDC computers) or 30-BIT (for32 bit machines). The next item specifies the type of output file. The options are OLD, NORMAL, and SOLAR. The code-word OLD produces a DOE-1 compatible file. NORMAL

```
PACK
COLLEGE STATION, TX
TMY   94846 -999    6 30.6 96.40 30-BITSOLAR    4  20. 0.025
1.00  1.00  1.00  1.00  1.00  1.00  1.00  1.00  1.00  1.00  1.00  1.00
-999.
LIST
PACKED -999 -999    1   12
STAT
END
```

Figure 4.36 Example of a DOE-2 Weather Processor Instruction File.

```
STATION NAME        COLLEGE STATION, TX
TAPE TYPE           TMY
STATION NUMBER      94846
TIME ZONE           6
LATITUDE            30.600
LONGITUDE           96.400
WORD SIZE           30-BIT
FILE TYPE           SOLAR
INTERP INTERVAL     4
MAX TEMPCHANGE      20.000
SOIL DIFFUSIVITY    0.025
CLEARNESS NUMBER ( 1)  1.000
CLEARNESS NUMBER ( 2)  1.000
CLEARNESS NUMBER ( 3)  1.000
 ----------
CLEARNESS NUMBER (11)  1.000
CLEARNESS NUMBER (12)  1.000
```

Figure 4.37 Description of the DOE-2 Weather Processor Instruction File.

produces a normal DOE-2 file and SOLAR creates a file containing additional solar information. The interpolation interval, the maximum dry-bulb temperature change allowed in one hour need to be input.

The next line contains the 12 clearness numbers for 12 months. The next line is used for the 12 monthly-average ground temperatures. As we can see in Figure 4.36, the number –999 is used when the ground temperatures are not available. The command 'LIST' specifies the options used for the list of the output file. The first item in the next line is the input file type. Options are PACKED, OTHER, TRY, CTZ, WYEC, TMY, etc. The next tow items are the year of weather data and station number. When the input file is set to PACKED, these values should be –999. The next two values are the beginning and ending months of the listing.

The batch program running in the MS-DOS environment, 'WTHPACK.BAT' produces three output files as the results of the DOE-2 weather packing process as listed in Table 4.7. The 'WEATHR.TMP' file is the binary weather file which can be used for the DOE-2 weather input. The 'Filename.OUT' file is the log file that contains the information of the instruction file and hourly weather report in IP units. Figure 4.38 shows an example of an hourly weather report in the log file (*.out). For a more description of the DOE-2 weather file packing process, refer to Appendix VIII.C in the DOE-2 Reference Manual (LBL 1982a).

This chapter described the graphical methods and equations used for displaying shading and solar data, the methods to calculate solar heat gain through window glazing, experimental validation using a test box, development of finite difference models of the experimental box, and the method to create DOE-2 input files and to pack a weather file for DOE-2 simulations. In

the following chapter, a proposed computer model for shading and thermal analysis of fenestration systems will be discussed.

Table 4.7 Output File Created by the DOE-2 Weather Processor.

File Name	Description
WEATHR.TMP	The packed weather file for DOE-2 weather input file, with binary file format
Filename.OUT	The LOG file that shows the contents of the instruction file and hourly weather report with header on each day. This file is saved in ASCII test file format.
Filename.WTH	The weather file converted in a binary format, which is copy of the packed weather file 'WEATHR.TMP'.

-----MAR 22-----

HOUR	WBT	DBT	PRESS	CLOUDS	SNOW	RAIN	WNDDIR	HUMID	DENSITY	ENTH	THZSOL	DNMSOL	CTYPE	WSPEED
1	49.	50.	29.2	10.	0	0	0	0.0073	0.075	20.0	0.0	0.0	2	2.
2	45.	49.	29.2	10.	0	0	0	0.0055	0.076	18.0	0.0	0.0	2	1.
3	41.	49.	29.2	10.	0	0	0	0.0037	0.076	16.0	0.0	0.0	2	1.
4	40.	48.	29.2	10.	0	0	0	0.0037	0.076	15.5	0.0	0.0	2	2.
5	40.	47.	29.2	10.	0	0	0	0.0037	0.076	15.5	0.0	0.0	2	3.
6	39.	46.	29.2	10.	0	0	0	0.0037	0.076	15.0	0.0	0.0	2	3.
7	40.	47.	29.2	10.	0	0	0	0.0037	0.076	15.5	0.0	0.0	2	3.
8	42.	51.	29.2	10.	0	0	0	0.0037	0.075	16.0	3.0	16.0	2	3.
9	45.	56.	29.2	10.	0	0	0	0.0037	0.075	17.5	22.0	53.0	2	3.
10	47.	61.	29.2	10.	0	0	0	0.0037	0.074	18.5	46.0	79.0	2	4.
11	50.	67.	29.2	10.	0	0	0	0.0037	0.073	20.0	64.0	88.0	2	5.
12	51.	71.	29.2	10.	0	0	0	0.0037	0.073	21.0	77.0	93.0	2	6.
13	54.	72.	29.2	10.	0	0	0	0.0049	0.072	22.5	84.0	96.0	2	7.
14	59.	74.	29.2	10.	0	0	0	0.0074	0.072	26.0	85.0	97.0	2	8.
15	60.	75.	29.2	10.	0	0	0	0.0078	0.072	26.5	80.0	96.0	2	8.
16	61.	74.	29.2	10.	0	0	0	0.0087	0.072	27.5	69.0	93.0	2	8.
17	60.	74.	29.2	10.	0	0	0	0.0081	0.072	26.5	51.0	87.0	2	7.
18	60.	72.	29.2	10.	0	0	0	0.0085	0.072	26.5	26.0	74.0	2	5.
19	58.	69.	29.2	10.	0	0	0	0.0080	0.072	25.5	1.0	17.0	2	4.
20	58.	66.	29.2	10.	0	0	0	0.0087	0.073	25.5	0.0	0.0	2	5.
21	58.	64.	29.2	10.	0	0	0	0.0091	0.073	25.5	0.0	0.0	2	5.
22	59.	63.	29.2	10.	0	0	0	0.0100	0.073	26.0	0.0	0.0	2	4.
23	59.	62.	29.2	10.	0	0	0	0.0102	0.073	26.0	0.0	0.0	2	5.
24	59.	61.	29.2	10.	0	0	0	0.0104	0.073	26.0	0.0	0.0	2	5.

Figure 4.38 Example of Hourly Weather Report in the OUT Log File.

CHAPTER V

THE SHADED FENESTRATION DESIGN (SFD) MODEL

The 'Shaded Fenestration Design (SFD) Model' is a user-friendly computerized program for energy-efficient shaded fenestration system design. The SFD program has several functions including: 1) calculation of solar angles for the given solar or civil time, 2) calculation of direct, diffuse and reflected solar radiation on a clear day either on a horizontal surface or on a vertical surface, 3) window glazing and shading device design, 4) calculation of heat gains and losses through the window system, 5) management of weather data, and 6) graphical display of weather information.

The SFD program is a composite program having the structure of numerous subroutines in the main program and three add-in programs including the 'Solar Data Calculator', the 'Weather Data Converter', and the 'Weather Data Displayer'. The overall program was developed using the 'Microsoft Visual Basic 5.0' (Microsoft 1997) computer language and runs under Windows 3.1, 95, 98, or NT environment. Although the Visual Basic has limitations in memory handling and processing speed, the useful structure of an object-oriented modules for coding and a powerful graphical user interface make it a suitable program for a graphic-oriented self-instructional simulation program. Figure 5.1 shows the flowchart of the major functions in the SFD program and various sub-programs. This chapter describes the major functions of the main program and add-in programs. The Visual Basic source codes of selected subroutines are included in Appendix D.

5.1 The Main Program

The SFD program has several functions. The major functions of the program are the window and shading device design, thermal performance of an unshaded fenestration system, and graphical display of shading and solar radiation data. The functions of the program become more beneficial and diverse when the program is used along with the add-in programs.

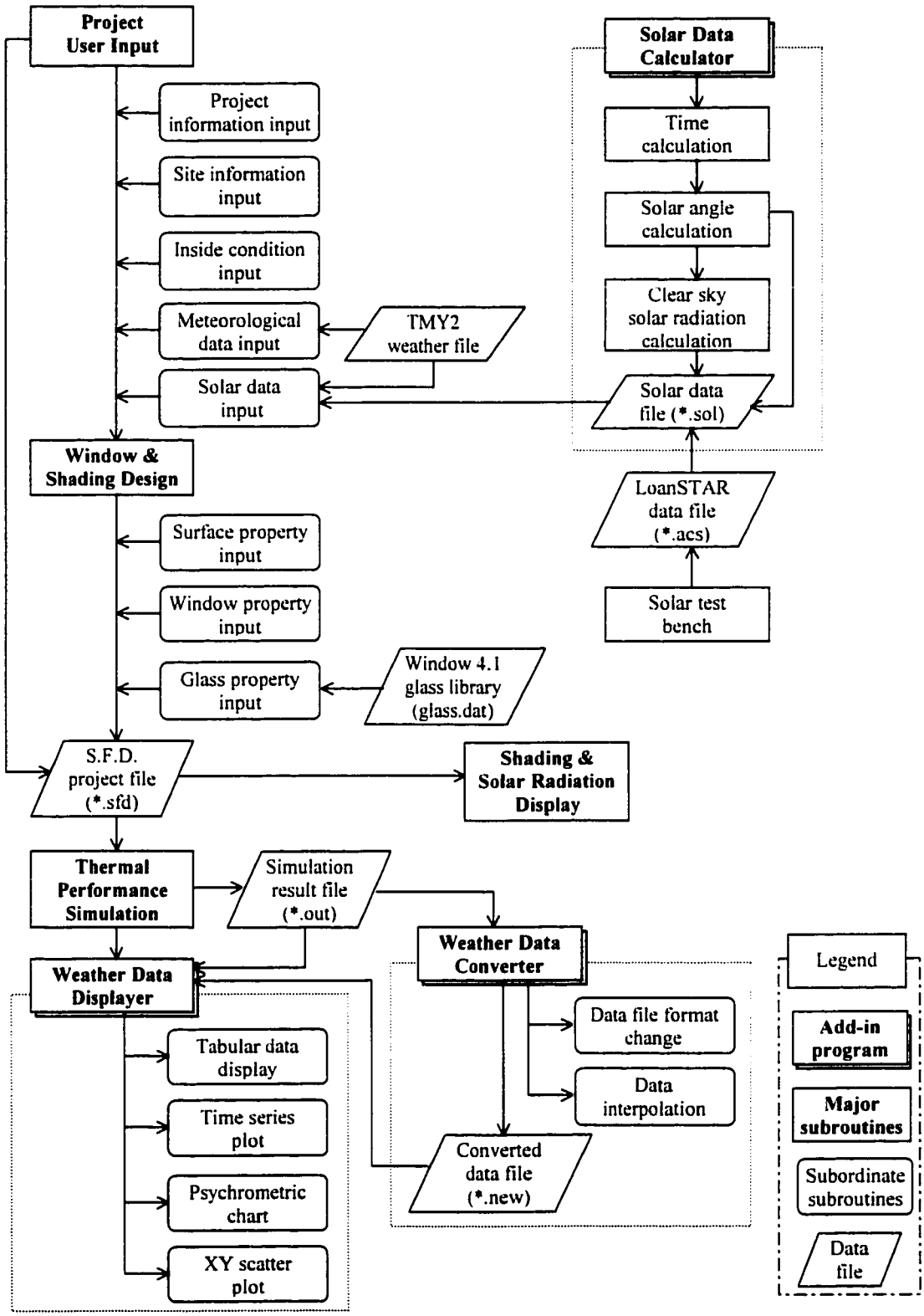

Figure 5.1 Shaded Fenestration Design Model Flow Chart. This figure shows the subroutines in the SFD program and three add-in programs.

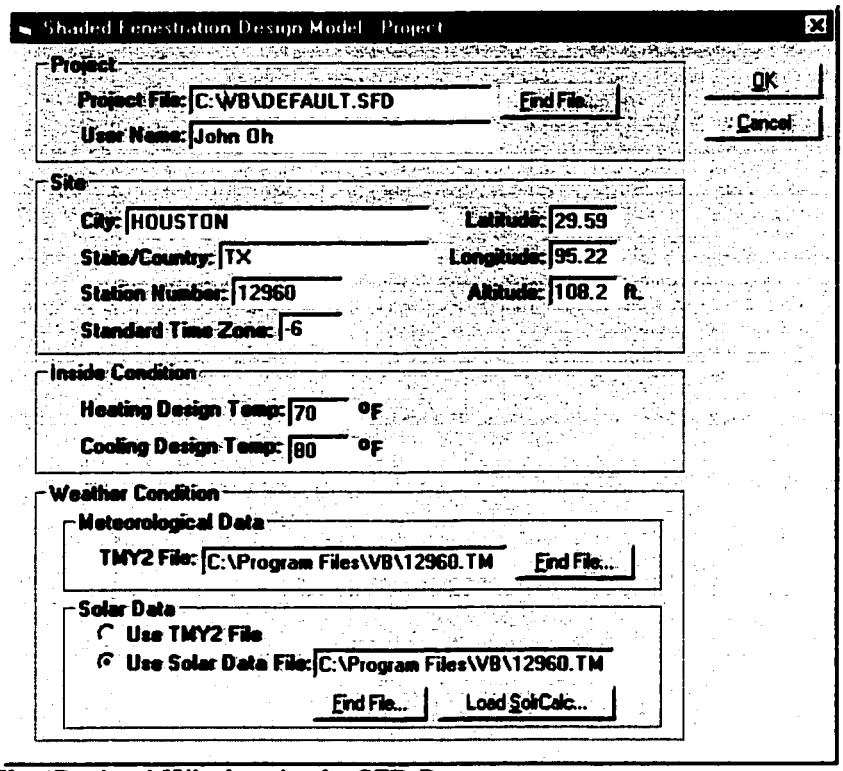

Figure 5.2 The 'Project' Window in the SFD Program.

The SFD program starts with the 'Introduction' window, which is followed by the 'Project' window (Figure 5.2). The Project window is the highest level of user input in the main program. This window allows the user to input the simulation environment for the shading analysis and thermal performance, including: the project information, the site information (i.e., the name of city, latitude, longitude, time zone, etc.), the inside condition (heating and cooling design temperatures), and the outside weather condition. The outside weather condition is separated into meteorological data and solar data. Currently, the SFD program uses only TMY2 weather file for the meteorological data input file. However, the solar data file can be either a TMY2 file or a solar data file created by the add-in program 'Solar Data Calculator (SolrCalc)'. When the user selects a TMY2 file for solar data input, the program will use the same TMY2 file used for meteorological data. The solar data file created by the SolrCalc program has a file extension of '.sol' and will be explained in detail in the following section.

The main program has three major functions: 1) the window and shading device design, 2) shading and solar radiation display, and 3) the thermal performance simulation (i.e., the heat gain and loss calculation through unshaded fenestration systems). As the shading device design is the default function, the user will see the four subordinate windows for shading device design

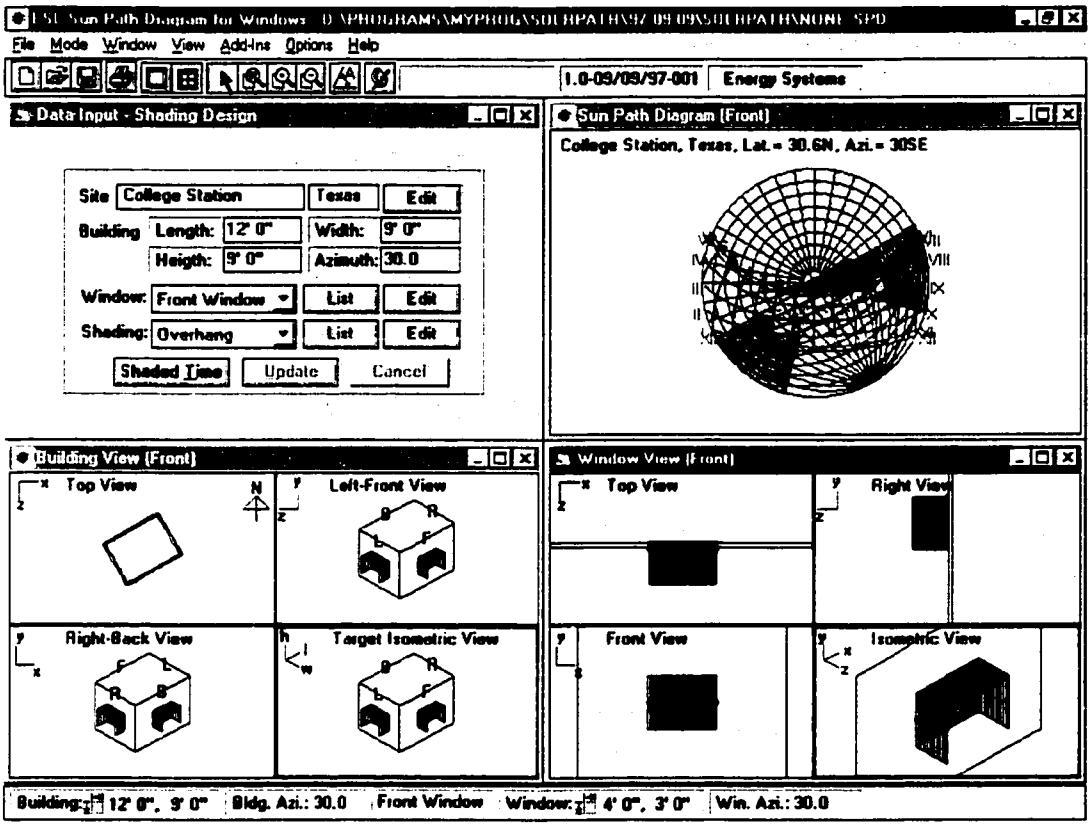

Figure 5.3 The Main Window of the SFD Program. This figure shows the Main window with the four subordinate windows including the 'Data Input', 'Sunpath Diagram', 'Building View', and 'Window View' windows.

when the 'Main' window (Figure 5.3) is loaded. The four subordinate windows are the 'Data Input', 'Sunpath Diagram', 'Building View', and 'Window View'.

The 'window and shading device design' subroutine provides an interactive user interface to design a window and shading devices and plots the shading effects instantly in various formats on the sunpath diagrams. A user-friendly graphical interface can provide the appropriate design solutions for the window glazing and shading devices.

The geometrical information and thermal property of the windows and shading devices are also saved along with project information in the project file with file extension of '.sfd'. Whenever the user adds a new item (i.e., window or shading device), the Input Data window will ask the user to input the geometrical information and thermal property of the item. The geometrical information includes the coordinates of the reference point and the size of the item (see Section 4.1). The shape of the shading devices can be any kind of trapezoids with a

specified tilt angle. Since shading devices can be separated from the wall, it can also be used as an external wall, or for analyzing the effects of neighboring buildings or the surrounding objects.

The thermal property of the window glass includes: thickness, solar transmittance, solar reflectance, and thermal conductivity. The user can type the values or load the values from the library of glass products (i.e., 'glass.dat') provided by the Window 4.1 (LBL 1994) program. The 'glass.dat' file also has values for the thermal infrared transmittance, visible transmittance and reflectance, and infrared emittance of the glass. Figure 5.4 shows the example of the 'glass.dat' file used for the library of window glazing properties.

```
WINDOW 4.1 Glass Library  Format Revision 2
CLEAR             1 A  8.501E-001 7.451E-002 7.451E-002 9.007E-001 8.120E-002 8.120E-002
0.000E+000 8.400E-001 8.400E-001 2.500E+000 9.000E-001 0
CLEAR             2 A  8.370E-001 7.500E-002 7.500E-002 8.980E-001 8.100E-002 8.100E-002
0.000E+000 8.400E-001 8.400E-001 3.000E+000 9.000E-001 0
CLEAR             3 A  7.750E-001 7.100E-002 7.100E-002 8.810E-001 8.000E-002 8.000E-002
0.000E+000 8.400E-001 8.400E-001 6.000E+000 9.000E-001 0
CLEAR             4 A  6.530E-001 6.400E-002 6.400E-002 8.410E-001 7.700E-002 7.700E-002
0.000E+000 8.400E-001 8.400E-001 1.200E+001 9.000E-001 0
BRONZE            5 A  6.450E-001 6.200E-002 6.200E-002 6.850E-001 6.500E-002 6.500E-002
0.000E+000 8.400E-001 8.400E-001 3.000E+000 9.000E-001 0
BRONZE            6 A  4.820E-001 5.400E-002 5.400E-002 5.340E-001 5.700E-002 5.700E-002
0.000E+000 8.400E-001 8.400E-001 6.000E+000 9.000E-001 0
BRONZE            7 A  3.260E-001 4.800E-002 4.800E-002 3.790E-001 5.000E-002 5.000E-002
0.000E+000 8.400E-001 8.400E-001 1.000E+001 9.000E-001 0
GREY              8 A  6.260E-001 6.100E-002 6.100E-002 6.110E-001 6.100E-002 6.100E-002
0.000E+000 8.400E-001 8.400E-001 3.000E+000 9.000E-001 0
GREY              9 A  4.550E-001 5.300E-002 5.300E-002 4.310E-001 5.200E-002 5.200E-002
0.000E+000 8.400E-001 8.400E-001 6.000E+000 9.000E-001 0
GREY             10 A  2.170E-001 4.400E-002 4.400E-002 1.870E-001 4.500E-002 4.500E-002
0.000E+000 8.400E-001 8.400E-001 1.200E+001 9.000E-001 0
GREEN            11 A  6.350E-001 6.300E-002 6.300E-002 8.220E-001 7.500E-002 7.500E-002
0.000E+000 8.400E-001 8.400E-001 3.000E+000 9.000E-001 0
GREEN            12 A  4.870E-001 5.600E-002 5.600E-002 7.490E-001 7.000E-002 7.000E-002
0.000E+000 8.400E-001 8.400E-001 6.000E+000 9.000E-001 0
LOW IRON         13 A  9.040E-001 8.000E-002 8.000E-002 9.140E-001 8.300E-002 8.300E-002
0.000E+000 8.400E-001 8.400E-001 2.500E+000 9.000E-001 0
LOW IRON         14 A  8.990E-001 7.900E-002 7.900E-002 9.130E-001 8.200E-002 8.200E-002
```

Figure 5.4 Example of the 'Glass.dat' File.

The next major function 'shading and solar radiation display' provides the user the graphical presentation of shading effects and solar radiation in the various projections of the sunpath diagram. The projection methods of shading and solar radiation were described in Section 4.1.

The last major function of the SFD program is the 'thermal performance simulation'. This subroutine calculates the total heat gains and losses through an unshaded fenestration system to evaluate the optimum material design for window glazing, and allow the user to analyze the thermal impact of shading devices upon solar radiation incident upon on a window.

For the total heat transfer calculation, the amount of the transmitted and absorbed solar radiation, the conductive and convective heat transfer through the glazing are calculated based on the weather conditions provided by a TMY2 weather file.

To calculate the total solar gain through the window glazing, direct, diffuse and reflected solar radiation are utilized. This includes the beam, diffuse and reflected solar radiation penetrating through the window glazing. The amounts of beam radiation, diffuse radiation, and global radiation on a horizontal surface are provided from the add-in program 'Solar Data Calculator' or a TMY2 weather data.

The result of thermal simulation and solar data can be displayed in various modes using the add-in program 'Weather Data Displayer' that will be described in Section 5.4. For further analysis, these data can be manipulated using the add-in program 'Weather Data Converter' that will be described in Section 5.3.

5.2 The Solar Data Calculator (SolrCalc) Program

The add-in program 'Solar Data Calculator (SolrCalc)' has three major functions including: 1) the solar time calculation, 2) the solar angle calculation for the given solar or local time, and 3) the solar radiation calculation both on the horizon and on a tilted wall on clear days. Figure 5.5 shows the flow chart of the SolrCalc program.

The SolrCalc program can be used as an add-in program for the SFD program or a stand-alone program used for solar radiation calculations. The SolrCalc program simulates the solar radiation on a clear day using one of the three solar radiation estimation methods such as ASHRAE Handbook (1997), Duffie and Beckman (1991), or Kreider and Rabl (1994). The equations and the difference of their calculation results were previously described in detail in Section 2.3.

The program can be used either for the instantaneous solar intensity calculation at a given time or for the creation of a weather data file in a given period. Figure 5.6 shows a screen image of the SolrCalc program for the instantaneous solar radiation calculation. The solar angles and intensities of solar radiation are updated whenever the user types in new data or resets the time. Figure 5.7 shows a screen image of the SolrCalc program used to create a weather data file for the user-defined period and interval. The user can also select items that will

be included in the weather file. This subroutine creates a solar data file (*.sol) either from the previously described calculation or from the real data file collected from the solar test bench. When someone chooses to use solar data in TMY2 file, they do not need to use this program because the SFD program can directly load the solar data from the TMY2 file.

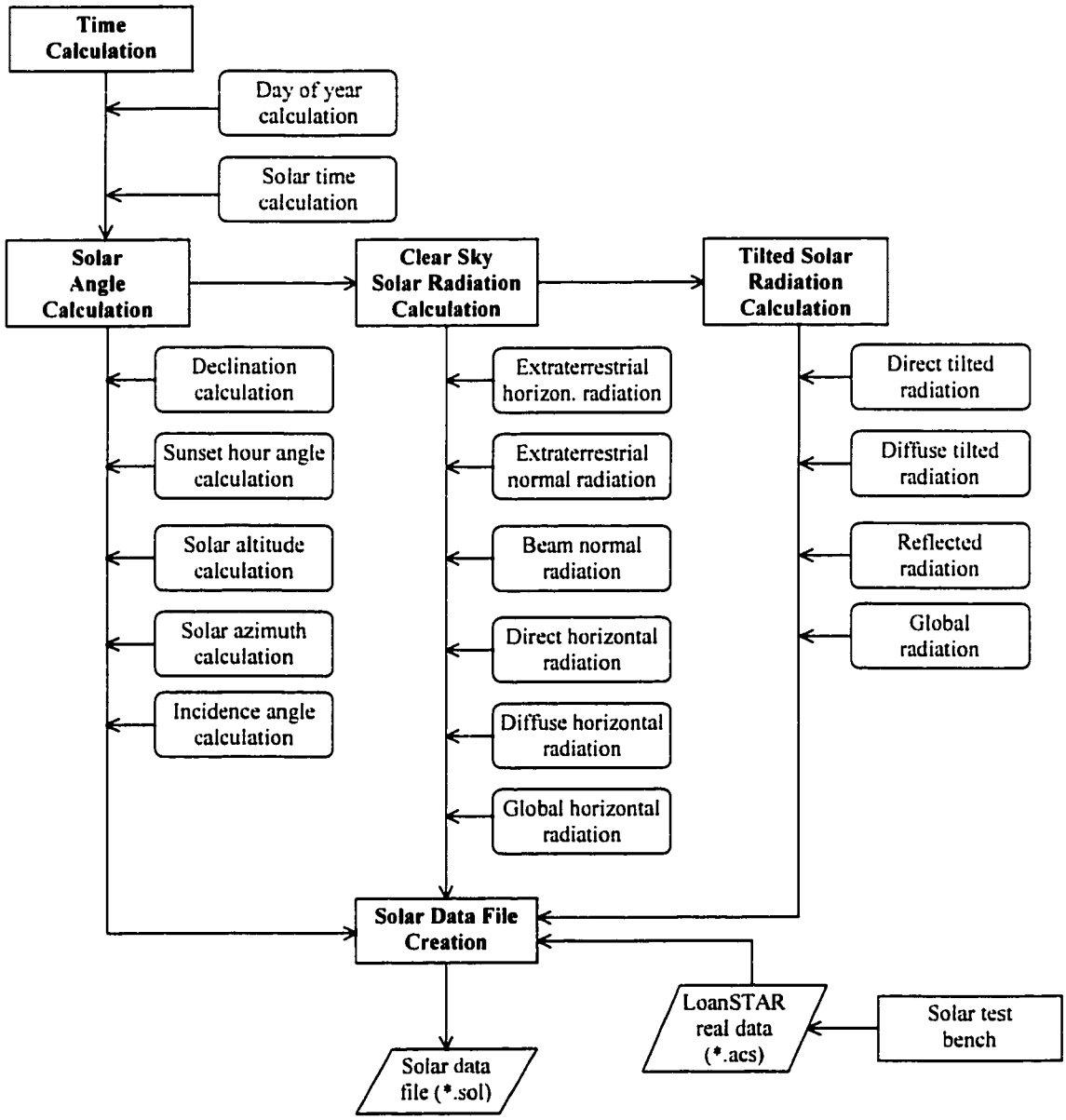

Figure 5.5 Flow Chart of the Solar Data Calculator (SolrCalc) Program. This figure shows the major subroutines in the SolrCalc program.

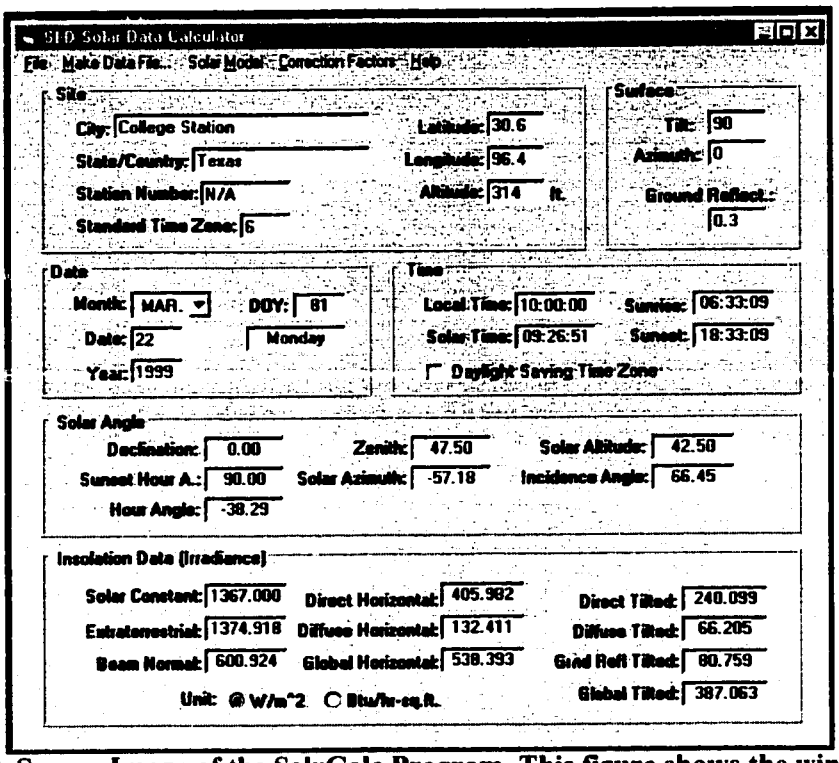

Figure 5.6 A Screen Image of the SolrCalc Program. This figure shows the window that displays the instantaneous solar radiation calculation.

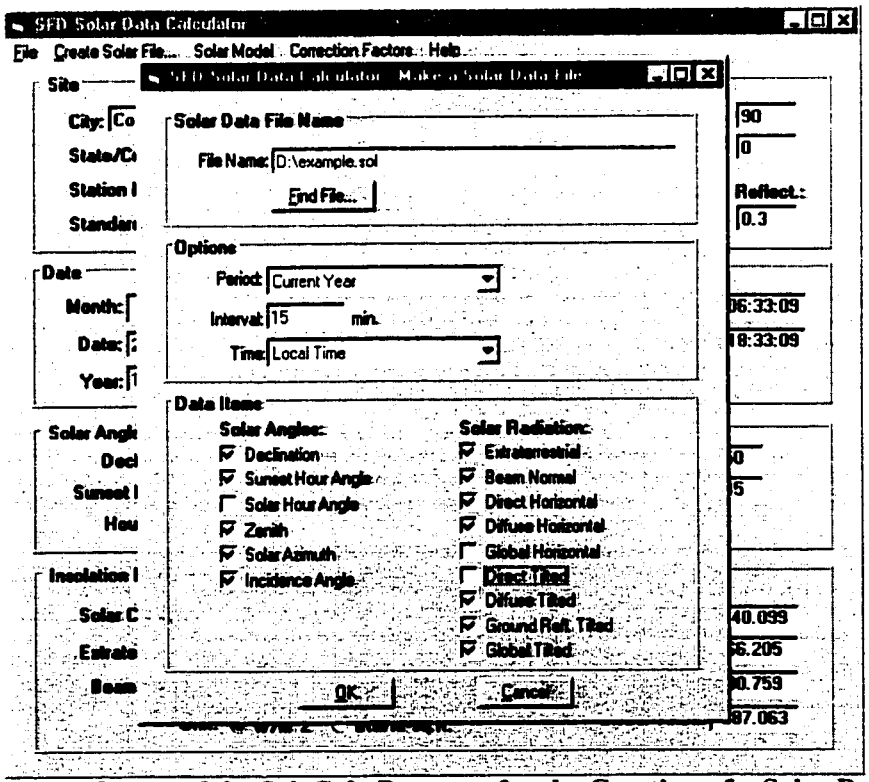

Figure 5.7 Screen Image of the SolrCalc Program for the Creation of a Solar Data File.

Table 5.1 Data Elements in the SOL Format Solar Data File.

Field #	Element	Format	Note
1	Station Number	XXXXX	0 if unused.
2	Year	YY	
3	Month	MM	
4	Day	DD	
5	Hour	HH	
6	Solar-local Time Difference	XX.XXX	Time difference in hours between the solar and local standard time.
7	Julian Date	YYDDD	
8	Decimal Date	XXXXX.XXXX	The days counted from the first day of January, 1900.
9	Solar Altitude	XXX.XXX	
10	Solar Azimuth	XXX.XXX	Degrees of due south, west is positive and east is negative.
11	Incidence Angle for South Vertical	XXX.XXX	The angle between the direct solar radiation and the outward normal of a vertical surface.
12	Extraterrestrial Horizontal Radiation	XXXX.XXX	All the solar data is in W/m^2.
13	Extraterrestrial Direct Normal Radiation	XXXX.XXX	
14	Global Horizontal Radiation	XXXX.XXX	
15	Direct Normal Radiation	XXXX.XXX	
16	Diffuse Horizontal Radiation	XXXX.XXX	
17	South Vertical Radiation	XXXX.XXX	

Table 5.1 lists the data elements in a solar data file created by the SolrCalc program to be used in the Main program.

5.3 The Weather Data Converter (DataConv) Program

These other add-in program 'Weather Data Converter (DataConv)' is used to change the format of the weather data file. This program can also change the data interval using linear interpolation, or shift the time stamp to local-solar time difference.

The SFD program works with three different data file formats, including TMY2 format (*.tm2), the LoanSTAR format (*.acs), and comma delimited variable format files (*.csv). The

DataConv program also makes it possible to convert from one format to another. The LoanSTAR data file is a text file having space delimited variables with space delimiters. It uses a decimal time with a reference year of 1980, whereas the '*.csv' file uses the decimal time having a reference year of 1900. As most computer programs use the year of 1900 as the reference year of time calculation, a '*.csv' file is usually easier to handle in most computer applications than the LoanSTAR file format.

The most important function of the DataConv program is the data interval change that uses the linear interpolation method. Figure 5.8 shows a screen image of the DataConv program asking the user to type the variable name and type. The data from the solar test bench at the Langford Architecture Center is stored in 15-minute intervals, whereas most weather data file including the TMY2 file has hourly data. Thus, to compare the solar bench data against the data from other sources, data conversion is needed. The finite difference model developed in this thesis used one-minute data converted from 15-minute data from the solar test bench using the DataConv program.

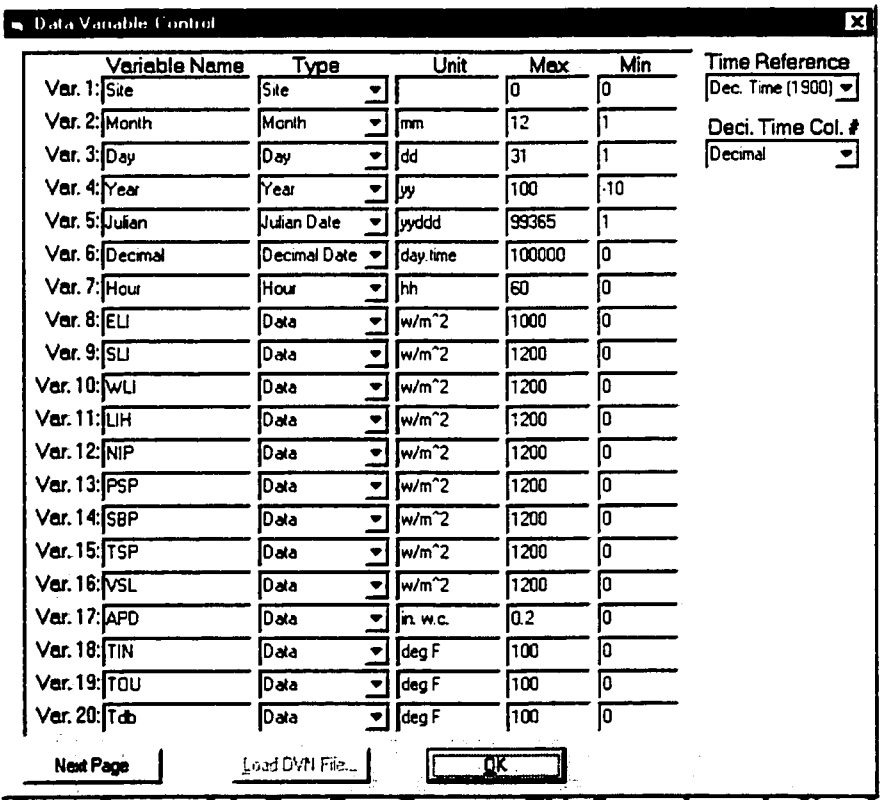

Figure 5.8 Screen Image of the DataConv Program. This figure shows the User Input window asking for the variable name and data type.

5.4 The Weather Data Displayer (WethDisp) Program

The last add-in program is the 'Weather Data Displayer (WethDisp)' program, which is a graphic viewer that provides four different graphic displays of the weather information. The four display methods are the tabular data display, time series plot, psychrometric chart, and XY scatter plot.

Figure 5.9 shows the screen image of the 'Tabular Display' window in the WethDisp program. The variable names and units in the first two rows of the table are given by the user and stored in a variable control file (*.vcn). The variable control file is created through the 'Data Variable Control' window (Figure 5.10) that is activated whenever the user opens a new data file. With this window, the user can set the display properties of each data item.

Figure 5.11 shows an example of the 'Time Series Plot' window. The maximum and minimum values of the display range of each data item are given by the data variable control window, and the display period (i.e., X-axis) is determined by the user input including one-day, one-week, one-month, or the selected days. The user can set the data items to be displayed or hidden.

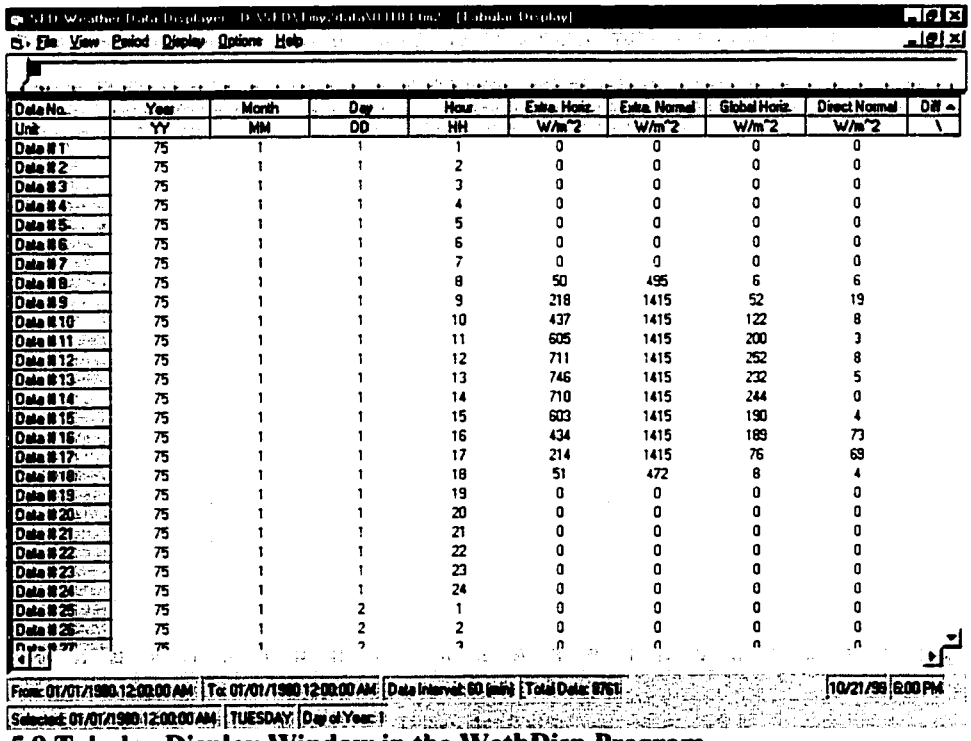

Figure 5.9 Tabular Display Window in the WethDisp Program.

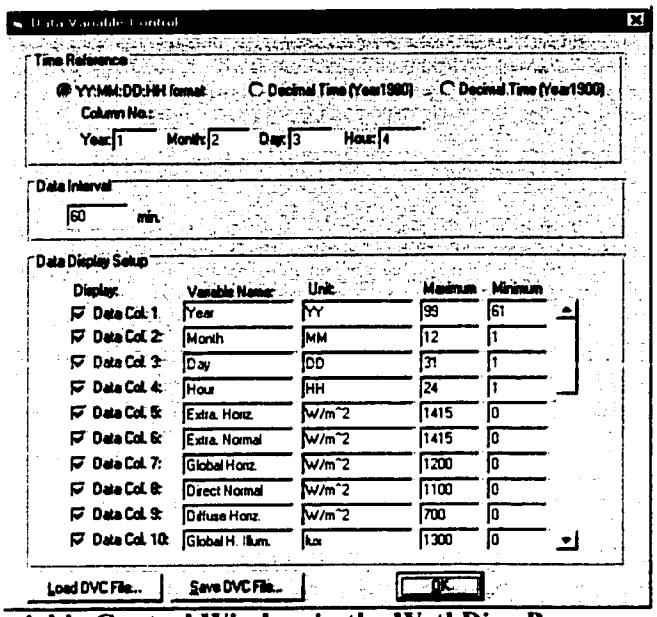

Figure 5.10 Data Variable Control Window in the WethDisp Program.

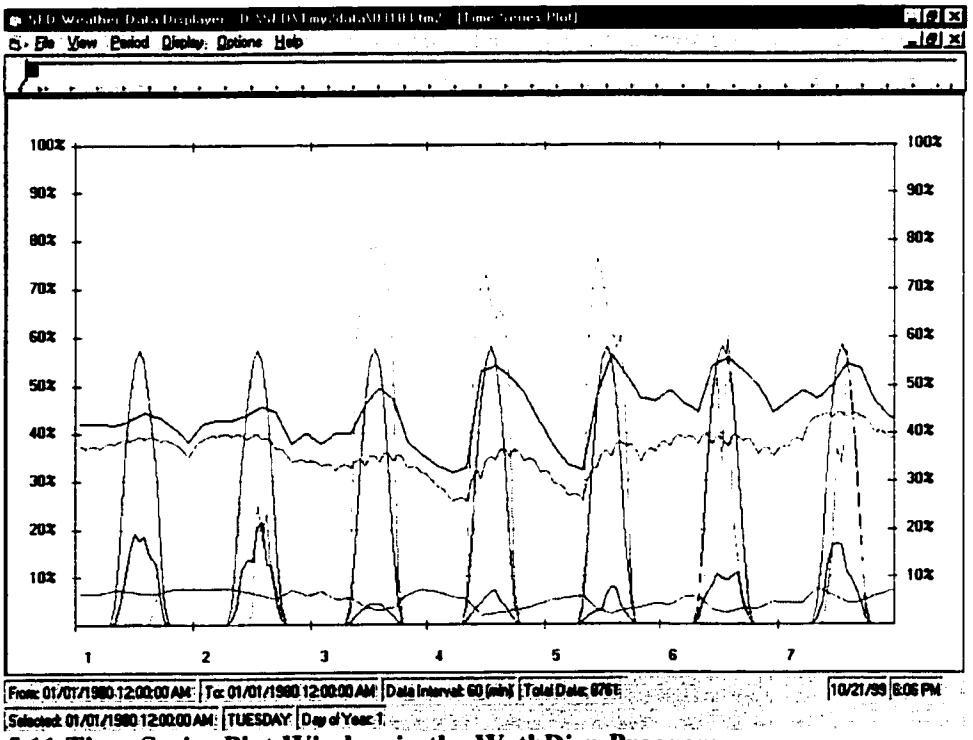

Figure 5.11 Time Series Plot Window in the WethDisp Program.

The 'Psychrometric Chart' (Figure 5.12) window in the WethDisp program plots two sets of data items (i.e., the major data set and the secondary data set) onto a psychrometric chart. Each data set needs to have either dry-bulb temperatures and RH or dry-bulb temperatures and

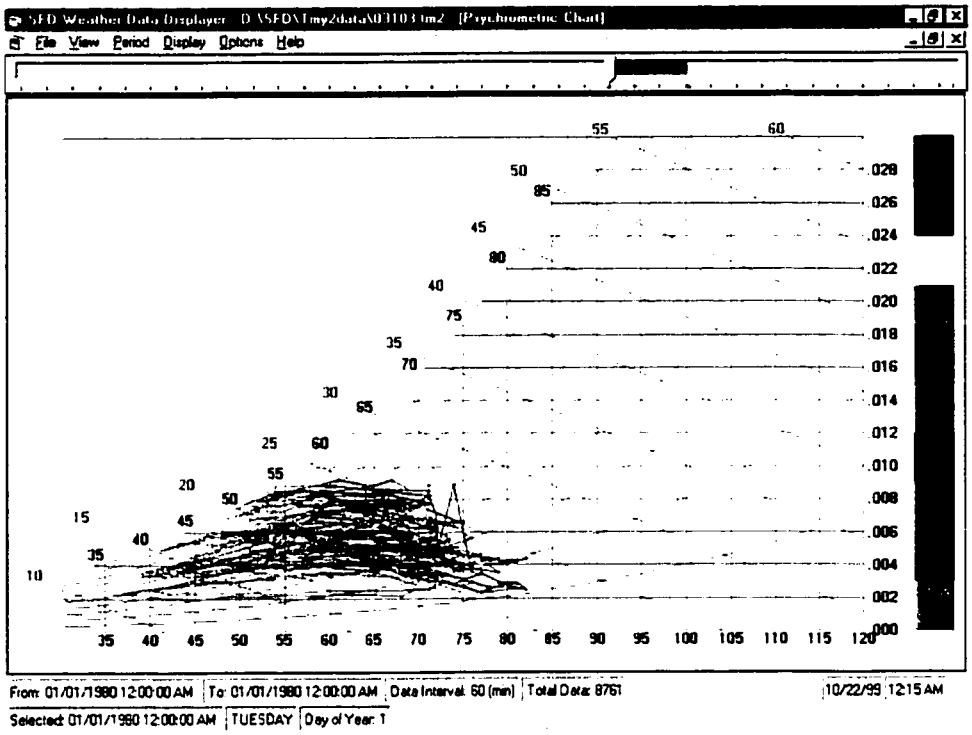

Figure 5.12 Psychrometric Chart Window in the WethDisp Program. This figure shows the intensities of extraterrestrial solar radiation plotted onto a psychrometric chart.

wet-bulb temperatures. A third set of weather information, such as the intensity of the solar radiation, can be displayed by plotting a line with a 'color scale' onto the psychrometric chart.

This chapter described the proposed computer model for shading and thermal analysis of fenestration systems. The SFD program consists of the Main program and three add-in programs. The major functions of the program are the window and shading device design, thermal performance simulation of unshaded fenestration systems, calculation of solar radiation, and graphical display of shading and solar data. The following chapter will discuss the results of the experimental and comparative validation of the proposed computer model.

CHAPTER VI

DATA ANALYSIS AND RESULTS

To validate the accuracy of the new thermal and shading analysis model, an experimental test box was constructed as described in Section 4.3. A total of eight different experiments were conducted with different experimental configurations. The first two experiments were performed in order to characterize the heat transfer properties of the highly insulated experimental box. The next experiment was conducted to validate the calculated transmittance of solar radiation through the window glazing of the box. The remaining experiments were conducted to develop test sets of measured data for various configurations of shading devices. Appendix B contains the graphical and tabular results of measured data from these experimental tests.

Before these experiments were conducted, all instruments were either calibrated at the ESL's Calibration Laboratory or calibrated on site as described in Section 4.3.2. Each simulation was conducted over a period of a week to assure that at least one clear day had been captured. From each data set, one clear day was selected for the data analysis of the experimental case. When a clear day did not exist during the experimental period, the experiment was continued until a clear day was acquired.

Simulations using the DOE-2 program were then conducted to simulate the experimental box and to serve as a secondary validation. For each experimental case, two versions of the DOE-2 simulations were conducted: one using a weather file and another using DESIGN-DAY instructions as described in Section 4.5. For the first three experimental cases, finite difference models were developed to calculate the dynamic heat transfer of the experimental test box. The following sections describe the results of the experiments and simulations as well as the comparison against the measured data, the simulated data from the model, and the DOE-2 simulation results for each experimental case.

6.1 Experimental Case 1: Heat Transfer through Highly Insulated Walls (Blocked Window)

The final target of this research was to estimate the heat gains and losses through a shaded window system. To reach this goal, we needed to extract the thermal performance

through the window aperture by eliminating the other thermal effects such as the dynamic heat transfer through walls and a roof of the experimental box. To accomplish this, two different experiments were conducted to empirically determine the heat transfer properties of the highly insulated walls.

6.1.1 Measured Results from the Experimental Box (Blocked Window)

The first experiment was conducted using the following procedure. First, the window aperture of the experimental box was blocked with the same thickness of Styrofoam insulation layers as in the walls of the box (Figure 6.1). Thus, there were no openings into the test box except the inlet and outlet portals used to circulate the air.

The inlet and outlet temperatures from the test chamber and the air pressure difference across the AMCA airflow nozzle were measured with a data logger. The diffuse and global horizontal solar radiation as well as vertical solar radiation on the south wall were also measured. Figures B.1 to B.5 in Appendix B show the measured data collected from the experimental box on a clear day for the first experimental period. The results highlight the impact of time delay caused by the highly insulated test box. As shown in Figure B.2, the outlet air temperature was about 5 ^{o}F lower than inlet temperature during the day, whereas it was about 2 or 3 ^{o}F higher during the night. The highly insulated walls therefore release the gained

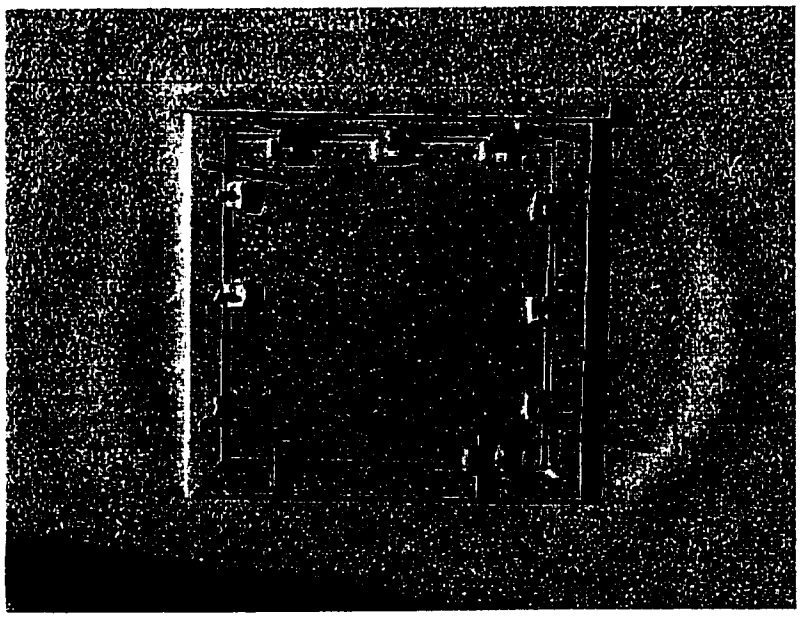

Figure 6.1 Insulation Block in the Window Aperture Area of the Experimental Box.

heat constantly through the night. The heat removed by the circulation fan (Q_{fan}) can be calculated from the air temperature difference between the inlet and outlet tubes and the airflow rate derived from the measured air pressure difference in the airflow chamber. Figure 6.2 shows the outlet-inlet temperature difference (T_{diff}) and the heat removed by the fan (Q_{fan}).

Figure 6.3 shows the volume flow rate ($\dot{V}_{fan}$) and the outlet-inlet heat removed by the fan (Q_{fan}).

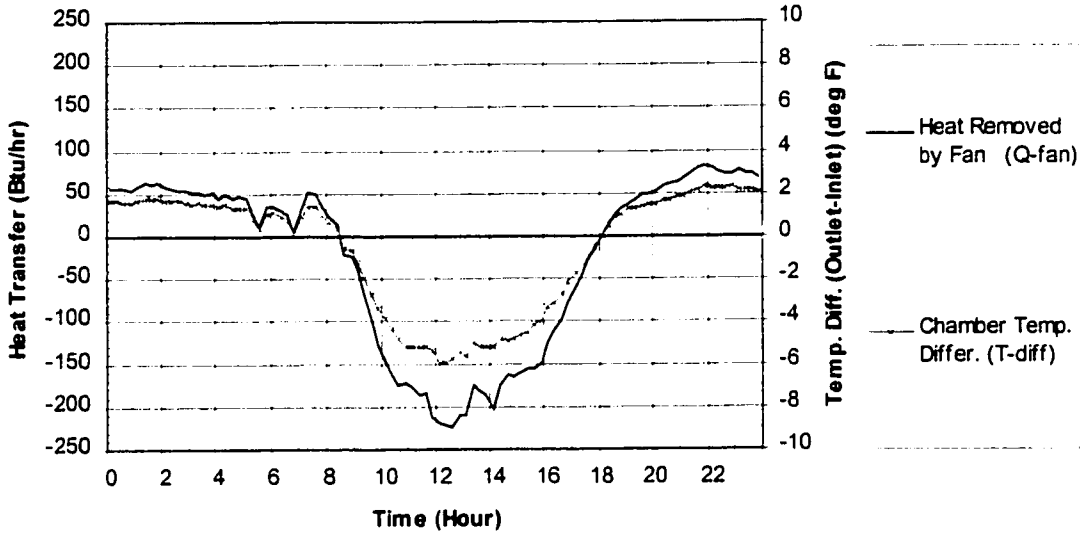

Figure 6.2 Outlet-Inlet Temperature Difference and Heat Removed by Fan (Case 1, 10/25/98, Blocked Window).

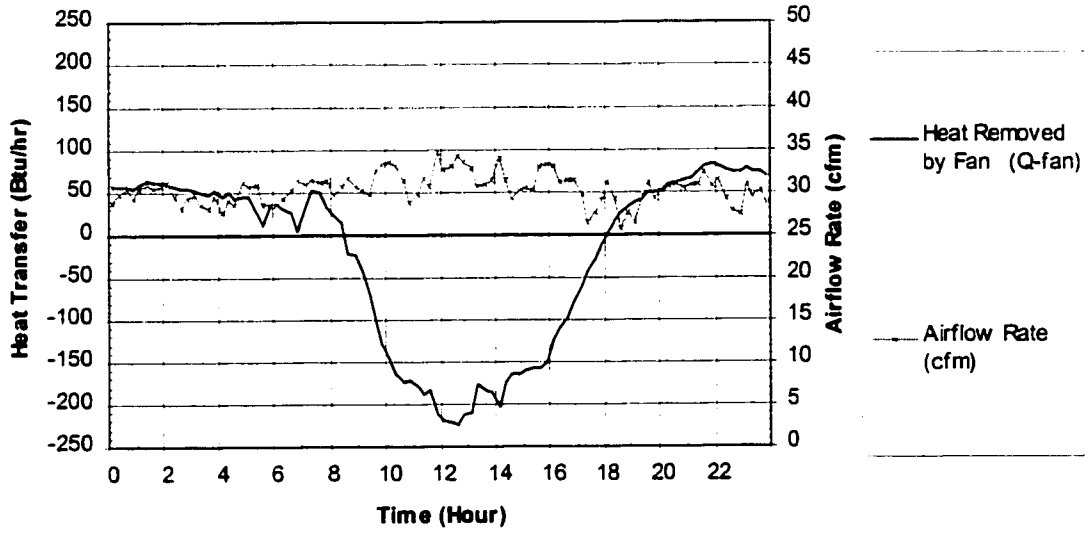

Figure 6.3 Airflow Rate and Heat Removed by Fan (Case 1, 10/25/98, Blocked Window).

As we can see from these figures, the amount of the heat transfer was driven mostly by the outlet-inlet temperature difference since the airflow rate was held almost constant. The test box absorbed a maximum of about 224 *Btu/hr* of heat from the inlet air around 12:30 p.m., and released a maximum of about 83 *Btu/hr* of heat into the outlet air at 9:45 p.m. Total heat gain (727 *Btu/day*) from the inlet air over a 24 hour period was about 600 *Btu* greater than heat loss (1,327 *Btu/day*) into the outlet air. This indicates that total heat transfer through walls should not be neglected in the experimental results. The heat absorption of walls occurred over a short time period, whereas the heat removed from the box occurred evenly throughout the night.

6.1.2 Results from the Finite Difference Model (Blocked Window)

A finite difference (F.D.) model was developed to calculate the dynamic heat transfer through the walls in order to simulate the test box. The objective of this model was to calculate the total convective heat transfer through the inside wall surfaces ($Q_{conv,w,in}$) and the outside wall surfaces ($Q_{conv,w,out}$) as well as the conductive heat transfer (Q_{cond}) through the walls. These values were derived empirically from the simulated values of the convection coefficient between the room air and the inside wall surfaces ($h_{w,in}$) and that between the ambient air and the outside wall surfaces ($h_{w,out}$) as well as the thermal conductivity of the insulation (k_{ins}). The method used to derive the values is described in Section 4.4. The application of the finite difference model to this experimental case was conducted using the following procedure.

First, the original 15-minute data was linearly interpolated into one-minute data using the Weather Data Converter program. Next, using these data, the heat removed by the circulation fan (Q_{fan}) was calculated every minute. A discrete distance (Δx) of 1 inch was used for the one-dimensional nodes. The thermal conductivity of plywood was set to 0.*0667 (Btu-ft/hr-ft*^{2}*-°F*). The initial values of $h_{w,in}$, $h_{w,out}$, and k_{ins} were set to 3.0 (*Btu/hr-ft*^{2}*-°F*), 3.0 (Btu/hr-ft^2-°F), and 0.0316 (*Btu-ft/hr-ft*^{2}*-°F*) respectively. From the conditions for the stability criterion, the discrete times were calculated at various nodes such as Δt_0 = 3 *min.*, Δt_m = 36 *min.*, and Δt_6 = 1.86 *min.* Thus, the minimum Δt was 1.86 minutes. As the actual data interval used in this model was one minute, the conditions for stability criterion were satisfied. The Biot numbers and Fourier numbers were then calculated.

The temperature at each node was calculated every minute using the finite difference equations described in Section 4.4. The simulated room temperatures for the 24 hour period

were then compared against the measured outlet temperatures. It was assumed that the outlet temperature was the same as the room air temperature. A linear regression analysis was then applied to obtain the maximum R^2 value between the simulated and the measured temperatures. A series of values for $h_{w,in}$, $h_{w,out}$, and k_{ins} were input into the model, and a set of values corresponding to the maximum R^2 value were chosen. Tables 6.1 to 6.3 show the values used to determine $h_{w,in}$, $h_{w,out}$, and k_{ins} and the calculated R^2 values for the case of the blocked window.

Table 6.1 Calculated R^2 Values for the Various k_{ins} Values (Case 1, Blocked Window).

k_{ins}	0.0316	0.035	0.037	0.038	0.039	0.04	0.041	0.045	0.05
R^2	0.9672	0.9768	0.9787	0.9788	0.9783	0.9774	0.9760	0.9673	0.9517

Table 6.2 Calculated R^2 Values for the Various $h_{w,in}$ Values (Case 1, Blocked Window).

$h_{w,in}$	1	2	2.1	2.2	2.3	2.4	2.5	3	4
R^2	0.9542	0.9791	0.9794	0.9796	0.9796	0.9796	0.9796	0.9788	0.9765

Table 6.3 Calculated R^2 Values for the Various $h_{w,out}$ Values (Case 1, Blocked Window).

$h_{w,out}$	3	5	7	9	9.5	9.6	9.7	9.8	10
R^2	0.9796	0.9802	0.9803	0.9803	0.9803	0.9803	0.9803	0.9803	0.9803

The final values calculated from this method were k_{ins} = 0.038 (Btu-ft/hr-ft^2-°F), $h_{w,in}$ = 2.3 (Btu/ hr-ft^2-°F), and $h_{w,out}$ = 9.6 (Btu/ hr-ft^2-°F). From these values, convective heat transfer through inside wall surfaces ($Q_{conv,w,in}$) and outside wall surfaces ($Q_{conv,w,out}$) as well as the total conductive heat transfer through the walls (Q_{cond}) were calculated. The total amount of the conductive heat transfer was calculated by accumulating the individual conductive heat transfers at each node. Figure 6.4 displays a measured room temperature and simulated temperatures at individual F.D. nodes. Figure 6.5 shows the calculated heat transfer of the experimental box.

The result shows that the peak heat gains from the outside surface convection occurred at around noon when the amount of the incident solar radiation reached the maximum value. However, the peak heat gains from the inside surface convection occurred at around 9:45 p.m. The peak conduction heat gain occurred at about 3:00 p.m.

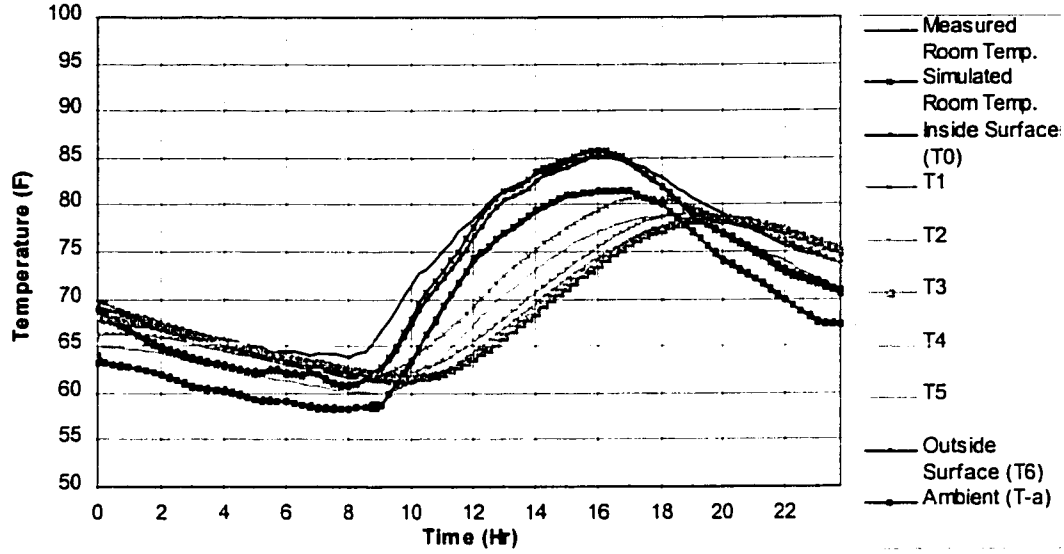

Figure 6.4 Measured Room Temperature and Finite Difference Model Calculated Temperatures at Individual Nodes (Case 1, 10/25/98, Blocked Window).

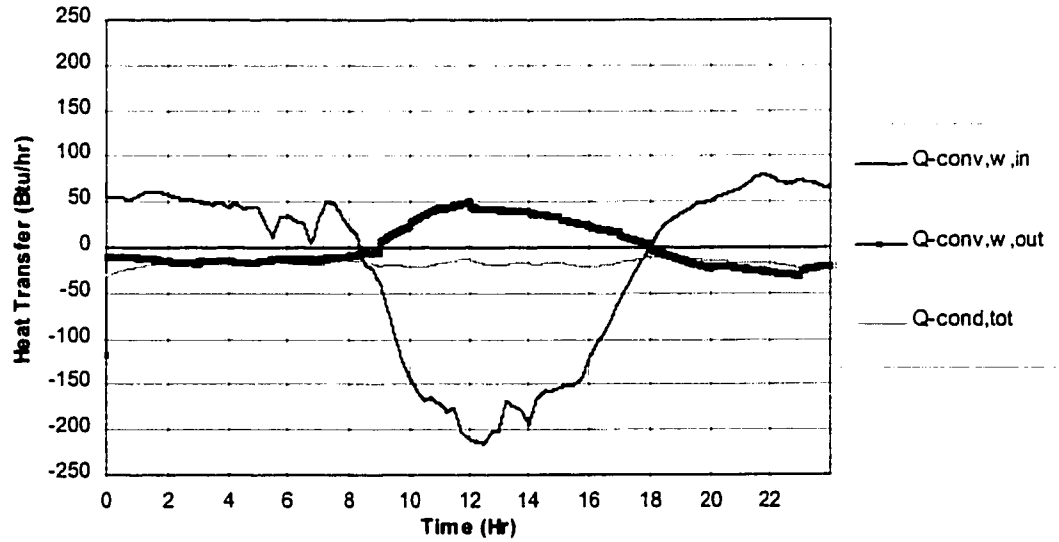

Figure 6.5 Finite Difference Model Calculated Heat Transfer of the Experimental Box (Case 1, 10/25/98, Blocked Window).

6.2 Experimental Case 2: Heat Transfer through Highly Insulated Walls with Periodic Heat Gain

This experiment was conducted to magnify the thermal storage effect of the insulated walls in the analysis of dynamic heat transfer. The experimental condition on this case is the same as in the previous case except that periodic heat gain occurred. In experiment case 2, a 100-Watt incandescent lamp was installed near to the entrance of the inlet tube (Figure 6.6) to act as a periodic heat source. The lamp was turned on and off every 2 hours using a programmable timer. The window aperture of the box remained blocked for this case, hence there was still no heat gain through the window. All the weather data were measured the same as in the previous case.

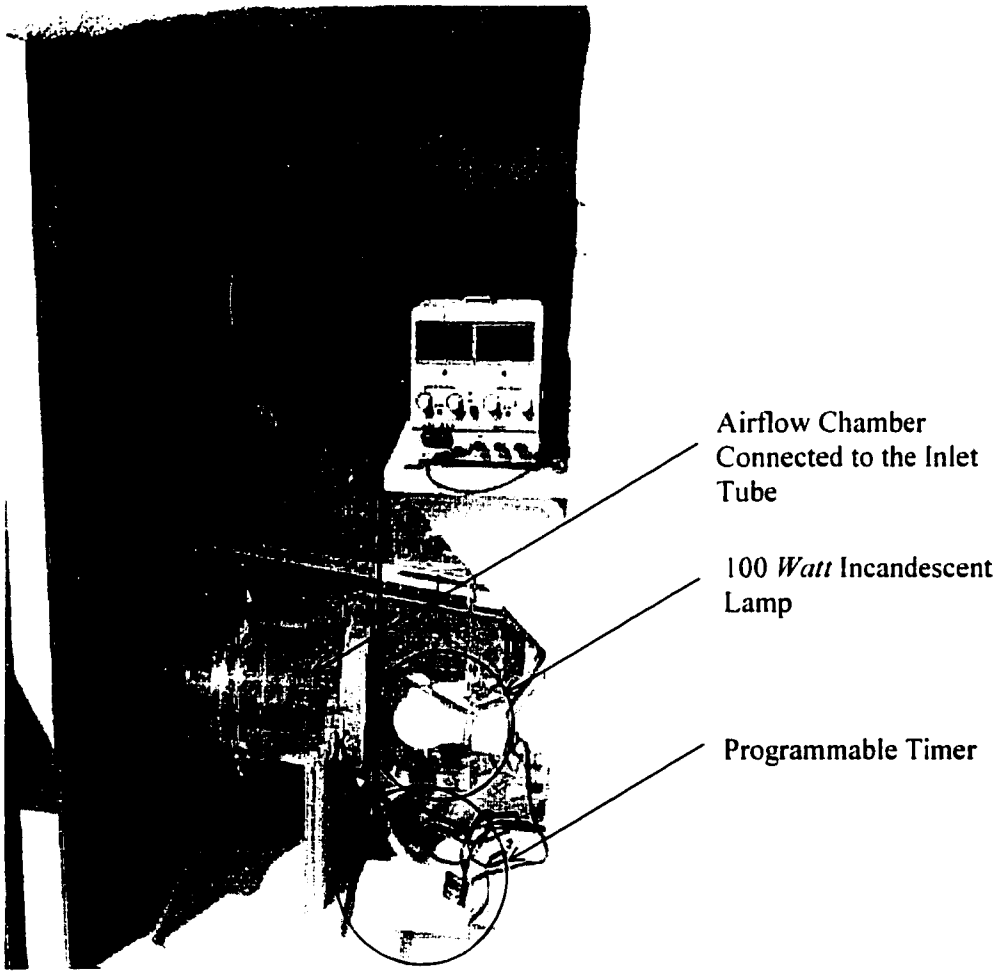

Figure 6.6 Instrument Room with a 100 Watt Incandescent Lamp and a Timer for the Thermal Storage Effect Test (Blocked Window with Periodic Heat Gain).

6.2.1 Measured Results from the Experimental Box (Blocked Window with Periodic Heat Gain)

Figures B.6 through B.10 in Appendix B show the measured data from test case 2. Figure 6.7 shows the inlet-outlet temperature difference (T_{diff}) and the heat removed by the fan (Q_{fan}). This figure displays the effects of the heat gain from the 100 W lamp as an increase in the outlet and inlet air temperature difference. The temperatures changed rapidly just after the lamp was turned on or turned off, and then followed a profile similar to what was seen in Figure 6.7.

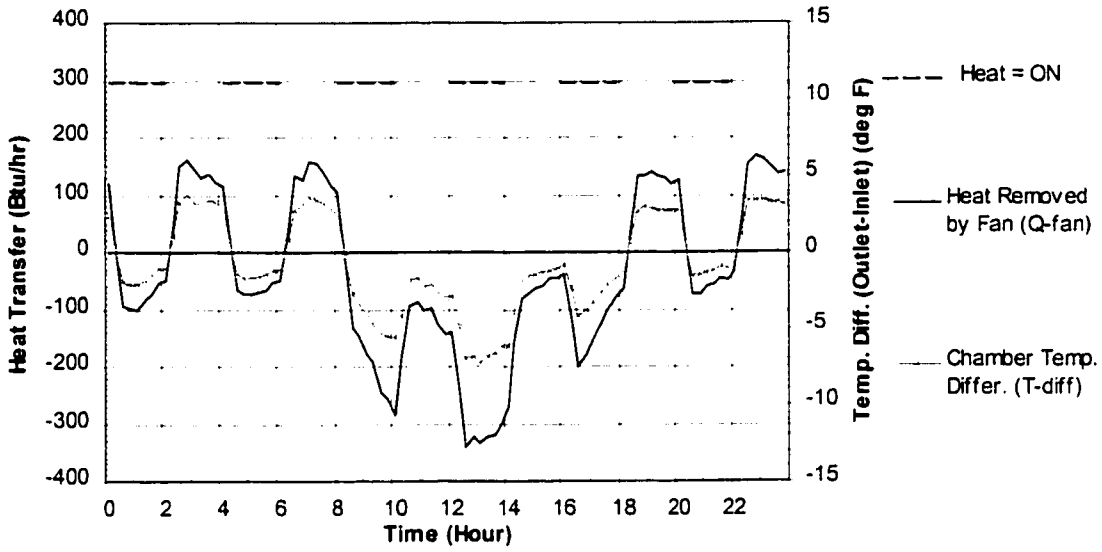

Figure 6.7 Outlet-Inlet Temperature Difference and Heat Removed by Fan (Case 2, 11/03/98, Blocked Window with Periodic Heat Gain).

Figure 6.8 shows the volume flow rate ($\dot{V}_{fan}$) and the measured heat removed by the fan (Q_{fan}). From these figures, we can see the amount of heat removed by the fan was definitely influenced by the outlet-inlet temperature difference. The walls of the experimental box gained the maximum heat of 341.8 *Btu/hr* at 12:30 p.m., released the maximum heat of 168.4 *Btu/hr* at 10:45 p.m. The total heat gained (1,966.2 *Btu/day*) from the delivered air was about 942.4 *Btu* greater than the total heat loss (1,023.9 *Btu/day*).

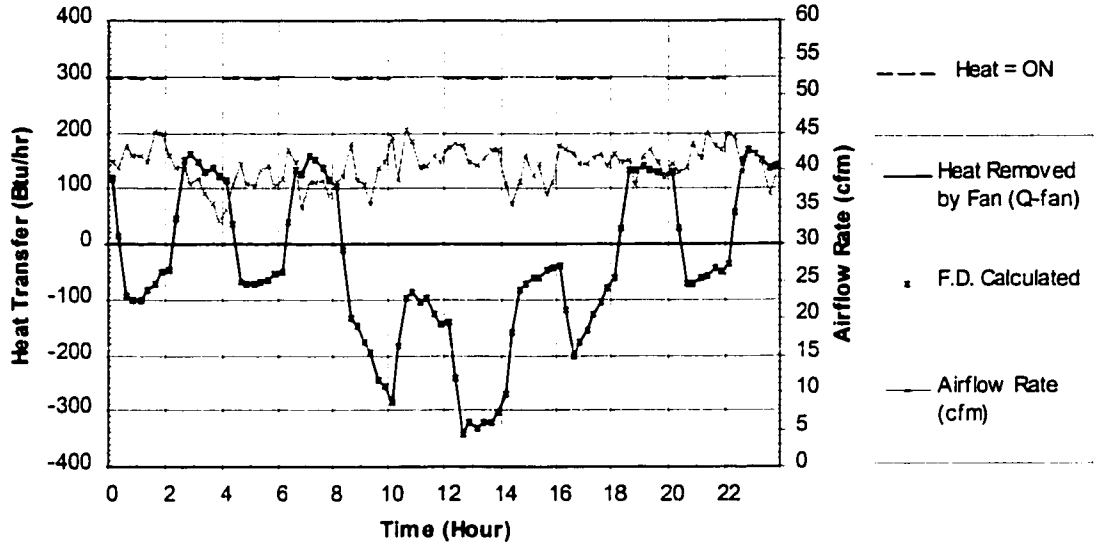

Figure 6.8 Heat Removed by Fan, Heat Transfer Calculated by a Finite Difference Model, and Airflow Rate (Case 2, 11/03/98, Blocked Window with Periodic Heat Gain).

6.2.2 Results from the Finite Difference Model (Blocked Window with Periodic Heat Gain)

A finite difference model was then developed using the same procedure described in Section 6.1.2. The values for the convection coefficient between the room air and the inside wall surface ($h_{w,in}$) and that between the ambient air and the outside wall surface ($h_{w,out}$) as well as the thermal conductivity of insulation (k_{ins}) were recalculated for the case of the blocked window with the on-off heat source.

The initial values of $h_{w,in}$, $h_{w,out}$, and k_{ins} were set to 3.0, 3.0, and 0.0316 respectively. From the conditions for the stability criterion, the discrete times were calculated at various nodes such as $\Delta t_0 = 5.5\ min.$, $\Delta t_m = 36.8\ min.$, and $\Delta t_6 = 5.5\ min.$ The minimum Δt was 5.5 minutes. As the actual data interval used in this model was one minute, the conditions for stability criterion were satisfied. Tables 6.4 to 6.6 show the values used to determine $h_{w,in}$, $h_{w,out}$, and k_{ins} and the calculated R^2 values.

Table 6.4 Calculated R^2 Values for the Various k_{ins} Values (Case 2, Blocked Window with Periodic Heat Gain).

k_{ins}	0.0316	0.035	0.04	0.045	0.05		0.052	0.053	0.055
R^2	0.8659	0.8831	0.8992	0.9071	0.9096		0.9096	0.9094	0.9088

Table 6.5 Calculated R^2 Values for the Various $h_{w,in}$ Values (Case 2, Blocked Window with Periodic Heat Gain).

$h_{w,in}$	2.5	3	3.1	3.2	[illegible]	3.4	3.5	3.7	4
R^2	0.9085	0.9096	0.9097	0.9097	[illegible]	0.9098	0.9097	0.9097	0.9094

Table 6.6 Calculated R^2 Values for the Various $h_{w,out}$ Values (Case 2, Blocked Window with Periodic Heat Gain).

$h_{w,out}$	0.5	0.9	[illegible]	1.1	1.2	1.5	2	2.5	3
R^2	0.9089	0.9115	[illegible]	0.9115	0.9114	0.9111	0.9105	0.9101	0.9098

The final values calculated from this test were k_{ins} = 0.051 (Btu-ft/hr-ft^2-°F), $h_{w,in}$ = 3.3 (Btu/ hr-ft^2-°F), and $h_{w,out}$ = 1.0 (Btu/ hr-ft^2-°F). Clearly the 34 % difference in the k_{ins}, 43 % difference in the $h_{w,in}$, and 860 % difference in the $h_{w,out}$ were cause for concern about the usefulness of the empirically determined coefficients. In the case of $h_{w,in}$ and $h_{w,in}$, the difference were somewhat larger than expected. The increase in the $h_{w,in}$ value seemed reasonable when one considers that the air velocity inside the test chamber increased 33 % from proximately 30 *cfm* to 40 *cfm*. However, the cause for the 34 % increase in k_{ins} remains unknown. The 880 % decrease in the $h_{w,out}$ value also remains a mystery.

From these problems with empirically determining k_{ins}, $h_{w,in}$, and $h_{w,out}$, it can be concluded that future efforts should utilize a velocity dependent $h_{w,in}$ and a $h_{w,out}$ that includes radiative and convective components. For the remainder of the dynamic F.D. calculation, the average values of 0.045 (Btu-ft/hr-ft^2-°F), 2.8 (Btu/ hr-ft^2-°F), and 5.25 (Btu/ hr-ft^2-°F) were used for k_{ins}, $h_{w,in}$, and $h_{w,out}$ respectively. Since this problem could not be adequately resolved in this dissertation, the SFD simulated solar heat gain was compared against the transmitted solar measurements using the Li-Cor sensor inside the window pane.

6.2.3 Results of Comparison of the SolrCalc Program versus Measured Solar Data

The proposed solar simulation program, the Solar Data Calculator (SolrCalc) program, is capable of using three different models for calculating solar radiation including the ASHRAE (1997), Duffie & Beckman (1991), and Kreider and Rabl (1994) methods as described in Chapters VI and V.

As the window area was blocked with insulation in experimental cases 1 and 2, the heat transfer through a window system was not compared. Thus, the measured data of the incident solar radiation on the south vertical surface was validated against the simulated results in this section. In the following section, the measured data was compared against the results from the DOE-2 program.

To compare the simulated data against the measured data, various solar radiation components including beam normal, global horizontal, diffuse horizontal and vertical south solar radiation were calculated in 15-minute intervals. The solar angles including declination, solar altitude, and solar azimuth angles were also calculated and included in the same file. In this case, the calculated time difference between the solar time and local standard time was minus 9 minutes 13 seconds and the declination angle was -15.96°. As the SolrCalc program itself calculated the solar time for each local standard time during the solar radiation calculation, the time shift was not needed.

Figures 6.9, 6.10 and 6.11 show the simulated solar radiation using the ASHRAE, Duffie & Beckman, and Kreider and Rabl methods plotted against the measured solar radiation respectively.

The ASHRAE (1997) method provided about a 10.5 percent larger value for the peak beam normal radiation than the measured radiation. It also provided 17.7 percent and 17.1 percent larger values than measured data for the peak global horizontal solar radiation and solar radiation on a south vertical surface respectively. The ASHRAE method, however, provided 9.9 percent smaller value for the peak diffuse solar radiation. Generally, the ASHRAE method provided over-estimated values for beam and global horizontal solar radiation as well as solar radiation on a vertical surface and an under-estimated value for diffuse solar radiation.

Duffie and Beckman (1991) and Kreider and Rabl (1994) provided very similar solutions for the solar radiation calculation when compared against each other as expected. Although these methods created much closer values to the measured solar radiation, there were still about 7 or 8 percent differences in the calculations of beam normal radiation. The simulated diffuse horizontal radiation had a 15 percent larger values than the measured data. In general, these methods provided more reliable global horizontal and vertical solar radiation calculations

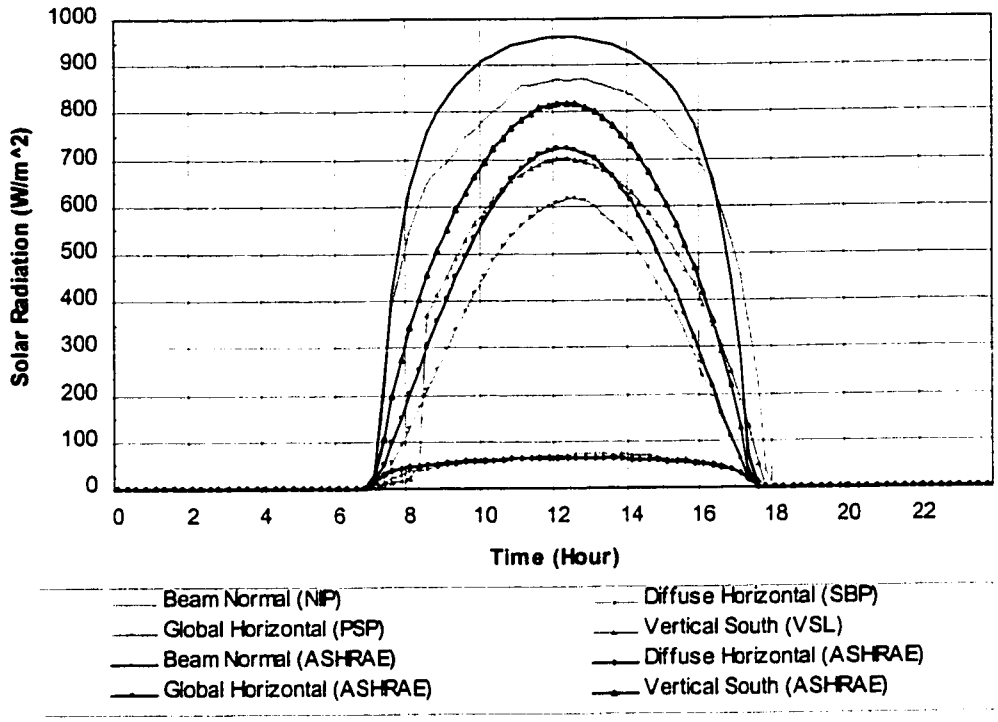

Figure 6.9 Solar Radiation Calculated Using the ASHRAE (1997) versus Measured Solar Radiation (Case 2, 11/03/98).

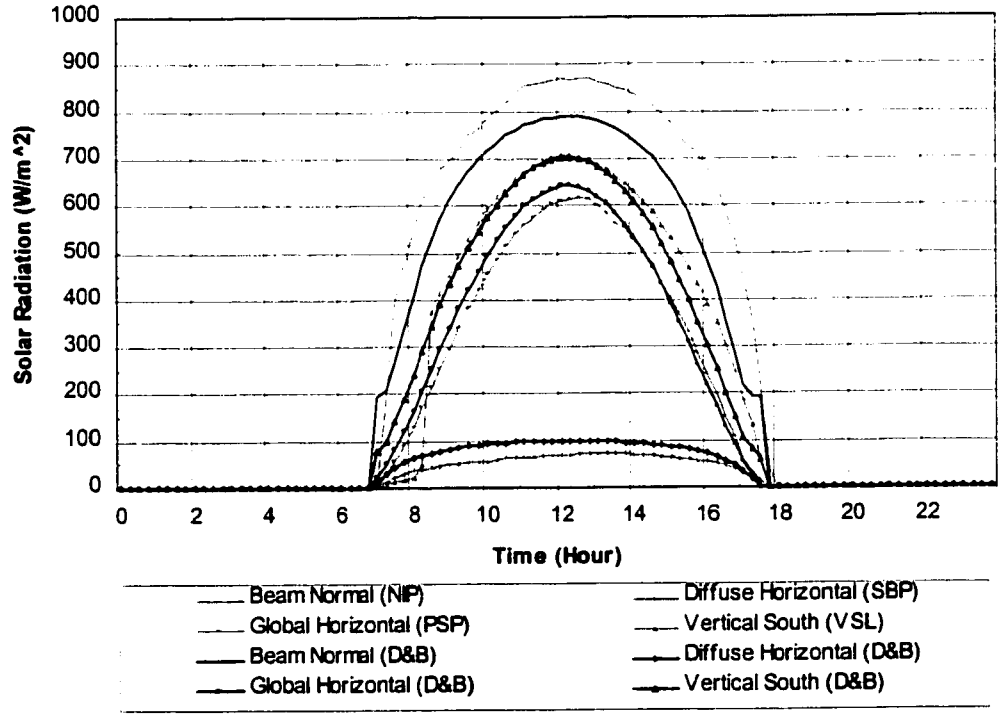

Figure 6.10 Solar Radiation Calculated Using Duffie and Beckman (1991) versus Measured Solar Radiation (Case 2, 11/03/98).

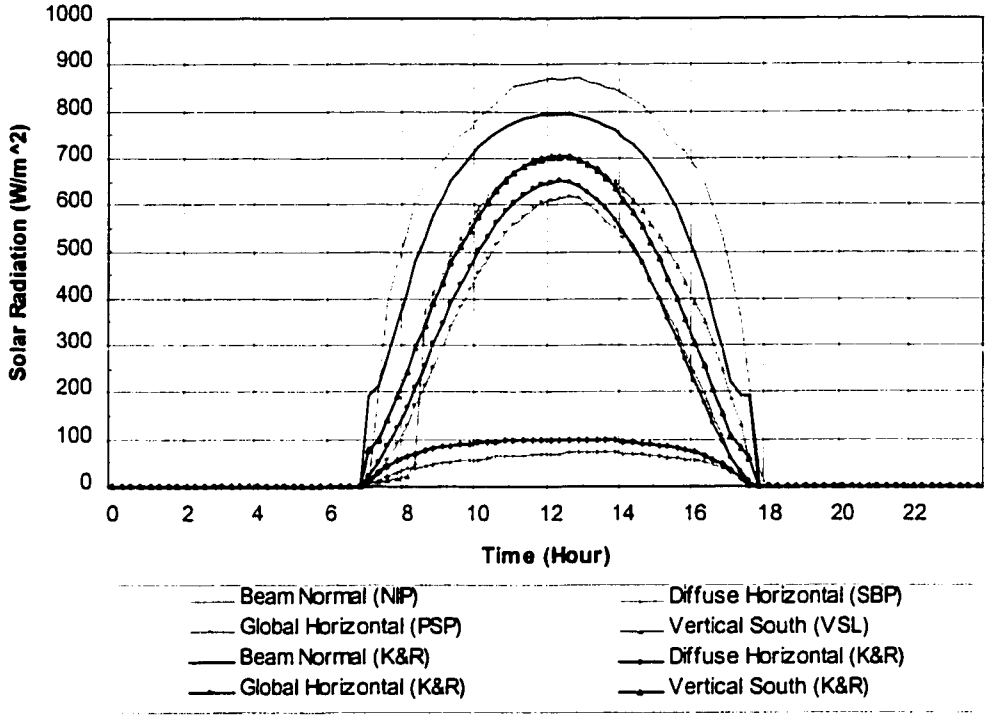

Figure 6.11 Solar Radiation Calculated Using Kreider and Rabl (1994) versus Measured Solar Radiation (Case 2, 11/03/98).

than the ASHRAE equations. However, it may be difficult to obtain very accurate beam normal radiation values from these methods.

6.2.4 Results of Comparison of the DOE-2 Program versus Measured Solar Data

As described in Section 4.5, two versions of DOE-2 simulations were compared against the measured data. The first DOE-2 simulation used a weather file created by overwriting the real data onto a TMY file as described in Section 4.5.3. When the weather file is packed, the DOE weather packer interpolates the data during the time conversion processes from the solar time data into the local standard time. Figure 6.12 shows the DOE-2 simulated solar radiation using a packed weather file plotted against the measured solar radiation. This figure clearly shows the smooth curves of the interpolated solar radiation data created by the DOE-2 weather packing processor. This version of the DOE-2 simulation provided most reliable results for horizontal and vertical solar radiation calculations. There were less than 2 percent differences between the DOE-2 simulated results and the measured solar data. However, as it does not provide the hourly report for diffuse horizontal radiation, there was no method to validate simulated diffuse solar radiation using this method.

The second DOE-2 simulation was conducted using the DESIGN-DAY instructions. From the measured weather data, the maximum and minimum outside weather conditions were given into the DOE-2 input file. When DESIGN-DAY instructions are given, the DOE-2 program itself calculates solar radiation and the heat transfer using the ASHRAE algorithms (ASHRAE 1997, LBL 1982b) described in Section 2.3. Figure 6.13 shows the DOE-2 simulated solar radiation using DESIGN-DAY instructions plotted against the measured solar radiation from the experiment. The result shows that there was about 11 percent differences in the maximum values of beam normal and diffuse horizontal calculations and about 20 percent differences in the other solar radiation calculations compared with the measured solar radiation.

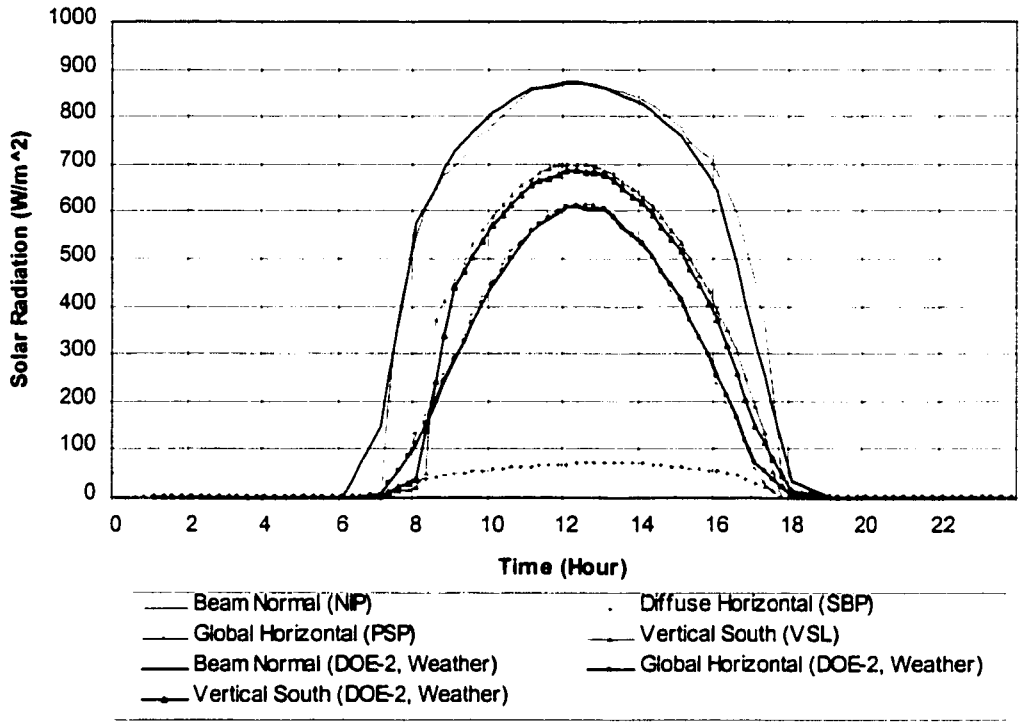

Figure 6.12 DOE-2 Simulated Solar Radiation Using the Packed Weather File versus Measured Solar Radiation (Case 2, 11/03/98).

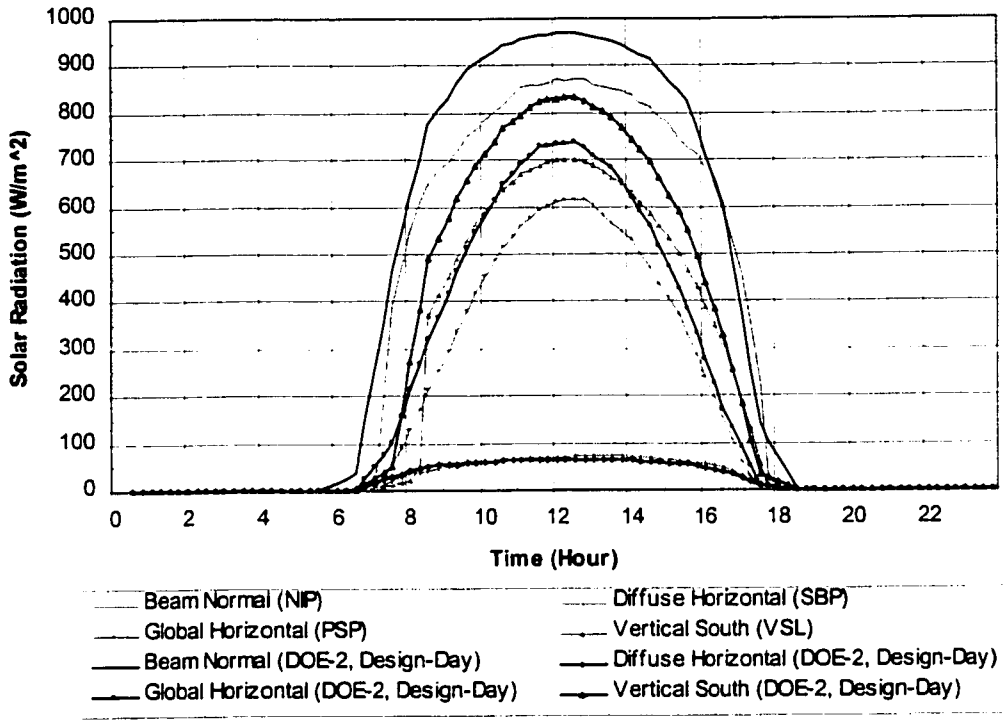

Figure 6.13 DOE-2 Simulated Solar Radiation Using the DESIGN-DAY Instructions versus Measured Solar Radiation (Case 2, 11/03/98).

6.2.5 Summary of Comparison of Horizontal and Vertical Solar Radiation Calculations

The previous sections described the measured data, the results from a finite difference model, the DOE-2 simulation results, and the simulation results from the proposed program

There are several features in the data that warrant further discussion. First, there was no significant difference between the measured data and the data in the packed file for the DOE-2 weather input. The data calculated by the ASHRAE method was very close to the DOE-2 simulated data using the DESIGN-DAY instructions. In general, these methods over-estimated the measured data by about 10 percent in beam normal calculations. In contrast, the results from Duffie and Beckman method and Kreider and Rabl method under-estimated the measured data by about 7 to 8 percent. Thus, when we have to use a simulated beam normal radiation, the simulation equation should be modified to obtain mid values from the ASHRAE method and Duffie and Beckman's method.

The calculation of horizontal global radiation is one of most important processes in the solar radiation simulation. Most weather data files contain only global horizontal radiation, and

the beam and diffuse components are calculated using Erb's equation as described in Section 4.2. The ASHRAE method, which is included in the DOE-2 simulation using the DESIGN-DAY instruction, resulted in about 20 percent over-estimation in the peak global radiation on a horizontal surface. However, the other simulation methods provided better results within about 5 percent of the measured data.

Usually, the calculation of diffuse solar radiation produces more errors comparing with other kinds of solar radiation. In the same fashion as the calculation of the beam normal radiation, the ASHRAE clear sky method under-estimated the amount of diffuse horizontal radiation, whereas Duffie and Beckman's method and Kreider and Rabl's method over-estimated it. The simulation error in this calculation was about twice as large as that used in the calculation of the beam normal radiation. None of these methods provides an estimate that is close enough to the measured data. Although there were large errors in the calculation of the diffuse solar radiation, in most cases it does not make a big difference in the total heat gain through a window system. The reason for this is that the amount of diffuse solar radiation represents a small portion of the transmitted solar radiation through the window glazing compared with the direct solar radiation transmitted.

Finally, since there was a significant difference in the estimation of horizontal solar radiation, this carries over into the vertical solar radiation calculation. The ASHRAE method produced about 20 percent over-estimation in the calculation of the peak values of vertical solar radiation compared with the measured data. However, Duffie and Beckman's method as well as Kreider and Rabl method provided better results within 3 percent differences.

Table 6.7 summarizes the peak solar radiation results to compare simulated values against the measured data for the experiment case 2. In general, Duffie and Beckman method provided the most reliable results except the DOE-2 simulation using a packed weather file, whereas the DOE-2 simulation created the worst results in the solar radiation calculation. Amazingly enough, Duffie and Beckman method created smaller difference in the calculation of south vertical solar radiation than in the calculation of global horizontal solar radiation and even normal beam radiation. This result is caused because the under-estimation of beam normal radiation is counter-balanced with the over-estimation of diffuse solar radiation.

Table 6.7 Peak Solar Radiation Simulated in Various Methods and Their Percentage Differences from the Measured Data (W/m^2) (Case 2, 11/03/98).

Calculation Method	Beam Normal	Diffuse Horizontal	Global Horizontal	Vertical South
Measured Data	869.8	72.0	616.0	700.8
DOE-2 / DESIGN-DAY	969.5 (11.5 %)	64.4 (-10.57 %)	739.5 (20.1 %)	833.5 (19.0 %)
DOE-2 / Weather file	873.9 (0.5 %)	- -	608.9 (-1.2 %)	688.6 (-2.0 %)
ASHRAE	960.8 (10.5 %)	64.9 (-9.9 %)	725.2 (17.7 %)	820.6 (17.1 %)
Duffie & Beckman	789.3 (-9.3 %)	99.7 (38.6 %)	642.2 (4.3 %)	703.2 (0.3 %)
Kreider & Rabl	795.0 (-8.6 %)	100.4 (39.5 %)	650.7 (5.6 %)	705.0 (0.6 %)

6.3 Experimental Case 3: Transmittance of Solar Radiation through Glazing

This experiment was focused on the calculation of the transmittance of incident solar radiation through a non-shaded window glazing. The main objective of this experiment was to validate how the proposed model's Fresnel equations perform against the measured data. The experiment was conducted using the following procedure.

A 1/8-inch single-pane glass was installed in the window aperture. Two Li-cor solar sensors were installed to measure the global solar radiation on a vertical surface and the transmitted solar radiation through window glazing. Thus, one of the sensors was installed at the center of the outside surface of the glazing and the other at a slightly higher position on the inside surface. A slight gap was left between the sensor and glass to prevent conductive heat gain from the glazing. These solar sensors were calibrated just before they were installed. No shading devices were installed during the experimental period.

6.3.1 Measured Results from the Experimental Box (Solar Transmittance Test)

Figures B.11 to B.15 in Appendix B show the measured data from this experimental case. Figure 6.14 shows the solar radiation values measured from the solar test bench and the experimental box that include the beam normal, the diffuse horizontal, the global horizontal, the

vertical south, and the transmitted solar radiation through the south facing window glazing. From this figure we can see the experimental box was blocked by the external objects until about 8:30 a.m. in the morning.

Figure 6.15 shows the solar transmittance of the south facing window glazing of the experimental box plotted against the predicted transmittance curve calculated by Fresnel's equation that was used in the SolrCalc program. The solar transmittance of the window glazing was derived by comparing the vertical solar radiation measured inside the glazing to the solar radiation measured outside the glazing. Fresnel's curve was plotted using Equation 2.26. The solar absorption (α) of the inside test chamber surfaces was calculated using Equation 2.27 by assuming that the value of the absorptance of the test chamber (α) equals 1.0. The value for the index of refraction (n) of glass for the solar spectrum was set to 1.526. The product of the extinction coefficient and the thickness of glazing (KL) provided the best result when it was set to 0.125. As we can see from the figure, the minimum solar incidence angle was about 58 degrees and its solar transmittance was about 0.7. A significant disagreement can be observed when the angle of incidence was larger than 70 degrees. This disagreement was caused by the shading of the external objects in the morning and the increase of the diffuse radiation fraction compared to the total incident solar radiation at sunrise and sunset hours.

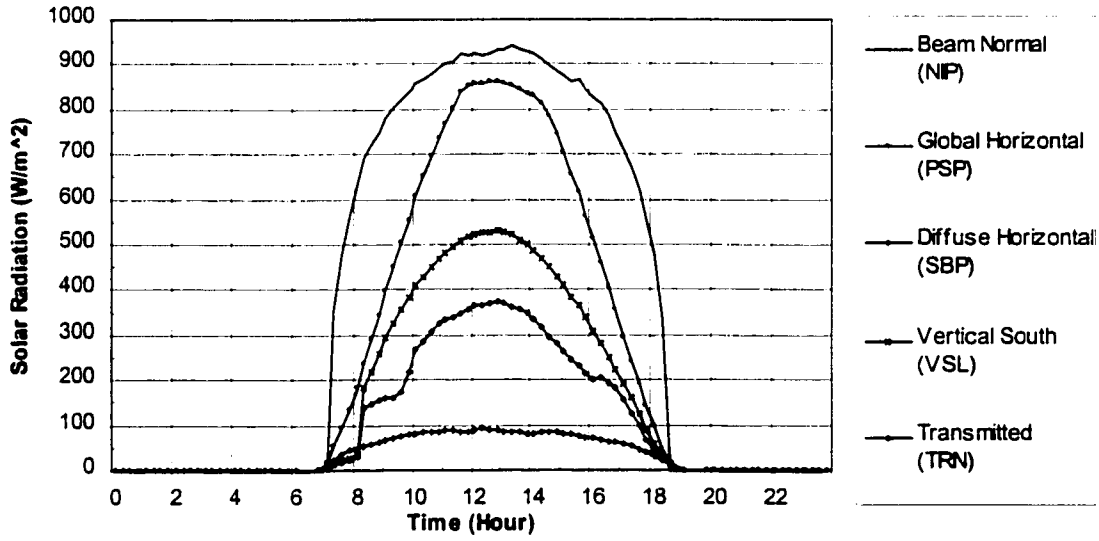

Figure 6.14 Measured Solar Radiation for the Solar Transmittance Test (Case 3, 03/22/99).

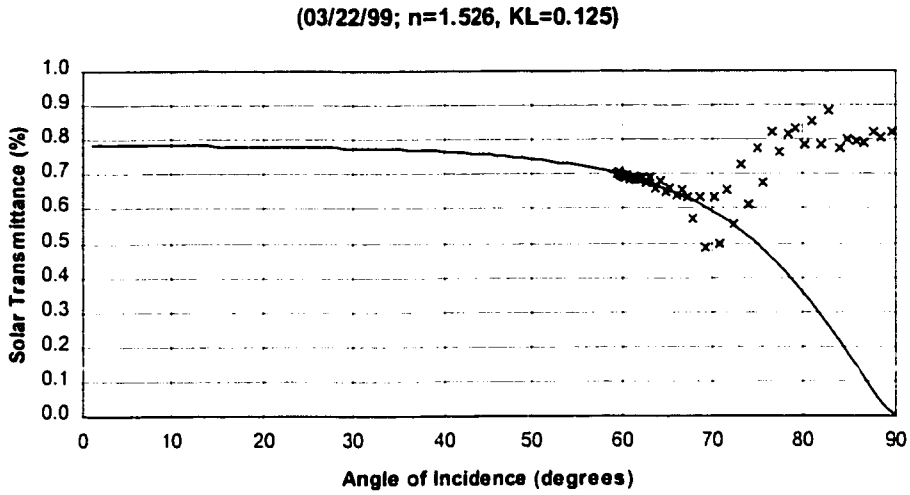

Figure 6.15 Solar Transmittance through a Single Glazing vs. Incidence Angles (Case 3, 03/22/99).

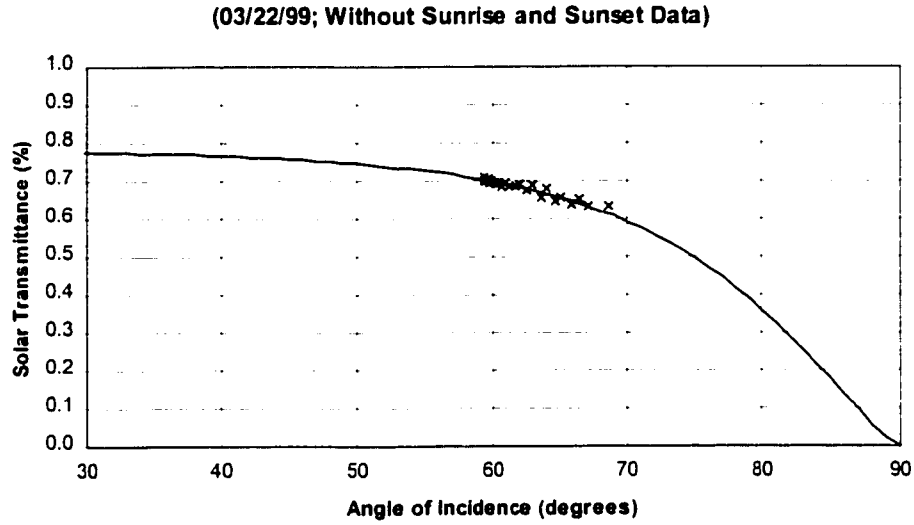

Figure 6.16 Solar Transmittance through Glazing vs. Incidence Angles after Data Cleaning (Case 3, 03/22/99).

Figure 6.16 shows how Fresnel's equation matches with the solar transmittance derived from the measured data when the data in the sunrise and sunset hours were removed. Figure 6.17 shows the transmittance of the window glazing for the incident solar radiation on a cloudy day. This figure clearly shows the diffuse solar radiation is not angle-dependent but constant with a value of 0.8. Thus, during those times when the solar incidence angle is very low, the actual transmitted solar radiation through vertical window glazing could be much larger than the simulated solar radiation using Fresnel's equation. Therefore, the estimation of the transmitted

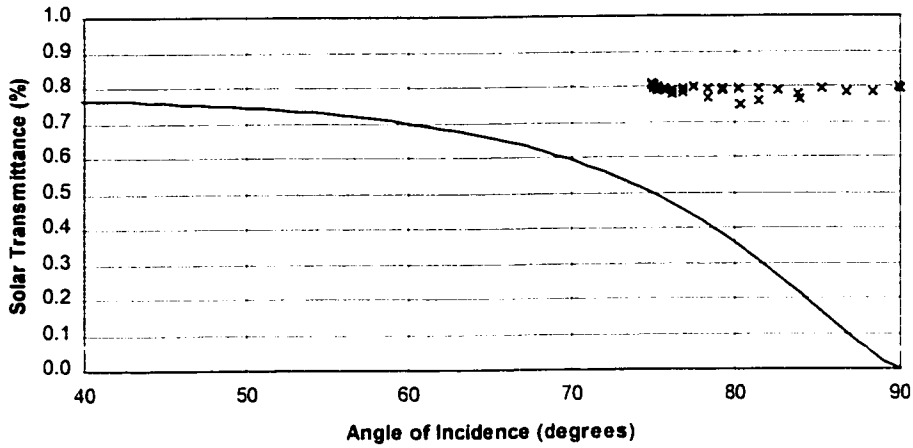

Figure 6.17 Solar Transmittance through Glazing vs. Incidence Angles on a Cloudy Day (05/03/99).

solar radiation on a cloudy day should be determined by the average solar property of the glazing for diffuse radiation not by the incidence angle dependent calculation.

6.3.2 Results from the Finite Difference Model (Solar Transmittance Test)

A finite difference model was developed following the same procedure described in Section 6.1.2. The values for the convection coefficient between the room air and the inside wall surface ($h_{w,in}$) and between the ambient air and the outside wall surface ($h_{w,out}$), as well as the thermal conductivity of insulation (k_{ins}) were set to the average values that were calculated in the Experimental Cases 1 and 2 (see Section 6.2.2). In contrast to the previous cases, this case had heat gain through the window glazing. To solve the problem, the inside convection coefficient ($h_{g,in}$) of the glazing was calculated in advance of the calculation of the temperatures at the nodes. A linear regression analysis was applied again as in the previous cases. Table 6.8 shows the values used to determine $h_{g,in}$ and the calculated values of R^2.

Figure 6.18 shows the calculated heat transfer including heat removed by the an. inside and outside convection of walls, conduction through walls, and the inside convection of the

Table 6.8 Calculated R^2 Values for the Various $h_{g,in}$ Values (Case 3, Solar Transmittance Test).

$h_{g,in}$	3	4	5	5.1	5.2	[illegible]	5.4	5.5	5.6
R^2	0.9607	0.9730	0.9763	0.9764	0.9764	[illegible]	0.9764	0.9763	0.9762

glazing. In general, the heat transfer calculated using a F.D. model matched the measured, transmitted solar heat gain within the error of this test box. The positive heat transfer values (i.e., about 50 *Btu/hr*) prior to sunrise and following sunset are due mostly to the drop in inlet temperature below the inside temperature of the test chamber which caused the chamber to slowly release heat throughout the night.

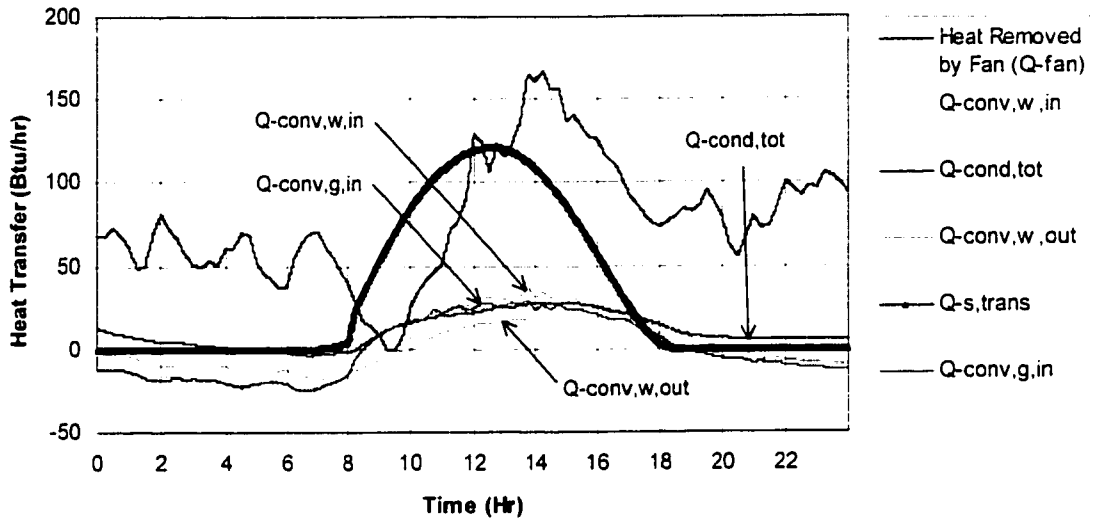

Figure 6.18 Finite Difference Model Calculated Heat Transfer of the Experimental Box (Case 3, 03/22/99).

6.3.3 Results of Comparison of Transmitted Solar Radiation Calculations

The SolrCalc program uses an anisotropic sky model (i.e., HDKR model) for the calculation of the transmitted solar radiation through a vertical window glazing. To compare the simulated result with the measured data, the transmitted solar radiation was calculated using the Equation 2.26. In this case, the calculation of the incident solar radiation on a vertical surface was calculated using the method outlined in Duffie and Beckman (1991).

Figure 6.19 shows the simulated transmitted solar radiation using the SolrCalc program and the DOE-2 program plotted with the measured transmitted solar radiation. From this figure, we can see the simulated solar radiation using the SolrCalc program over-estimates during mid-day and under-estimates at sunrise and sunset hours.

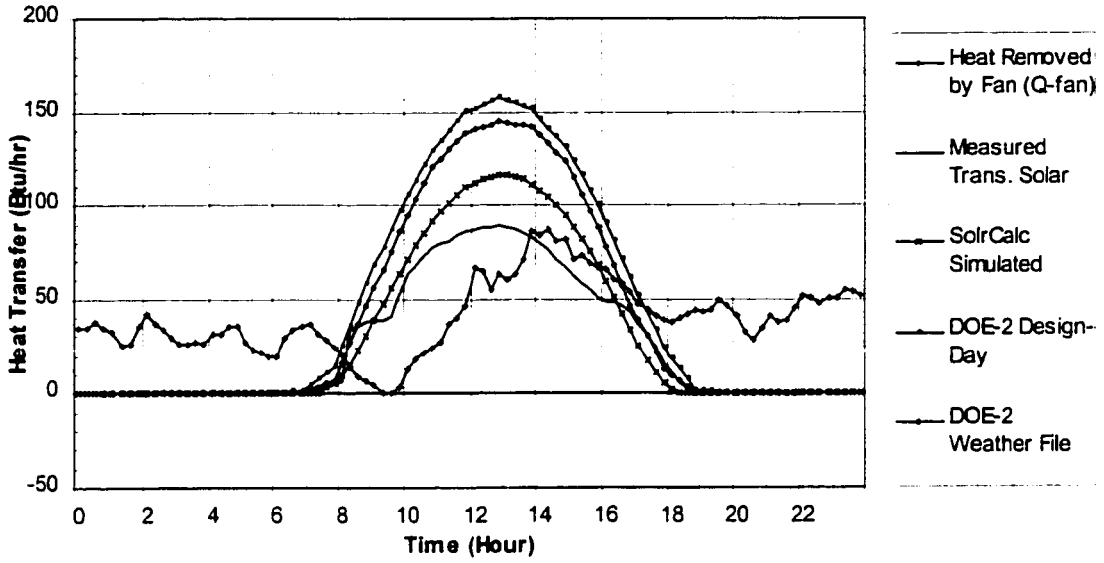

Figure 6.19 Transmitted Solar Radiation Simulated by the SolrCalc Program and the DOE-2 Program Plotted against Measured Transmitted Solar Radiation and Heat Removed by the Fan (Case 3, 03/22/99).

The transmitted solar radiation simulated by the DOE-2 program using the DESIGN-DAY instructions showed the largest difference in the calculation of the transmitted solar radiation. Even when the measured data were used, the DOE-2 simulation still showed a significant difference in the calculation of the transmitted solar radiation.

Table 6.9 shows the daily solar heat gains through glazing that were measured and simulated using the SolrCalc program and the DOE-2 program for March 22, 1999. In this table, the heat removed by the fan was calculated for the hours from sunrise to sunset to. This table clearly shows the SolrCalc program compares favorably with both the measured heat gain (Q_{fan}) and the measured, transmitted solar radiation. The transmitted solar radiation simulated using the SolrCalc program provided a 19.2 percent larger than the measured, transmitted solar radiation. The DOE-2 program provided more than a 50 percent difference in the transmitted solar radiation even when the packed weather file was used. The measured heat removed by the fan during the period from sunrise to sunset was 11.5 percent smaller than the measured transmitted solar radiation. The small shoulder in the early morning and late afternoon measured transmitted solar radiation is most likely due to reflected radiation. The heat gain before sunrise and after sunset represents dynamic effects of the experimental box.

Table 6.9 Daily Solar Heat Gains through the Glazing Using Measured and Various Simulated Methods (Btu/day) (Case 3, 03/22/99).

Calculation Method	Daily Total Radiation	Difference
Measured Transmitted Solar Radiation	613.1	-
Measured Heat Removed by the Fan	542.7	-70.4 (-11.5 %)
SolrCalc Simulated	730.7	117.6 (19.2 %)
DOE-2 / DESIGN-DAY	1,078.7	465.6 (75.9 %)
DOE-2 / Weather file	959.3	345.9 (56.4 %)

Note: Measured heat removed by the fan includes the period from sunrise to sunset.

6.4 Experimental Case 4: Heat Transfer of a Shaded Fenestration System (Left-fin Shade)

In the pervious experiments, no shading device was applied in the window. In other test cases, various configurations of shading devices were installed around the window to test the effects of shading devices including: an overhang shade (case 6), a right-fin shade (case 7), a left-fin shade (case 4), and compound shades of an overhang and side fins (case 8). All the measured results from these experiments as well as the transmitted solar radiation simulated using the DOE-2 program are included in Appendix B. In this section, the experiment case using a left-fin shade is described as an example of the heat transfer of a shaded fenestration system.

6.4.1 Measured Results from the Experimental Box (Left-fin Shade)

Figure 6.20 shows the experimental box with a left-fin shade. Using the SFD program, it was determined that a point at the midpoint of the bottom of the window was completely shaded from beam radiation at 1 p.m. in solar time. Figure 6.21 shows the measured temperatures from the test chamber and includes the glazing temperatures of the left and right half of the pane of glass. The results of the experiment show the left glazing temperature dropping at 1:00 p.m. and the right glazing temperature dropping at about 2-3 p.m. which agrees well with the shading projections from the SolrCalc program.

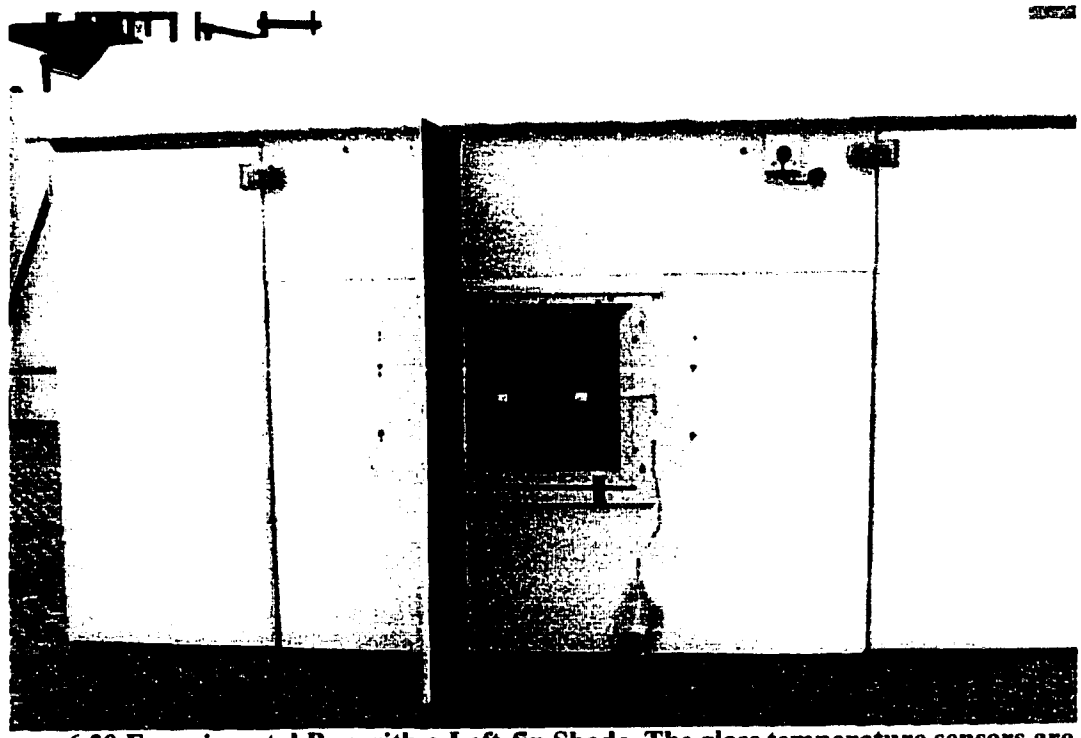

Figure 6.20 Experimental Box with a Left-fin Shade. The glass temperature sensors are the two white dots on the glass pane.

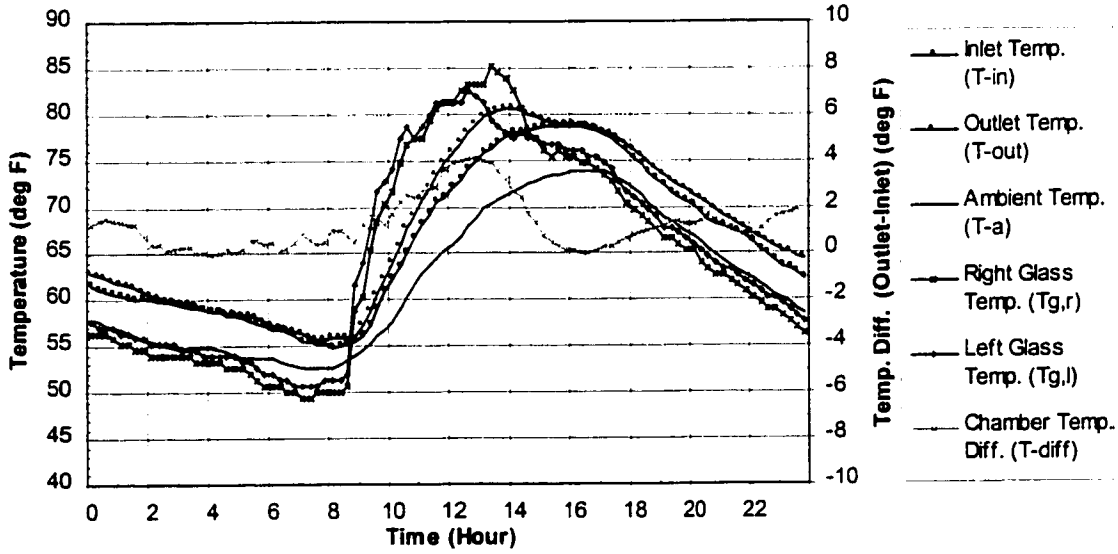

Figure 6.21 Measured Temperature from the Experimental Box with a Left-fin Shade (Case 4, 01/25/99).

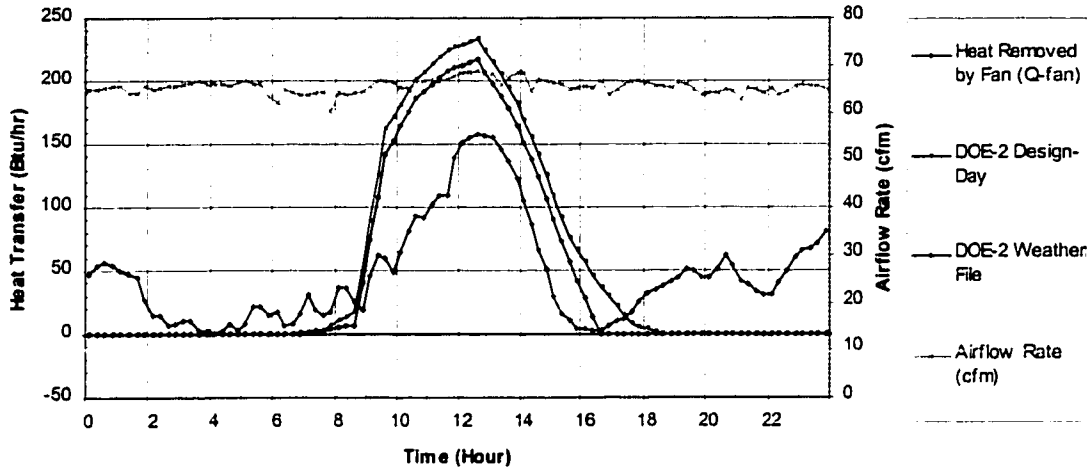

Figure 6.22 Transmitted Solar Radiation Simulated Using the DOE-2 Program Plotted against Heat Removed by Fan (Case 4, 01/25/99).

6.4.2 Results of Comparison of Heat Transfer of a Shaded Fenestration System

Figure 6.22 shows the transmitted solar radiation simulated using the DOE-2 program and the heat removed by the fan (Q_{fan}). The heat removed by the fan from sunset and sunrise was 719.9 *Btu/day*. The solar heat gains from the window calculated using the DOE-2 program were 1,298.2 *Btu/day* for the DESIGN-DAY instructions and 1,121.6 *Btu/day* for the weather file respectively (see Table B.2 in Appendix. B). The DOE-2 program appears to clearly overstate the transmitted solar gain through the window.

Figures B.28, B.33, and B.38 show the DOE-2 simulated transmitted solar radiation plotted against the measured heat removal by the fan for the shading cases of an overhang, a right-fin, and a compound shades respectively. The measured and simulated results of daily solar heat transfer through a shaded window of the experiment box for each configuration of shading devices are summarized in Table B.2 in Appendix B.

CHAPTER VII

SUMMARY AND CONCLUSIONS

7.1 Summary of Study Objectives

The goal of this study was to develop and validate a computer-aided simulation model for the shading and thermal analysis of a shaded fenestration system. To achieve this goal, several objectives had to be met: 1) to develop an accurate and visually effective methods to calculate and view the sun angles, solar radiation, and the thermal performance of the fenestration systems, 2) to develop and test a computerized shaded fenestration system design model which incorporates accurate, complex energy analysis into a window and shading device design tool, 3) to validate portions of the computerized solar simulation model against other models and against the measured data gathered from a specially constructed test box, and 4) to develop methods that help the user to clearly visualize the energy impacts with a proper self-guided user interface.

7.2 Summary of Methodology

The developed methodology includes: 1) graphical display methods for displaying solar data and shading devices; 2) the calculation of the total transmitted solar heat gain through a single glazed unshaded window; 3) validation of the simulation against measured data, and 4) a comparison of the model against a previously validated simulation program (i.e., DOE-2).

Five methods were developed to display the path of the sun, the shading of external surfaces, and solar data. These projection methods include: equidistant, orthographic, stereographic, gnomonic, and cylindrical projections. The geometrical descriptions and equations for plotting orthographic, stereographic, gnomonic, and cylindrical projections are believed to be original work. New techniques such as applying a color scale to display the various kinds of solar radiation onto a sun path diagram as well as onto a psychrometric chart are also presented.

Three different solar models were used in the development of a computer-aided simulation method. These methods include the methods developed by the ASHRAE Handbook (1997), Duffie and Beckman (1991), and Kreider and Rabl (1994). For the diffuse sky

simulation, an improved anisotropic model, the HDKR model (Reindl et al. 1990) was applied. The ray-tracing technique with Fresnel's equation was used to calculate the transmittance of the incident solar radiation through window glazing (Duffie and Beckman 1991). Methods used to calculate the sunlit factor (i.e., the factor of sunlit area to the total area of the surface) from the beam radiation were also reviewed. The calculation of the total heat gains and losses through a shaded window glazing, the convective and radiative heat transfer between the glazing and the room air were also reviewed.

7.3 Summary of the Computer Model

The proposed computer model, the Shaded Fenestration Design (SFD) model, is a combined program for the shading design and thermal analysis of windows using new techniques for the various graphical displays of solar, shading, thermal data. The SFD model provides four major functions including: 1) a design tool for window and shading devices, 2) display of solar and shading information, 3) thermal performance simulation of unshaded fenestration systems, and 4) weather data conversion.

The SFD model consists of the Main program and three add-in programs including the Solar Data Calculator (SolrCalc), the Weather Data Displayer (WethDisp), and the Weather Data Converter (DataConv). The Main program provides a user-friendly graphical interface for the design of window glazing and shading devices. These graphical interface includes the various projections of sunpath diagrams as well as display of solar data onto the sunpath diagram. The Main program also calculates the total heat gain and loss through window glazing. The various kinds of solar radiation can be calculated with the aid of the SolrCalc program and can be displayed in one of various graphical display modes or a tabular display mode using the WethDisp program. The DataConv program converts the intervals of data using the linear interpolation and changes time stamps between the solar time and the local standard time.

7.4 Summary of Validation

The experimental validation of the proposed model was a major task in this research. The validation was conducted through the experimental validation using the measured data from an experimental test box and a comparative validation against the previously validated simulation program, the DOE-2 program (LBL 1991).

The experimental box was constructed adjacent to a NIST-calibrated solar test bench (Munger 1997). Vertical solar radiation, the temperature difference between the inlet air and the outlet air, and the airflow as measured by the pressure difference measured across an AMCA airflow nozzle were collected as well as selected data sets that including the glass temperature and a transmitted solar measurement. A finite difference (F.D.) model was also developed and applied to calculate the dynamic heat transfer through the walls of the experimental box.

Selected results from the measured data were compared with the simulations from the SFD model as well as simulations from the DOE-2 program. The validation results showed that the solar simulation method developed by Duffie and Beckman provides closer results to the measured data than the methods used by the ASHRAE Handbook and the DOE-2 program. The comparison of the SFD model's transmitted solar radiation agreed reasonably well with both the measured, transmitted solar radiation and the measured heat gain (Q_{fan}), and outperformed the DOE-2 program.

7.5 Recommendations for Future Research

This experimental research was limited to a single-glazed window. Thus, the heat transfer through multi-pane glazing and window systems having the various thermal properties such as the effects of frames and dividers, the glazing type, and various weather conditions will need to be performed to provide more a widespread application of the SFD model.

Future improvements to the experimental test box include: 1) surface temperatures measured inside and outside the box, 2) continuous solar measurements at multiple points inside the glazing, 3) consideration of the specific heat of the moisture in the air, 4) development of a velocity dependent inside convection heat transfer coefficient, 5) consideration of wind and solar effects on the exterior surface coefficient, 6) improved glass temperature measurement (e.g., embedded thermocouples), 7) additional experiments on 2-pane and 3-pane windows, 8) extension of the F.D. equation to allow the calculation of a shaded fenestration.

REFERENCES

Abouella, N. and M. Milne. 1990. OPAQUE: A microcomputer tool for designing climate responsive opaque building elements. *Proceedings of the Fourth National Conference on Microcomputer Applications in Energy.* Tucson, AZ.

Anderson, E. E. 1983. *Fundamentals of Solar Energy Conversion.* Addison-Wesley Publishing Company, Reading, MA.

ANSI/AMCA. 1985. *Laboratory Methods of Testing Fans for Rating.* American National Standards Institute (ANSI)/ Air Movement and Control Association (AMCA) Standard 210-85 and ANSI/American Society of Heating, Refrigerating and Air-conditioning Engineers (ASHRAE) Standard 51-1985, Atlanta, GA.

Arasteh, D. K., E. U. Finlayson, and C. Huizenga. 1994. *Window 4.1: A PC Program for Analyzing the Thermal Performance of Fenestration Products.* Lawrence Berkeley Laboratory, LBL-35298, March, Berkeley, CA.

Aronin, J. E. 1953. *Climate & Architecture.* Reinhold Publishing Corporation, New York, NY.

ASHRAE. 1997. *1997 ASHRAE Handbook - Fundamentals.* American Society of Heating, Refrigerating and Air-conditioning Engineers Inc., Atlanta, GA.

ASHRAE. 1991. *HVAC Applications.* American Society of Heating, Refrigerating and Air-conditioning Engineers Inc., Atlanta, GA.

ASHRAE. 1977. *1977 ASHRAE Handbook - Fundamentals.* American Society of Heating, Refrigerating and Air-conditioning Engineers Inc., Atlanta, GA.

ASHRAE. 1976. Procedures for Determining Heating and Cooling Loads for Computerized Energy Calculations: Algorithms for Building Heat Transfer Subroutines. American Society of Heating, Refrigerating and Air-conditioning Engineers, Atlanta, GA.

ASHRAE. 1975. *Subroutine Algorithms for Heating and Cooling Loads to Determine Building Energy Requirements.* Compiled by Subcommittee for Heating and Cooling Loads. ASHRAE Task Group on Energy Requirements, Atlanta, GA.

Baecker, R.M, J. Grudin, W. A. S. Buxton, and S. Greenberg. 1995. *Readings in Human-Computer Interaction: Toward the Year 2000.* 2nd ed. Morgan Kaufmann Publishers, Inc., San Francisco, CA.

Baltrip, K. 1997. The effect of fan and heat sink design on heat removal from microprocessor chips. M.S. Thesis, Texas A&M University, College Station, TX (December).

Beckman, W. A., S. A. Klein, and J. A. Duffie. 1977. *Solar Heating Design by the f-Chart Method.* John Wiley & Sons, Inc., New York.

Bennett, R. 1978. *Sun Angles for Design,* Robert Bennett, Bala Cynwyd, PA.

Bird, R. E. and R. L. Hulstrom. 1981. *A Simplified Clear Sky Model for Direct and Diffuse Insolation on Horizontal Surfaces.* SERI/TR-642-761. Solar Energy Research Institute, Golden, CO.

Boecker, C. 1997. *Calibration Procedure for Solar Sensors,* Memorandum for Energy Systems Laboratory, Texas A&M University, College Station, TX.

Bou-Saada, T. E. 1994. An improved procedure for developing a calibrated hourly simulation model of an electrically heated and cooled commercial building. M.S. Thesis, Texas A&M University, College Station, TX. (Also available Energy Systems Laboratory Report No. ESL-TH-94/12-01).

Bronson, J. D. 1992. Calibrating DOE-2 to weather and non-weather-dependent loads for a commercial building. M.S. Thesis, Texas A&M University, College Station, TX. (Also available Energy Systems Laboratory Report No. ESL-TH-92/04-01, Volume I).

BSO. 1993. *BLAST User Reference*. Blast Support Office. Department of Mechanical and Industrial Engineering, University of Illinois at Urbana-Champaign.

CEN. 1995. *Thermal Performance of Buildings - Internal Temperature in Summer of a Room without Mechanical Cooling - General Criteria and Calculation Procedures*. CEN TC89. European Committee for Standardization, Brussels.

Clarke, J. A. 1982. Computer applications in the design of energy-conscious buildings. *Computer Aided Design* 14(1): 3-9.

Clarke, J. P., J. Hand, J. Hensen, C. Pernot, and E. Aasem. 1993. *ESP-r, A Program for Building Energy Simulation Version 8 Series*. ESRU Energy Simulation Research Unit, University of Strathclyde, Glasgow, Scotland.

Cockroft, J. P. 1982. Validation of buildings and systems energy prediction using real measurement. *Computer Aided Design* 14(1): 39-44.

Curcija, D. and W. P. Gross. 1994. Two-dimensional finite-element model heat transfer in complete fenestration systems. *ASHRAE Transactions* 100(2): 1207-1221.

Dale, J. D. 1985. A study of passive solar heating in northern climate. *Solar Engineering*. R. B. Nannerot, ed. The American Society of Mechanical Engineers, New York: 48-56.

Danz, A. 1967. *Sun Protection: An International Architectural Survey*. Fredrick A. Praeger, Publishers, New York.

Dave, J. V. 1978. Extensive datasets of the diffuse radiation in realistic atmospheric models with aerosols and common absorbing gases. *Solar Energy* 21: 361-369.

Degelman, L. O. 1994. *EnerCAD Users Manual. Energy-based Computer Aided Design for Buildings Version 94.08*. Department of Architecture, Texas A&M University, College Station, TX.

Degelman, L. O. and V. I. Soebarto. 1995. Software description of ENER-WIN: A visual interface model for hourly energy simulation in buildings. *Proceedings of Building Simulation '95 Fourth International Conference*. International Building Performance Simulation Association, Madison, WI: 692-696.

Diamond, S. C., C. C. Cappiello, and B. D. Hunn. 1985. User-effect validation tests of the DOE-2 building energy analysis computer program. *ASHRAE Transactions* 91(2): 712-724.

Diamond, S. C. and B. D. Hunn. 1981. Comparison of DOE-2 computer program simulations to metered data for seven commercial buildings. *ASHRAE Transactions* 87(1) 1222-1231.

Dickinson, W. C. and P. N. Cheremisinoff. 1980. *Solar Energy Technology Handbook*. Marcel Dekker, Inc., New York.

Duffie, J.A. and W.A. Beckman. 1991. *Solar Engineering of Thermal Processes.* John Wiley & Sons, Inc. , New York.

Enderle, G., K. Kansy, and G. Pfaff. 1987. *Computer Graphics Programming,* 2nd ed., Springer-Verlag, Berlin.

Enermodel Engineering Limited. 1992. *FRAME: A Computer Program to Evaluate the Thermal Performance of Window Frame Systems. Version 3.0 User's Manual,* Denver, CO.

Fry M. and J. Drew. 1982. *Tropical Architecture in the Dry and Humid Zones.* 2nd ed., Robert E. Krieger Publishing Company, Malabar, FL.

Grau, K and K. Johnsen. 1995. General shading model for solar building design. *ASHRAE Transactions* 101(2): 1298-1310.

Groth, C. G. and M. Lokmanhekim. 1969. SHADOW – A new technique for the calculation of shadow shapes and areas by digital computer. *Proceedings Hawaii 2nd International Conference on System Sciences,* University of Hawaii: 471-474.

Gueymard, C. 1993. *Shading Calculations for Hourly Building Simulations: Survey of Existing Methods and New Simplified Algorithm.* FSEC-PF-250-93. Florida Solar Energy Center, Cocoa, FL.

Haberl, J, R. Lopez, and R. Sparks. 1992. *LoanSTAR Monitoring and Analysis Program: Building Energy Monitoring Workbook.* Energy Systems Laboratory Report No. ESL-TR-92/06-02, TEES, Texas A&M University, College Station, TX.

Harkness, E. L. and M. L. Metha. 1978. *Solar Radiation Control in Buildings.* Applied Science Publishers Ltd., London.

Harrison, S. J. and S. J. van Wonderen. 1994. A test method for the determination of window solar heat gain coefficient. *ASHRAE Transactions* 100(1): 1057-1064.

Hartson, H. R., D. Hix, and T. M. Kraly. 1990. Developing human-computer interface models and representation techniques. *Software - Practice and Experience* 20 (5): 425-457.

Hay, J. E. 1979. Calculation of monthly mean solar radiation for horizontal and inclined surfaces. *Solar Energy* 23: 301-307.

Hiller, M. 1996. TRNSHD - a program for shading and insolation calculations. M.S. Thesis, University of Wisconsin, Madison.

Hottel, H.C. 1976. A simple model for estimating the transmissivity of direct solar radiation through clear atmosphere. *Solar Energy* 18: 129134.

Huang, T., L. O. Degelman, and T. R. Larsen. 1992. A visualization model for computerized energy evaluation during the conceptual design stage (ENERGRAPH). *ACADIA-1992:* 195-206.

Hwang, S. 1987. SOLAR-6, a computer aided passive solar design tool. M.Arch. Thesis, University of California, Los Angeles.

Incropera, F. P. and D. P. DeWitt. 1996. *Fundamentals of Heat and Mass Transfer.* John Wiley & Sons, New York.

Irving, S. J. 1982. Energy program validation: Conclusions of IEA Annex I. *Computer Aided Design* 14(1): 33-38.

Johnson, S. A. 1985. Solar Test (SOLTST): Subroutine to solar graphics. M.Arch. & U.P. Thesis. University of Wisconsin, Milwaukee.

Judkoff, R. and J. Neymark. 1995. *International Energy Agency Building Energy Simulation Test (BESTEST) and Diagnostic Method.* National Renewable Energy Laboratory (NREL). Golden, CO.

Kerrisk, J. F., J. E. Moore, N. M. Schnurr, and B. D. Hunn. 1980. Passive-solar design calculations with the DOE-2 computer program. *Proceedings of the 5th National Passive Solar Conference.* American Solar Energy Society: 116-120.

Kim, B. S. 1992. An interface model for building energy performance simulation in an integrated computer-aided design environment. Ph.D. Dissertation, Texas A&M University, College Station, TX.

Klein, S. A. 1977. Calculation of monthly average insolation on tilted surfaces. *Solar Energy* 19: 325-329.

Klucher, T. M. 1979. Evaluating model to predict insolation on tilted surfaces. *Solar Energy* 23: 111-114.

Kreider, J. F. and A. Rabl. 1994. *Heating and Cooling of Buildings.* McGraw-Hill.

Kreider, J. F., C. J. Hoogendoorn, and F. Kreith. 1989. *Solar Design: Components, Systems, Economics.* Hemisphere Publishing Corporation, New York.

Kreider, J. F. and F. Kreith. 1981. *Solar Energy Handbook,* McGraw-Hill Book Company, New York.

Kreith, F. and Kreider, J. F. 1978. *Principles of Solar Engineering,* McGraw-Hill Book Company, New York.

LBL. 1993. *DOE-2 Supplement, Version 2.1E.* Lawrence Berkeley Laboratory and Los Alamos National Laboratory, LBL-8706 Rev. 6. Berkeley, CA.

LBL. 1982a. *DOE-2.1 Reference Manual, Rev. 2.1A.* Lawrence Berkeley Laboratory and Los Alamos National Laboratory, LBL-8706 Rev. 2. Berkeley, CA.

LBL. 1982b. *DOE-2 Engineers Manual Version 2.1A.* Lawrence Berkeley Laboratory and Los Alamos National Laboratory, LBL-11353 Rev. 2. Berkeley, CA.

Life, M. A., C. S. Narborough-Hall, and W. I. Hamilton. 1990. *Simulation and the User Interface*, Taylor & Francis, London.

Liming, R. A. 1979. *Mathematics for Computer Graphics,* Aero Publishers, Inc., Fallbrook, CA.

Liu, B. Y. and R. C. Jordan. 1963. The long-term average performance of flat-plate solar energy collectors. *Solar Energy* 7(2): 53-74.

Liu, B. Y. and R. C. Jordan. 1960. The interrelationship and characteristic distribution of direct, diffuse and total solar radiation. *Solar Energy* 4(3): 1.

LOF. 1974. *Sun Angle Calculator,* Libbey-Owens-Ford Company, Toledo, OH.

Marion, W. and K. Urban. 1995. *User's Manual for TMY2s: Typical Meteorological Years.* National Renewable Energy Laboratory (NREL). Golden, CO.

Markus, T. A. and E. N. Morris. 1980. *Buildings, Climate and Energy,* Pitman Publishing Ltd., London.

Mazria, E. 1979. *The Passive Solar Energy Book*, Rodale Press, Emmaus, PA.

McCluney, R. 1995. Software for window solar gain analysis. *Fourth International Conference Proceedings*, International Building Performance Simulation Association, Madison, WI: 653-660.

McWatters, K. and J. Haberl. 1995. A procedure for plotting of a sun-path diagram, and shading mask protractor, *Journal of Solar Energy Engineering, ASME Transactions*, 117: 153-156. (Also available Energy Systems Laboratory Report No. ESL-PA-94/07-04).

McWatters, K. and J. Haberl. 1994a. Development of procedures for the computerized plotting of a sun-path diagram and shading mask protractor, *Proceedings of the ASME/JSME/JSEE Solar Energy Conference*, San Francisco, CA, (March): 483-491.

McWatters, K. and J. Haberl. 1994b. *SOLRPATH V1.0: A Computerized Procedure forPplotting a Sun-Path Diagram and Shading Mask Protractor, Energy System Laboratory Software*, Texas A&M University, College Station, TX (March).

Messadi, M. T. 1990. Experimental validation of the procedure to determine the internal sunlit configurations. *Proceedings of the 15th National Passive Solar Conference.* American Solar Energy Society, Austin, TX: 251-256.

Milne, M., M. Vasser, and Vijay Sehgal. 1988. SOLAR-5 update: Work in progress for the new release. *Proceedings of the Third National Conference of Microcomputer Applications in Energy Conservation*, Tucson, AZ (November): 92-96.

Munger, B. and J. Haberl. 1994. An improved multipyronometer array for the measurement of direct and diffuse solar radiation, *Proceedings of the Ninth Symposium on Improving Building Systems in Hot and Humid Climates.* Dallas, TX (May): 125-131. (Also available Energy Systems Laboratory Report No. ESL-PA-94/05-04).

NFRC. 1991. *A Procedure for Determining the Thermal Properties of Fenestration Products (Currently Limited to U-values).* Standard 100-91, National Fenestration Rating Council. Silver Spring, MD.

Norman, D. 1990. Human error and the design of computer systems. *Communications of the ACM* 33(1): 4-5, 7.

Oh, J. K. and J. Haberl. 1997. New educational software for teaching the sunpath diagram and shading mask protractor. *Fifth International Building Performance Simulation Association (IBPSA) Conference*, Prague, Czech Republic, (September): I307-313.

Oh, J. K. and J. Haberl. 1996. A new MS-Windows-based educational software for teaching the sunpath diagram and shading mask protractor. *Proceedings of the 10th Symposium on Improving Building Systems in Hot and Humid Climates*, Texas Building Energy Institute, Austin, TX, (May): 262-268. Energy Systems Laboratory Report No. ESL-PA-96/05-11.

Olgyay, V. and A. Olgyay. 1963. *Design with Climate: Biological Approach to Architectural Regionalism.* Princeton University Press, Princeton, NJ.

Olgyay, V. and A. Olgyay. 1957. *Solar Control and Shading Devices*, Princeton University Press, Princeton, NJ.

Radford, A. and G. Stevens. 1987. *CADD Made Easy: A Comprehensive Guide for Architects and Designers*, McGraw Hill Book Company, New York.

Ramsey, C. G. and H. R. Sleeper. 1970. *AIA Architectural Graphic Standards*, 6th ed., John Wiley and Sons, New York: 67-76.

Rapp, D. 1981. *Solar Energy*. Prentice-Hall, Inc., Englewood Cliffs, NJ.

Reindl, D. T., W. A. Beckman, and J. A. Duffie. 1990. Evaluation of hourly tilted surface radiation model. *Solar Energy* 45: 9-17.

Schnieders, J., A. Eicker, and F. D. Heidt. 1997. SOMBRERO - Shadow calculations on arbitrarily oriented surfaces as a preprocessor for simulation programs. *Fifth International Building Performance Simulation Association (IBPSA) Conference*, Prague, Czech Republic (September): I363-368.

Schuler, M., H. Meyer, A. Knirsch, S. Holst, M. Hiller, W. A. Beckmann, and N. Blair. 1997. TRNSYS 14 goes Windows and Window 4.1 - Tool for energetic and visual building simulation. *Fifth International Building Performance Simulation Association (IBPSA) Conference*, Prague, Czech Republic (September): I33-40.

Seehof, J. M. and W. O. Evans. 1967. Automated layout design program. *Journal of Industrial Engineering* 8(12): 690-695.

SEL. 1995. *TRNSYS Manual Version 14.1*. Solar Energy Lab., University of Wisconsin-Madison.

Sheu, C. 1986. A computer aided window shading design tool: SOLAR-2.PC. M.Arch. Thesis, University of California, Los Angeles.

Soebarto, V. I. 1996. Development of calibration methodology for hourly building energy simulation models using disaggregated energy use data from existing buildings. Ph.D. Dissertation, Texas A&M University, College Station, TX.

Solar Energy Lab. 1990. *TRNSYS. A TRaNsient SYstem Simulation program*, University of Wisconsin, Madison, (September).

Sparks, R., S. Katipamula, J. Spadaro, J. Mahoney, and J. Haberl. 1993. *Documentation Manual Air, Version 1.5β*. Energy Systems Laboratory, Texas A&M University, College Station, TX.

Synergistic Control System, Inc. 1993. *Installation Manual; Survey Meter/Recorder; Model C180E, Revision A*. Synergistic Control System, Inc, Metairie, LA.

Townsend, C. and D. Feucht. 1986. *Designing and Programming Personal Expert Systems*, TAB Books Inc., Blue Ridge Summit, PA.

Trumbly, J. E., K. P. Arnett, and M. P. Martin. 1993. Performance effect of matching computer interface characteristics and user skill level. *International Journal of Man-Machine Studies* 38(5): 713-24.

Walton, G. N. 1979. The application of homogeneous coordinates to shadowing calculations. *ASHRAE Transactions* 85(1): 174-180.

Weiler, K and P. Atherton. 1977. Hidden surface removal using polygon area sorting. *Computer Graphics* 11: 214-222.

Wooldridge, M. J. and S. K. Mouer. 1982. Working in progress: Estimation of building energy use. *Computer Aided Design* 14(1): 23-26.

Wright, J. L. 1995. Summary and comparison of methods to calculate solar heat gain. *ASHRAE Transactions* 101(1): 802-818.

APPENDIX A

EXPERIMENTAL BOX

A.1 Pictures of Experimental Box and Solar Test Bench

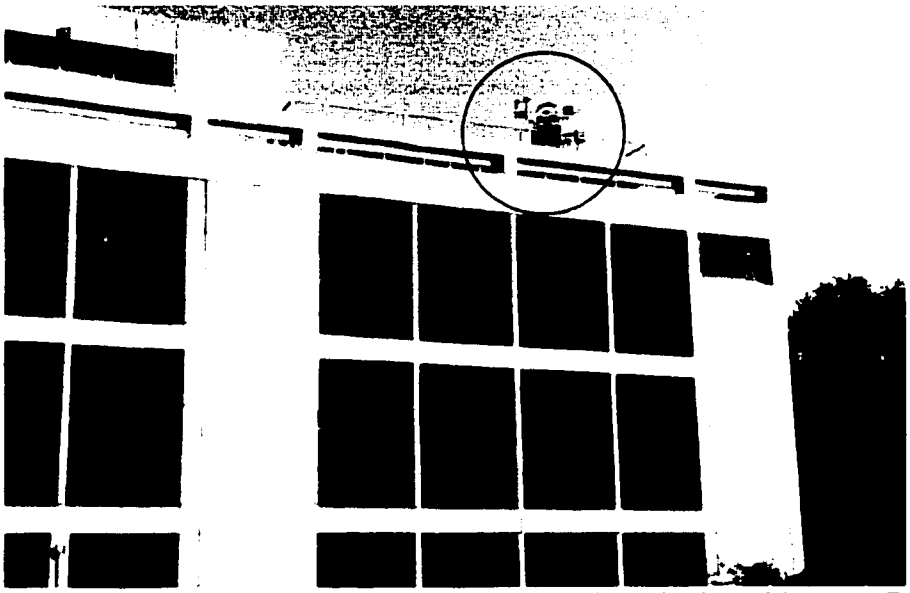

Figure A.1 Solar Test Bench Located on the Roof of the Langford Architecture Building, Texas A&M University. This figure is the view of the solar test bench from the northwest.

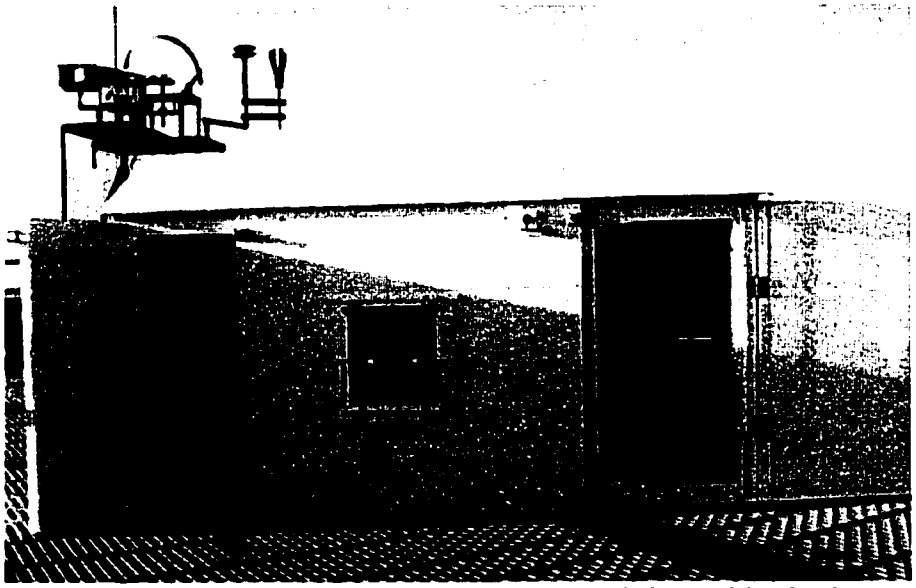

Figure A.2 South View of the Experimental Box. The box is located in the front of Langford Architecture Center solar test bench. The right side contains the air measurement equipment. The left side contains extra storage. The test chamber is in the center.

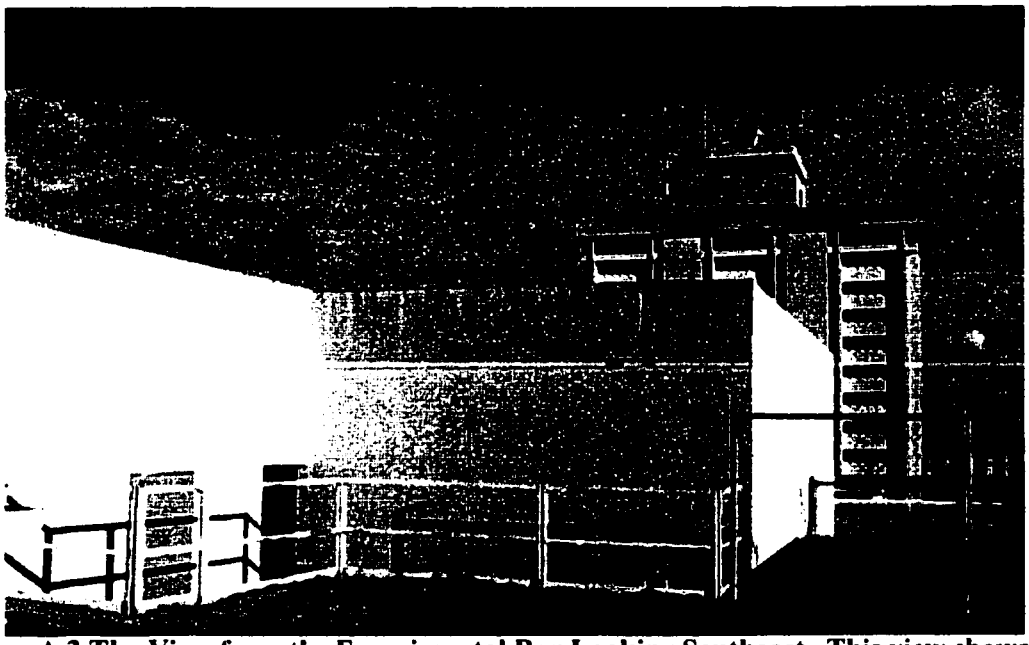

Figure A.3 The View from the Experimental Box Looking Southeast. This view shows a penthouse of the Langford Architecture Center and a nearby high rise building (O&M building) which partially shade the experimental box from the direct sunlit in the early morning for about one hour.

Figure A.4 Southwest View from the Experimental Box. The buildings in the southwest of the experimental box remain low on the horizon.

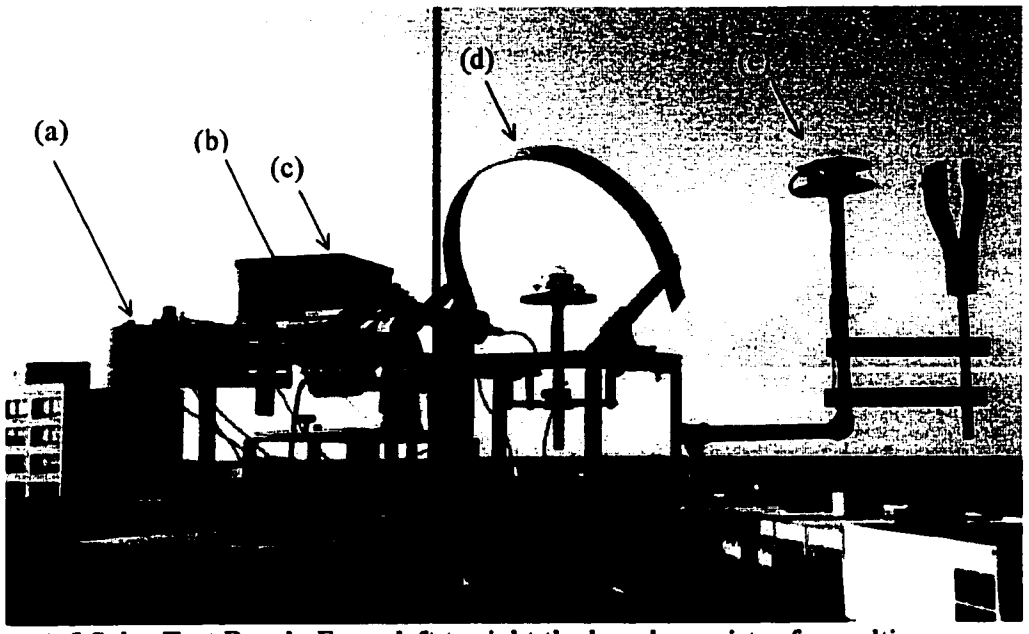

Figure A.5 Solar Test Bench. From left to right the bench consists of a multi-pyranometer array with an artificial horizon (a), an Eppley normal incidence pyrheliometer (b), a horizontal solar transmittance test box (c), an Eppley shadow band pyranometer (d), an Eppley precision spectral pyranometer (e), and test stand for calibrating pyranometers.

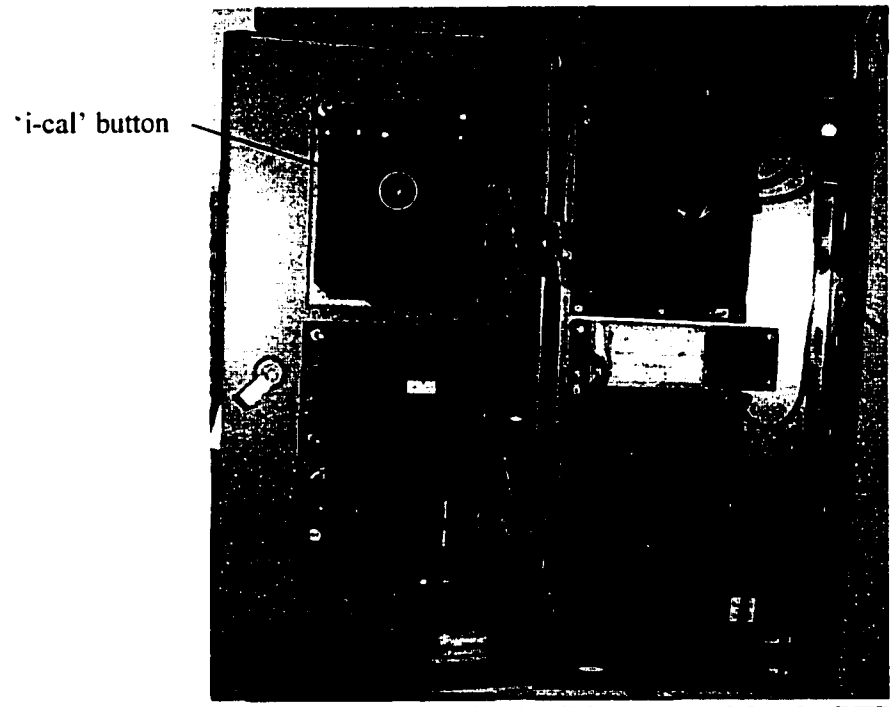

Figure A.6 Synergistic Data Logger. The 'i-cal' button used for the RTD sensor calibration is located on the center of the upper board in the logger box cover.

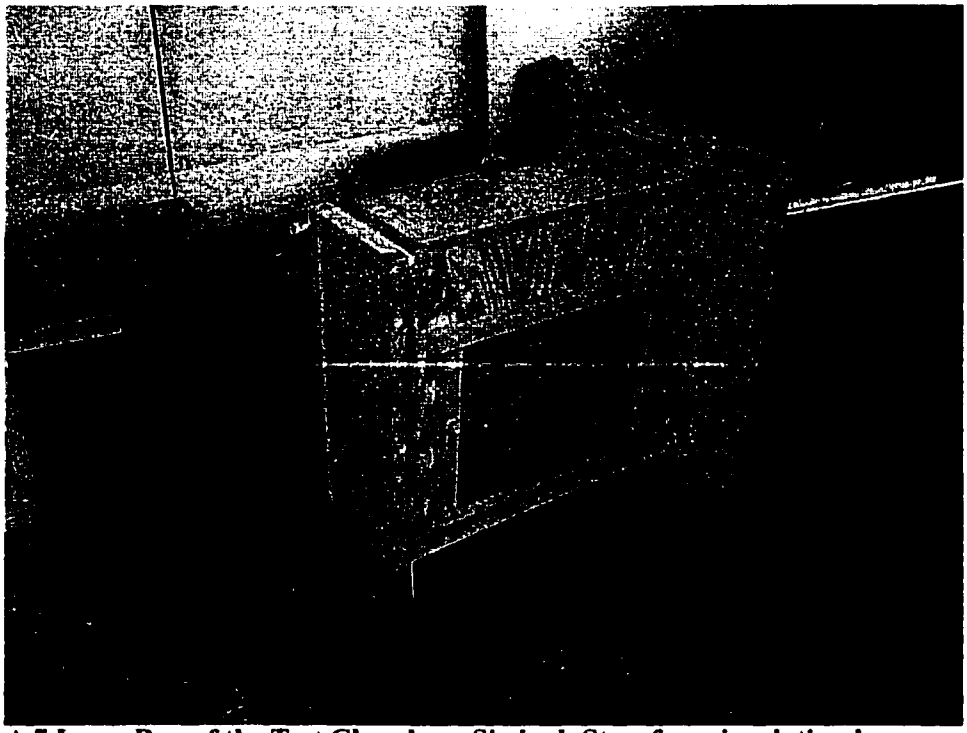

Figure A.7 Inner Box of the Test Chamber. Six inch Styrofoam insulation layers were installed between walls of this inner box and outer walls of the experimental box.

Figure A.8 Experimental Box under Construction. The box was divided to make three rooms. The figure shows the access hole between the main room and the instrument room where a wall having inlet and outlet tubes was later installed.

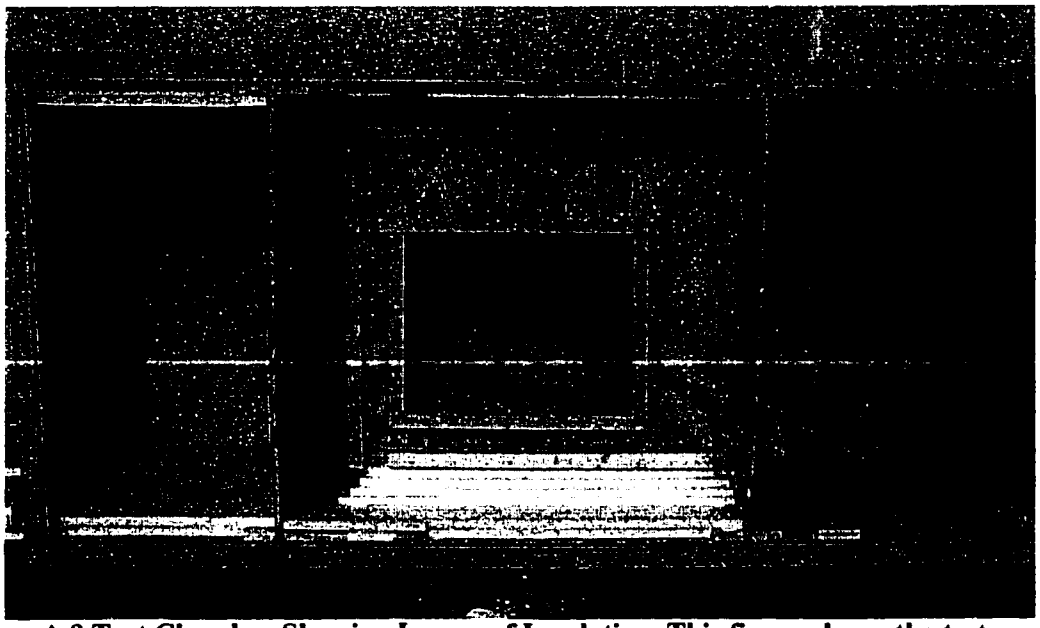

Figure A.9 Test Chamber Showing Layers of Insulation. This figure shows the test chamber as the surrounding insulation was glued into place.

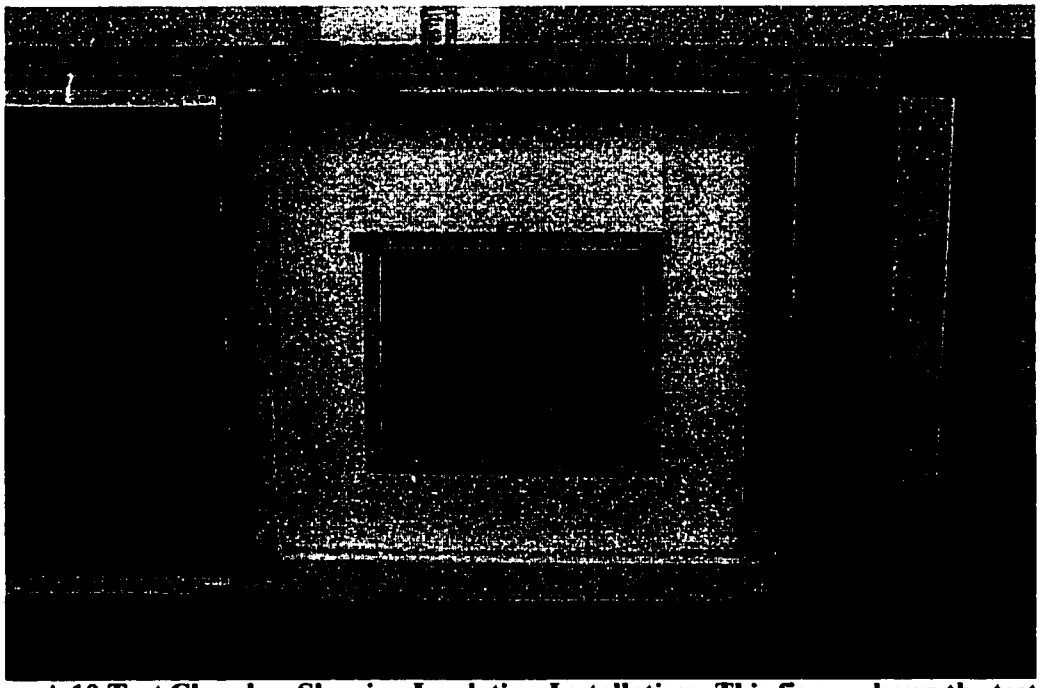

Figure A.10 Test Chamber Showing Insulation Installation. This figure shows the test chamber with all insulation installed as seen from the front of the box. The remaining 6 inches taper toward the 12 in. by 12 in. window.

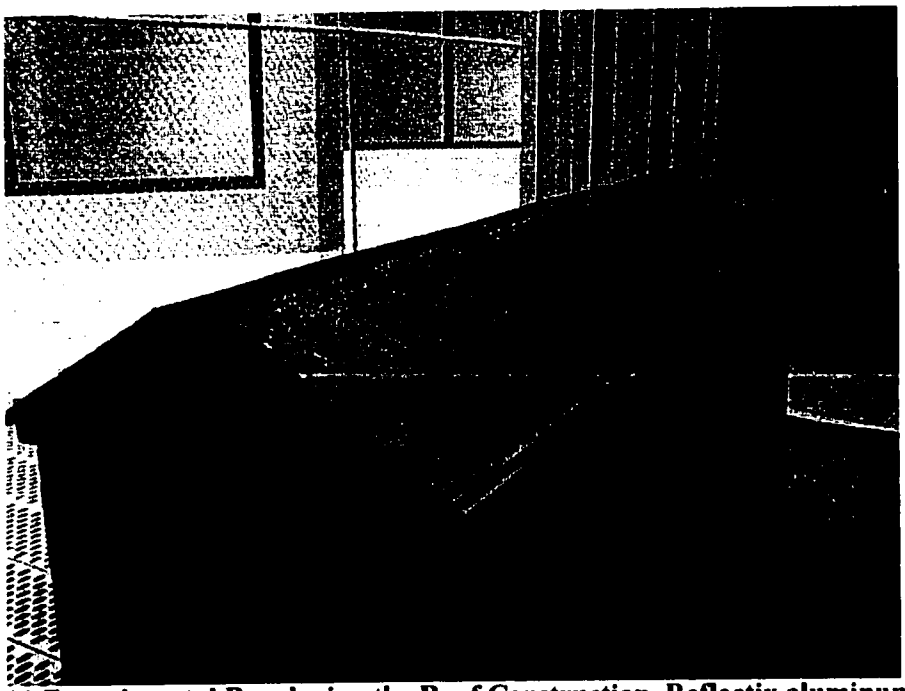

Figure A.11 Experimental Box during the Roof Construction. Reflectix aluminum foil insulation was added on the top of the 9 in. Styrofoam insulation surrounding the test box.

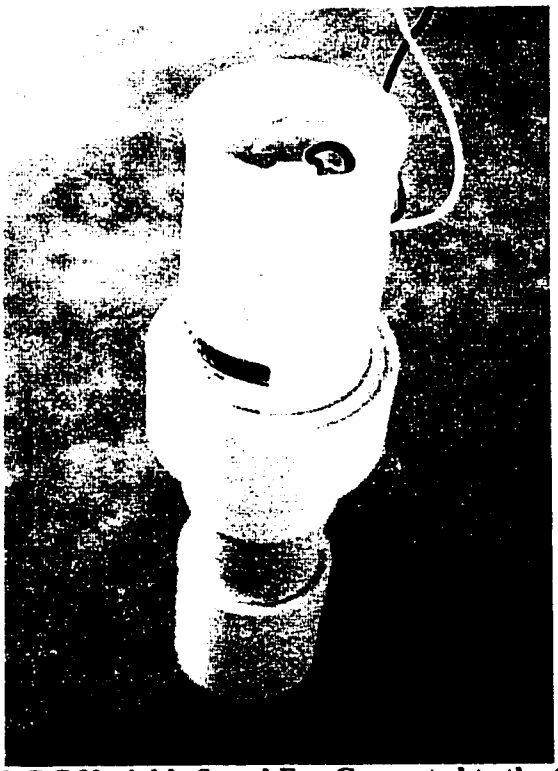

Figure A.12 Twelve Volt DC Variable Speed Fan Connected to the Outlet Tube. The speed of this fan is controlled by a variable AC/DC power supply.

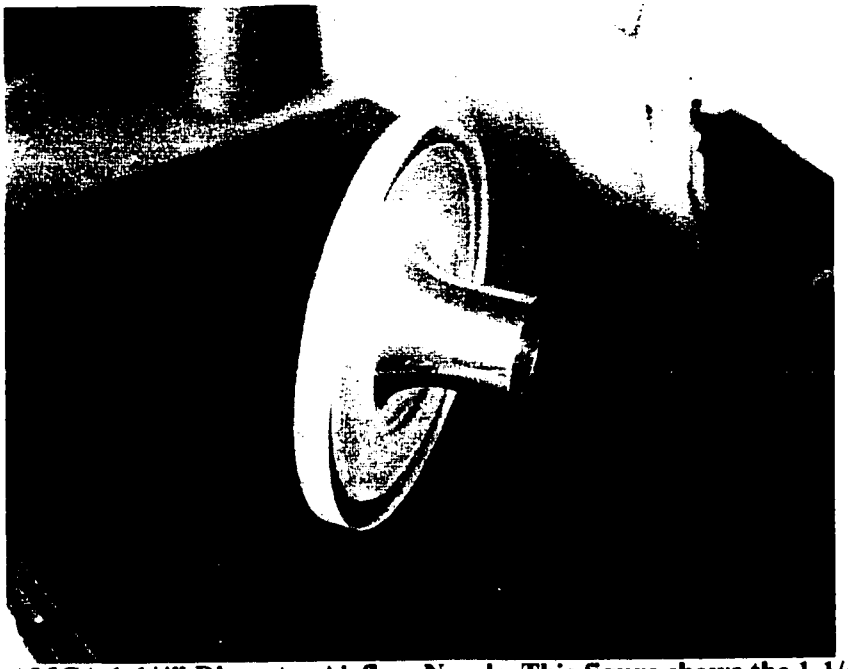

Figure A.13 AMCA 1-1/4" Diameter Airflow Nozzle. This figure shows the 1-1/4" diameter AMCA airflow nozzle installed into supporting Plexiglass collar.

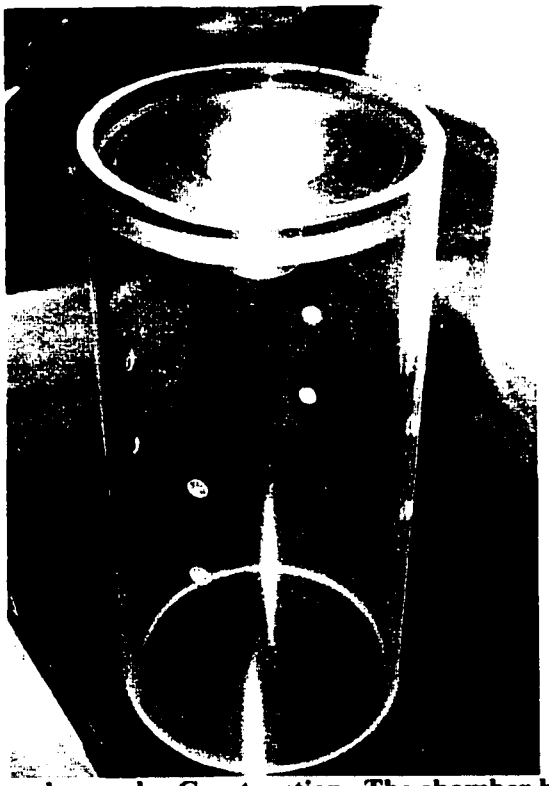

Figure A.14 Airflow Chamber under Construction. The chamber has 6 in. diameter and consists of an AMCA airflow nozzle in the center and four ports on each side of the nozzle to measure the average air pressure difference.

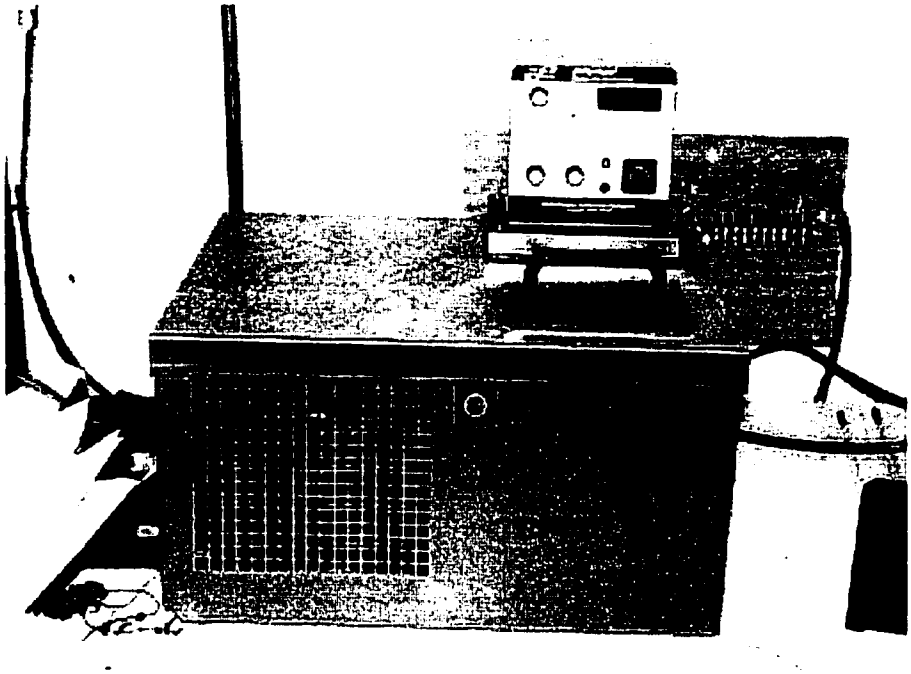

Figure A.15 Constant-temperature Thermometer Calibration Bath. This oil bath was used to generate a series of constant temperatures to calibrate the temperature sensors.

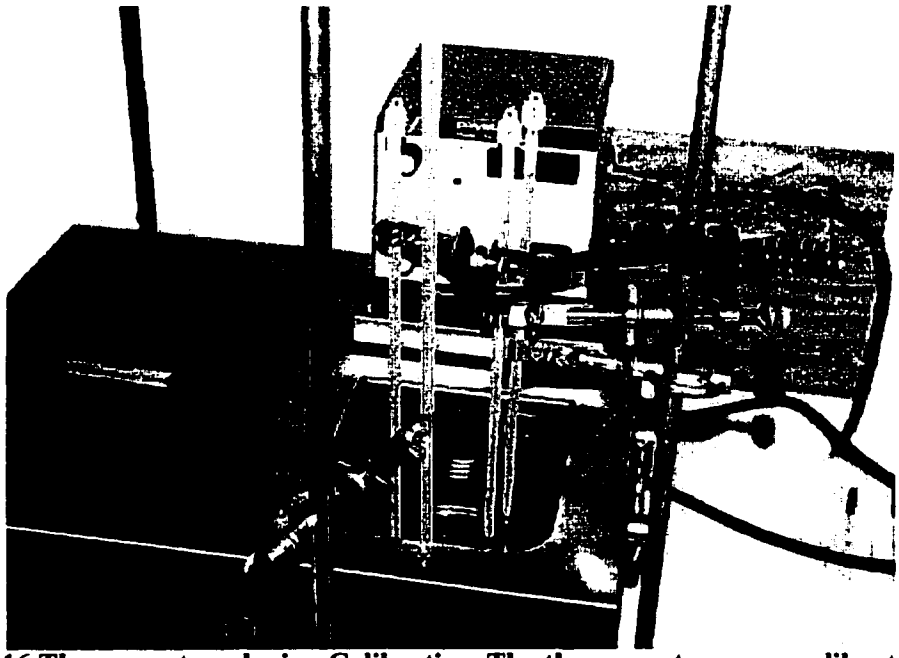

Figure A.16 Thermometers during Calibration. The thermometers were calibrated against ASTM certified partial-immersion thermometers in a constant-temperature oil bath.

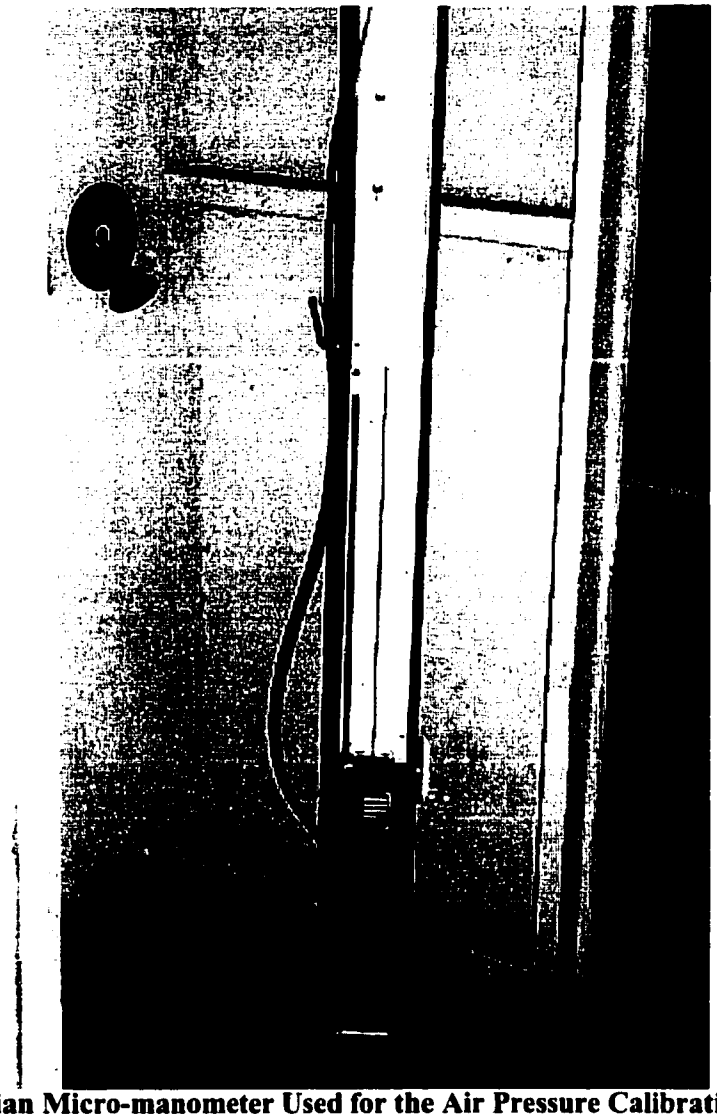

Figure A.17 Merian Micro-manometer Used for the Air Pressure Calibration. This figure shows a one-thousand scale Merian micro-manometer (model 34FB2TM) used to calibrate the Setra pressure transducer, and the u-inclined manometer.

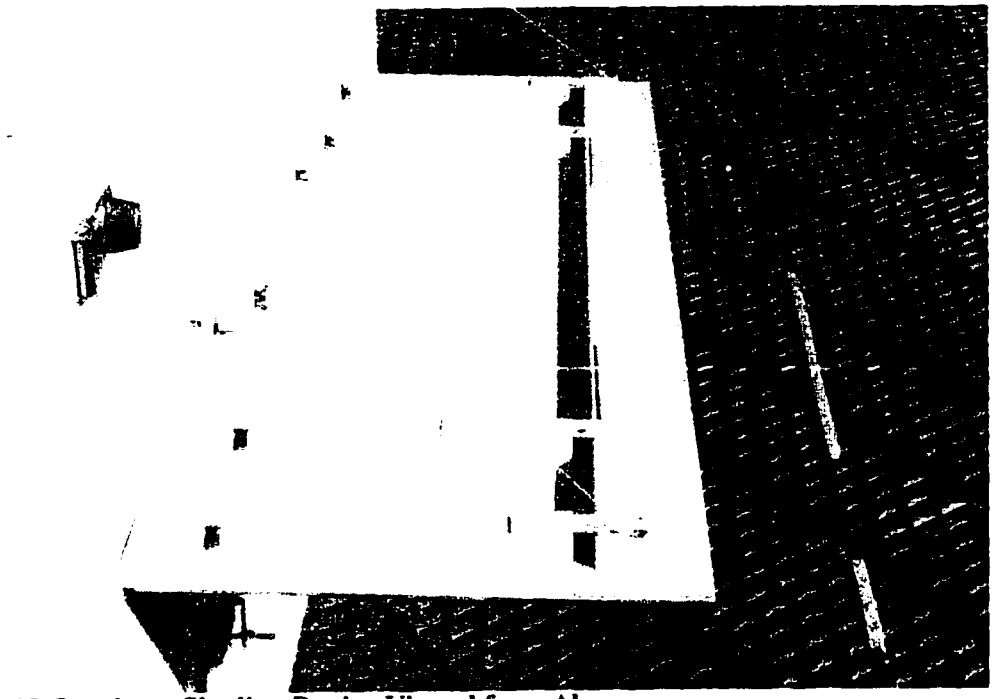

Figure A.18 Overhang Shading Device Viewed from Above.

Figure A.19 Overhang Shading Device View from Below. The window aperture is to the left of the overhang.

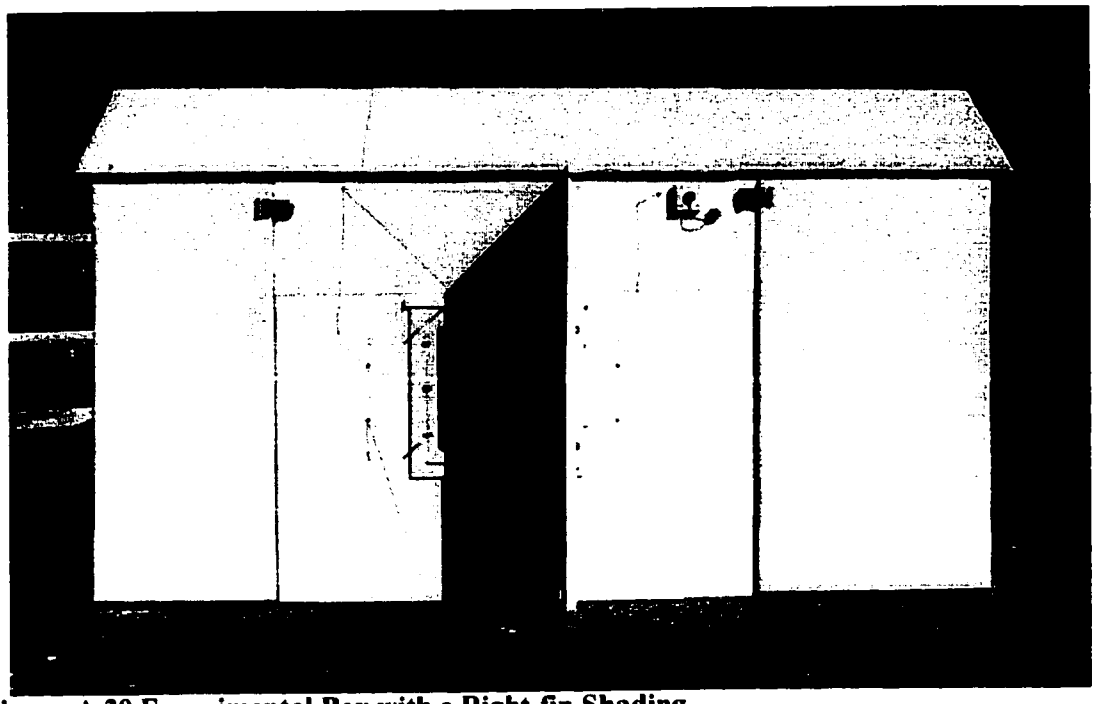

Figure A.20 Experimental Box with a Right-fin Shading.

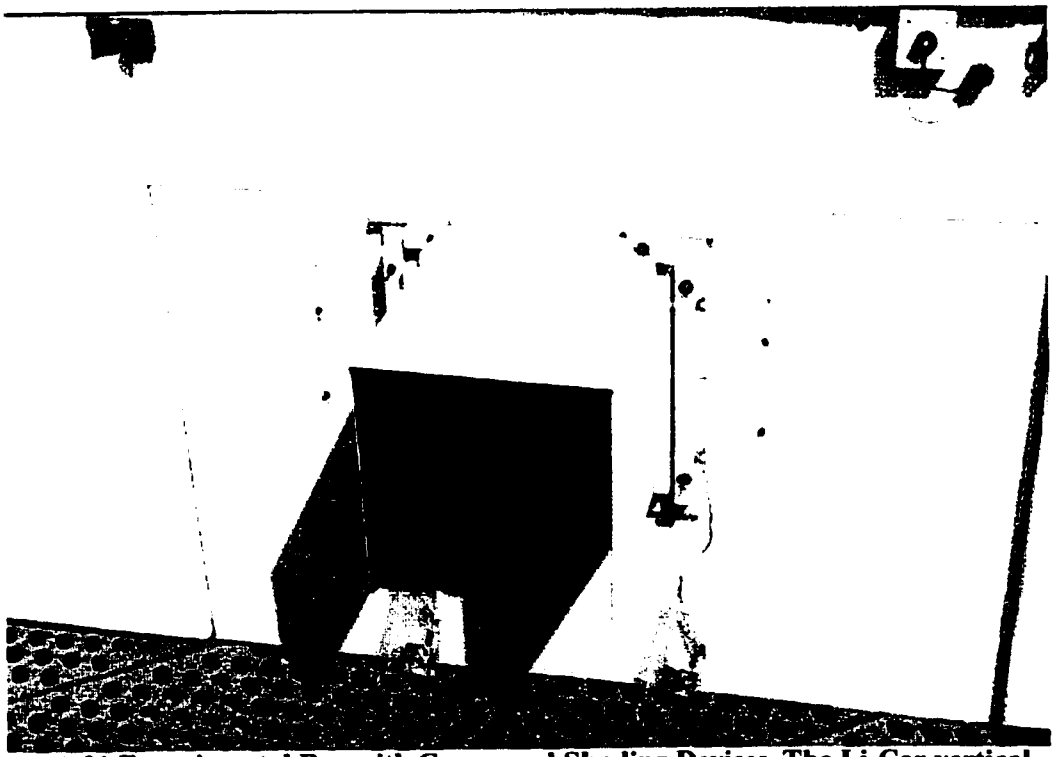

Figure A.21 Experimental Box with Compound Shading Devices. The Li-Cor vertical solar sensor can be seen to the upper right.

A.2 List of Instruments Used for the Experiments

Table A.1 shows the list of instruments used to collect the data from the test box that was construceted for the experimental validation of the proposed computer model. Section 4.3 describes the experimental validation using the test box. Most of these instruments were calibrated either in a calibration laboratory or on a site following the authorized calibration procedures as described in Section 4.3.2.

Table A.1 List of Instruments Used for the Experiments.

Item	Vendor	Note
LI-200SA Pyranometer Sensor	LI-COR	PY32029
2-wire Millivolt Transmitter	Moore Industries	MVX/10-20MVFS/4-20/12-42DC(FL)
AMCA Airflow Nozzle	Helander Metal Spinning Company	1.250" w/o taps, bore D -1.25, flange D-4.0
Pressure Transducer	Setra	Model 264; 0-1" w.g., 12-28 VDC
1127 Dual Range Flex-Tube U-inclined Manometer	Dwyer	Range 0-16" w.g. vertical, 0.2-2.6" inclined.
Variable AC/DC Power Supply	Mid-State Electronic Supply, Inc.	For fan speed control.
RTD Sensor	Kele & Associates (Technologies, Inc.)	1,000 ohm platinum.
Data & Signal Line Protector	Joslyn	1820 series.
Laboratory Glass Thermometer	Taylor	Model 6321, 0-230 °F range, 12" length

A.3 Parameter Set for the Data Logger

A Synergistic data logger (model C180E; Figure A.6) was used as the data acquisition system for collecting data from the experimental box as well as the Langford Architecture Center solar test bench. This data logger has channels for 16 current transformer inputs for electrical metering, 16 digital input, and 15 analog inputs. Among these channels, only 12 analog channels were used for the experiments. The analog channels store 0 to +5.00 volts direct current inputs using built-in precision shunt resistors accommodating 4 to 20 mA instrumentation loops.

A Synergistic data logger can be remotely configured using a computer program called Parset that is supplied by the manufacturer. The Parset program was used either for setting the data logger or for downloading the data from the logger. The following computer printout shows the parameter configuration information for the data logger. The first five lines show that all the channels were set to 15-minute intervals. The configuration of analog channels and their descriptions follow. For the detailed information about the Synergistic data logger and the Parset program, refer to the Installation Manual, Model C180E (Synergistic Control System, Inc. 1993).

```
                        -----  INTEGRATION PERIODS  -----

      AM                                          PM
From: 12  1  2  3  4  5  6  7  8  9 10 11 12  1  2  3  4  5  6  7  8  9 10 11
  To:  1  2  3  4  5  6  7  8  9 10 11 12  1  2  3  4  5  6  7  8  9 10 11 12

Flag:  1  1  1  1  1  1  1  1  1  1  1  1  1  1  1  1  1  1  1  1  1  1  1  1
Mins: 15 15 15 15 15 15 15 15 15 15 15 15 15 15 15 15 15 15 15 15 15 15 15 15

                          -----  ANALOG CHANNELS  -----

Chan   Description      Search String    STA Scale   Offset   Units     T S G
---- ---------------- ---------------- --- ------- ------- --------  - - -
 A 0 60 EAST OF SOUTH ELI              ON  319.93  -255.93 W/m^2      *
 A 1 DUE SOUTH        SLI              ON  394.14  -317.38 W/m^2      *
 A 2 60 WEST OF SOUTH WLI              ON  368.3   -295.65 W/m^2      *
 A 3 HORIZONTAL       LIH              ON  420.43  -332.72 W/m^2      *
 A 4 PYRHELIOMETER    NIP              ON  553.42  -442.74 W/m^2      *
 A 5 PSP              PSP              ON  521.75  -417.39 W/m^2      *
 A 6 BLACK & WHITE    SBP              ON  454.66  -363.73 W/m^2      *
 A 7 TRANSMITTANCE    TSP              ON  592.93  -465.25 W/m^2      *
 A 8 LICOR SOUTH      LIS              ON  420.43  -332.72 W/m^2      *
 A 9 AIR PRESS.       APD              ON  5         .1     Volts DC  *
 A10 TEMP. INLET      TI               ON  1         0      Deg F     *
 A11 TEMP. OUTLET     TO               ON  1         0      Deg F     *
 A12 CALIBRATION 5                     ON  1         0      Volts DC  *
 A13 CALIBRATION 6                     ON  1         0      Volts DC  *
 A14 CALIBRATION 7                     ON  1         0      Volts DC  *
```

A15 NOT USED! OFF 1 0

Chan	CType	Field Notes
A 0	+5 VDC	Licor array, 40 tilt 60 east of south
A 1	+5 VDC	Licor array, 40 tilt due south
A 2	+5 VDC	Licor array, 40 tilt 60 west of south
A 3	+5 VDC	Licor array horizontal (no tilt)
A 4	+5 VDC	Normal Incidence Pyrheliometer
A 5	+5 VDC	Total Horizontal Precision Spectral Pyranometer
A 6	+5 VDC	Shadow Band with Eppley Black & White Pyranometer
A 7	+5 VDC	Precision Spectral Pyranometer for transmittance tests
A 8	+5 VDC	Single Licor facing south
A 9	+5 VDC	Air Pressure Difference in Chamber
A10	1K RTD	Temperature for Chamber Inlet
A11	1K RTD	Temperature for Chamber Outlet
A12	+5 VDC	
A13	+5 VDC	
A14	+5 VDC	
A15	OFF	

A.4 Solar Sensor Calibration Worksheet

Li-Cor pyranometer sensors (model LI-200SA) were used to measure vertical solar radiation and transmitted solar radiation through window glazing of the experimental box. These solar sensors were linearly calibrated against the Epply PSP pyranometer installed the Langford Architecture Center solar test bench. The methods to calibrate the solar sensors are described in Section 4.3.2. The following information shows the result of the solar sensor calibration.

The Licor solar sensor linear calibration results shows

$$\text{Watts/SquareMeter} = 76.6044 * \text{mA} - 303.898 \quad \text{(A.1)}$$

$$\text{R Squared} = 0.998796 \quad \text{(A.2)}$$

If sensor output (mA) is forced through a resistor, the resulting voltage drop can be used to calculate solar radiation intensity using the linear calibrations listed below:

$$\text{200 ohm} \quad \text{Watts/SquareMeter} = 383.022 * \text{Volts} - 303.898 \quad \text{(A.3)}$$

$$\text{250 ohm} \quad \text{Watts/SquareMeter} = 306.4176 * \text{Volts} - 303.898 \quad \text{(A.4)}$$

Table A.2 Information Table for Solar Calibration.

Solar Sensor	
Manufacturer:	LI-COR
Model#:	LI-200SA Pyranometer Sensor
Serial#:	PY22696
Transmitter	
Manufacturer:	Moore Industries
Model#:	MVX/10-20MVFS/4-20MA/12-42DC FL
Serial#:	873480
Project:	John Oh's Experiment
Date Calibrated:	20-Oct-98
Calibrated By:	Jon Kie-Whan Oh

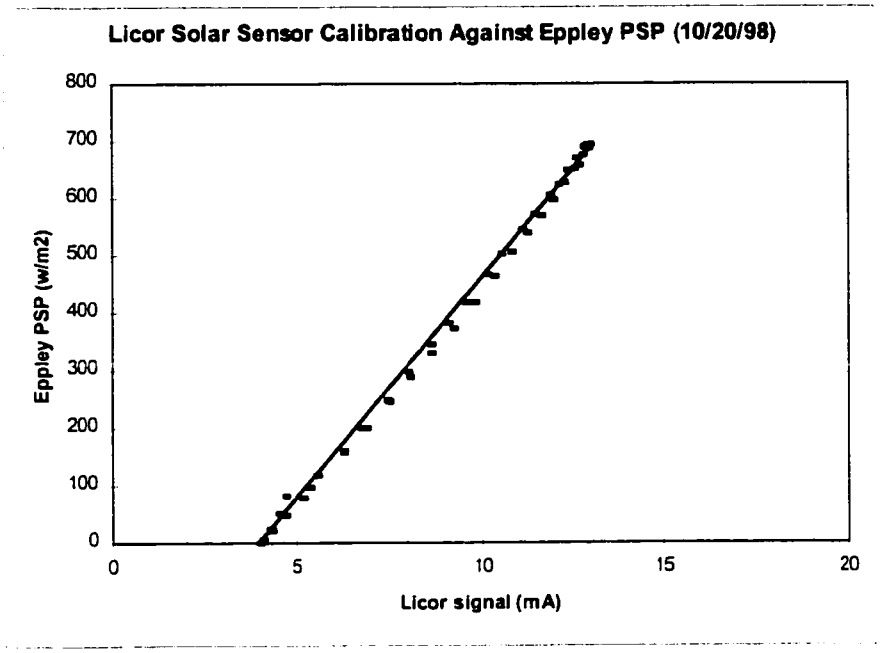

Figure A.22 Li-Cor Solar Sensor Calibration against Eppley PSP.

Table A.3 Solar Sensor Calibration Output Summary.

Regression Statistics	
Multiple R	0.999398
R Square	0.998796
Adjusted R Square	0.998784
Standard Error	8.949889
Observations	96

A.5 Procedures of AMCA Airflow Measurement

An AMCA airflow nozzle (1.250" w/o taps, bore D -1.25, flange D-4.0) was used to measure the airflow into the test chamber. This airflow nozzle was located in the entrance of the inlet tube of the test chamber to measure the airflow rate through the tube. The calculated airflow rate is used for calculating the heat removed by the circulation fan. Figure A.23 shows the inlet chamber setup of an AMCA airflow test chamber. The following sections explain the procdeures used to calculate the airflow rate and the heat removed by the fan from the measured air pressure difference data. For a more detailed description of these calculations, refer to the 'Laboratory Methods of Testing Fans fro Rating' (ANSI/AMCA 1985).

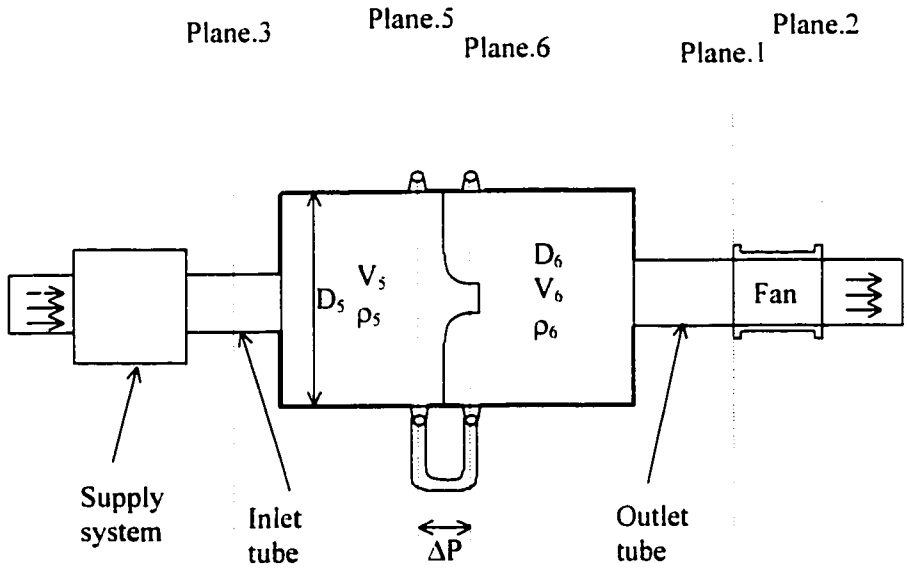

Figure A.23 AMCA Airflow Test Chamber (Inlet Chamber Setup).

A.5.1 Atmospheric Air Density (ρ_o)

The density of air (ρ) is determined from the measurements of dry-bulb temperature (T_{do}), wet-bulb temperature (T_{wo}), and barometric pressure (P_b). The gas constant (R_g) may be taken as 53.35 (ft-lb/lbm-°R) for air. Thus, the atmospheric air density (ρ_o) is calculated from

$$P_e = 2.96 \times 10^{-4} T_{wo}^{\ 2} - 1.59 \times 10^{-2} T_{wo} + 0.41 \qquad \text{(A.5)}$$

$$P_p = P_e - P_b\left(\frac{T_{do} - T_{wo}}{2700}\right), \text{ and} \tag{A.6}$$

$$\rho_o = \frac{70.73\left(P_b - 0.378P_p\right)}{R_g\left(T_{do} + 459.7\right)}. \tag{A.7}$$

where P_e is saturated vapor pressure (in. Hg) at a given wet-bulb temperature (T_w), and P_p is partial vapor pressure (in. Hg). The atmospheric air density (ρ_o) is also calculated as function of altitude above sea level (H) and the air temperature (T_{do}) using

$$\rho_o = 39.8\frac{e^{-H/27,000}}{T_{do} + 459.7} \tag{A.8}$$

where H is the of altitude above sea level in feet.

A.5.2 Chamber Air Density (ρ_5)

The density of air (ρ_x) in the airflow chamber at the given measurement point (*5*) may be calculated by correcting the density of atmospheric air (ρ_o) for the static pressure (P_{s5}) and temperature (T_{d5}) at the plane 5 in Figure A.23 using

$$\rho_5 = \rho_o\left(\frac{T_{do} + 459.7}{T_{d5} + 459.7}\right)\left(\frac{P_{s5} + 13.63P_b}{13.63P_b}\right). \tag{A.9}$$

If P_{s5} is numerically less than 4 in. w.g, ρ_5 may be considered equal to ρ_o.

A.5.3 Static Pressure Ratio for a Airflow Nozzle (R_a)

The static pressure ratio for a airflow nozzle (R_a) is the ratio of absolute nozzle exit pressure (P_6) to absolute approach pressure (P_5), and is given by

$$R_a = 1 - \frac{5.187\Delta P}{\rho_5 R_g\left(T_{d5} + 459.7\right)}. \tag{A.10}$$

A.5.4 Diameter Ratio for a Airflow Nozzle (R_β)

The diameter ratio for a airflow nozzle (R_β) is the ratio of nozzle exit diameter (D_6) to the approach duct diameter (D_5), and calculated from

$$R_\beta = \frac{D_6}{D_5}. \tag{A.11}$$

For a chamber approach, R_β may be taken as zero.

A.5.5 Expansion Factor (Y)

The nozzle expansion factor (Y) for air may be approximated with sufficient accuracy using

$$Y = 1 - \left(0.548 + 0.71 R_\beta^{\ 4}\right)\left(1 - R_\alpha\right) \tag{A.12}$$

A.5.6 Reynolds Number (R_e)

The Reynolds Number (R_e) based on nozzle exit diameter (D_6) in feet shall be calculated from

$$R_e = \frac{D_6 V_6 \rho_6}{60 \mu_6}. \tag{A.13}$$

where V_6, ρ_6, and μ_6 are the volume flow rate (cfm), density (lb_m/ft^3) of the air, and air viscosity (lb_m/ft-s) measured at the exit of the airflow nozzle (Plane 6 in Figure A.23) in the air chamber respectively. A simplified approximation suitable for the range of temperature from 40°F to 100°F is

$$R_e = 1{,}363{,}000 D_6 \sqrt{\Delta P \rho_5}. \tag{A.14}$$

A.5.7 Discharge Coefficient (C)

For the case when Reynolds Number (R_e) is 12,000 and above, the nozzle discharge coefficient (C) is determined from

$$C = 0.9986 - \frac{7.006}{\sqrt{R_e}} + \frac{134.6}{R_e} \text{ for } \frac{L_t}{D_t} = 0.6 \qquad \text{(A.15)}$$

where D_t and L_t are the throat diameter and throat length of the airflow nozzle.

A.5.8 Air Velocity in Chamber (v_5)

The average velocity of air (v_5) measured at the entrance to a nozzle or multiple nozzles shall be calculated from

$$v_5 = 1096Y\sqrt{\frac{\Delta P}{\rho_5}}. \qquad \text{(A.16)}$$

A.5.9 Flow Rate for Chamber Nozzle (V_5)

The volume flow rate (V_5) at the entrance to a nozzle or multiple nozzles shall be calculated from

$$V_5 = 1096Y\sqrt{\frac{\Delta P}{\rho_5}}\sum(CA_{c,6}). \qquad \text{(A.17)}$$

The area of cross section ($A_{c,6}$) is measured at the plane of the throat traps or the nozzle exit for nozzles without throat traps.

A.5.10 Heat Transfer by Fan (Q_{fan})

The heat removed by the ventilation fan (Q_{fan}) is the calculated from

$$Q_{fan} = \dot{m} \cdot c_{p,air}(T_{outlet} - T_{inlet}) \qquad \text{(A.18)}$$

and

$$Q_{fan} = \dot{V}_5 \times \rho_5 \times 60 \times c_{p,air} \left(T_{outlet} - T_{inlet}\right) \qquad \text{(A.19)}$$

where the value of the specific heat of air ($c_{p,air}$) is 0.240 (Btu/lb_m-°F), and $\dot{V}_5$ and ρ_5 are the volume flow rate (cfm) and density (lb_m/ft^3) of the air measured at the entrance of the airflow nozzle in the air chamber.

APPENDIX B

SOLAR TEST BENCH RESULTS

This appendix contains the graphical and tabular list of the measured data taken at the ESL solar lab as results of the experimental tests. The data were collected from the ESL's solar lab on the top of Langford Architecture Center. Additional data were collected from the weather station atop the Zachry Engineering Center and from the College Station National Weather Service (CLL). The data listed in columns 8 to 15 are various kinds of solar radiation collected from the solar lab and the data in columns from 16 to 19, 27, and 28 are the data measured from the experimental box. The data listed in columns from 20 to 23 is weather data collected at the Zachry building, and the data in columns from 24 to 26 is the weather data collected from CLL. Table B.1 shows the list of data elements collected for the experimental validation. The parameter set for the data logger is listed in Appendix A.3.

A total of eight different cases of tests were conducted using the experimental box with different experimental conditions. Table B.2 shows the daily summary of the results of all the experimental tests.

Table B.1 Data Elements Collected for the Experimental Validation.

Column #	Heading	Description	Units
1	Site	Site number.	XXXXX
2	Month	Month of the year.	MM
3	Day	Day of the month.	DD
4	Year	Year.	YY
5	Julian	Julian date.	YYDDD
6	Decimal	Decimal date counted from January 1, 1980.	XXXX.XX
7	Hour	Hour of day in local standard time. The date and time indicates the starting time of the experiment.	HHMM
8	ELI	Licor array, 40° tilt and 60 ° east of south.	W/m^2
9	SLI	Licor array, 40° tilt and due south.	W/m^2
10	WLI	Licor array, 40° tilt and 60 ° west of south.	W/m^2
11	LIH	Horizontal licor array without tilt.	W/m^2
12	NIP	Normal incidence pyrheliometer.	W/m^2
13	PSP	Total horizontal precision spectral pyranometer.	W/m^2
14	SBP	Shadow band with Eppley black and white pyranometer.	W/m^2
15	TSP	Precision spectral pyranometer for transmittance tests.	W/m^2
16	SVL	Licor for vertical solar radiation, due south.	W/m^2
17	APD	Air pressure difference across the AMCA airflow nozzle in the airflow chamber.	" w.g.
18	TI	Air temperature in the inlet tube.	°F
19	TO	Air temperature in the outlet tube.	°F
20	Tdb	Dry-bulb temperature collected on the top of Zachry.	°F
21	RH	Relative humidity collected on the top of Zachry.	%
22	GHR	Total horizontal solar radiation collected on the top of Zachry.	W/m^2
23	Wind	Wind speed collected on the top of Zachry.	mph
24	Tdb2	Dry-bulb temperature	°F
25	Tdew	Dew point temperature	°F
26	Wind2	Wind speed	mph
27	Tg,r	Surface temperature of the right side of the glazing.	°F
28	Tg,l	Surface temperature of the left side of the glazing.	°F

Table B.2 Summary of the Results of Experimental Tests (Btu/day). This figure shows daily solar heat gains transmitted through glazing measured and simulated using various methods.

Case # (Date)	Description	Measured Heat Removed by Fan Daily Total (Day Time Only)	Measured Vertical South Solar	Measured Transmitted Solar Radiation	SolrCalc Simulated Solar Gain through Glazing	DOE-2 Simulated Solar Gain through Glazing (Design-Day)	DOE-2 Simulated Solar Gain through Glazing (Weather File)
1 (10/25/98)	Blocked window	726.5 (52.8)	1,151.7	N/A	N/A	N/A	N/A
2 (11/03/98)	Blocked window w/ periodic heat gain	1,024.0 (167.3)	1,178.3	N/A	N/A	N/A	N/A
3 (03/22/99)	Glazing solar transmittance	972.3 (542.7)	906.8	613.1	730.7	1,078.7	959.3
4 (01/25/99)	Left-fin shade	1,146.8 (719.9)	1,283.6	N/A	N/A	1,298.2	1,121.6
5 (12/01/98)	No shading	1,269.3 (460.0)	1,252.7	950.2	871.8	1,161.0	976.7
6 (12/15/98)	Overhang shade	1,047.4 (667.4)	1,272.6	N/A	N/A	866.3	668.0
7 (01/18/99)	Right-fin shade	1,643.2 (922.2)	1,293.4	N/A	N/A	1,393.7	1,078.0
8 (02/12/99)	Overhang and side fins shades	530.1 (100.6)	1,300.8	N/A	N/A	280.8	46.5

Note: Measured heat removed by the fan only includes values from sunrise to sunset for values indicated as (Day Time Only).

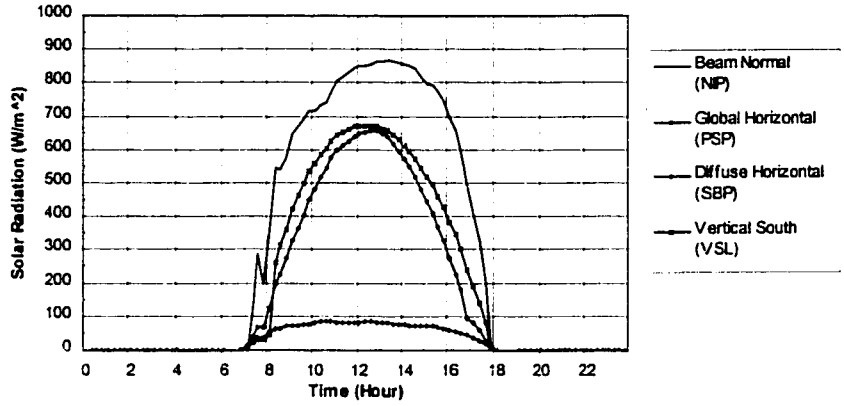

Figure B.1. Measured Beam Normal, Global Horizontal, Diffuse Horizontal and Vertical South Solar Radiation (Case 1, 10/25/98, Blocked Window).

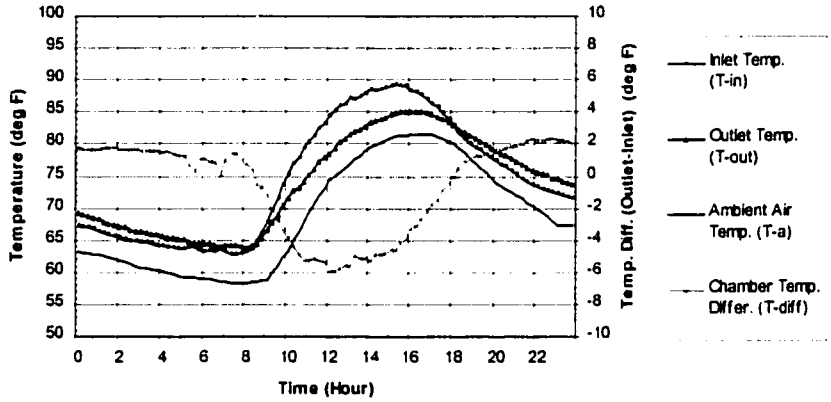

Figure B.2. Measured Chamber Inlet and Outlet Temperature, Ambient Air Temperature, and Air Temperature Difference between Chamber Outlet and Inlet (Case 1, 10/25/98, Blocked Window).

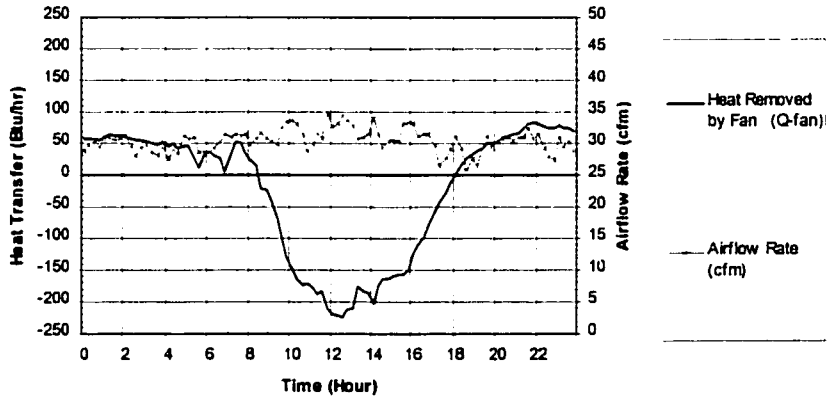

Figure B.3. Heat Transfer of the Experimental Box and Calculated Airflow Rate (Case 1, 10/25/98, Blocked Window).

1	2	3	4	5	6	7	8	9	10	11	12	13	14
Site	Month	Day	Year	Julian	Decimal	Hour	ELI	SLI	WLI	LIH	NIP	PSP	SBP
0	10	25	98	98298	6872.000	0	1.312	-1.101	1.074	-1.745	-7.958	-3.308	-6.172
0	10	25	98	98298	6872.010	15	1.696	-0.627	1.812	-1.576	-7.958	-1.427	-5.262
0	10	25	98	98298	6872.021	30	1.824	-0.311	2.107	-1.576	-7.958	-1.009	-4.897
0	10	25	98	98298	6872.031	45	1.824	-0.311	2.107	-1.576	-7.958	-1.218	-4.897
0	10	25	98	98298	6872.042	100	1.824	-0.311	2.255	-1.576	-7.958	-1.218	-4.897
0	10	25	98	98298	6872.052	115	1.953	-0.311	2.107	-1.576	-7.736	-1.218	-5.079
0	10	25	98	98298	6872.063	130	1.824	-0.469	2.107	-1.576	-7.736	-1.009	-5.079
0	10	25	98	98298	6872.073	145	1.824	-0.469	2.107	-1.576	-7.736	-0.800	-5.079
0	10	25	98	98298	6872.083	200	1.824	-0.469	2.107	-1.576	-7.736	-0.382	-4.897
0	10	25	98	98298	6872.094	215	1.953	-0.469	2.255	-1.576	-7.958	-1.009	-5.079
0	10	25	98	98298	6872.104	230	1.824	-0.469	2.107	-1.576	-7.736	-0.591	-4.897
0	10	25	98	98298	6872.115	245	1.824	-0.469	2.107	-1.576	-7.736	-0.382	-4.897
0	10	25	98	98298	6872.125	300	1.953	-0.311	2.255	-1.576	-7.515	0.036	-4.897
0	10	25	98	98298	6872.135	315	1.953	-0.311	2.107	-1.576	-7.736	-0.173	-4.897
0	10	25	98	98298	6872.146	330	1.953	-0.311	2.107	-1.576	-7.736	-0.173	-4.715
0	10	25	98	98298	6872.156	345	1.953	-0.311	2.255	-1.576	-7.736	-0.382	-4.715
0	10	25	98	98298	6872.167	400	1.824	-0.469	2.107	-1.576	-7.958	-0.591	-4.715
0	10	25	98	98298	6872.177	415	1.953	-0.311	2.255	-1.576	-7.736	-0.591	-4.533
0	10	25	98	98298	6872.188	430	1.953	-0.311	2.255	-1.576	-7.736	-0.800	-4.533
0	10	25	98	98298	6872.198	445	1.953	-0.311	2.255	-1.576	-7.736	-0.173	-4.533
0	10	25	98	98298	6872.208	500	1.953	-0.311	2.255	-1.408	-7.736	0.036	-4.533
0	10	25	98	98298	6872.219	515	1.953	-0.311	2.255	-1.408	-7.736	0.036	-4.351
0	10	25	98	98298	6872.229	530	1.953	-0.311	2.255	-1.576	-7.736	-0.173	-4.351
0	10	25	98	98298	6872.240	545	1.953	-0.311	2.255	-1.576	-7.736	0.036	-4.351
0	10	25	98	98298	6872.250	600	1.953	-0.311	2.255	-1.576	-7.736	0.036	-4.351
0	10	25	98	98298	6872.260	615	1.568	-1.259	1.222	-1.576	-7.958	-1.009	-5.444
0	10	25	98	98298	6872.271	630	2.465	-0.627	1.369	-1.240	-7.958	-2.472	-5.079
0	10	25	98	98298	6872.281	645	7.592	3.478	4.320	1.961	-7.958	1.081	-1.801
0	10	25	98	98298	6872.292	700	25.793	17.374	13.321	12.235	-7.515	13.205	8.764
0	10	25	98	98298	6872.302	715	141.404	76.114	28.666	44.238	137.265	42.469	27.889
0	10	25	98	98298	6872.313	730	320.845	163.276	35.453	84.999	286.257	67.970	36.268
0	10	25	98	98298	6872.323	745	250.607	141.485	33.978	77.251	197.128	67.970	35.540
0	10	25	98	98298	6872.333	800	433.637	257.070	46.667	144.962	364.744	127.751	52.662
0	10	25	98	98298	6872.344	815	614.616	383.077	53.750	218.400	545.219	196.312	62.133
0	10	25	98	98298	6872.354	830	632.047	419.710	55.225	244.676	539.011	225.158	64.319
0	10	25	98	98298	6872.365	845	700.235	490.450	58.766	293.522	575.173	273.234	70.148
0	10	25	98	98298	6872.375	900	777.138	571.297	80.899	346.747	648.982	326.745	70.877
0	10	25	98	98298	6872.385	915	814.565	630.036	140.214	386.835	672.927	365.206	71.427
0	10	25	98	98298	6872.396	930	844.301	683.723	203.661	424.565	692.438	407.011	75.248
0	10	25	98	98298	6872.406	945	870.961	736.147	255.599	460.947	715.496	450.488	77.070
0	10	25	98	98298	6872.417	1000	884.291	779.728	308.717	491.265	718.157	483.933	81.441
0	10	25	98	98298	6872.427	1015	898.646	826.467	365.376	522.257	714.120	516.541	85.084
0	10	25	98	98298	6872.438	1030	896.595	858.680	417.904	543.817	742.989	544.132	87.270
0	10	25	98	98298	6872.448	1045	900.697	895.945	473.974	569.419	769.594	575.068	84.356
0	10	25	98	98298	6872.458	1100	900.697	929.420	529.862	593.000	804.182	600.151	81.077
0	10	25	98	98298	6872.469	1115	888.392	949.632	578.439	607.822	818.172	614.365	81.441
0	10	25	98	98298	6872.479	1130	871.986	967.317	626.836	620.623	833.448	627.743	81.077
0	10	25	98	98298	6872.490	1145	851.478	978.686	672.282	630.055	845.864	641.121	82.898
0	10	25	98	98298	6872.500	1200	824.819	986.265	713.596	634.772	852.959	648.646	82.898
0	10	25	98	98298	6872.510	1215	792.519	986.265	750.188	634.772	850.299	651.154	85.813
0	10	25	98	98298	6872.521	1230	758.682	987.528	787.171	634.098	854.733	657.007	85.084
0	10	25	98	98298	6872.531	1245	722.793	988.791	822.193	630.729	862.715	657.007	82.898
0	10	25	98	98298	6872.542	1300	683.316	985.002	852.293	623.992	864.488	647.910	81.263
0	10	25	98	98298	6872.552	1315	642.301	979.949	880.623	613.886	868.923	637.776	79.255
0	10	25	98	98298	6872.563	1330	593.596	962.895	898.329	597.716	864.488	616.874	78.527
0	10	25	98	98298	6872.573	1345	542.327	939.526	910.723	577.504	859.167	593.463	78.163
0	10	25	98	98298	6872.583	1400	489.007	912.998	918.986	554.596	855.620	570.052	76.705
0	10	25	98	98298	6872.594	1415	436.200	883.944	923.708	529.668	851.185	547.477	72.334
0	10	25	98	98298	6872.604	1430	380.830	847.311	921.147	501.171	840.543	517.377	71.969
0	10	25	98	98298	6872.615	1445	324.434	804.361	912.494	468.358	821.012	481.424	71.791
0	10	25	98	98298	6872.625	1500	269.064	756.359	898.329	433.997	798.861	444.636	71.062
0	10	25	98	98298	6872.635	1515	216.257	713.409	890.656	403.005	794.427	411.191	71.605
0	10	25	98	98298	6872.646	1530	162.681	659.722	862.917	361.907	771.142	370.640	65.412
0	10	25	98	98298	6872.656	1545	98.082	602.245	828.685	320.135	747.423	327.581	61.405
0	10	25	98	98298	6872.667	1600	55.016	531.505	771.435	270.952	697.759	274.906	56.669
0	10	25	98	98298	6872.677	1615	48.607	468.976	721.268	228.506	656.077	227.248	53.390
0	10	25	98	98298	6872.688	1630	44.249	398.235	652.805	183.702	598.431	180.844	49.019
0	10	25	98	98298	6872.698	1645	40.148	310.757	544.208	135.193	496.442	92.635	43.190
0	10	25	98	98298	6872.708	1700	36.303	238.122	450.366	96.453	411.304	42.184	36.997
0	10	25	98	98298	6872.719	1715	31.945	170.855	353.572	57.376	329.270	57.100	28.618
0	10	25	98	98298	6872.729	1730	23.998	94.430	211.134	25.036	197.571	26.583	17.325
0	10	25	98	98298	6872.740	1745	11.437	21.479	43.126	8.361	21.087	5.680	4.757
0	10	25	98	98298	6872.750	1800	3.875	2.057	5.206	0.613	-9.510	-2.681	-4.169
0	10	25	98	98298	6872.760	1815	1.568	-0.943	1.812	-1.576	-9.510	-3.517	-6.719
0	10	25	98	98298	6872.771	1830	1.312	-1.417	1.222	-1.913	-9.288	-3.099	-6.901
0	10	25	98	98298	6872.781	1845	1.184	-1.417	1.074	-1.913	-9.288	-2.681	-6.901
0	10	25	98	98298	6872.792	1900	1.184	-1.575	1.074	-1.913	-9.288	-2.054	-6.901
0	10	25	98	98298	6872.802	1915	1.568	-1.101	1.369	-1.576	-8.845	-1.845	-6.537
0	10	25	98	98298	6872.813	1930	1.440	-1.259	1.369	-1.745	-8.845	-2.054	-6.537
0	10	25	98	98298	6872.823	1945	1.440	-1.259	1.222	-1.745	-8.845	-2.054	-6.537
0	10	25	98	98298	6872.833	2000	1.312	-1.259	1.222	-1.913	-8.845	-2.054	-6.537
0	10	25	98	98298	6872.844	2015	1.440	-1.259	1.222	-1.745	-8.845	-1.427	-6.537
0	10	25	98	98298	6872.854	2030	1.568	-1.259	1.369	-1.745	-8.845	-1.427	-6.537
0	10	25	98	98298	6872.865	2045	1.568	-1.259	1.369	-1.745	-8.623	-1.009	-6.354
0	10	25	98	98298	6872.875	2100	1.696	-1.417	1.369	-1.576	-8.845	-1.218	-6.354
0	10	25	98	98298	6872.885	2115	1.568	-1.259	1.369	-1.745	-8.623	-1.636	-6.354
0	10	25	98	98298	6872.896	2130	1.568	-1.417	1.369	-1.408	-8.623	-1.427	-6.354
0	10	25	98	98298	6872.906	2145	1.568	-1.417	1.222	-1.745	-8.623	-1.218	-6.172
0	10	25	98	98298	6872.917	2200	1.568	-1.417	1.222	-1.576	-8.623	-0.591	-6.172
0	10	25	98	98298	6872.927	2215	1.568	-1.259	1.222	-1.576	-8.623	-0.800	-6.172
0	10	25	98	98298	6872.938	2230	1.440	-1.259	1.222	-1.576	-8.623	-1.009	-6.354
0	10	25	98	98298	6872.948	2245	1.440	-1.259	1.222	-1.576	-8.401	-1.009	-6.172
0	10	25	98	98298	6872.958	2300	1.440	-1.259	1.074	-1.576	-8.401	-1.009	-6.172
0	10	25	98	98298	6872.969	2315	1.440	-1.259	1.222	-1.576	-8.401	-1.009	-6.172
0	10	25	98	98298	6872.979	2330	1.568	-1.259	1.074	-1.576	-8.623	-1.218	-6.172
0	10	25	98	98298	6872.990	2345	1.440	-1.253	1.074	-1.576	-8.401	-1.636	-6.172

Figure B.4. Measured Data from the Solar Test Bench (Case 1, 10/25/98, Blocked Window; Part 1).

15	16	17	18	19	20	21	22	23	24	25	26	27	28
TSP	SVL	APD	TI	TO	Tdb	RH	GHR	Wind	Tdb2	Tdew	Wind2	Tg,r	Tg,l
-2.516	-3.609	0.051	67.342	69.085	63.266	75.293	-99.000	3.745	-99.000	-99.000	-99.000	-99.000	-99.000
-2.278	-3.609	0.055	67.173	68.860	63.131	75.810	-99.000	3.451	-99.000	-99.000	-99.000	-99.000	-99.000
-2.753	-3.992	0.057	67.005	68.635	62.996	76.326	-99.000	3.156	-99.000	-99.000	-99.000	-99.000	-99.000
-2.753	-3.609	0.053	66.780	68.410	62.862	76.842	-99.000	2.862	-99.000	-99.000	-99.000	-99.000	-99.000
-2.753	-3.609	0.057	66.443	68.129	62.727	77.359	-99.000	2.568	-99.000	-99.000	-99.000	-99.000	-99.000
-2.753	-3.609	0.059	66.049	67.848	62.525	78.039	-99.000	2.800	-99.000	-99.000	-99.000	-99.000	-99.000
-2.991	-3.609	0.057	65.824	67.623	62.323	78.719	-99.000	3.031	-99.000	-99.000	-99.000	-99.000	-99.000
-2.753	-3.609	0.058	65.600	67.398	62.121	79.400	-99.000	3.263	-99.000	-99.000	-99.000	-99.000	-99.000
-2.516	-3.609	0.060	65.431	67.117	61.919	80.080	-99.000	3.495	-99.000	-99.000	-99.000	-99.000	-99.000
-2.753	-3.609	0.054	65.262	66.949	61.604	80.886	-99.000	3.445	-99.000	-99.000	-99.000	-99.000	-99.000
-2.278	-3.609	0.049	64.981	66.668	61.290	81.692	-99.000	3.394	-99.000	-99.000	-99.000	-99.000	-99.000
-2.041	-3.609	0.053	64.813	66.443	60.975	82.498	-99.000	3.344	-99.000	-99.000	-99.000	-99.000	-99.000
-1.803	-3.609	0.055	64.756	66.274	60.661	83.304	-99.000	3.294	-99.000	-99.000	-99.000	-99.000	-99.000
-1.803	-3.609	0.050	64.588	66.162	60.549	83.480	-99.000	3.169	-99.000	-99.000	-99.000	-99.000	-99.000
-1.328	-3.609	0.049	64.475	65.993	60.437	83.657	-99.000	3.444	-99.000	-99.000	-99.000	-99.000	-99.000
-1.803	-3.609	0.054	64.250	65.768	60.324	83.834	-99.000	3.520	-99.000	-99.000	-99.000	-99.000	-99.000
-2.278	-3.609	0.047	64.138	65.600	60.212	84.010	-99.000	3.595	-99.000	-99.000	-99.000	-99.000	-99.000
-2.516	-3.609	0.052	63.913	65.431	59.988	84.741	-99.000	4.058	-99.000	-99.000	-99.000	-99.000	-99.000
-2.516	-3.609	0.050	63.969	65.318	59.763	85.471	-99.000	4.522	-99.000	-99.000	-99.000	-99.000	-99.000
-2.041	-3.609	0.060	63.857	65.150	59.538	86.201	-99.000	4.985	-99.000	-99.000	-99.000	-99.000	-99.000
-1.566	-3.609	0.058	63.801	65.094	59.314	86.932	-99.000	5.448	-99.000	-99.000	-99.000	-99.000	-99.000
-1.328	-3.609	0.059	64.026	64.756	59.247	87.310	-99.000	4.791	-99.000	-99.000	-99.000	-99.000	-99.000
-1.328	-3.609	0.050	64.082	64.419	59.179	87.688	-99.000	4.133	-99.000	-99.000	-99.000	-99.000	-99.000
-1.566	-3.609	0.050	63.463	64.531	59.112	88.065	-99.000	3.476	-99.000	-99.000	-99.000	-99.000	-99.000
-1.566	-3.609	0.050	63.351	64.475	59.045	88.443	-99.000	2.818	-99.000	-99.000	-99.000	-99.000	-99.000
-2.041	-3.609	0.053	63.520	64.419	58.888	88.997	-99.000	2.868	-99.000	-99.000	-99.000	-99.000	-99.000
-1.566	-3.226	0.056	63.351	64.138	58.730	89.551	-99.000	2.918	-99.000	-99.000	-99.000	-99.000	-99.000
2.235	-0.545	0.061	63.857	63.969	58.573	90.106	-99.000	2.969	-99.000	-99.000	-99.000	-99.000	-99.000
13.162	7.882	0.059	63.182	64.138	58.416	90.660	-99.000	3.019	-99.000	-99.000	-99.000	-99.000	-99.000
33.591	22.920	0.061	62.789	64.250	58.394	90.383	-99.000	2.543	-99.000	-99.000	-99.000	-99.000	-99.000
69.697	30.863	0.060	62.845	64.250	58.371	90.106	-99.000	2.068	-99.000	-99.000	-99.000	-99.000	-99.000
74.923	29.331	0.061	63.014	63.969	58.348	89.829	-99.000	1.592	-99.000	-99.000	-99.000	-99.000	-99.000
137.159	43.503	0.055	63.182	63.857	58.326	89.552	-99.000	1.116	-99.000	-99.000	-99.000	-99.000	-99.000
206.047	261.442	0.058	63.745	64.138	58.418	89.275	-99.000	1.197	-99.000	-99.000	-99.000	-99.000	-99.000
235.502	316.215	0.062	65.037	64.475	58.550	88.997	-99.000	1.279	-99.000	-99.000	-99.000	-99.000	-99.000
284.436	362.560	0.058	66.105	65.431	58.661	88.720	-99.000	1.360	-99.000	-99.000	-99.000	-99.000	-99.000
338.596	422.695	0.056	67.792	66.611	58.775	88.441	99.900	1.441	59.000	55.000	1.000	-99.000	-99.000
380.404	464.444	0.055	69.703	67.679	59.920	85.622	158.309	2.267	60.750	55.500	4.000	-99.000	-99.000
418.411	500.831	0.065	71.614	68.916	61.065	82.900	216.717	3.093	62.500	56.000	4.000	-99.000	-99.000
455.467	534.537	0.068	73.638	70.265	62.211	79.979	275.126	1.920	64.250	56.500	4.000	-99.000	-99.000
485.873	559.817	0.069	75.437	71.558	63.356	77.158	333.535	4.746	66.000	57.000	4.000	-99.000	-99.000
516.278	586.245	0.067	77.011	72.682	64.618	75.470	384.437	4.827	-99.000	-99.000	-99.000	-99.000	-99.000
539.083	601.481	0.061	78.079	73.244	66.120	73.782	435.339	4.909	-99.000	-99.000	-99.000	-99.000	-99.000
566.638	624.164	0.051	79.428	74.200	67.802	72.094	486.241	4.990	-99.000	-99.000	-99.000	-99.000	-99.000
592.292	643.315	0.055	80.383	75.156	69.284	70.406	537.143	5.072	-99.000	-99.000	-99.000	-99.000	-99.000
608.445	654.806	0.062	81.283	76.111	70.541	68.328	573.604	5.335	-99.000	-99.000	-99.000	-99.000	-99.000
621.747	662.850	0.058	82.519	77.292	71.799	66.249	610.065	5.598	-99.000	-99.000	-99.000	-99.000	-99.000
633.150	668.978	0.074	83.250	77.910	73.057	64.171	646.525	5.861	-99.000	-99.000	-99.000	-99.000	-99.000
638.851	672.908	0.065	84.262	78.360	74.314	62.093	682.986	6.124	75.000	61.000	7.000	-99.000	-99.000
637.900	670.893	0.067	85.218	79.315	75.010	59.813	703.862	6.187	76.000	61.000	6.500	-99.000	-99.000
636.950	670.893	0.072	85.948	80.215	75.706	57.534	724.737	6.249	77.000	61.000	6.000	-99.000	-99.000
634.100	668.978	0.069	86.342	80.933	76.402	55.254	745.612	6.312	78.000	61.000	5.500	-99.000	-99.000
626.498	663.999	0.066	87.129	81.508	77.098	52.974	766.488	6.374	79.000	61.000	5.000	-99.000	-99.000
616.997	658.636	0.058	86.904	81.901	77.704	51.488	769.062	6.080	-99.000	-99.000	-99.000	-99.000	-99.000
599.894	644.464	0.059	87.410	82.238	78.311	50.001	771.635	5.786	-99.000	-99.000	-99.000	-99.000	-99.000
578.040	629.144	0.061	87.860	82.688	78.918	48.515	774.209	5.491	-99.000	-99.000	-99.000	-99.000	-99.000
552.185	611.908	0.071	88.534	83.306	79.524	47.029	776.783	5.197	-99.000	-99.000	-99.000	-99.000	-99.000
527.680	593.523	0.061	88.422	83.587	79.906	45.179	764.057	4.840	-99.000	-99.000	-99.000	-99.000	-99.000
498.700	571.307	0.053	88.703	83.812	80.288	43.329	751.332	4.484	-99.000	-99.000	-99.000	-99.000	-99.000
464.969	546.794	0.056	88.928	84.150	80.669	42.079	738.607	4.127	-99.000	-99.000	-99.000	-99.000	-99.000
431.713	518.450	0.057	89.096	84.487	81.051	40.429	725.881	3.770	-99.000	-99.000	-99.000	-99.000	-99.000
402.733	493.554	0.056	89.321	84.768	81.163	39.623	695.425	4.102	-99.000	-99.000	-99.000	-99.000	-99.000
363.301	461.380	0.067	89.152	84.993	81.275	38.816	664.970	4.434	-99.000	-99.000	-99.000	-99.000	-99.000
320.068	426.525	0.068	89.096	85.161	81.388	38.010	634.515	4.765	-99.000	-99.000	-99.000	-99.000	-99.000
269.233	383.626	0.067	88.478	85.161	81.500	37.204	604.059	5.097	81.000	55.000	5.000	-99.000	-99.000
225.526	345.324	0.060	88.197	85.105	81.478	37.166	560.449	5.066	81.000	55.500	5.500	-99.000	-99.000
179.917	300.511	0.061	87.691	84.993	81.455	37.129	516.839	5.035	81.000	56.000	6.000	-99.000	-99.000
130.033	240.376	0.061	86.960	84.768	81.433	37.091	473.230	5.003	81.000	56.500	6.500	-99.000	-99.000
91.076	189.434	0.055	86.286	84.543	81.410	37.053	429.620	4.972	81.000	57.000	7.000	-99.000	-99.000
47.843	140.408	0.043	85.667	84.206	81.073	38.225	373.795	4.916	80.000	57.000	6.500	-99.000	-99.000
16.408	79.507	0.047	84.768	83.868	80.737	39.396	317.969	4.859	79.000	57.000	6.000	-99.000	-99.000
4.610	11.712	0.052	83.812	83.419	80.400	40.567	262.114	4.802	78.000	57.000	5.500	-99.000	-99.000
-3.704	-2.077	0.060	82.857	82.857	80.063	41.739	206.279	4.746	77.000	57.000	5.000	-99.000	-99.000
-5.166	-3.992	0.053	81.732	82.238	79.322	43.855	160.024	4.634	-99.000	-99.000	-99.000	-99.000	-99.000
-4.416	-3.992	0.041	80.833	81.732	78.581	45.971	113.769	4.521	-99.000	-99.000	-99.000	-99.000	-99.000
-4.179	-3.992	0.047	80.158	81.226	77.839	48.087	67.514	4.408	-99.000	-99.000	-99.000	-99.000	-99.000
-3.229	-3.992	0.043	79.428	80.721	77.098	50.203	21.259	4.296	-99.000	-99.000	-99.000	-99.000	-99.000
-2.991	-3.609	0.054	79.034	80.327	76.335	52.521	-99.000	4.290	-99.000	-99.000	-99.000	-99.000	-99.000
-2.991	-3.992	0.060	78.472	79.877	75.572	54.838	-99.000	4.283	-99.000	-99.000	-99.000	-99.000	-99.000
-2.753	-3.992	0.053	77.854	79.371	74.808	57.155	-99.000	4.277	-99.000	-99.000	-99.000	-99.000	-99.000
-2.516	-3.992	0.057	77.460	78.978	74.045	59.473	-99.000	4.271	68.000	61.000	0.000	-99.000	-99.000
-2.278	-3.609	0.058	76.842	78.528	73.551	60.745	-99.000	4.427	67.500	61.000	1.000	-99.000	-99.000
-2.516	-3.609	0.059	76.448	78.191	73.057	62.017	-99.000	4.584	67.000	61.000	2.000	-99.000	-99.000
-2.278	-3.609	0.057	75.886	77.741	72.563	63.290	-99.000	4.740	66.500	61.000	3.000	-99.000	-99.000
-2.516	-3.609	0.059	75.380	77.292	72.069	64.562	-99.000	4.897	66.000	61.000	4.000	-99.000	-99.000
-2.516	-3.609	0.059	74.762	76.842	71.507	66.338	-99.000	4.897	65.500	61.000	3.750	-99.000	-99.000
-2.516	-3.609	0.064	74.200	76.392	70.946	68.114	-99.000	4.897	65.000	61.000	3.500	-99.000	-99.000
-2.516	-3.609	0.058	73.582	75.943	70.384	69.890	-99.000	4.897	64.500	61.000	3.250	-99.000	-99.000
-2.041	-3.609	0.061	73.357	75.605	69.823	71.666	-99.000	4.897	64.000	61.000	3.000	-99.000	-99.000
-1.566	-3.609	0.053	73.076	75.324	69.217	73.820	-99.000	4.790	-99.000	-99.000	-99.000	-99.000	-99.000
-1.803	-3.609	0.048	72.738	75.043	68.611	75.973	-99.000	4.684	-99.000	-99.000	-99.000	-99.000	-99.000
-1.803	-3.609	0.046	72.401	74.762	68.004	78.127	-99.000	4.578	-99.000	-99.000	-99.000	-99.000	-99.000
-1.803	-3.609	0.059	72.345	74.537	67.398	80.281	-99.000	4.471	-99.000	-99.000	-99.000	-99.000	-99.000
-1.803	-3.609	0.054	72.064	74.256	67.331	81.087	-99.000	4.584	-99.000	-99.000	-99.000	-99.000	-99.000
-2.041	-3.609	0.056	71.895	74.031	67.263	81.893	-99.000	4.696	-99.000	-99.000	-99.000	-99.000	-99.000
-2.278	-3.609	0.051	71.670	73.750	67.195	82.700	-99.000	4.809	-99.000	-99.000	-99.000	-99.000	-99.000

Figure B.5. Measured Data from the Solar Test Bench (Case 1, 10/25/98, Blocked Window; Part 2).

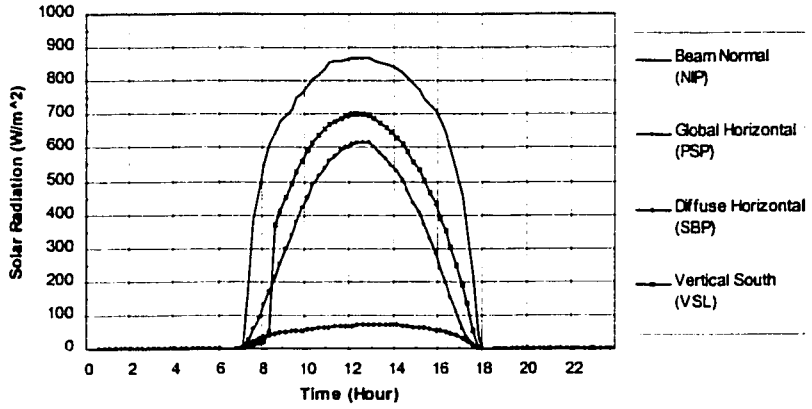

Figure B.6. Measured Beam Normal, Global Horizontal, Diffuse Horizontal and Vertical South Solar Radiation (Case 2, 11/03/98, Blocked Window w/ Periodic Heat Gain).

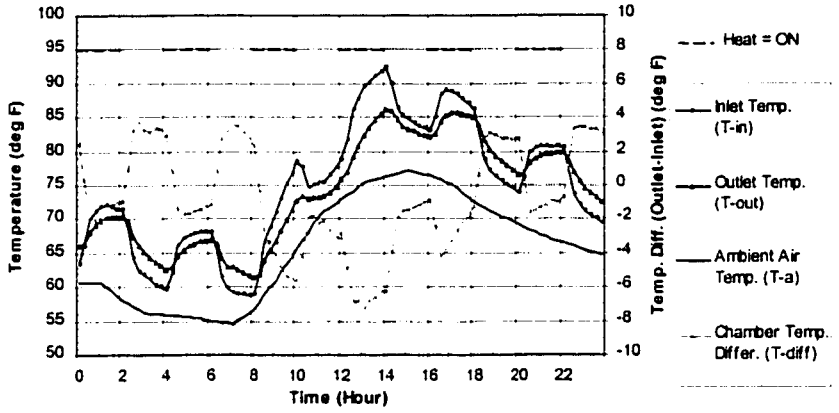

Figure B.7. Measured Chamber Inlet and Outlet Temperature, Ambient Air Temperature, and Air Temperature Difference between Chamber Outlet and Inlet (Case 2, 11/03/98, Blocked Window w/ Periodic Heat Gain).

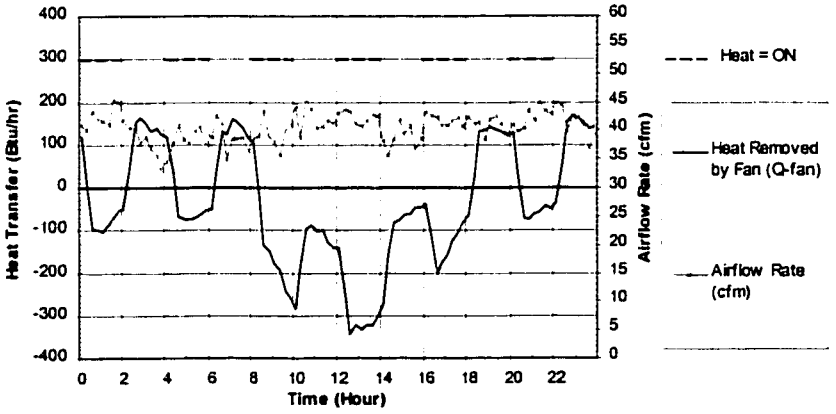

Figure B.8. Heat Transfer of the Experimental Box and Calculated Airflow Rate (Case 2, 11/03/98, Blocked Window w/ Periodic Heat Gain).

1	2	3	4	5	6	7	8	9	10	11	12	13	14
Site	Month	Day	Year	Julian	Decimal	Hour	ELI	SLI	WLI	LIH	NIP	PSP	SBP
0	10	25	98	98298	6872.000	0	1.312	-1.101	1.074	-1.745	-7.958	-3.308	-6.172
0	10	25	98	98298	6872.010	15	1.696	-0.627	1.812	-1.576	-7.958	-1.427	-5.262
0	10	25	98	98298	6872.021	30	1.824	-0.311	2.107	-1.576	-7.958	-1.009	-4.897
0	10	25	98	98298	6872.031	45	1.824	-0.311	2.107	-1.576	-7.958	-1.218	-4.897
0	10	25	98	98298	6872.042	100	1.824	-0.311	2.255	-1.576	-7.958	-1.218	-4.897
0	10	25	98	98298	6872.052	115	1.953	-0.311	2.107	-1.576	-7.736	-1.218	-5.079
0	10	25	98	98298	6872.063	130	1.824	-0.469	2.107	-1.576	-7.736	-1.009	-5.079
0	10	25	98	98298	6872.073	145	1.824	-0.469	2.107	-1.576	-7.736	-0.800	-5.079
0	10	25	98	98298	6872.083	200	1.824	-0.469	2.107	-1.576	-7.736	-0.382	-4.897
0	10	25	98	98298	6872.094	215	1.953	-0.469	2.255	-1.576	-7.958	-1.009	-5.079
0	10	25	98	98298	6872.104	230	1.824	-0.469	2.107	-1.576	-7.736	-0.591	-4.897
0	10	25	98	98298	6872.115	245	1.824	-0.469	2.107	-1.576	-7.736	-0.382	-4.897
0	10	25	98	98298	6872.125	300	1.953	-0.311	2.255	-1.576	-7.515	0.036	-4.897
0	10	25	98	98298	6872.135	315	1.953	-0.311	2.107	-1.576	-7.736	-0.173	-4.897
0	10	25	98	98298	6872.146	330	1.953	-0.311	2.107	-1.576	-7.736	-0.173	-4.715
0	10	25	98	98298	6872.156	345	1.953	-0.311	2.255	-1.576	-7.736	-0.382	-4.715
0	10	25	98	98298	6872.167	400	1.824	-0.469	2.107	-1.576	-7.958	-0.591	-4.715
0	10	25	98	98298	6872.177	415	1.953	-0.311	2.255	-1.576	-7.736	-0.591	-4.533
0	10	25	98	98298	6872.188	430	1.953	-0.311	2.255	-1.576	-7.736	-0.800	-4.533
0	10	25	98	98298	6872.198	445	1.953	-0.311	2.255	-1.576	-7.736	-0.173	-4.533
0	10	25	98	98298	6872.209	500	1.953	-0.311	2.255	-1.408	-7.736	0.036	-4.351
0	10	25	98	98298	6872.219	515	1.953	-0.311	2.255	-1.408	-7.736	0.036	-4.351
0	10	25	98	98298	6872.229	530	1.953	-0.311	2.255	-1.576	-7.736	-0.173	-4.351
0	10	25	98	98298	6872.240	545	1.953	-0.311	2.255	-1.576	-7.736	0.036	-4.351
0	10	25	98	98298	6872.250	600	1.953	-0.311	2.255	-1.576	-7.736	0.036	-4.351
0	10	25	98	98298	6872.260	615	1.568	-1.259	1.222	-1.576	-7.958	-1.009	-5.444
0	10	25	98	98298	6872.271	630	2.465	-0.627	1.369	-1.240	-7.958	-2.472	-5.079
0	10	25	98	98298	6872.281	645	7.592	3.478	4.320	1.961	-7.958	1.081	-1.801
0	10	25	98	98298	6872.292	700	25.793	17.374	13.321	12.235	-7.515	13.205	9.764
0	10	25	98	98298	6872.302	715	141.404	76.114	28.666	44.238	137.265	42.469	27.889
0	10	25	98	98298	6872.313	730	320.845	163.276	35.453	84.999	286.257	67.970	36.268
0	10	25	98	98298	6872.323	745	250.607	141.485	33.978	77.251	197.128	67.970	35.540
0	10	25	98	98298	6872.333	800	433.617	257.070	46.667	144.962	364.744	127.751	52.662
0	10	25	98	98298	6872.344	815	614.616	383.077	53.750	218.400	545.219	196.312	62.133
0	10	25	98	98298	6872.354	830	632.047	419.710	55.225	244.676	539.011	225.158	64.319
0	10	25	98	98298	6872.365	845	700.235	490.450	58.766	293.522	575.173	273.234	70.148
0	10	25	98	98298	6872.375	900	777.138	571.297	60.899	346.747	648.982	326.745	70.877
0	10	25	98	98298	6872.385	915	814.565	630.036	140.214	386.635	672.927	365.206	73.427
0	10	25	98	98298	6872.396	930	844.301	683.723	203.661	424.565	692.438	407.011	75.248
0	10	25	98	98298	6872.406	945	870.961	736.147	255.599	460.947	715.496	450.488	77.070
0	10	25	98	98298	6872.417	1000	884.291	779.728	308.717	491.265	718.157	483.933	91.441
0	10	25	98	98298	6872.427	1015	898.646	826.467	365.376	522.257	734.120	516.541	95.084
0	10	25	98	98298	6872.438	1030	896.595	858.680	417.904	543.817	742.989	544.132	87.270
0	10	25	98	98298	6872.448	1045	900.697	895.945	473.974	569.419	769.594	575.068	94.356
0	10	25	98	98298	6872.458	1100	900.697	929.420	528.862	593.000	804.182	600.151	81.077
0	10	25	98	98298	6872.469	1115	888.392	949.632	578.439	607.822	818.372	614.365	81.441
0	10	25	98	98298	6872.479	1130	871.986	967.317	626.836	620.623	833.448	627.743	81.077
0	10	25	98	98298	6872.490	1145	851.478	978.686	672.282	630.055	845.864	641.121	82.898
0	10	25	98	98298	6872.500	1200	824.819	986.265	713.596	634.772	852.959	648.646	82.898
0	10	25	98	98298	6872.510	1215	792.519	986.265	750.188	634.772	850.299	651.154	85.813
0	10	25	98	98298	6872.521	1230	758.682	987.528	787.171	634.098	854.733	657.007	85.084
0	10	25	98	98298	6872.531	1245	722.793	988.791	822.193	630.729	862.715	657.007	82.898
0	10	25	98	98298	6872.542	1300	683.316	985.002	852.293	623.992	864.488	647.810	83.263
0	10	25	98	98298	6872.552	1315	642.301	979.949	880.623	613.886	868.923	637.776	79.255
0	10	25	98	98298	6872.563	1330	593.596	962.895	898.329	597.716	864.488	616.874	78.527
0	10	25	98	98298	6872.573	1345	542.327	939.526	910.723	577.504	859.167	593.463	78.163
0	10	25	98	98298	6872.583	1400	489.007	912.998	918.986	554.596	855.620	570.052	76.705
0	10	25	98	98298	6872.594	1415	436.200	883.944	923.708	529.668	851.185	547.477	72.334
0	10	25	98	98298	6872.604	1430	380.830	847.311	921.347	501.171	840.543	517.377	71.969
0	10	25	98	98298	6872.615	1445	324.434	804.361	912.494	468.358	821.032	481.424	71.791
0	10	25	98	98298	6872.625	1500	269.064	756.359	898.329	433.997	798.861	444.636	71.062
0	10	25	98	98298	6872.635	1515	216.257	713.409	890.656	403.005	794.427	411.191	71.605
0	10	25	98	98298	6872.646	1530	162.681	659.722	862.917	361.907	773.142	370.640	65.412
0	10	25	98	98298	6872.656	1545	98.082	602.245	828.685	320.135	747.423	327.581	61.405
0	10	25	98	98298	6872.667	1600	55.016	531.505	771.435	270.952	697.759	274.906	56.669
0	10	25	98	98298	6872.677	1615	48.607	468.976	721.268	228.506	656.377	227.248	51.390
0	10	25	98	98298	6872.688	1630	44.249	398.235	652.405	183.702	590.431	180.844	49.019
0	10	25	98	98298	6872.698	1645	40.148	310.757	544.208	135.193	496.442	92.635	43.190
0	10	25	98	98298	6872.708	1700	36.303	238.122	450.366	96.453	411.304	82.184	36.997
0	10	25	98	98298	6872.719	1715	31.945	170.855	353.572	57.376	329.270	57.100	28.618
0	10	25	98	98298	6872.729	1730	23.998	94.430	211.334	25.036	197.571	26.583	17.325
0	10	25	98	98298	6872.740	1745	11.437	21.479	43.126	0.161	21.087	5.680	4.757
0	10	25	98	98298	6872.750	1800	3.875	2.057	5.206	0.613	-9.510	-2.661	-4.169
0	10	25	98	98298	6872.760	1815	1.568	-0.943	1.812	-1.576	-9.510	-3.517	-6.719
0	10	25	98	98298	6872.771	1830	1.312	-1.417	1.222	-1.913	-9.288	-3.099	-6.901
0	10	25	98	98298	6872.781	1845	1.184	-1.417	1.074	-1.913	-9.288	-2.681	-6.901
0	10	25	98	98298	6872.792	1900	1.184	-1.575	1.074	-1.913	-9.288	-2.054	-6.901
0	10	25	98	98298	6872.802	1915	1.568	-1.101	1.369	-1.576	-8.845	-1.845	-6.537
0	10	25	98	98298	6872.813	1930	1.440	-1.259	1.369	-1.745	-8.845	-2.054	-6.537
0	10	25	98	98298	6872.823	1945	1.440	-1.259	1.222	-1.745	-8.845	-2.054	-6.537
0	10	25	98	98298	6872.833	2000	1.312	-1.259	1.222	-1.913	-8.845	-2.054	-6.537
0	10	25	98	98298	6872.844	2015	1.440	-1.259	1.222	-1.745	-8.845	-1.427	-6.537
0	10	25	98	98298	6872.854	2030	1.568	-1.259	1.369	-1.745	-8.845	-1.427	-6.537
0	10	25	98	98298	6872.865	2045	1.568	-1.259	1.369	-1.745	-8.623	-1.009	-6.354
0	10	25	98	98298	6872.875	2100	1.696	-1.417	1.369	-1.576	-8.845	-1.218	-6.354
0	10	25	98	98298	6872.885	2115	1.568	-1.259	1.369	-1.745	-8.623	-1.636	-6.354
0	10	25	98	98298	6872.896	2130	1.568	-1.417	1.369	-1.408	-8.623	-1.427	-6.354
0	10	25	98	98298	6872.906	2145	1.568	-1.417	1.222	-1.745	-8.623	-1.218	-6.172
0	10	25	98	98298	6872.917	2200	1.568	-1.417	1.222	-1.576	-8.623	-0.591	-6.172
0	10	25	98	98298	6872.927	2215	1.568	-1.259	1.222	-1.576	-8.623	-0.800	-6.172
0	10	25	98	98298	6872.938	2230	1.440	-1.259	1.222	-1.576	-8.623	-1.009	-6.354
0	10	25	98	98298	6872.948	2245	1.440	-1.259	1.222	-1.576	-8.401	-1.009	-6.172
0	10	25	98	98298	6872.958	2300	1.440	-1.259	1.074	-1.576	-8.401	-1.009	-6.172
0	10	25	98	98298	6872.969	2315	1.440	-1.259	1.222	-1.576	-8.401	-1.009	-6.172
0	10	25	98	98298	6872.979	2330	1.568	-1.259	1.074	-1.576	-8.623	-1.218	-6.172
0	10	25	98	98298	6872.990	2345	1.440	-1.259	1.074	-1.576	-8.401	-1.636	-6.172

Figure B.9. Measured Data from the Solar Test Bench (Case 2, 11/03/98, Blocked Window w/ Periodic Heat Gain; Part 1).

15	16	17	18	19	20	21	22	23	24	25	26	27	28
TSP	SVL	APD	TI	TO	Tdb	RH	GHR	Wind	Tdb2	Tdew	Wind2	Tq,r	Tq,l
-2.516	-3.609	0.051	67.342	69.085	63.266	75.293	-99.000	3.745	-99.000	-99.000	-99.000	-99.000	-99.000
-2.278	-3.609	0.055	67.173	68.860	63.131	75.810	-99.000	3.451	-99.000	-99.000	-99.000	-99.000	-99.000
-2.753	-3.992	0.057	67.005	68.635	62.996	76.326	-99.000	3.156	-99.000	-99.000	-99.000	-99.000	-99.000
-2.753	-3.609	0.053	66.780	68.410	62.862	76.842	-99.000	2.862	-99.000	-99.000	-99.000	-99.000	-99.000
-2.753	-3.609	0.057	66.443	68.129	62.727	77.359	-99.000	2.568	-99.000	-99.000	-99.000	-99.000	-99.000
-2.753	-3.609	0.059	66.049	67.848	62.525	78.039	-99.000	2.800	-99.000	-99.000	-99.000	-99.000	-99.000
-2.991	-3.609	0.057	65.824	67.623	62.323	78.719	-99.000	3.031	-99.000	-99.000	-99.000	-99.000	-99.000
-2.753	-3.609	0.058	65.600	67.398	62.121	79.400	-99.000	3.263	-99.000	-99.000	-99.000	-99.000	-99.000
-2.516	-3.609	0.060	65.431	67.117	61.919	80.080	-99.000	3.495	-99.000	-99.000	-99.000	-99.000	-99.000
-2.753	-3.609	0.054	65.262	66.949	61.604	80.886	-99.000	3.445	-99.000	-99.000	-99.000	-99.000	-99.000
-2.278	-3.609	0.049	64.981	66.668	61.290	81.692	-99.000	3.394	-99.000	-99.000	-99.000	-99.000	-99.000
-2.041	-3.609	0.053	64.813	66.443	60.975	82.498	-99.000	3.344	-99.000	-99.000	-99.000	-99.000	-99.000
-1.803	-3.609	0.055	64.756	66.274	60.661	83.304	-99.000	3.294	-99.000	-99.000	-99.000	-99.000	-99.000
-1.803	-3.609	0.050	64.588	66.162	60.549	83.480	-99.000	3.369	-99.000	-99.000	-99.000	-99.000	-99.000
-1.328	-3.609	0.049	64.475	65.993	60.437	83.657	-99.000	3.444	-99.000	-99.000	-99.000	-99.000	-99.000
-1.803	-3.609	0.054	64.250	65.768	60.324	83.834	-99.000	3.520	-99.000	-99.000	-99.000	-99.000	-99.000
-2.278	-3.609	0.047	64.138	65.600	60.212	84.010	-99.000	3.595	-99.000	-99.000	-99.000	-99.000	-99.000
-2.516	-3.609	0.052	63.913	65.431	59.988	84.741	-99.000	4.058	-99.000	-99.000	-99.000	-99.000	-99.000
-2.516	-3.609	0.050	63.969	65.318	59.763	85.471	-99.000	4.522	-99.000	-99.000	-99.000	-99.000	-99.000
-2.041	-3.609	0.060	63.857	65.150	59.538	86.201	-99.000	4.985	-99.000	-99.000	-99.000	-99.000	-99.000
-1.566	-3.609	0.058	63.801	65.094	59.314	86.332	99.000	5.119	-99.000	-99.000	-99.000	-99.000	-99.000
-1.328	-3.609	0.059	64.026	64.756	59.247	87.310	-99.000	4.791	-99.000	-99.000	-99.000	-99.000	-99.000
-1.328	-3.609	0.050	64.082	64.419	59.179	87.888	-99.000	4.133	-99.000	-99.000	-99.000	-99.000	-99.000
-1.566	-3.609	0.050	63.463	64.531	59.112	88.065	-99.000	3.476	-99.000	-99.000	-99.000	-99.000	-99.000
-1.566	-3.609	0.050	63.351	64.475	59.045	88.443	-99.000	2.818	-99.000	-99.000	-99.000	-99.000	-99.000
-2.041	-3.609	0.053	63.520	64.419	58.888	88.997	-99.000	2.868	-99.000	-99.000	-99.000	-99.000	-99.000
-1.566	-3.226	0.056	63.351	64.138	58.730	89.551	-99.000	2.918	-99.000	-99.000	-99.000	-99.000	-99.000
2.235	-0.545	0.061	63.857	63.969	58.571	90.106	-99.000	2.969	-99.000	-99.000	-99.000	-99.000	-99.000
13.162	7.882	0.059	63.182	64.138	58.416	90.660	-99.000	3.019	-99.000	-99.000	-99.000	-99.000	-99.000
33.591	22.820	0.061	62.789	64.250	58.394	90.383	-99.000	2.543	-99.000	-99.000	-99.000	-99.000	-99.000
69.697	30.863	0.060	62.845	64.250	58.371	90.106	-99.000	2.068	-99.000	-99.000	-99.000	-99.000	-99.000
74.923	29.331	0.061	63.014	63.969	58.348	89.829	-99.000	1.592	-99.000	-99.000	-99.000	-99.000	-99.000
137.159	43.503	0.055	63.182	63.857	58.326	89.552	-99.000	1.116	-99.000	-99.000	-99.000	-99.000	-99.000
206.047	261.442	0.058	63.745	64.138	58.438	89.275	-99.000	1.197	-99.000	-99.000	-99.000	-99.000	-99.000
235.502	316.215	0.062	65.017	64.475	58.550	88.997	-99.000	1.279	-99.000	-99.000	-99.000	-99.000	-99.000
284.436	362.560	0.058	66.105	65.431	58.663	88.720	-99.000	1.360	-99.000	-99.000	-99.000	-99.000	-99.000
338.596	422.695	0.056	67.792	66.611	58.775	88.443	99.900	1.441	59.000	55.000	4.000	-99.000	-99.000
380.404	464.444	0.055	69.703	67.679	59.920	85.622	158.309	2.267	60.750	55.500	4.000	-99.000	-99.000
418.411	500.831	0.065	71.614	68.916	61.065	82.800	216.717	3.093	62.500	56.000	4.000	-99.000	-99.000
455.467	534.537	0.068	73.638	70.265	62.211	79.979	275.126	3.920	64.250	56.500	4.000	-99.000	-99.000
485.873	559.817	0.069	75.437	71.558	63.356	77.158	333.535	4.746	66.000	57.000	4.000	-99.000	-99.000
516.278	586.245	0.067	77.011	72.682	64.838	75.470	384.437	4.827	-99.000	-99.000	-99.000	-99.000	-99.000
539.083	603.481	0.061	78.079	73.244	66.320	73.782	435.339	4.909	-99.000	-99.000	-99.000	-99.000	-99.000
566.638	624.164	0.051	79.428	74.200	67.802	72.094	486.241	4.990	-99.000	-99.000	-99.000	-99.000	-99.000
592.292	643.315	0.055	80.383	75.156	69.284	70.406	537.143	5.072	-99.000	-99.000	-99.000	-99.000	-99.000
608.445	654.806	0.062	81.283	76.111	70.541	68.328	573.604	5.335	-99.000	-99.000	-99.000	-99.000	-99.000
621.747	662.850	0.058	82.519	77.292	71.799	66.249	610.065	5.598	-99.000	-99.000	-99.000	-99.000	-99.000
633.150	668.978	0.074	83.250	77.910	73.057	64.171	646.525	5.861	-99.000	-99.000	-99.000	-99.000	-99.000
638.851	672.808	0.065	84.262	78.360	74.314	62.093	682.986	6.124	75.000	61.000	7.000	-99.000	-99.000
637.900	670.893	0.067	85.218	79.315	75.010	59.813	703.862	6.187	76.000	61.000	6.500	-99.000	-99.000
636.950	670.893	0.072	85.948	80.215	75.706	57.534	724.737	6.249	77.000	61.000	6.000	-99.000	-99.000
634.100	668.978	0.069	86.342	80.833	76.402	55.254	745.612	6.312	78.000	61.000	5.500	-99.000	-99.000
626.498	663.999	0.066	87.129	81.508	77.098	52.974	766.488	6.374	79.000	61.000	5.000	-99.000	-99.000
616.997	658.636	0.058	86.904	81.901	77.704	51.488	769.062	6.080	-99.000	-99.000	-99.000	-99.000	-99.000
599.894	644.464	0.059	87.410	82.238	78.311	50.001	771.635	5.786	-99.000	-99.000	-99.000	-99.000	-99.000
578.040	629.144	0.061	87.860	82.688	78.918	48.515	774.209	5.491	-99.000	-99.000	-99.000	-99.000	-99.000
552.385	611.908	0.071	88.534	83.306	79.524	47.029	776.783	5.197	-99.000	-99.000	-99.000	-99.000	-99.000
527.680	593.523	0.061	88.422	83.587	79.906	45.379	764.057	4.840	-99.000	-99.000	-99.000	-99.000	-99.000
498.700	571.107	0.053	88.703	83.812	80.288	43.729	751.332	4.484	-99.000	-99.000	-99.000	-99.000	-99.000
464.969	546.794	0.056	88.928	84.150	80.669	42.079	738.607	4.127	-99.000	-99.000	-99.000	-99.000	-99.000
431.713	518.450	0.057	89.096	84.487	81.051	40.429	725.881	3.770	-99.000	-99.000	-99.000	-99.000	-99.000
402.733	493.554	0.056	89.321	84.768	81.163	39.623	695.425	4.102	-99.000	-99.000	-99.000	-99.000	-99.000
363.301	461.380	0.067	89.152	84.993	81.275	38.816	664.970	4.434	-99.000	-99.000	-99.000	-99.000	-99.000
320.068	426.525	0.068	89.096	85.161	81.388	38.010	634.515	4.765	-99.000	-99.000	-99.000	-99.000	-99.000
269.233	383.626	0.067	88.478	85.161	81.500	37.204	604.059	5.097	81.000	55.000	5.000	-99.000	-99.000
225.526	345.324	0.060	88.197	85.105	81.478	37.166	560.449	5.066	81.000	55.500	5.500	-99.000	-99.000
179.917	300.511	0.061	87.691	84.993	81.455	37.129	516.839	5.035	81.000	56.000	6.000	-99.000	-99.000
130.033	240.376	0.061	86.960	84.768	81.433	37.091	473.230	5.003	81.000	56.500	6.500	-99.000	-99.000
91.076	189.434	0.055	86.286	84.543	81.410	37.053	429.620	4.972	81.000	57.000	7.000	-99.000	-99.000
47.843	140.408	0.043	85.667	84.206	81.073	38.225	373.785	4.916	80.000	57.000	6.500	-99.000	-99.000
16.488	79.507	0.047	84.768	83.868	80.737	39.396	317.949	4.859	79.000	57.000	6.000	-99.000	-99.000
4.610	11.712	0.052	83.812	83.419	80.400	40.567	262.114	4.802	78.000	57.000	5.500	-99.000	-99.000
-1.704	-2.077	0.060	82.857	82.857	80.063	41.739	206.279	4.746	77.000	57.000	5.000	-99.000	-99.000
-5.166	-1.992	0.053	81.732	82.239	79.322	43.855	160.924	4.634	-99.000	-99.000	-99.000	-99.000	-99.000
-4.416	-1.992	0.041	80.833	81.732	78.581	45.971	113.769	4.521	-99.000	-99.000	-99.000	-99.000	-99.000
-4.179	-1.992	0.047	80.158	81.226	77.839	48.087	67.514	4.408	-99.000	-99.000	-99.000	-99.000	-99.000
-3.229	-1.992	0.043	79.428	80.721	77.098	50.203	21.259	4.296	-99.000	-99.000	-99.000	-99.000	-99.000
-2.991	-3.609	0.054	79.034	80.327	76.335	52.521	-99.000	4.290	-99.000	-99.000	-99.000	-99.000	-99.000
-2.991	-3.992	0.060	78.472	79.877	75.572	54.838	-99.000	4.283	-99.000	-99.000	-99.000	-99.000	-99.000
-2.753	-3.992	0.053	77.854	79.371	74.808	57.155	-99.000	4.277	-99.000	-99.000	-99.000	-99.000	-99.000
-2.516	-3.992	0.057	77.460	78.978	74.045	59.473	-99.000	4.271	68.000	61.000	0.000	-99.000	-99.000
-2.278	-3.609	0.058	76.842	78.528	73.551	60.745	-99.000	4.427	67.500	61.000	1.000	-99.000	-99.000
-2.516	-3.609	0.059	76.448	78.191	73.057	62.017	-99.000	4.584	67.000	61.000	2.000	-99.000	-99.000
-2.278	-3.609	0.057	75.886	77.741	72.563	63.290	-99.000	4.740	66.500	61.000	3.000	-99.000	-99.000
-2.516	-3.609	0.059	75.380	77.292	72.069	64.562	-99.000	4.897	66.000	61.000	4.000	-99.000	-99.000
-2.516	-3.609	0.059	74.762	76.842	71.507	66.338	-99.000	4.897	65.500	61.000	3.750	-99.000	-99.000
-2.516	-3.609	0.064	74.200	76.392	70.946	68.114	-99.000	4.897	65.000	61.000	3.500	-99.000	-99.000
-2.516	-3.609	0.058	73.582	75.943	70.384	69.890	-99.000	4.897	64.500	61.000	3.250	-99.000	-99.000
-2.041	-3.609	0.061	73.357	75.605	69.823	71.666	-99.000	4.897	64.000	61.000	3.000	-99.000	-99.000
-1.566	-3.609	0.053	73.076	75.324	69.217	73.820	-99.000	4.790	-99.000	-99.000	-99.000	-99.000	-99.000
-1.803	-3.609	0.048	72.738	75.043	68.611	75.973	-99.000	4.684	-99.000	-99.000	-99.000	-99.000	-99.000
-1.803	-3.609	0.046	72.401	74.762	68.004	78.127	-99.000	4.578	-99.000	-99.000	-99.000	-99.000	-99.000
-1.803	-3.609	0.059	72.345	74.537	67.398	80.281	-99.000	4.471	-99.000	-99.000	-99.000	-99.000	-99.000
-1.803	-3.609	0.054	72.064	74.256	67.331	81.087	-99.000	4.584	-99.000	-99.000	-99.000	-99.000	-99.000
-2.041	-3.609	0.056	71.895	74.031	67.263	81.893	-99.000	4.696	-99.000	-99.000	-99.000	-99.000	-99.000
-2.278	-3.609	0.051	71.670	73.750	67.195	82.700	-99.000	4.809	-99.000	-99.000	-99.000	-99.000	-99.000

Figure B.10. Measured Data from the Solar Test Bench (Case 2, 11/03/98, Blocked Window w/ Periodic Heat Gain; Part 2).

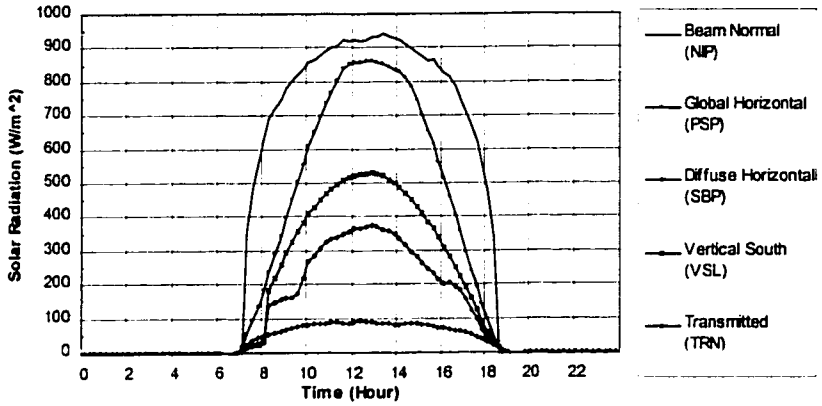

Figure B.11. Measured Beam Normal, Global Horizontal, Diffuse Horizontal and Vertical South Solar Radiation (Case 3, 03/22/99, Glazing Solar Transmittance).

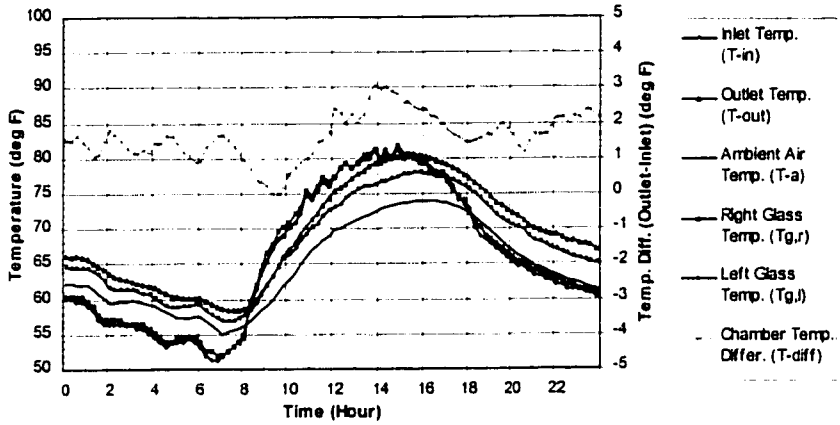

Figure B.12. Measured Chamber Inlet and Outlet Temperature, Ambient Air Temperature, and Air Temperature Difference between Chamber Outlet and Inlet (Case 3, 03/22/99, Glazing Solar Transmittance).

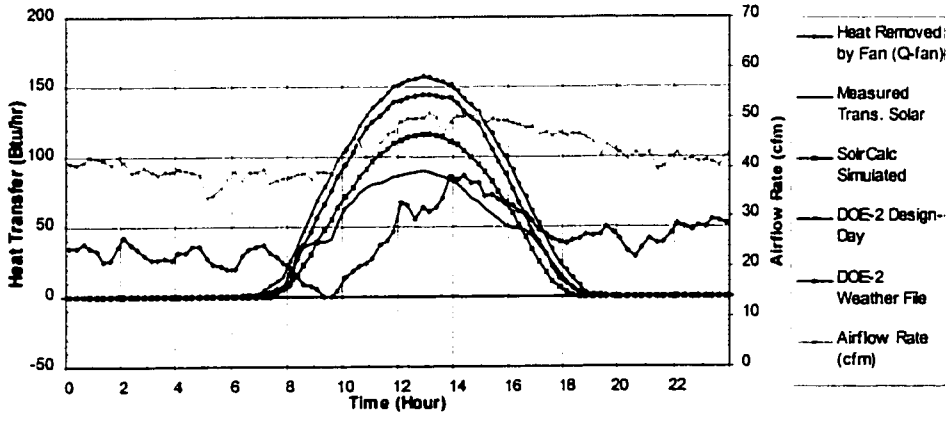

Figure B.13. Heat Transfer of the Experimental Box and Calculated Airflow Rate (Case 3, 03/22/99, Glazing Solar Transmittance).

1	2	3	4	5	6	7	8	9	10	11	12	13	14
Site	Month	Day	Year	Julian	Decimal	Hour	ELI	SLI	WLI	LIH	NIP	PSP	SBP
0	10	25	98	98298	6872.000	0	1.312	-1.101	1.074	-1.745	-7.958	-3.308	-6.172
0	10	25	98	98298	6872.010	15	1.696	-0.627	1.812	-1.576	-7.958	-1.427	-5.262
0	10	25	98	98298	6872.021	30	1.824	-0.311	2.107	-1.576	-7.958	-1.009	-4.897
0	10	25	98	98298	6872.031	45	1.824	-0.311	2.107	-1.576	-7.958	-1.218	-4.897
0	10	25	98	98298	6872.042	100	1.824	-0.311	2.255	-1.576	-7.958	-1.218	-4.897
0	10	25	98	98298	6872.052	115	1.953	-0.311	2.107	-1.576	-7.736	-1.218	-5.079
0	10	25	98	98298	6872.063	130	1.824	-0.469	2.107	-1.576	-7.736	-1.009	-5.079
0	10	25	98	98298	6872.073	145	1.824	-0.469	2.107	-1.576	-7.736	-0.800	-5.079
0	10	25	98	98298	6872.083	200	1.824	-0.469	2.107	-1.576	-7.736	-0.382	-4.897
0	10	25	98	98298	6872.094	215	1.953	-0.469	2.255	-1.576	-7.958	-1.009	-5.079
0	10	25	98	98298	6872.104	230	1.824	-0.469	2.107	-1.576	-7.736	-0.591	-4.897
0	10	25	98	98298	6872.115	245	1.824	-0.469	2.107	-1.576	-7.736	-0.382	-4.897
0	10	25	98	98298	6872.125	300	1.953	-0.311	2.255	-1.576	-7.515	0.036	-4.897
0	10	25	98	98298	6872.135	315	1.953	-0.311	2.107	-1.576	-7.736	-0.173	-4.897
0	10	25	98	98298	6872.146	330	1.953	-0.311	2.107	-1.576	-7.736	-0.173	-4.715
0	10	25	98	98298	6872.156	345	1.953	-0.311	2.255	-1.576	-7.736	-0.382	-4.715
0	10	25	98	98298	6872.167	400	1.824	-0.469	2.107	-1.576	-7.958	-0.591	-4.715
0	10	25	98	98298	6872.177	415	1.953	-0.311	2.255	-1.576	-7.736	-0.591	-4.533
0	10	25	98	98298	6872.188	430	1.953	-0.311	2.255	-1.576	-7.736	-0.800	-4.533
0	10	25	98	98298	6872.198	445	1.953	-0.311	2.255	-1.576	-7.736	-0.173	-4.533
0	10	25	98	98298	6872.208	500	1.953	-0.311	2.255	-1.408	-7.736	0.036	-4.533
0	10	25	98	98298	6872.219	515	1.953	-0.311	2.255	-1.408	-7.736	0.036	-4.351
0	10	25	98	98298	6872.229	530	1.953	-0.311	2.255	-1.576	-7.736	-0.173	-4.351
0	10	25	98	98298	6872.240	545	1.953	-0.311	2.255	-1.576	-7.736	0.036	-4.351
0	10	25	98	98298	6872.250	600	1.953	-0.311	2.255	-1.576	-7.736	0.036	-4.351
0	10	25	98	98298	6872.260	615	1.568	-1.259	1.222	-1.576	-7.958	-3.099	-5.444
0	10	25	98	98298	6872.271	630	2.465	-0.627	1.369	-1.240	-7.958	-2.472	-5.079
0	10	25	98	98298	6872.281	645	7.592	3.478	4.320	1.961	-7.958	1.081	-1.801
0	10	25	98	98298	6872.292	700	25.793	17.371	13.321	12.235	-7.515	13.205	8.764
0	10	25	98	98298	6872.302	715	141.404	76.114	28.666	44.238	137.265	42.469	27.889
0	10	25	98	98298	6872.313	730	320.845	163.276	35.453	84.999	286.257	67.970	36.268
0	10	25	98	98298	6872.323	745	250.607	141.485	33.978	77.251	197.128	67.970	35.540
0	10	25	98	98298	6872.333	800	433.637	257.070	46.667	144.962	364.744	127.751	52.662
0	10	25	98	98298	6872.344	815	614.616	383.077	53.750	218.400	545.219	196.312	62.133
0	10	25	98	98298	6872.354	830	632.047	419.710	55.225	244.676	539.011	225.158	64.319
0	10	25	98	98298	6872.365	845	700.235	490.450	58.766	293.522	575.373	273.234	70.148
0	10	25	98	98298	6872.375	900	777.138	571.297	80.999	346.747	648.982	326.745	70.877
0	10	25	98	98298	6872.385	915	814.565	630.036	140.214	386.835	672.927	365.206	73.427
0	10	25	98	98298	6872.396	930	844.301	683.723	203.661	424.565	692.438	407.011	75.248
0	10	25	98	98298	6872.406	945	870.961	736.147	255.599	460.947	715.496	450.488	77.070
0	10	25	98	98298	6872.417	1000	884.291	779.728	308.717	491.265	718.157	483.933	81.441
0	10	25	98	98298	6872.427	1015	898.646	826.467	365.176	522.257	734.120	516.541	85.084
0	10	25	98	98298	6872.438	1030	896.595	858.680	417.904	543.817	742.989	544.132	87.270
0	10	25	98	98298	6872.448	1045	900.697	895.945	473.974	569.419	769.594	575.068	84.356
0	10	25	98	98298	6872.458	1100	900.697	929.420	528.862	593.000	804.182	600.151	81.077
0	10	25	98	98298	6872.469	1115	888.392	949.632	578.439	607.822	818.372	614.365	81.441
0	10	25	98	98298	6872.479	1130	871.986	967.317	626.836	620.623	833.448	627.743	81.077
0	10	25	98	98298	6872.490	1145	851.478	978.686	672.282	630.055	845.864	641.121	82.898
0	10	25	98	98298	6872.500	1200	824.819	986.265	713.596	634.772	852.959	648.646	82.998
0	10	25	98	98298	6872.510	1215	792.519	986.265	750.188	634.772	850.299	651.154	85.813
0	10	25	98	98298	6872.521	1230	758.682	967.528	787.371	634.098	854.733	657.007	85.084
0	10	25	98	98298	6872.531	1245	722.793	968.791	822.193	630.729	862.715	657.007	82.898
0	10	25	98	98298	6872.542	1300	683.316	985.002	852.293	623.992	864.488	647.910	83.263
0	10	25	98	98298	6872.552	1315	642.301	979.949	880.623	613.886	868.921	637.776	79.255
0	10	25	98	98298	6872.563	1330	593.596	962.895	898.329	597.716	864.488	616.874	78.527
0	10	25	98	98298	6872.573	1345	542.327	939.526	910.723	577.504	859.167	593.463	78.163
0	10	25	98	98298	6872.583	1400	489.007	912.998	918.986	554.596	855.620	570.052	76.705
0	10	25	98	98298	6872.594	1415	436.200	883.944	923.708	529.668	851.185	547.477	72.334
0	10	25	98	98298	6872.604	1430	380.830	847.311	921.347	501.371	840.543	517.377	71.969
0	10	25	98	98298	6872.615	1445	324.434	804.361	912.494	468.358	821.032	481.424	73.791
0	10	25	98	98298	6872.625	1500	269.064	756.359	898.329	433.997	798.861	444.636	73.062
0	10	25	98	98298	6872.635	1515	216.257	713.409	890.656	403.005	794.427	411.191	71.605
0	10	25	98	98298	6872.646	1530	162.681	659.722	862.917	361.907	773.142	370.640	65.412
0	10	25	98	98298	6872.656	1545	98.082	602.245	828.685	320.135	747.423	327.581	61.405
0	10	25	98	98298	6872.667	1600	55.016	531.505	771.435	270.952	697.759	274.906	56.669
0	10	25	98	98298	6872.677	1615	48.607	468.976	721.268	228.506	656.077	227.248	53.390
0	10	25	98	98298	6872.688	1630	44.249	398.235	652.805	183.702	598.431	190.844	49.019
0	10	25	98	98298	6872.698	1645	40.146	310.757	544.208	135.193	496.442	92.635	43.190
0	10	25	98	98298	6872.708	1700	36.303	238.122	450.366	96.453	411.304	42.184	36.997
0	10	25	98	98298	6872.719	1715	31.945	170.855	353.572	57.376	329.270	57.100	28.618
0	10	25	98	98298	6872.729	1730	23.998	94.430	211.334	25.036	197.571	26.583	17.325
0	10	25	98	98298	6872.740	1745	11.437	21.479	43.126	8.361	21.087	5.680	4.757
0	10	25	98	98298	6872.750	1800	3.875	2.057	5.206	0.613	-4.510	-2.681	-4.169
0	10	25	98	98298	6872.760	1815	1.568	-0.943	1.812	-1.576	-4.510	-3.517	-6.719
0	10	25	98	98298	6872.771	1830	1.312	-1.417	1.222	-1.913	-4.288	-3.099	-6.901
0	10	25	98	98298	6872.781	1845	1.184	-1.417	1.074	-1.913	-4.288	-2.681	-6.901
0	10	25	98	98298	6872.792	1900	1.184	-1.575	1.074	-1.913	-4.288	-2.054	-6.901
0	10	25	98	98298	6872.802	1915	1.568	-1.101	1.369	-1.576	-8.845	-1.845	-6.537
0	10	25	98	98298	6872.813	1930	1.440	-1.259	1.369	-1.745	-8.845	-2.054	-6.537
0	10	25	98	98298	6872.823	1945	1.440	-1.259	1.222	-1.745	-8.845	-2.054	-6.537
0	10	25	98	98298	6872.833	2000	1.312	-1.259	1.222	-1.913	-8.845	-2.054	-6.537
0	10	25	98	98298	6872.844	2015	1.440	-1.259	1.222	-1.745	-8.845	-1.427	-6.537
0	10	25	98	98298	6872.854	2030	1.568	-1.259	1.369	-1.745	-8.845	-1.427	-6.537
0	10	25	98	98298	6872.865	2045	1.568	-1.259	1.369	-1.745	-8.623	-1.009	-6.354
0	10	25	98	98298	6872.875	2100	1.696	-1.417	1.369	-1.576	-8.845	-1.218	-6.354
0	10	25	98	98298	6872.885	2115	1.568	-1.259	1.369	-1.745	-8.623	-1.636	-6.354
0	10	25	98	98298	6872.896	2130	1.568	-1.417	1.369	-1.408	-8.623	-1.427	-6.354
0	10	25	98	98298	6872.906	2145	1.568	-1.417	1.222	-1.745	-8.623	-1.218	-6.172
0	10	25	98	98298	6872.917	2200	1.568	-1.417	1.222	-1.576	-8.623	-0.591	-6.172
0	10	25	98	98298	6872.927	2215	1.568	-1.259	1.222	-1.576	-8.623	-0.800	-6.172
0	10	25	98	98298	6872.938	2230	1.440	-1.259	1.222	-1.576	-8.623	-1.009	-6.354
0	10	25	98	98298	6872.948	2245	1.440	-1.259	1.222	-1.576	-8.401	-1.009	-6.172
0	10	25	98	98298	6872.958	2300	1.440	-1.259	1.074	-1.576	-8.401	-1.009	-6.172
0	10	25	98	98298	6872.969	2315	1.440	-1.259	1.222	-1.576	-8.401	-1.009	-6.172
0	10	25	98	98298	6872.979	2330	1.568	-1.259	1.074	-1.576	-8.623	-1.218	-6.172
0	10	25	98	98298	6872.990	2345	1.440	-1.259	1.074	-1.576	-8.401	-1.636	-6.172

Figure B.14. Measured Data from the Solar Test Bench (Case 3, 03/22/99, Glazing Solar Transmittance; Part 1).

15	16	17	18	19	20	21	22	23	24	25	26	27	28
TSP	SVL	APD	TI	TO	Tdb	RH	GHR	Wind	Tdb2	Tdew	Wind2	Tg,c	Tg,1
-2.516	-3.609	0.051	67.342	69.085	63.266	75.293	-99.000	3.745	-99.000	-99.000	-99.000	-99.000	-99.000
-2.278	-3.609	0.055	67.173	68.860	63.131	75.810	-99.000	3.451	-99.000	-99.000	-99.000	-99.000	-99.000
-2.753	-3.992	0.057	67.005	68.635	62.996	76.326	-99.000	3.156	-99.000	-99.000	-99.000	-99.000	-99.000
-2.753	-3.609	0.053	66.780	68.410	62.862	76.842	-99.000	2.862	-99.000	-99.000	-99.000	-99.000	-99.000
-2.753	-3.609	0.057	66.443	68.129	62.727	77.359	-99.000	2.568	-99.000	-99.000	-99.000	-99.000	-99.000
-2.753	-3.609	0.059	66.049	67.848	62.525	78.039	-99.000	2.800	-99.000	-99.000	-99.000	-99.000	-99.000
-2.991	-3.609	0.057	65.824	67.623	62.323	78.719	-99.000	3.031	-99.000	-99.000	-99.000	-99.000	-99.000
-2.753	-3.609	0.058	65.600	67.398	62.121	79.400	-99.000	3.263	-99.000	-99.000	-99.000	-99.000	-99.000
-2.516	-3.609	0.060	65.431	67.117	61.919	80.080	-99.000	3.495	-99.000	-99.000	-99.000	-99.000	-99.000
-2.753	-3.609	0.054	65.262	66.949	61.604	80.886	-99.000	3.445	-99.000	-99.000	-99.000	-99.000	-99.000
-2.278	-3.609	0.049	64.981	66.668	61.290	81.692	-99.000	3.394	-99.000	-99.000	-99.000	-99.000	-99.000
-2.041	-3.609	0.053	64.813	66.443	60.975	82.498	-99.000	3.344	-99.000	-99.000	-99.000	-99.000	-99.000
-1.803	-3.609	0.055	64.756	66.274	60.661	83.304	-99.000	3.294	-99.000	-99.000	-99.000	-99.000	-99.000
-1.803	-3.609	0.050	64.588	66.162	60.549	83.580	-99.000	3.169	-99.000	-99.000	-99.000	-99.000	-99.000
-1.328	-3.609	0.049	64.475	65.993	60.437	83.657	-99.000	3.444	-99.000	-99.000	-99.000	-99.000	-99.000
-1.803	-3.609	0.054	64.250	65.768	60.324	83.834	-99.000	3.520	-99.000	-99.000	-99.000	-99.000	-99.000
-2.278	-3.609	0.047	64.138	65.600	60.212	84.010	-99.000	3.595	-99.000	-99.000	-99.000	-99.000	-99.000
-2.516	-3.609	0.052	63.913	65.431	59.988	84.741	-99.000	4.058	-99.000	-99.000	-99.000	-99.000	-99.000
-2.516	-3.609	0.050	63.969	65.318	59.763	85.471	-99.000	4.522	-99.000	-99.000	-99.000	-99.000	-99.000
-2.041	-3.609	0.060	63.857	65.150	59.538	86.201	-99.000	4.985	-99.000	-99.000	-99.000	-99.000	-99.000
-1.566	-3.609	0.058	63.801	65.094	59.314	86.932	-99.000	5.448	-99.000	-99.000	-99.000	-99.000	-99.000
-1.328	-3.609	0.059	64.026	64.756	59.247	87.310	-99.000	4.791	-99.000	-99.000	-99.000	-99.000	-99.000
-1.328	-3.609	0.050	64.082	64.419	59.179	87.688	-99.000	4.133	-99.000	-99.000	-99.000	-99.000	-99.000
-1.566	-3.609	0.050	63.463	64.531	59.112	88.065	-99.000	3.476	-99.000	-99.000	-99.000	-99.000	-99.000
-1.566	-3.609	0.050	63.351	64.475	59.045	88.443	-99.000	2.818	-99.000	-99.000	-99.000	-99.000	-99.000
-2.041	-3.609	0.053	63.520	64.419	58.888	88.997	-99.000	2.868	-99.000	-99.000	-99.000	-99.000	-99.000
-1.566	-3.226	0.056	63.351	64.138	58.730	89.551	-99.000	2.918	-99.000	-99.000	-99.000	-99.000	-99.000
2.235	-0.545	0.061	63.857	63.969	58.573	90.106	-99.000	2.969	-99.000	-99.000	-99.000	-99.000	-99.000
13.162	7.882	0.059	63.182	64.138	58.416	90.660	-99.000	3.019	-99.000	-99.000	-99.000	-99.000	-99.000
33.591	22.820	0.061	62.789	64.250	58.394	90.383	-99.000	2.543	-99.000	-99.000	-99.000	-99.000	-99.000
69.697	30.863	0.060	62.845	64.250	58.371	90.106	-99.000	2.068	-99.000	-99.000	-99.000	-99.000	-99.000
74.923	29.331	0.061	62.014	63.969	58.348	89.829	-99.000	1.592	-99.000	-99.000	-99.000	-99.000	-99.000
137.159	43.503	0.055	62.182	63.857	58.326	89.552	-99.000	1.116	-99.000	-99.000	-99.000	-99.000	-99.000
206.047	261.442	0.058	63.745	64.138	58.438	89.275	-99.000	1.197	-99.000	-99.000	-99.000	-99.000	-99.000
235.502	316.215	0.062	65.017	64.475	58.550	88.997	-99.000	1.279	-99.000	-99.000	-99.000	-99.000	-99.000
284.436	362.560	0.058	66.105	65.431	58.663	88.720	-99.000	1.360	-99.000	-99.000	-99.000	-99.000	-99.000
338.596	422.695	0.056	67.792	66.611	58.775	88.443	-99.900	1.441	59.000	55.000	4.000	-99.000	-99.000
380.404	464.444	0.055	69.703	67.673	59.920	85.622	158.309	2.267	60.750	55.500	4.000	-99.000	-99.000
418.411	500.831	0.065	71.614	68.916	61.065	82.800	216.717	3.093	62.500	56.000	4.000	-99.000	-99.000
455.467	534.537	0.068	73.638	70.265	62.211	79.979	275.126	3.920	64.250	56.500	4.000	-99.000	-99.000
485.873	559.817	0.069	75.437	71.558	63.356	77.158	333.535	4.746	66.000	57.000	4.000	-99.000	-99.000
516.278	586.245	0.067	77.011	72.682	64.838	75.470	384.437	4.827	-99.000	-99.000	-99.000	-99.000	-99.000
539.083	603.481	0.061	78.079	73.244	66.320	73.782	435.339	4.909	-99.000	-99.000	-99.000	-99.000	-99.000
566.638	624.164	0.051	79.428	74.200	67.802	72.094	486.241	4.990	-99.000	-99.000	-99.000	-99.000	-99.000
592.292	643.315	0.055	80.383	75.156	69.284	70.406	537.143	5.072	-99.000	-99.000	-99.000	-99.000	-99.000
608.445	654.406	0.062	81.281	76.111	70.541	68.328	573.604	5.335	-99.000	-99.000	-99.000	-99.000	-99.000
621.747	662.850	0.058	82.519	77.292	71.799	66.249	610.065	5.598	-99.000	-99.000	-99.000	-99.000	-99.000
633.150	668.978	0.074	83.250	77.910	73.057	64.171	646.525	5.861	-99.000	-99.000	-99.000	-99.000	-99.000
638.851	672.808	0.065	84.262	78.860	74.314	62.093	682.986	6.124	75.000	61.000	7.000	-99.000	-99.000
637.900	670.893	0.067	85.218	79.315	75.010	59.813	703.862	6.187	76.000	61.000	6.500	-99.000	-99.000
636.950	670.893	0.072	85.948	80.215	75.706	57.534	724.737	6.249	77.000	61.000	6.000	-99.000	-99.000
634.100	668.978	0.069	86.342	80.933	76.402	55.254	745.612	6.312	78.000	61.000	5.500	-99.000	-99.000
626.498	663.999	0.066	87.129	81.508	77.098	52.974	766.488	6.374	79.000	61.000	5.000	-99.000	-99.000
616.997	658.636	0.058	86.904	81.901	77.704	51.488	769.062	6.080	-99.000	-99.000	-99.000	-99.000	-99.000
599.894	644.464	0.059	87.410	82.238	78.311	50.001	771.635	5.786	-99.000	-99.000	-99.000	-99.000	-99.000
578.040	629.144	0.061	87.860	82.688	78.918	48.515	774.209	5.491	-99.000	-99.000	-99.000	-99.000	-99.000
552.385	611.908	0.071	88.534	83.306	79.524	47.029	776.783	5.197	-99.000	-99.000	-99.000	-99.000	-99.000
527.680	593.523	0.061	88.422	83.587	79.906	45.379	764.057	4.840	-99.000	-99.000	-99.000	-99.000	-99.000
498.700	571.307	0.053	88.703	83.812	80.288	43.729	751.332	4.484	-99.000	-99.000	-99.000	-99.000	-99.000
464.969	546.794	0.056	88.928	84.150	80.669	42.079	738.607	4.127	-99.000	-99.000	-99.000	-99.000	-99.000
431.713	518.450	0.057	89.096	84.487	81.051	40.429	725.881	3.770	-99.000	-99.000	-99.000	-99.000	-99.000
402.733	493.554	0.056	89.321	84.768	81.163	39.623	695.425	4.102	-99.000	-99.000	-99.000	-99.000	-99.000
361.301	461.180	0.067	89.152	84.993	81.275	38.816	664.970	4.434	-99.000	-99.000	-99.000	-99.000	-99.000
320.068	426.525	0.068	89.096	85.161	81.388	38.010	634.515	4.765	-99.000	-99.000	-99.000	-99.000	-99.000
269.233	383.626	0.067	88.478	85.161	81.500	37.204	604.059	5.097	81.000	55.000	5.000	-99.000	-99.000
225.526	345.324	0.060	88.197	85.105	81.478	37.166	560.449	5.066	81.000	55.500	5.500	-99.000	-99.000
179.917	300.511	0.061	87.691	84.993	81.455	37.129	516.839	5.035	81.000	56.000	6.000	-99.000	-99.000
130.033	240.376	0.061	86.960	84.768	81.433	37.091	473.230	5.003	81.000	56.500	6.500	-99.000	-99.000
91.076	189.434	0.055	86.286	84.543	81.410	37.053	429.620	4.972	81.000	57.000	7.000	-99.000	-99.000
47.843	140.408	0.043	85.667	84.206	81.073	38.225	373.785	4.916	80.000	57.000	6.500	-99.000	-99.000
16.488	79.507	0.047	84.768	83.868	80.737	39.396	317.949	4.859	79.000	57.000	6.000	-99.000	-99.000
4.610	11.712	0.052	83.812	83.419	80.400	40.567	262.114	4.802	78.000	57.000	5.500	-99.000	-99.000
-3.704	-2.077	0.060	82.857	82.857	80.063	41.739	206.279	4.746	77.000	57.000	5.000	-99.000	-99.000
-5.366	-3.992	0.053	81.732	82.238	79.322	43.855	160.024	4.634	-99.000	-99.000	-99.000	-99.000	-99.000
-4.416	-3.992	0.041	80.833	81.732	78.581	45.971	113.769	4.521	-99.000	-99.000	-99.000	-99.000	-99.000
-4.179	-3.992	0.047	80.158	81.226	77.839	48.087	67.514	4.408	-99.000	-99.000	-99.000	-99.000	-99.000
-3.229	-3.992	0.043	79.428	80.721	77.098	50.203	21.259	4.296	-99.000	-99.000	-99.000	-99.000	-99.000
-2.991	-3.609	0.054	79.034	80.327	76.335	52.521	-99.000	4.290	-99.000	-99.000	-99.000	-99.000	-99.000
-2.991	-3.992	0.060	78.472	79.877	75.572	54.838	-99.000	4.283	-99.000	-99.000	-99.000	-99.000	-99.000
-2.753	-3.992	0.053	77.854	79.371	74.808	57.155	-99.000	4.277	-99.000	-99.000	-99.000	-99.000	-99.000
-2.516	-3.992	0.057	77.460	78.978	74.045	59.473	-99.000	4.271	68.000	61.000	0.000	-99.000	-99.000
-2.278	-3.609	0.058	76.842	78.528	73.551	60.745	-99.000	4.427	67.500	61.000	1.000	-99.000	-99.000
-2.516	-3.609	0.059	76.448	78.191	73.057	62.017	-99.000	4.584	67.000	61.000	2.000	-99.000	-99.000
-2.278	-3.609	0.057	75.886	77.741	72.563	63.290	-99.000	4.740	66.500	61.000	3.000	-99.000	-99.000
-2.516	-3.609	0.059	75.380	77.292	72.069	64.562	-99.000	4.897	66.000	61.000	4.000	-99.000	-99.000
-2.516	-3.609	0.059	74.762	76.842	71.507	66.338	-99.000	4.897	65.500	61.000	3.750	-99.000	-99.000
-2.516	-3.609	0.064	74.200	76.392	70.946	68.114	-99.000	4.897	65.000	61.000	3.500	-99.000	-99.000
-2.516	-3.609	0.058	73.582	75.943	70.384	69.890	-99.000	4.897	64.500	61.000	3.250	-99.000	-99.000
-2.041	-3.609	0.061	73.357	75.605	69.823	71.666	-99.000	4.897	64.000	61.000	3.000	-99.000	-99.000
-1.566	-3.609	0.053	73.076	75.324	69.217	73.820	-99.000	4.790	-99.000	-99.000	-99.000	-99.000	-99.000
-1.803	-3.609	0.048	72.738	75.043	68.611	75.973	-99.000	4.684	-99.000	-99.000	-99.000	-99.000	-99.000
-1.803	-3.609	0.046	72.401	74.762	68.004	78.127	-99.000	4.578	-99.000	-99.000	-99.000	-99.000	-99.000
-1.803	-3.609	0.059	72.345	74.537	67.398	80.281	-99.000	4.471	-99.000	-99.000	-99.000	-99.000	-99.000
-1.803	-3.609	0.054	72.064	74.256	67.331	81.087	-99.000	4.584	-99.000	-99.000	-99.000	-99.000	-99.000
-2.041	-3.609	0.056	71.895	74.031	67.263	81.893	-99.000	4.696	-99.000	-99.000	-99.000	-99.000	-99.000
-2.278	-3.609	0.051	71.670	73.750	67.195	82.700	-99.000	4.809	-99.000	-99.000	-99.000	-99.000	-99.000

Figure B.15. Measured Data from the Solar Test Bench (Case 3, 03/22/99, Glazing Solar Transmittance; Part 2).

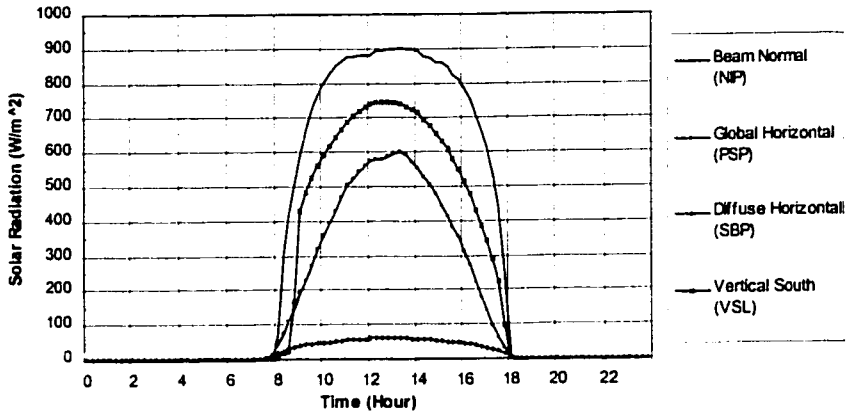

Figure B.16. Measured Beam Normal, Global Horizontal, Diffuse Horizontal and Vertical South Solar Radiation (Case 4, 01/25/99, Left-fin Shade).

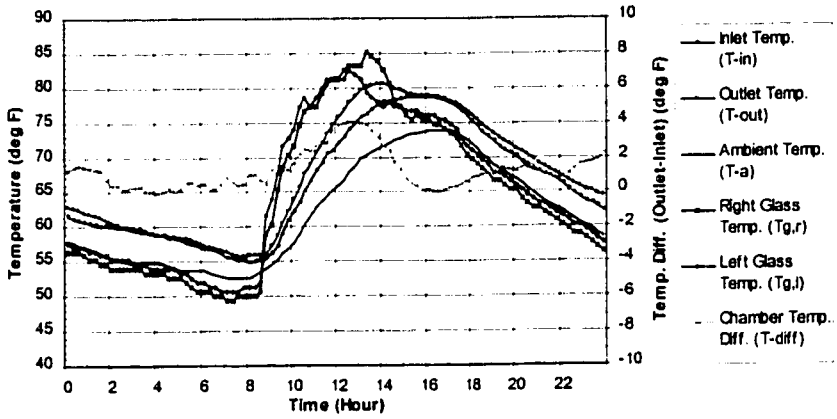

Figure B.17. Measured Chamber Inlet and Outlet Temperature and Outside Air Temperature (Case 4, 01/25/99, Left-fin Shade).

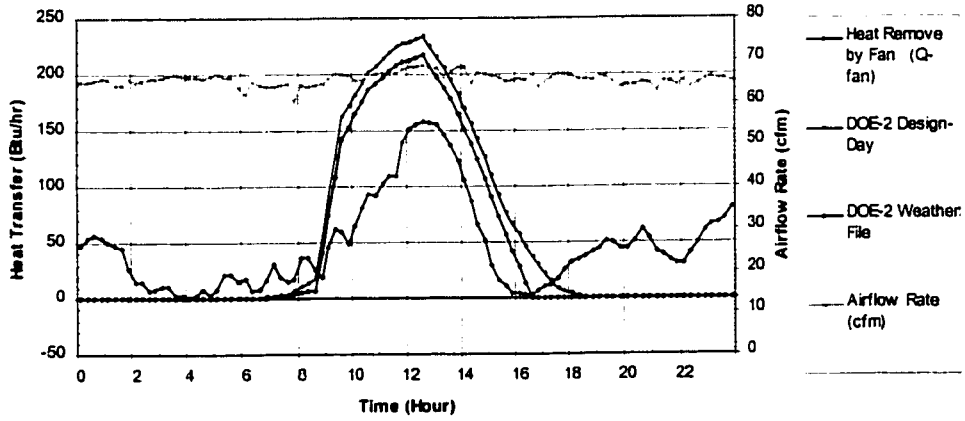

Figure B.18. Heat Transfer of the Experimental Box and Calculated Airflow Rate (Case 4, 01/25/99, Left-fin Shade).

1	2	3	4	5	6	7	8	9	10	11	12	13	14
Site	Month	Day	Year	Julian	Decimal	Hour	ELI	SLI	WLI	LIH	NIP	PSP	SHP
0	1	25	99	99025	6964.000	0	1.953	-1.259	1.959	-1.408	-8.401	-1.218	-5.444
0	1	25	99	99025	6964.010	15	1.953	-1.417	1.812	-1.576	-8.401	-0.800	-5.262
0	1	25	99	99025	6964.021	30	2.081	-1.259	2.255	-1.071	-8.180	-0.173	-4.897
0	1	25	99	99025	6964.031	45	2.081	-1.259	2.107	-1.240	-8.180	-0.382	-5.079
0	1	25	99	99025	6964.042	100	2.081	-1.101	2.107	-1.240	-8.180	-0.591	-5.079
0	1	25	99	99025	6964.052	115	2.081	-1.101	2.107	-1.240	-8.180	-0.591	-5.079
0	1	25	99	99025	6964.063	130	2.081	-1.101	2.107	-1.408	-8.180	-0.591	-5.079
0	1	25	99	99025	6964.073	145	2.081	-1.101	2.107	-1.240	-8.180	-1.009	-5.079
0	1	25	99	99025	6964.083	200	2.081	-1.101	2.107	-1.240	-8.180	-1.009	-5.079
0	1	25	99	99025	6964.094	215	2.081	-1.101	2.107	-1.240	-7.958	-0.800	-4.897
0	1	25	99	99025	6964.104	230	2.081	-1.101	2.107	-1.240	-7.958	-0.382	-4.897
0	1	25	99	99025	6964.115	245	2.081	-1.101	2.107	-1.240	-8.180	-0.591	-4.897
0	1	25	99	99025	6964.125	300	2.081	-1.101	2.107	-1.240	-8.180	-0.591	-4.897
0	1	25	99	99025	6964.135	315	2.081	-1.101	2.255	-1.240	-7.958	-0.382	-4.897
0	1	25	99	99025	6964.146	330	2.081	-1.101	2.255	-1.240	-7.958	-0.173	-4.715
0	1	25	99	99025	6964.156	345	2.081	-1.101	2.107	-1.240	-8.180	-0.173	-4.897
0	1	25	99	99025	6964.167	400	2.081	-1.101	2.107	-1.240	-8.180	0.036	-4.897
0	1	25	99	99025	6964.177	415	2.081	-1.101	2.107	-1.240	-8.180	0.036	-4.715
0	1	25	99	99025	6964.188	430	2.081	-1.101	2.107	-1.240	-8.180	0.036	-4.715
0	1	25	99	99025	6964.198	445	2.081	-1.259	2.107	-1.240	-8.180	0.036	-4.715
0	1	25	99	99025	6964.208	500	2.081	-1.101	2.107	-1.408	-8.401	0.036	-4.897
0	1	25	99	99025	6964.219	515	2.081	-1.259	2.107	-1.408	-8.401	-0.591	-4.897
0	1	25	99	99025	6964.229	530	2.081	-1.259	2.107	-1.408	-8.401	-0.382	-4.897
0	1	25	99	99025	6964.240	545	2.081	-1.259	2.107	-1.408	-8.401	-0.591	-4.897
0	1	25	99	99025	6964.250	600	2.209	-1.259	1.959	-1.408	-8.180	-0.173	-4.897
0	1	25	99	99025	6964.260	615	2.209	-1.417	1.959	-1.408	-8.180	0.036	-4.897
0	1	25	99	99025	6964.271	630	2.081	-1.417	1.959	-1.408	-8.401	-0.591	-4.897
0	1	25	99	99025	6964.281	645	2.081	-1.417	1.959	-1.408	-8.401	-0.382	-4.897
0	1	25	99	99025	6964.292	700	2.209	-1.417	1.812	-1.408	-8.401	-0.173	-4.897
0	1	25	99	99025	6964.302	715	2.850	-1.101	2.107	-0.903	-8.401	0.245	-4.715
0	1	25	99	99025	6964.313	730	6.823	2.215	4.763	1.624	-8.401	1.590	-1.983
0	1	25	99	99025	6964.323	745	16.821	11.689	14.206	9.024	-8.180	13.623	5.485
0	1	25	99	99025	6964.333	800	45.788	30.322	21.584	21.668	67.647	42.887	16.596
0	1	25	99	99025	6964.344	815	478.753	252.017	30.732	98.137	306.211	73.404	23.154
0	1	25	99	99025	6964.354	830	573.088	330.021	36.044	139.572	407.757	107.685	30.440
0	1	25	99	99025	6964.365	845	643.839	402.025	39.290	174.944	498.216	146.564	35.540
0	1	25	99	99025	6964.375	900	700.235	470.870	41.651	215.705	586.015	190.477	39.547
0	1	25	99	99025	6964.385	915	747.403	535.926	43.126	256.803	660.511	229.756	42.461
0	1	25	99	99025	6964.396	930	789.443	597.193	62.013	296.891	722.591	271.562	44.647
0	1	25	99	99025	6964.406	945	820.717	653.406	119.952	334.957	767.821	319.638	47.197
0	1	25	99	99025	6964.417	1000	846.352	706.461	188.611	371.339	801.521	361.025	48.290
0	1	25	99	99025	6964.427	1015	865.834	755.095	239.958	405.700	829.014	394.887	48.654
0	1	25	99	99025	6964.438	1030	879.164	801.835	292.782	437.366	849.412	430.422	51.205
0	1	25	99	99025	6964.448	1045	889.417	846.679	347.670	467.010	865.375	469.719	54.119
0	1	25	99	99025	6964.458	1100	893.519	887.102	403.740	493.286	875.131	502.327	55.940
0	1	25	99	99025	6964.469	1115	890.443	918.683	457.448	514.846	877.791	524.066	57.398
0	1	25	99	99025	6964.479	1130	884.291	948.368	510.566	534.384	883.112	543.296	58.490
0	1	25	99	99025	6964.490	1145	869.935	968.580	560.143	548.533	882.225	560.454	58.855
0	1	25	99	99025	6964.500	1200	852.504	985.002	607.950	560.660	879.565	573.396	59.219
0	1	25	99	99025	6964.510	1215	831.996	998.897	653.395	570.093	894.641	577.577	59.948
0	1	25	99	99025	6964.521	1230	804.311	1006.477	695.299	574.809	896.415	579.249	59.948
0	1	25	99	99025	6964.531	1245	772.524	1009.003	733.072	576.156	899.076	589.282	60.312
0	1	25	99	99025	6964.542	1300	737.149	1009.003	767.304	573.461	898.189	596.807	60.676
0	1	25	99	99025	6964.552	1315	701.773	1009.003	802.126	570.093	901.716	600.988	60.312
0	1	25	99	99025	6964.563	1330	659.733	1000.160	830.456	560.660	899.076	590.118	60.312
0	1	25	99	99025	6964.573	1345	616.154	988.791	854.654	548.533	898.189	571.724	57.762
0	1	25	99	99025	6964.583	1400	569.499	972.170	874.131	533.037	893.755	551.657	55.940
0	1	25	99	99025	6964.594	1415	515.154	941.421	890.623	510.130	875.131	525.738	54.855
0	1	25	99	99025	6964.604	1430	464.911	917.419	892.427	489.244	873.357	503.399	53.576
0	1	25	99	99025	6964.615	1445	410.053	882.049	893.607	462.294	860.941	477.244	52.483
0	1	25	99	99025	6964.625	1500	356.733	848.574	895.968	436.018	858.280	444.636	51.933
0	1	25	99	99025	6964.635	1515	301.363	806.887	890.066	405.026	846.751	412.864	50.112
0	1	25	99	99025	6964.646	1530	246.249	755.727	871.770	369.952	826.353	381.510	48.290
0	1	25	99	99025	6964.656	1545	196.518	709.619	856.425	335.968	813.051	357.263	46.469
0	1	25	99	99025	6964.667	1600	139.097	654.038	826.914	297.228	785.558	311.695	44.647
0	1	25	99	99025	6964.677	1615	76.805	594.666	790.312	257.477	755.405	272.398	42.461
0	1	25	99	99025	6964.688	1630	41.942	526.452	737.204	215.705	706.628	224.322	41.004
0	1	25	99	99025	6964.698	1645	37.072	458.870	681.135	174.944	660.511	180.844	36.997
0	1	25	99	99025	6964.708	1700	34.508	395.077	624.475	138.562	615.281	138.621	32.625
0	1	25	99	99025	6964.719	1715	31.689	319.600	541.847	95.442	539.898	98.488	27.889
0	1	25	99	99025	6964.729	1730	28.100	238.122	436.201	50.638	440.570	61.281	21.696
0	1	25	99	99025	6964.740	1745	21.947	126.958	248.811	19.646	252.556	29.927	13.682
0	1	25	99	99025	6964.750	1800	10.156	11.373	18.928	6.508	12.218	7.352	3.664
0	1	25	99	99025	6964.760	1815	4.132	1.741	5.648	0.613	-9.510	0.036	-3.440
0	1	25	99	99025	6964.771	1830	1.953	-1.417	2.255	-1.576	-9.288	-2.054	-5.626
0	1	25	99	99025	6964.781	1845	1.696	-1.732	1.812	-1.745	-9.288	-1.845	-5.626
0	1	25	99	99025	6964.792	1900	1.824	-1.732	1.812	-1.745	-9.288	-1.845	-5.626
0	1	25	99	99025	6964.802	1915	1.824	-1.732	1.812	-1.576	-9.067	-1.845	-5.444
0	1	25	99	99025	6964.813	1930	1.824	-1.732	1.812	-1.576	-8.845	-1.427	-5.444
0	1	25	99	99025	6964.823	1945	1.824	-1.732	1.812	-1.576	-8.845	-1.427	-5.444
0	1	25	99	99025	6964.833	2000	1.824	-1.732	1.959	-1.576	-8.845	-1.218	-5.262
0	1	25	99	99025	6964.844	2015	1.953	-1.732	1.812	-1.408	-8.845	-1.218	-5.444
0	1	25	99	99025	6964.854	2030	1.824	-1.732	1.812	-1.576	-8.845	-1.427	-5.444
0	1	25	99	99025	6964.865	2045	1.824	-1.732	1.812	-1.576	-8.845	-1.427	-5.444
0	1	25	99	99025	6964.875	2100	1.824	-1.732	1.812	-1.576	-8.623	-1.009	-5.444
0	1	25	99	99025	6964.885	2115	1.953	-1.732	1.812	-1.408	-8.623	-0.800	-5.444
0	1	25	99	99025	6964.896	2130	1.953	-1.732	1.812	-1.408	-8.623	-0.800	-5.444
0	1	25	99	99025	6964.906	2145	1.953	-1.732	1.812	-1.408	-8.623	-1.009	-5.444
0	1	25	99	99025	6964.917	2200	1.953	-1.732	1.812	-1.408	-8.623	-1.009	-5.262
0	1	25	99	99025	6964.927	2215	1.953	-1.732	1.812	-1.408	-8.623	-0.800	-5.262
0	1	25	99	99025	6964.938	2230	1.953	-1.732	1.812	-1.408	-8.623	-1.009	-5.262
0	1	25	99	99025	6964.948	2245	1.953	-1.890	1.812	-1.408	-8.623	-0.800	-5.262
0	1	25	99	99025	6964.958	2300	1.953	-1.890	1.664	-1.408	-8.623	-0.800	-5.262
0	1	25	99	99025	6964.969	2315	1.953	-1.732	1.812	-1.408	-8.623	-1.009	-5.262
0	1	25	99	99025	6964.979	2330	1.953	-1.732	1.812	-1.408	-8.401	-1.009	-5.079
0	1	25	99	99025	6964.990	2345	1.953	-1.732	1.664	-1.408	-8.401	-1.009	-5.262

Figure B.19. Measured Data from the Solar Test Bench (Case 4, 01/25/99, Left-fin Shade; Part 1).

15	16	17	18	19	20	21	22	23	24	25	26	27	28
TSP	SVL	APD	TI	TO	Tdb	RH	GHR	Wind	Tdb2	Tdew	Wind2	Tg,r	Tg,l
-1.091	-3.992	0.252	61.721	63.014	57.877	76.755	-99.000	7.476	55.000	48.000	4.000	56.470	57.740
-2.041	-3.992	0.251	61.215	62.676	57.608	77.712	-99.000	7.507	54.500	48.000	3.750	56.470	57.100
-1.566	-3.609	0.255	60.934	62.452	57.338	78.670	-99.000	7.539	54.000	48.000	3.500	56.470	57.100
-1.803	-3.609	0.256	60.653	62.114	57.069	79.627	-99.000	7.570	53.500	48.000	3.250	55.840	57.100
-1.803	-3.609	0.257	60.484	61.833	56.799	80.584	-99.000	7.601	53.000	48.000	3.000	55.200	56.470
-1.803	-3.609	0.246	60.316	61.608	56.462	81.894	-99.000	7.589	52.750	48.000	3.000	55.200	56.470
-2.041	-3.609	0.246	60.091	61.327	56.126	83.204	-99.000	7.576	52.500	48.000	3.000	54.560	55.840
-2.041	-3.609	0.257	60.203	60.934	55.789	84.513	-99.000	7.564	52.250	48.000	3.000	54.560	55.840
-2.041	-3.609	0.251	60.147	60.540	55.452	85.823	-99.000	7.551	52.000	48.000	3.000	53.930	55.200
-1.566	-3.609	0.255	59.866	60.259	55.272	86.730	-99.000	7.138	51.500	47.750	3.000	53.930	55.200
-1.091	-3.609	0.258	59.810	59.978	55.093	87.637	-99.000	7.126	51.000	47.500	3.000	53.930	55.200
-1.328	-3.609	0.256	59.697	59.922	54.913	88.544	-99.000	6.913	50.500	47.250	3.000	53.930	55.200
-1.803	-3.609	0.259	59.472	59.753	54.733	89.451	-99.000	6.700	50.000	47.000	3.000	53.930	54.560
-1.328	-3.609	0.262	59.304	59.585	54.756	90.156	-99.000	6.894	50.000	47.250	3.250	53.930	54.560
-0.853	-3.609	0.264	59.304	59.360	54.778	90.862	-99.000	7.088	50.000	47.500	3.500	53.290	54.560
-1.091	-3.609	0.259	59.023	59.079	54.801	91.567	-99.000	7.282	50.000	47.750	3.750	53.290	53.930
-0.853	-3.609	0.259	58.798	58.798	54.823	92.272	-99.000	7.476	50.000	48.000	4.000	53.290	53.930
-1.091	-3.609	0.259	58.742	58.798	54.576	92.524	-99.000	7.426	49.250	47.500	3.000	53.290	53.930
-1.328	-3.609	0.257	58.404	58.629	54.329	92.776	-99.000	7.376	48.500	47.000	2.000	52.650	53.930
-1.328	-3.609	0.262	58.404	58.461	54.082	93.028	-99.000	7.325	47.750	46.500	1.000	52.650	53.930
-1.328	-3.609	0.266	58.180	58.404	53.835	93.280	-99.000	7.275	47.000	46.000	0.000	52.650	53.290
-2.278	-3.609	0.260	57.786	58.348	53.790	93.280	-99.000	6.724	46.750	45.750	0.000	52.360	53.290
-2.278	-3.609	0.260	57.533	58.123	53.745	93.280	-99.000	6.174	46.500	45.500	0.000	51.360	52.650
-2.516	-3.609	0.240	57.280	57.674	53.700	93.280	-99.000	5.623	46.250	45.250	0.000	50.710	52.000
-2.041	-3.609	0.230	56.830	57.308	53.655	93.280	-99.000	5.072	46.000	45.000	0.000	50.710	52.000
-1.566	-3.609	0.251	56.915	57.083	53.386	93.582	-99.000	4.434	46.000	45.000	0.000	50.710	51.360
-2.041	-3.609	0.246	56.549	56.774	53.117	93.885	-99.000	3.795	46.000	45.000	0.000	50.070	51.360
-2.041	-3.609	0.243	56.156	56.606	52.847	94.187	-99.000	3.157	46.000	45.000	0.000	50.070	50.710
-1.803	-3.609	0.242	55.509	56.381	52.578	94.489	-99.000	2.518	46.000	45.000	0.000	49.420	50.710
-1.091	-3.226	0.245	55.425	55.959	52.600	94.766	-99.000	2.725	46.000	44.750	0.000	49.420	50.710
1.997	-0.928	0.249	55.313	55.706	52.623	95.044	-99.000	2.931	46.000	44.500	0.000	50.070	50.710
9.361	4.818	0.216	55.285	55.791	52.645	95.321	-99.000	3.138	46.000	44.250	0.000	50.070	51.360
25.989	10.563	0.247	54.947	55.959	52.667	95.598	20.687	3.344	46.000	44.000	0.000	50.070	51.360
72.548	18.224	0.244	55.004	56.015	53.139	94.464	70.946	3.138	48.000	46.000	0.000	50.070	51.360
110.080	23.203	0.246	55.285	55.987	53.611	93.331	121.205	2.931	50.000	48.000	0.000	50.710	52.000
151.887	167.985	0.248	55.509	56.015	54.082	92.197	171.463	2.725	52.000	50.000	0.000	59.000	61.520
206.522	430.738	0.258	56.072	57.308	54.554	91.063	221.722	2.518	54.000	52.000	0.000	60.260	64.040
268.283	482.829	0.264	57.168	58.798	55.317	89.930	273.268	3.088	55.750	52.250	1.250	65.300	67.820
299.164	526.494	0.264	58.966	60.540	56.081	88.796	324.813	3.658	57.500	52.500	2.500	68.440	71.570
321.018	560.966	0.261	60.990	62.283	56.844	87.663	376.359	4.227	59.250	52.750	1.750	70.320	72.830
366.626	592.757	0.253	62.171	63.913	57.607	86.529	427.904	4.797	61.000	53.000	5.000	71.570	74.100
402.258	620.334	0.254	63.576	65.768	58.955	83.065	469.369	5.041	62.000	52.750	5.250	74.740	77.320
435.514	644.847	0.264	65.206	67.679	60.302	79.602	510.835	5.285	63.000	52.500	5.500	76.680	78.610
466.394	668.212	0.266	66.724	69.141	61.650	76.138	552.300	5.529	64.000	52.250	5.750	77.320	77.320
492.524	689.661	0.269	68.073	70.771	62.997	72.674	593.765	5.773	65.000	52.000	6.000	77.320	78.610
519.129	706.514	0.266	69.253	72.120	63.738	71.024	620.646	5.761	66.000	52.250	5.750	79.250	79.900
543.833	721.069	0.267	70.602	73.469	64.479	69.374	647.527	5.748	67.000	52.500	5.500	80.540	81.190
558.086	731.410	0.273	71.108	74.706	65.220	67.723	674.407	5.736	68.000	52.750	5.250	81.190	81.190
566.638	739.071	0.278	72.008	75.886	65.961	66.073	701.288	5.723	69.000	53.000	5.000	81.190	81.190
575.189	745.199	0.279	72.907	76.898	66.927	63.592	710.725	5.567	70.000	52.750	6.000	82.480	81.190
577.089	747.497	0.282	73.975	78.022	67.892	61.111	720.162	5.410	71.000	52.500	7.000	83.130	82.480
565.687	746.731	0.277	74.875	78.922	68.858	58.629	729.599	5.254	72.000	52.250	4.000	83.130	81.830
536.232	743.667	0.276	75.774	79.765	69.823	56.148	739.036	5.097	73.000	52.000	9.000	83.130	81.190
514.378	742.518	0.259	76.336	80.215	70.295	54.120	732.173	5.560	73.250	51.750	9.750	85.100	79.250
508.677	734.475	0.270	76.954	80.496	70.766	52.092	725.310	6.024	73.500	51.500	9.500	84.450	78.610
522.930	725.282	0.278	77.460	80.608	71.238	50.064	718.446	6.487	73.750	51.250	9.250	83.790	77.970
535.282	713.025	0.280	77.910	80.608	71.709	48.036	711.583	6.950	74.000	51.000	8.000	82.480	77.320
506.777	691.576	0.249	77.966	80.327	72.068	47.671	686.418	6.894	74.250	50.750	9.500	80.540	77.970
469.245	675.872	0.267	78.103	80.046	72.428	47.306	661.253	6.838	74.500	50.500	9.000	77.970	77.320
440.740	652.891	0.264	78.360	79.709	72.787	46.940	636.088	6.781	74.750	50.250	9.500	77.320	77.320
429.813	633.357	0.262	78.585	79.371	73.146	46.575	610.923	6.725	75.000	50.000	10.000	76.030	76.680
415.560	608.077	0.259	78.641	79.090	73.326	45.870	572.175	6.882	75.000	50.500	9.500	75.390	76.680
374.228	577.053	0.252	78.641	78.922	73.506	45.165	533.426	7.038	75.000	51.000	9.000	76.030	76.680
341.922	549.858	0.253	78.697	78.809	73.685	44.459	494.678	7.195	75.000	51.500	8.500	75.390	76.030
303.440	515.001	0.256	78.753	78.866	73.865	43.754	455.929	7.351	75.000	52.000	8.000	75.390	76.030
262.582	477.467	0.255	78.697	78.753	73.843	44.321	405.456	6.988	74.500	52.000	4.500	74.740	76.030
220.775	431.504	0.264	78.529	78.585	73.820	44.888	354.983	6.625	74.000	52.000	9.000	74.740	75.390
178.967	385.925	0.244	78.191	78.360	73.798	45.454	304.509	6.261	73.500	52.000	9.500	74.100	75.390
139.060	343.026	0.250	77.798	78.079	73.775	46.021	254.036	5.898	73.000	52.000	10.000	73.470	74.740
98.202	287.871	0.260	77.348	77.685	73.326	47.142	203.634	5.723	71.750	52.000	9.000	72.830	74.100
42.142	223.906	0.266	76.786	77.235	72.877	48.263	153.233	5.548	70.500	52.000	8.000	71.570	72.830
16.250	96.743	0.264	76.055	76.730	72.428	49.384	102.831	5.372	69.250	52.000	7.000	70.320	71.570
5.085	4.435	0.263	75.212	76.055	71.979	50.505	-99.000	5.197	68.000	52.000	6.000	69.700	70.950
-2.041	-2.077	0.258	74.425	75.380	71.193	52.306	-99.000	4.746	66.500	52.000	5.750	69.070	70.320
-3.941	-3.992	0.258	73.694	74.706	70.407	54.108	-99.000	4.296	65.000	52.000	5.500	68.440	69.700
-3.941	-4.375	0.254	72.963	74.088	69.621	55.909	-99.000	3.845	63.500	52.000	5.250	67.820	69.070
-3.941	-4.375	0.261	72.289	73.469	68.835	57.710	-99.000	3.394	62.000	52.000	5.000	66.560	67.820
-3.704	-4.375	0.260	71.502	72.851	68.341	59.070	-99.000	3.494	61.750	52.000	5.250	66.560	67.820
-3.466	-4.375	0.251	70.940	72.289	67.847	60.431	-99.000	3.595	61.500	52.000	5.500	65.930	67.190
-3.229	-4.375	0.243	70.546	71.783	67.353	61.791	-99.000	3.695	61.250	52.000	5.750	65.300	66.560
-2.753	-4.375	0.245	70.040	71.277	66.859	63.151	-99.000	3.795	61.000	52.000	6.000	65.300	65.930
-2.753	-4.375	0.246	69.366	70.771	66.185	64.889	-99.000	3.927	60.250	51.750	5.750	64.040	65.300
-3.229	-4.375	0.252	68.635	70.321	65.512	66.628	-99.000	4.058	59.500	51.500	5.500	63.410	64.670
-3.229	-3.992	0.249	68.241	69.703	64.838	68.366	-99.000	4.190	58.750	51.250	5.250	62.780	64.040
-2.516	-3.992	0.235	67.960	69.141	64.164	70 104	-99.000	4.321	58.000	51.000	5.000	62.780	63.410
-2.041	-3.992	0.254	67.567	68.635	63.670	71.641	-99.000	5.116	57.750	51.250	4.750	62.150	63.410
-2.041	-3.992	0.250	67.286	68.185	63.176	73.178	-99.000	5.911	57.500	51.500	4.500	61.520	62.780
-2.041	-3.992	0.245	66.892	67.736	62.682	74.714	-99.000	6.706	57.250	51.750	4.250	60.890	62.150
-2.278	-3.992	0.253	66.274	67.117	62.188	76.251	-99.000	7.501	57.000	52.000	4.000	60.260	61.520
-2.991	-3.992	0.244	65.431	66.555	61.649	77.813	-99.000	6.643	56.500	51.750	4.250	59.630	60.890
-2.991	-3.992	0.249	64.813	66.162	61.111	79.375	-99.000	5.786	56.000	51.500	4.500	59.000	60.260
-2.991	-3.992	0.258	64.194	65.824	60.572	80.936	-99.000	4.928	55.500	51.250	4.750	59.000	60.260
-2.991	-3.992	0.260	63.688	65.431	60.033	82.498	-99.000	4.070	55.000	51.000	5.000	58.370	59.630
-2.753	-3.992	0.256	63.295	65.094	59.561	83.632	-99.000	4.220	54.500	51.000	4.750	57.740	59.000
-2.753	-3.992	0.257	62.845	64.756	59.090	84.766	-99.000	4.371	54.000	51.000	4.500	57.100	58.370
-2.991	-3.995	0.250	62.339	64.531	58.618	85.899	-99.000	4.521	53.500	51.000	4.250	56.470	57.740

Figure B.20. Measured Data from the Solar Test Bench (Case 4, 01/25/99, Left-fin Shade; Part 2).

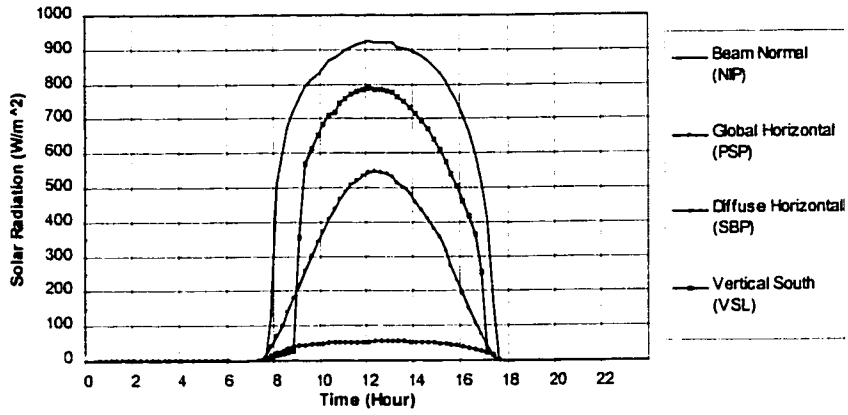

Figure B.21. Measured Beam Normal, Global Horizontal, Diffuse Horizontal and Vertical South Solar Radiation (Case 5, 12/01/98, No Shading).

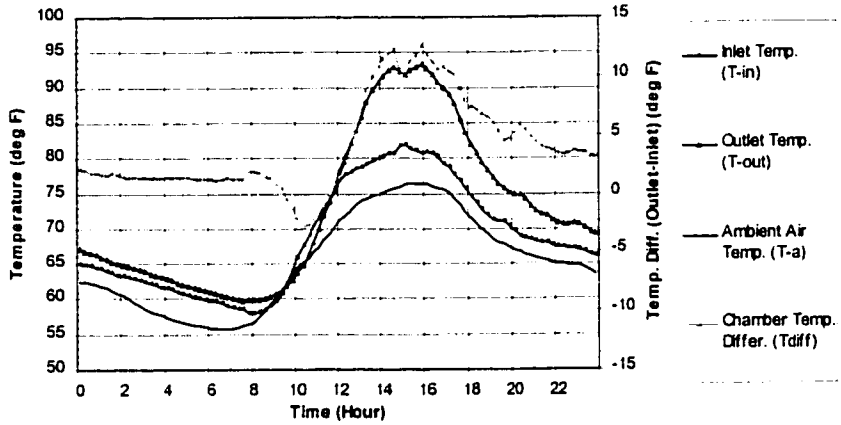

Figure B.22. Measured Chamber Inlet and Outlet Temperature and Outside Air Temperature (Case 5, 12/01/98, No Shading).

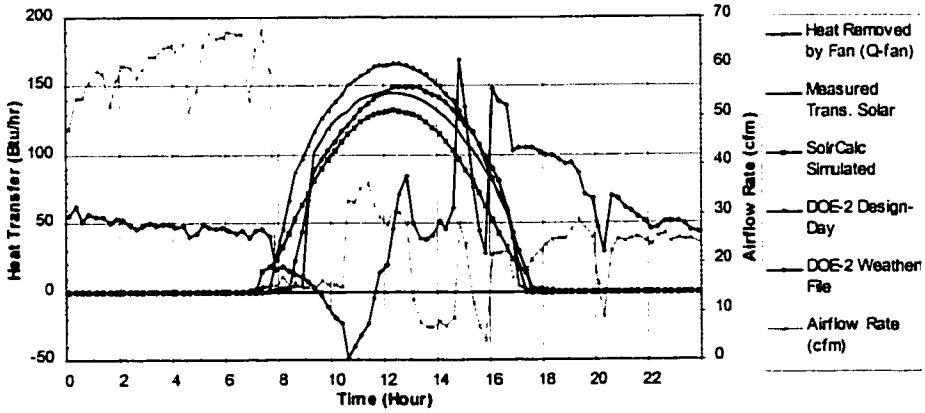

Figure B.23. Heat Transfer of the Experimental Box and Calculated Airflow Rate (Case 5, 12/01/98, No Shading).

1	2	3	4	5	6	7	8	9	10	11	12	13	14
Site	Month	Day	Year	Julian	Decimal	Hour	ELI	SLI	WLI	LIH	NIP	PSP	SBP
0	12	1	98	98335	6909.000	0	1.953	-3.785	-0.696	-2.587	-8.180	-4.562	-4.897
0	12	1	98	98335	6909.010	15	1.824	-2.364	0.484	-2.250	-7.958	-3.517	-4.897
0	12	1	98	98335	6909.021	30	1.824	-0.785	2.107	-1.576	-7.958	-1.636	-4.897
0	12	1	98	98335	6909.031	45	1.824	-0.785	2.107	-1.576	-7.958	-1.427	-4.533
0	12	1	98	98335	6909.042	100	1.824	-0.785	2.255	-1.576	-7.958	-1.636	-4.351
0	12	1	98	98335	6909.052	115	1.824	-0.627	2.255	-1.576	-7.958	-1.636	-4.351
0	12	1	98	98335	6909.063	130	1.824	-0.627	2.255	-1.408	-7.958	-1.427	-4.351
0	12	1	98	98335	6909.073	145	1.824	-0.627	2.255	-1.408	-7.736	-1.218	-4.351
0	12	1	98	98335	6909.083	200	1.824	-0.785	2.255	-1.408	-7.958	-1.009	-4.351
0	12	1	98	98335	6909.094	215	1.824	-0.785	2.255	-1.576	-7.958	-1.218	-4.533
0	12	1	98	98335	6909.104	230	1.824	-0.785	2.255	-1.576	-8.180	-1.009	-4.533
0	12	1	98	98335	6909.115	245	1.696	-0.785	2.107	-1.745	-8.180	-1.218	-4.715
0	12	1	98	98335	6909.125	300	1.824	-0.627	2.255	-1.745	-8.180	-1.009	-4.533
0	12	1	98	98335	6909.135	315	1.824	-0.785	2.107	-1.745	-8.180	-1.218	-4.533
0	12	1	98	98335	6909.146	330	1.824	-0.627	2.255	-1.745	-8.180	-1.427	-4.533
0	12	1	98	98335	6909.156	345	1.824	-0.627	2.107	-1.745	-8.180	-1.218	-4.533
0	12	1	98	98335	6909.167	400	1.824	-0.627	2.107	-1.745	-7.958	-1.009	-4.533
0	12	1	98	98335	6909.177	415	1.824	-0.627	2.255	-1.576	-7.958	-1.009	-4.533
0	12	1	98	98335	6909.188	430	1.824	-0.627	2.107	-1.576	-8.180	-1.218	-4.533
0	12	1	98	98335	6909.198	445	1.824	-0.627	2.255	-1.576	-7.958	-1.009	-4.351
0	12	1	98	98335	6909.208	500	1.824	-0.627	2.255	-1.576	-8.180	-1.009	-4.533
0	12	1	98	98335	6909.219	515	1.824	-0.785	2.255	-1.576	-7.958	-1.009	-4.533
0	12	1	98	98335	6909.229	530	1.824	-0.785	2.255	-1.576	-8.180	-0.800	-4.533
0	12	1	98	98335	6909.240	545	1.824	-0.627	2.255	-1.576	-8.180	-0.800	-4.533
0	12	1	98	98335	6909.250	600	1.824	-0.943	1.812	-1.913	-7.958	-1.218	-4.715
0	12	1	98	98335	6909.260	615	1.696	-1.417	0.779	-2.755	-8.401	-3.099	-5.262
0	12	1	98	98335	6909.271	630	1.696	-1.417	0.779	-2.755	-8.401	-3.099	-5.262
0	12	1	98	98335	6909.281	645	1.824	-1.417	0.779	-2.587	-8.401	-3.308	-5.079
0	12	1	98	98335	6909.292	700	2.593	-0.943	1.222	-2.250	-8.401	-2.681	-4.715
0	12	1	98	98335	6909.302	715	6.823	2.531	4.173	0.950	-8.401	1.290	-1.436
0	12	1	98	98335	6909.313	730	15.026	10.426	12.436	6.845	-8.401	10.696	6.032
0	12	1	98	98335	6909.323	745	31.432	25.585	19.813	16.951	118.198	39.124	35.139
0	12	1	98	98335	6909.333	800	455.682	272.960	27.486	94.326	510.632	68.388	22.425
0	12	1	98	98335	6909.344	815	539.251	342.653	34.273	124.750	604.639	102.668	28.254
0	12	1	98	98335	6909.354	830	622.306	424.131	35.749	165.511	673.814	140.293	32.990
0	12	1	98	98335	6909.365	845	680.240	491.082	39.290	204.925	723.478	179.172	37.161
0	12	1	98	98335	6909.375	900	726.895	553.611	43.716	244.002	759.839	216.379	41.733
0	12	1	98	98335	6909.385	915	766.885	614.246	81.489	281.732	792.651	257.766	43.919
0	12	1	98	98335	6909.396	930	798.159	669.828	147.887	318.114	813.937	302.498	46.104
0	12	1	98	98335	6909.406	945	822.768	720.357	208.384	351.901	829.014	340.540	47.926
0	12	1	98	98335	6909.417	1000	841.225	767.096	260.025	384.140	848.525	371.476	49.383
0	12	1	98	98335	6909.427	1015	855.580	812.572	314.619	413.111	866.262	406.175	50.476
0	12	1	98	98335	6909.438	1030	861.732	852.363	368.918	439.387	878.678	437.947	51.569
0	12	1	98	98335	6909.448	1045	861.732	886.470	423.216	462.294	887.547	463.866	53.026
0	12	1	98	98335	6909.458	1100	858.656	918.051	476.334	483.180	897.302	487.277	53.755
0	12	1	98	98335	6909.469	1115	851.478	944.579	528.272	501.371	907.057	507.344	53.755
0	12	1	98	98335	6909.479	1130	839.174	967.317	577.849	516.193	915.926	521.557	54.483
0	12	1	98	98335	6909.490	1145	820.717	982.475	624.475	526.973	922.134	533.263	54.119
0	12	1	98	98335	6909.500	1200	797.133	993.844	667.560	533.037	925.681	543.296	54.119
0	12	1	98	98335	6909.510	1215	765.347	995.107	703.562	533.711	920.160	546.641	54.847
0	12	1	98	98335	6909.521	1230	734.073	997.634	738.974	534.384	922.134	545.805	55.940
0	12	1	98	98335	6909.531	1245	699.722	997.634	771.435	531.689	921.247	538.280	56.305
0	12	1	98	98335	6909.542	1300	662.296	993.844	802.126	525.626	919.473	529.919	55.940
0	12	1	98	98335	6909.552	1315	616.667	977.422	822.193	512.151	908.831	514.869	55.212
0	12	1	98	98335	6909.563	1330	571.550	961.000	841.670	498.002	903.510	499.819	54.847
0	12	1	98	98335	6909.573	1345	523.870	940.789	857.015	480.485	899.963	480.588	54.119
0	12	1	98	98335	6909.583	1400	472.089	913.630	865.278	458.925	891.094	457.177	54.483
0	12	1	98	98335	6909.594	1415	419.282	882.049	869.409	434.671	880.452	432.512	52.662
0	12	1	98	98335	6909.604	1430	365.962	846.679	868.819	407.721	868.923	408.265	51.933
0	12	1	98	98335	6909.615	1445	310.079	801.835	857.605	376.729	850.299	382.146	50.840
0	12	1	98	98335	6909.625	1500	256.246	754.464	844.030	344.053	831.675	355.172	49.383
0	12	1	98	98335	6909.635	1515	203.952	701.303	822.193	308.344	808.616	314.203	47.562
0	12	1	98	98335	6909.646	1530	151.658	649.616	794.453	271.962	782.010	269.889	45.740
0	12	1	98	98335	6909.656	1545	89.366	595.929	763.173	235.580	750.970	231.429	43.190
0	12	1	98	98335	6909.667	1600	45.531	535.295	721.268	197.851	711.949	190.877	40.276
0	12	1	98	98335	6909.677	1615	15.790	468.976	666.970	159.448	661.398	149.072	36.268
0	12	1	98	98335	6909.688	1630	13.739	400.130	602.638	122.392	595.770	109.357	31.897
0	12	1	98	98335	6909.698	1645	30.920	319.284	512.927	77.588	512.406	74.241	26.797
0	12	1	98	98335	6909.708	1700	26.562	234.016	403.149	38.174	407.313	39.960	20.604
0	12	1	98	98335	6909.719	1715	18.102	97.904	175.922	13.246	171.409	10.069	11.496
0	12	1	98	98335	6909.729	1730	6.823	1.794	7.124	1.961	-9.288	-5.190	-0.932
0	12	1	98	98335	6909.740	1745	2.722	-1.732	1.074	-1.745	-9.732	-7.907	-3.987
0	12	1	98	98335	6909.750	1800	1.696	-3.469	-0.696	-2.924	-9.510	-6.462	-5.079
0	12	1	98	98335	6909.760	1815	1.696	-3.627	-0.844	-2.924	-9.288	-5.608	-5.079
0	12	1	98	98335	6909.771	1830	1.696	-3.627	-0.844	-2.755	-9.288	-4.981	-4.897
0	12	1	98	98335	6909.781	1845	1.696	-3.627	-0.844	-2.755	-9.288	-4.771	-4.897
0	12	1	98	98335	6909.792	1900	1.568	-3.943	-1.139	-3.092	-9.510	-4.771	-5.079
0	12	1	98	98335	6909.802	1915	1.568	-3.785	-0.992	-2.924	-9.288	-4.353	-5.079
0	12	1	98	98335	6909.813	1930	1.696	-3.785	-0.844	-2.755	-9.067	-4.144	-4.997
0	12	1	98	98335	6909.823	1945	2.081	-3.469	-0.549	-2.250	-8.623	-3.099	-4.533
0	12	1	98	98335	6909.833	2000	2.081	-3.469	-0.401	-2.250	-8.401	-3.099	-4.533
0	12	1	98	98335	6909.844	2015	2.081	-3.311	-0.401	-2.250	-8.401	-3.308	-4.351
0	12	1	98	98335	6909.854	2030	1.953	-3.469	-0.549	-2.250	-8.401	-3.308	-4.533
0	12	1	98	98335	6909.865	2045	1.953	-3.469	-0.549	-2.419	-8.401	-3.099	-4.533
0	12	1	98	98335	6909.875	2100	1.953	-3.469	-0.549	-2.419	-8.401	-2.681	-4.533
0	12	1	98	98335	6909.885	2115	1.953	-3.469	-0.696	-2.419	-8.180	-2.472	-4.533
0	12	1	98	98335	6909.896	2130	1.953	-3.469	-0.549	-2.419	-8.180	-2.681	-4.533
0	12	1	98	98335	6909.906	2145	1.953	-3.469	-0.696	-2.419	-8.401	-3.099	-4.715
0	12	1	98	98335	6909.917	2200	1.953	-3.627	-0.696	-2.587	-8.401	-3.099	-4.715
0	12	1	98	98335	6909.927	2215	1.953	-3.627	-0.696	-2.419	-8.401	-2.681	-4.715
0	12	1	98	98335	6909.938	2230	2.081	-3.627	-0.549	-2.419	-8.401	-2.890	-4.715
0	12	1	98	98335	6909.948	2245	1.953	-3.627	-0.549	-2.419	-8.401	-3.308	-4.897
0	12	1	98	98335	6909.958	2300	1.953	-3.627	-0.696	-2.419	-8.401	-3.099	-4.897
0	12	1	98	98335	6909.969	2315	2.081	-3.627	-0.696	-2.419	-8.623	-3.308	-4.897
0	12	1	98	98335	6909.979	2330	2.081	-3.785	-0.696	-2.419	-8.401	-3.517	-4.897
0	12	1	98	98335	6909.990	2345	1.953	-3.785	-0.696	-2.419	-8.623	-3.308	-4.715

Figure B.24. Measured Data from the Solar Test Bench (Case 5, 12/01/98, No Shading; Part 1).

15	16	17	18	19	20	21	22	23	24	25	26	27	28
TSP	SVL	APD	TI	TO	Tdb	RH	GHR	Wind	Tdb2	Tdew	Wind2	Tg, r	Tg, l
-2.278	-3.609	0.134	65.037	67.117	62.548	71.515	-99.000	1.642	52.000	51.000	0.000	-99.000	-99.000
-2.278	-3.992	0.174	64.756	66.780	62.368	71.855	-99.000	1.454	51.750	50.750	0.000	-99.000	-99.000
-2.516	-3.992	0.174	64.813	66.499	62.188	72.195	-99.000	1.266	51.500	50.500	0.000	-99.000	-99.000
-2.041	-3.992	0.194	64.475	66.218	62.009	72.535	-99.000	1.078	51.250	50.250	0.000	-99.000	-99.000
-2.516	-3.992	0.209	64.307	65.937	61.829	72.875	-99.000	0.890	51.000	50.000	0.000	-99.000	-99.000
-2.991	-3.992	0.205	64.026	65.656	61.492	73.870	-99.000	1.328	51.250	50.000	1.000	-99.000	-99.000
-2.278	-3.992	0.161	63.632	65.318	61.155	74.865	-99.000	1.766	51.500	50.000	2.000	-99.000	-99.000
-1.566	-3.992	0.197	63.351	64.981	60.819	75.860	-99.000	2.205	51.750	50.000	3.000	-99.000	-99.000
-1.803	-3.992	0.217	63.239	64.756	60.482	76.855	-99.000	2.643	52.000	50.000	4.000	-99.000	-99.000
-2.516	-3.992	0.214	63.126	64.531	59.988	78.140	-99.000	3.469	52.750	50.250	4.000	-99.000	-99.000
-2.753	-3.992	0.199	62.958	64.363	59.494	79.424	-99.000	4.295	53.500	50.500	4.000	-99.000	-99.000
-3.229	-3.992	0.213	62.676	64.082	59.000	80.709	-99.000	5.122	54.250	50.750	4.000	-99.000	-99.000
-2.991	-3.992	0.230	62.452	63.857	58.506	81.994	-99.000	5.948	55.000	51.000	4.000	-99.000	-99.000
-3.229	-3.992	0.230	62.227	63.576	58.214	82.800	-99.000	5.610	55.000	51.000	4.000	-99.000	-99.000
-3.466	-3.992	0.244	61.946	63.295	57.922	83.607	-99.000	5.272	55.000	51.000	4.000	-99.000	-99.000
-3.229	-3.992	0.246	61.665	63.014	57.630	84.413	-99.000	4.934	55.000	51.000	4.000	-99.000	-99.000
-2.991	-3.992	0.239	61.496	62.789	57.338	85.219	-99.000	4.596	55.000	51.000	4.000	-99.000	-99.000
-2.991	-3.609	0.251	61.271	62.564	57.136	85.698	-99.000	4.484	54.750	50.750	4.000	-99.000	-99.000
-3.229	-3.992	0.156	60.934	62.339	56.934	86.176	-99.000	4.171	54.500	50.500	4.000	-99.000	-99.000
-2.516	-3.609	0.182	60.709	62.058	56.732	86.655	-99.000	4.259	54.250	50.250	4.000	-99.000	-99.000
-2.753	-3.609	0.246	60.484	61.833	56.530	87.133	-99.000	4.146	54.000	50.000	4.000	-99.000	-99.000
-2.753	-3.609	0.266	60.316	61.552	56.328	87.561	-99.000	4.290	54.000	50.250	4.750	-99.000	-99.000
-2.516	-3.609	0.258	60.091	61.327	56.125	87.990	-99.000	4.434	54.000	50.500	5.500	-99.000	-99.000
-2.278	-3.609	0.260	59.922	61.159	55.923	88.418	-99.000	4.577	54.000	50.750	6.250	-99.000	-99.000
-1.803	-3.609	0.268	59.753	60.934	55.721	88.846	-99.000	4.721	54.000	51.000	7.000	-99.000	-99.000
-1.328	-3.609	0.265	59.585	60.709	55.743	88.619	-99.000	4.634	54.500	51.000	6.500	-99.000	-99.000
-1.566	-3.609	0.264	59.360	60.540	55.766	88.393	-99.000	4.546	55.000	51.000	6.000	-99.000	-99.000
-1.803	-3.609	0.169	59.023	60.316	55.789	88.166	-99.000	4.458	55.500	51.000	5.500	-99.000	-99.000
-1.566	-3.226	0.241	58.798	60.035	55.811	87.939	-99.000	4.371	56.000	51.000	5.000	-99.000	-99.000
1.760	-0.545	0.271	58.685	59.866	56.013	87.360	-99.000	4.308	56.250	51.250	5.250	-99.000	-99.000
9.361	4.818	0.211	58.517	59.697	56.215	86.781	-99.000	4.246	56.500	51.500	5.500	-99.000	-99.000
18.625	10.180	0.014	57.955	59.810	56.417	86.201	-99.000	4.183	56.750	51.750	5.750	-99.000	-99.000
62.571	14.010	0.018	58.011	59.866	56.619	85.622	56.433	4.121	57.000	52.000	6.000	-99.000	-99.000
112.455	17.074	0.015	58.236	59.922	57.472	83.959	108.479	3.933	58.000	52.250	6.250	-99.000	-99.000
154.738	20.905	0.016	58.629	60.091	58.326	82.297	160.525	3.745	59.000	52.500	6.500	-99.000	-99.000
196.545	24.735	0.014	59.023	60.316	59.180	80.634	212.571	3.557	60.000	52.750	6.750	-99.000	-99.000
235.502	355.283	0.014	59.753	60.653	60.033	78.971	264.617	3.369	61.000	53.000	7.000	-99.000	-99.000
270.184	569.192	0.013	60.709	61.103	61.133	76.968	312.302	3.901	62.000	53.250	7.000	-99.000	-99.000
307.240	613.623	0.017	62.171	61.721	62.233	74.966	359.987	4.434	63.000	53.500	7.000	-99.000	-99.000
348.098	651.742	0.015	64.026	62.676	63.334	72.964	407.672	4.966	64.000	53.750	7.000	-99.000	-99.000
384.204	685.448	0.015	65.937	63.401	64.434	70.961	455.357	5.498	65.000	54.000	7.000	-99.000	-99.000
414.610	708.812	0.014	67.623	64.869	65.197	69.600	490.960	5.661	65.750	54.250	7.000	-99.000	-99.000
440.265	719.920	0.065	69.141	66.499	65.961	68.240	526.563	5.824	66.500	54.500	7.000	-99.000	-99.000
463.069	746.348	0.064	70.321	68.129	66.725	66.880	562.165	5.986	67.250	54.750	7.000	-99.000	-99.000
483.973	760.520	0.076	71.502	69.872	67.488	65.519	597.768	6.149	68.000	55.000	7.000	-99.000	-99.000
502.026	772.777	0.080	72.963	71.839	68.431	63.554	618.072	5.723	68.750	55.000	6.750	-99.000	-99.000
516.278	781.203	0.062	74.088	73.806	69.374	61.589	638.375	5.298	69.500	55.000	6.500	-99.000	-99.000
525.780	786.183	0.053	75.380	76.224	70.317	59.624	658.679	4.872	70.250	55.000	6.250	-99.000	-99.000
534.332	789.247	0.048	76.899	78.135	71.260	57.659	678.983	4.446	71.000	55.000	6.000	-99.000	-99.000
534.332	785.034	0.057	77.685	80.327	71.956	55.996	681.842	3.864	71.500	54.750	5.250	-99.000	-99.000
534.332	781.884	0.056	78.079	82.238	72.652	54.334	684.702	3.282	72.000	54.500	4.500	-99.000	-99.000
528.631	779.288	0.049	78.585	83.868	73.349	52.672	687.562	2.699	72.500	54.250	3.750	-99.000	-99.000
521.029	774.692	0.010	78.753	85.836	74.045	51.009	690.421	2.117	73.000	54.000	3.000	-99.000	-99.000
506.302	761.669	0.004	79.203	88.084	74.337	49.800	675.837	2.136	73.250	53.750	3.000	-99.000	-99.000
492.049	748.646	0.003	79.653	89.602	74.628	48.590	661.253	2.155	73.500	53.500	3.000	-99.000	-99.000
475.896	733.326	0.003	79.990	90.783	74.920	47.381	646.668	2.173	73.750	53.250	3.000	-99.000	-99.000
454.992	713.791	0.004	80.215	91.738	75.212	46.172	632.084	2.192	74.000	53.000	3.000	-99.000	-99.000
430.763	691.491	0.003	80.664	92.525	75.481	45.996	601.485	2.230	74.250	53.250	3.250	-99.000	-99.000
404.633	670.127	0.005	80.664	92.975	75.751	45.819	570.887	2.267	74.500	53.500	3.500	-99.000	-99.000
372.802	640.634	0.049	81.789	92.300	76.021	45.643	540.289	2.305	74.750	53.750	3.750	-99.000	-99.000
338.596	609.992	0.035	81.901	91.907	76.290	45.467	509.690	2.343	75.000	54.000	4.000	-99.000	-99.000
303.915	575.521	0.009	81.226	92.525	76.290	45.391	465.651	2.105	75.000	53.750	3.000	-99.000	-99.000
266.858	538.750	0.003	81.114	92.862	76.290	45.316	421.612	1.867	75.000	53.500	2.000	-99.000	-99.000
230.276	502.746	0.001	80.721	93.168	76.290	45.241	377.574	1.629	75.000	53.250	1.000	-99.000	-99.000
191.794	461.380	0.030	80.945	92.906	76.290	45.165	333.535	1.391	75.000	53.000	0.000	-99.000	-99.000
151.412	415.417	0.030	80.608	91.794	76.021	45.278	284.134	1.685	74.250	53.250	0.000	-99.000	-99.000
113.405	365.624	0.032	80.271	90.939	75.751	45.392	234.734	1.980	73.500	53.500	0.000	-99.000	-99.000
76.348	256.080	0.018	79.259	89.996	75.481	45.505	185.333	2.274	72.750	53.750	0.000	-99.000	-99.000
21.713	23.203	0.020	78.697	89.096	75.212	45.618	135.932	2.568	72.000	54.000	0.000	-99.000	-99.000
7.461	12.095	0.021	77.685	87.803	74.269	47.986	-99.000	2.337	69.500	54.750	0.000	-99.000	-99.000
-1.803	0.221	0.027	76.730	85.667	73.326	50.354	-99.000	2.105	67.000	55.500	0.000	-99.000	-99.000
-6.792	-3.226	0.032	75.774	83.700	72.383	52.722	-99.000	1.873	64.500	56.250	0.000	-99.000	-99.000
-6.554	-4.375	0.035	74.706	82.070	71.440	55.090	-99.000	1.642	62.000	57.000	0.000	-99.000	-99.000
-5.604	-4.375	0.038	73.638	80.721	70.699	57.471	-99.000	1.698	61.500	56.750	0.000	-99.000	-99.000
-4.416	-3.992	0.039	72.738	79.484	69.958	59.851	-99.000	1.754	61.000	56.500	0.000	-99.000	-99.000
-3.941	-4.375	0.039	71.839	78.360	69.217	62.231	-99.000	1.811	60.500	56.250	0.000	-99.000	-99.000
-3.704	-4.375	0.045	71.221	77.348	68.476	64.612	-99.000	1.967	60.000	56.000	0.000	-99.000	-99.000
-3.466	-4.375	0.051	71.108	76.392	68.094	65.506	-99.000	2.011	59.500	55.750	0.000	-99.000	-99.000
-3.229	-4.375	0.046	71.052	75.661	67.712	66.400	-99.000	2.155	59.000	55.500	0.000	-99.000	-99.000
-2.041	-3.609	0.040	70.434	75.156	67.331	67.295	-99.000	2.299	58.500	55.250	0.000	-99.000	-99.000
-1.803	-3.609	0.016	69.647	74.818	66.949	68.189	-99.000	2.443	58.000	55.000	0.000	-99.000	-99.000
-1.566	-3.609	0.005	68.916	74.818	66.657	68.945	-99.000	2.575	58.250	55.500	0.000	-99.000	-99.000
-1.566	-3.609	0.032	68.691	74.144	66.365	69.701	-99.000	2.706	58.500	56.000	0.000	-99.000	-99.000
-1.328	-3.609	0.038	68.410	73.244	66.073	70.456	-99.000	2.838	58.750	56.500	0.000	-99.000	-99.000
-1.091	-3.609	0.037	68.241	72.626	65.781	71.212	-99.000	2.969	59.000	57.000	0.000	-99.000	-99.000
-1.091	-3.609	0.039	68.073	72.176	65.602	71.892	-99.000	2.982	59.000	56.500	0.750	-99.000	-99.000
-1.091	-3.609	0.040	68.017	71.783	65.422	72.572	-99.000	2.994	59.000	56.000	1.500	-99.000	-99.000
-1.091	-3.609	0.037	67.679	71.333	65.243	73.253	-99.000	3.007	59.000	55.500	2.250	-99.000	-99.000
-1.091	-3.609	0.035	67.455	70.827	65.063	73.933	-99.000	3.019	59.000	55.000	3.000	-99.000	-99.000
-1.091	-3.609	0.040	67.398	70.659	64.973	74.412	-99.000	3.075	59.000	55.250	2.250	-99.000	-99.000
-1.328	-3.609	0.042	67.230	70.659	64.883	74.891	-99.000	3.132	59.000	55.500	1.500	-99.000	-99.000
-1.803	-3.609	0.037	67.061	70.715	64.793	75.369	-99.000	3.188	59.000	55.750	0.750	-99.000	-99.000
-1.328	-3.609	0.039	67.005	70.602	64.703	75.848	-99.000	3.244	59.000	56.000	0.000	-99.000	-99.000
-1.091	-3.609	0.038	66.780	70.265	64.344	76.981	-99.000	3.457	58.750	55.750	0.000	-99.000	-99.000
-1.091	-3.609	0.038	66.386	69.591	63.985	78.115	-99.000	3.669	58.500	55.500	0.000	-99.000	-99.000
-1.328	-3.609	0.036	66.049	69.253	63.625	79.249	-99.000	3.882	58.250	55.250	0.000	-99.000	-99.000

Figure B.25. Measured Data from the Solar Test Bench (Case 5, 12/01/98, No Shading; Part 2).

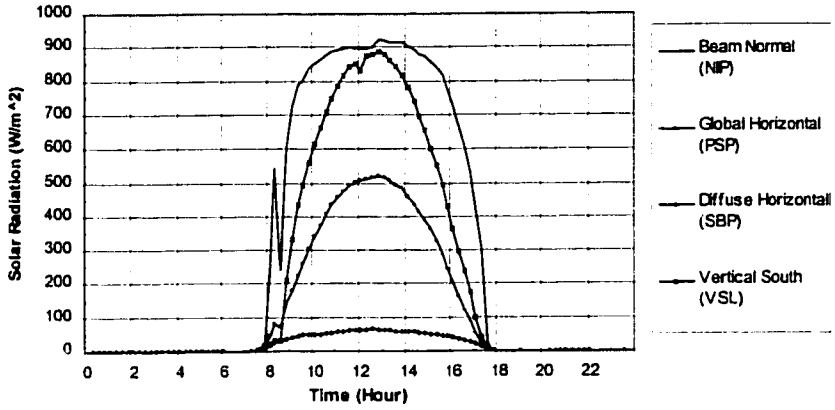

Figure B.26. Measured Beam Normal, Global Horizontal, Diffuse Horizontal and Vertical South Solar Radiation (Case 6, 12/15/98, Overhang Shade).

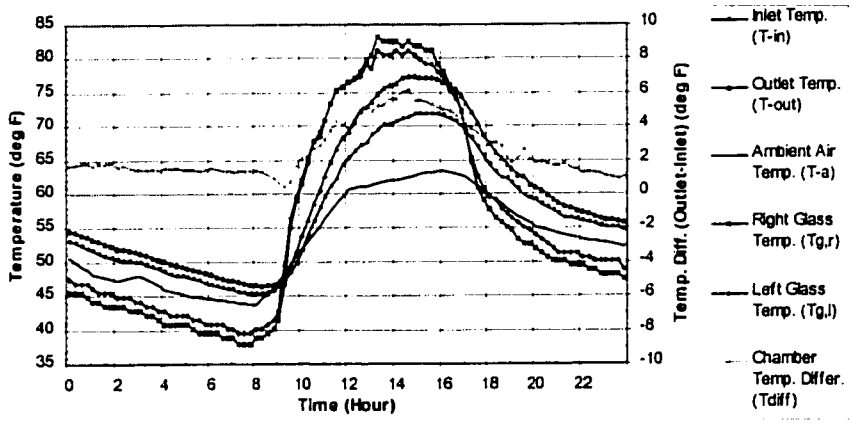

Figure B.27. Measured Chamber Inlet and Outlet Temperature and Outside Air Temperature (Case 6, 12/15/98, Overhang Shade).

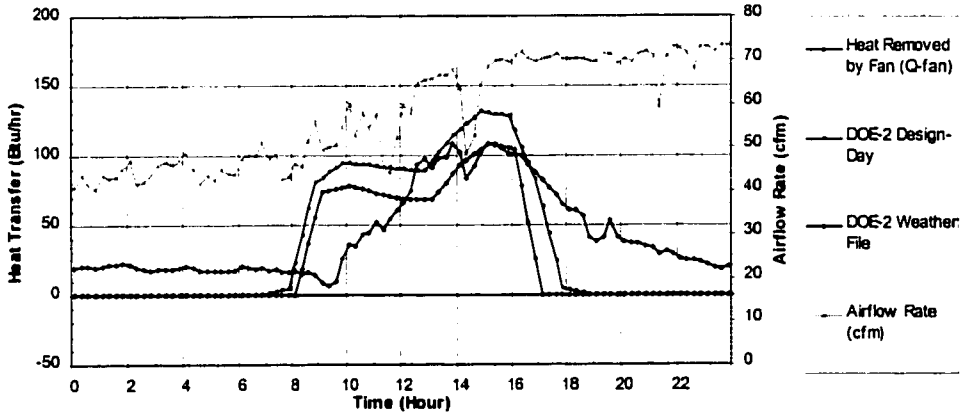

Figure B.28. Heat Transfer of the Experimental Box and Calculated Airflow Rate (Case 6, 12/15/98, Overhang Shade).

1	2	3	4	5	6	7	8	9	10	11	12	13	14
Site	Month	Day	Year	Julian	Decimal	Hour	ELI	SLI	WLI	LIH	NIP	PSP	SBP
0	12	15	98	98349	6923.000	0	1.696	-4.575	-2.762	-3.766	-7.736	-2.472	-4.533
0	12	15	98	98349	6923.010	15	2.081	-2.996	-0.549	-2.419	-7.515	-1.636	-4.351
0	12	15	98	98349	6923.021	30	1.953	-0.311	2.107	-1.240	-7.293	-1.009	-4.351
0	12	15	98	98349	6923.031	45	1.953	-0.311	2.107	-1.408	-7.293	-1.009	-4.533
0	12	15	98	98349	6923.042	100	1.953	-0.311	2.107	-1.240	-7.293	-1.009	-4.351
0	12	15	98	98349	6923.052	115	1.953	-0.311	2.107	-1.240	-7.293	-0.800	-4.351
0	12	15	98	98349	6923.063	130	1.953	-0.311	2.107	-1.240	-7.293	-0.382	-4.351
0	12	15	98	98349	6923.073	145	1.953	-0.311	2.107	-1.240	-7.293	-0.591	-4.351
0	12	15	98	98349	6923.083	200	1.953	-0.311	2.107	-1.240	-7.293	-0.591	-4.351
0	12	15	98	98349	6923.094	215	1.953	-0.311	2.107	-1.240	-7.071	-0.591	-4.169
0	12	15	98	98349	6923.104	230	1.953	-0.311	2.107	-1.240	-7.071	-0.591	-4.169
0	12	15	98	98349	6923.115	245	1.953	-0.311	2.107	-1.240	-7.071	-0.382	-4.169
0	12	15	98	98349	6923.125	300	1.953	-0.311	2.107	-1.240	-7.071	-0.382	-4.169
0	12	15	98	98349	6923.135	315	1.953	-0.311	2.107	-1.240	-7.071	-0.591	-4.169
0	12	15	98	98349	6923.146	330	1.953	-0.311	2.107	-1.240	-7.071	-0.800	-4.169
0	12	15	98	98349	6923.156	345	1.953	-0.311	2.107	-1.240	-7.071	-1.009	-4.351
0	12	15	98	98349	6923.167	400	1.953	-0.311	2.107	-1.071	-7.071	-0.800	-4.351
0	12	15	98	98349	6923.177	415	1.953	-0.311	2.107	-1.071	-7.071	-0.382	-4.169
0	12	15	98	98349	6923.188	430	1.953	-0.311	2.107	-1.071	-7.071	-0.591	-4.169
0	12	15	98	98349	6923.198	445	2.081	-0.153	2.107	-1.071	-7.071	-0.173	-4.169
0	12	15	98	98349	6923.208	500	2.081	-0.311	2.107	-1.071	-7.071	0.036	-4.169
0	12	15	98	98349	6923.219	515	2.081	-0.311	2.107	-1.071	-7.071	-0.173	-4.169
0	12	15	98	98349	6923.229	530	1.953	-0.311	2.107	-1.071	-7.071	-0.382	-4.169
0	12	15	98	98349	6923.240	545	1.953	-0.469	2.107	-1.240	-7.293	-0.800	-4.169
0	12	15	98	98349	6923.250	600	1.953	-0.943	1.222	-1.913	-7.071	-0.800	-4.169
0	12	15	98	98349	6923.260	615	1.568	-1.469	-2.024	-4.271	-7.293	-2.263	-4.351
0	12	15	98	98349	6923.271	630	1.568	-1.469	-2.024	-4.271	-7.293	-2.263	-4.351
0	12	15	98	98349	6923.281	645	1.696	-1.469	-2.024	-4.271	-7.293	-2.472	-4.351
0	12	15	98	98349	6923.292	700	1.696	-1.311	-2.024	-4.103	-7.293	-2.263	-4.351
0	12	15	98	98349	6923.302	715	3.747	-2.364	-0.944	-2.419	-7.293	-0.173	-3.258
0	12	15	98	98349	6923.313	730	9.643	3.005	1.878	1.624	-7.293	4.426	1.296
0	12	15	98	98349	6923.323	745	19.640	12.005	12.140	8.530	-7.515	18.221	9.675
0	12	15	98	98349	6923.333	800	135.764	98.536	20.108	31.774	246.348	47.067	19.146
0	12	15	98	98349	6923.344	815	463.885	281.703	27.781	91.400	540.785	79.257	28.254
0	12	15	98	98349	6923.354	830	209.592	142.117	29.256	59.734	240.140	72.150	30.804
0	12	15	98	98349	6923.365	845	542.840	379.918	35.749	147.320	600.205	144.474	35.904
0	12	15	98	98349	6923.375	900	676.139	504.977	38.700	207.283	726.138	177.500	39.911
0	12	15	98	98349	6923.385	915	742.276	583.929	58.176	252.424	789.105	223.486	44.283
0	12	15	98	98349	6923.396	930	765.859	633.826	112.770	285.437	803.295	260.692	47.197
0	12	15	98	98349	6923.406	945	803.286	695.092	181.824	323.167	840.543	303.752	49.019
0	12	15	98	98349	6923.417	1000	825.844	744.990	234.647	356.517	852.072	339.704	50.112
0	12	15	98	98349	6923.427	1015	841.225	789.202	287.175	386.161	865.375	372.311	51.569
0	12	15	98	98349	6923.438	1030	850.453	831.520	341.178	412.437	876.904	406.593	52.662
0	12	15	98	98349	6923.448	1045	854.555	869.417	394.887	436.018	886.660	434.602	54.847
0	12	15	98	98349	6923.458	1100	852.504	901.629	448.595	456.230	893.755	458.013	57.033
0	12	15	98	98349	6923.469	1115	846.352	930.052	501.713	474.421	897.302	477.244	59.948
0	12	15	98	98349	6923.479	1130	837.123	955.948	551.880	490.591	901.736	493.130	62.498
0	12	15	98	98349	6923.490	1145	812.514	964.790	593.785	497.329	898.189	500.655	61.769
0	12	15	98	98349	6923.500	1200	789.930	974.896	636.279	504.066	896.415	508.180	63.591
0	12	15	98	98349	6923.510	1215	764.834	982.475	675.233	509.456	897.302	513.196	64.684
0	12	15	98	98349	6923.521	1230	736.616	988.791	713.005	511.477	900.849	517.377	65.048
0	12	15	98	98349	6923.531	1245	714.078	1005.213	750.451	516.867	923.021	522.394	63.591
0	12	15	98	98349	6923.542	1300	677.164	1001.424	788.551	511.477	918.587	516.541	63.955
0	12	15	98	98349	6923.552	1315	635.616	991.318	812.750	499.350	913.265	505.671	63.591
0	12	15	98	98349	6923.563	1330	593.596	979.949	836.948	487.222	913.265	494.802	60.312
0	12	15	98	98349	6923.573	1345	548.479	962.895	855.244	472.400	913.265	482.260	58.855
0	12	15	98	98349	6923.583	1400	495.159	932.579	861.736	450.167	901.736	458.950	58.126
0	12	15	98	98349	6923.594	1415	441.840	900.997	865.278	425.912	891.094	435.957	56.669
0	12	15	98	98349	6923.604	1430	386.982	862.469	861.736	398.962	877.791	412.028	54.483
0	12	15	98	98349	6923.615	1445	334.688	820.994	863.507	374.034	874.244	391.125	53.026
0	12	15	98	98349	6923.625	1500	279.830	782.886	851.113	341.694	854.733	362.697	51.205
0	12	15	98	98349	6923.635	1515	228.048	738.673	838.719	310.029	840.543	327.581	49.019
0	12	15	98	98349	6923.646	1530	177.036	686.250	813.340	274.320	813.937	286.194	46.833
0	12	15	98	98349	6923.656	1545	114.488	630.036	781.469	237.602	776.689	245.642	44.283
0	12	15	98	98349	6923.667	1600	59.630	564.349	733.663	198.525	728.799	204.673	40.640
0	12	15	98	98349	6923.677	1615	37.072	492.977	675.233	159.111	664.945	160.360	37.361
0	12	15	98	98349	6923.688	1630	34.508	427.921	620.344	124.413	604.639	122.317	32.990
0	12	15	98	98349	6923.698	1645	31.176	354.654	547.159	82.304	531.030	98.036	27.989
0	12	15	98	98349	6923.708	1700	28.869	270.018	445.644	42.554	429.928	52.920	22.061
0	12	15	98	98349	6923.719	1715	21.435	171.171	303.700	14.593	303.994	21.148	14.046
0	12	15	98	98349	6923.729	1730	10.412	20.532	32.502	1.624	21.973	0.454	4.392
0	12	15	98	98349	6923.740	1745	4.132	0.478	1.959	-3.935	-8.845	-4.353	-2.165
0	12	15	98	98349	6923.750	1800	1.696	-2.680	-1.729	-6.124	-8.623	-4.771	-4.533
0	12	15	98	98349	6923.760	1815	1.696	-3.469	-2.320	-5.787	-8.180	-3.726	-4.715
0	12	15	98	98349	6923.771	1830	1.696	-3.311	-2.320	-5.956	-7.958	-2.890	-4.715
0	12	15	98	98349	6923.781	1845	1.824	-3.154	-2.172	-5.956	-7.958	-2.472	-4.715
0	12	15	98	98349	6923.792	1900	1.824	-3.154	-2.172	-5.956	-7.736	-2.054	-4.533
0	12	15	98	98349	6923.802	1915	1.824	-2.996	-2.172	-5.956	-7.958	-2.681	-4.351
0	12	15	98	98349	6923.813	1930	1.696	-3.154	-2.172	-5.787	-7.958	-2.681	-4.351
0	12	15	98	98349	6923.823	1945	1.696	-3.154	-2.172	-5.787	-7.515	-2.681	-4.169
0	12	15	98	98349	6923.833	2000	1.696	-3.154	-2.172	-5.619	-7.515	-2.263	-4.169
0	12	15	98	98349	6923.844	2015	1.824	-2.996	-2.172	-5.787	-7.293	-1.636	-4.169
0	12	15	98	98349	6923.854	2030	1.824	-2.996	-2.172	-5.619	-7.293	-1.218	-4.351
0	12	15	98	98349	6923.865	2045	1.953	-2.680	-2.024	-5.956	-7.293	-1.218	-4.533
0	12	15	98	98349	6923.875	2100	1.824	-2.996	-2.024	-5.787	-7.293	-1.218	-4.533
0	12	15	98	98349	6923.885	2115	1.824	-2.838	-2.172	-5.787	-7.515	-1.636	-4.715
0	12	15	98	98349	6923.896	2130	1.824	-3.154	-2.172	-5.450	-7.293	-1.845	-4.715
0	12	15	98	98349	6923.906	2145	1.824	-3.311	-2.172	-5.282	-7.515	-1.427	-4.897
0	12	15	98	98349	6923.917	2200	1.824	-3.469	-2.320	-4.945	-7.515	-1.845	-4.897
0	12	15	98	98349	6923.927	2215	1.824	-3.627	-2.467	-4.945	-7.736	-2.263	-4.897
0	12	15	98	98349	6923.938	2230	1.696	-4.101	-2.467	-4.608	-7.736	-2.890	-4.897
0	12	15	98	98349	6923.948	2245	1.824	-4.101	-2.615	-4.777	-7.736	-2.681	-4.897
0	12	15	98	98349	6923.958	2300	1.824	-4.417	-2.615	-4.608	-7.515	-2.890	-4.715
0	12	15	98	98349	6923.969	2315	1.824	-4.417	-2.615	-4.608	-7.515	-2.472	-4.715
0	12	15	98	98349	6923.979	2330	1.824	-4.417	-2.467	-4.440	-7.515	-2.054	-4.533
0	12	15	98	98349	6923.990	2345	1.953	-4.417	-2.615	-4.608	-7.515	-2.472	-4.533

Figure B.29. Measured Data from the Solar Test Bench (Case 6, 12/15/98, Overhang Shade; Part 1).

15	16	17	18	19	20	21	22	23	24	25	26	27	28
TSP	SVL	APD	TI	TO	Tdb	RH	GHR	Wind	Tdb2	Tdew	Wind2	Tg,r	Tg,l
-0.378	-5.484	0.100	53.008	54.722	50.601	59.476	-99.000	2.493	38.000	37.000	0.000	45.480	47.460
-0.616	-5.484	0.114	52.755	54.413	49.995	61.765	-99.000	2.900	38.000	37.000	0.000	45.480	46.800
-1.328	-5.484	0.104	52.333	54.076	49.389	63.655	-99.000	3.307	38.000	37.000	0.000	45.480	46.800
-1.328	-5.484	0.099	51.996	53.739	48.782	65.544	-99.000	3.714	38.000	37.000	0.000	44.810	46.800
-1.328	-5.484	0.114	51.715	53.401	48.176	67.434	-99.000	4.121	38.000	37.000	0.000	44.140	46.140
-1.091	-5.484	0.111	51.294	53.064	47.974	67.887	-99.000	3.676	38.000	37.000	0.750	44.140	45.480
-1.091	-5.484	0.113	50.928	52.727	47.772	68.341	-99.000	3.232	38.000	37.000	1.500	43.470	45.480
-0.853	-5.484	0.122	50.647	52.390	47.570	68.795	-99.000	2.787	38.000	37.000	2.250	43.470	45.480
-0.853	-5.484	0.134	50.422	52.052	47.368	69.248	-99.000	2.343	38.000	37.000	3.000	43.470	44.810
-0.616	-5.484	0.104	50.197	51.856	47.525	68.857	-99.000	2.374	38.250	37.000	2.250	43.470	44.810
-0.616	-5.484	0.108	50.113	51.659	47.683	68.467	-99.000	2.405	38.500	37.000	1.500	42.800	44.810
-0.378	-5.484	0.114	50.029	51.462	47.840	68.076	-99.000	2.437	38.750	37.000	0.750	42.800	44.140
-0.378	-5.484	0.127	49.860	51.265	47.997	67.686	-99.000	2.468	39.000	37.000	0.000	42.800	44.140
-0.378	-5.484	0.132	49.579	50.984	47.503	69.122	-99.000	2.349	39.500	37.000	1.500	42.120	43.470
-0.616	-5.484	0.128	49.298	50.731	47.009	70.557	-99.000	2.230	40.000	37.000	3.000	42.120	43.470
-0.853	-4.833	0.133	48.961	50.422	46.515	71.993	-99.000	2.111	40.500	37.000	4.500	41.440	42.800
-0.853	-4.833	0.141	48.567	50.085	46.021	73.429	-99.000	1.992	41.000	37.000	6.000	40.760	42.800
-0.616	-4.833	0.121	48.230	49.776	45.774	74.366	-99.000	2.236	41.000	36.750	5.500	40.760	42.120
-0.616	-4.833	0.104	48.005	49.495	45.527	75.344	-99.000	2.480	41.000	36.500	5.000	40.760	42.120
-0.140	-4.833	0.115	47.836	49.270	45.280	76.301	-99.000	2.725	41.000	36.250	4.500	40.760	42.120
-0.335	-4.833	0.112	47.640	49.073	45.033	77.258	-99.000	2.969	41.000	36.000	4.000	40.760	42.120
0.097	-4.833	0.121	47.443	48.848	44.921	77.737	-99.000	2.781	41.000	36.000	3.750	40.080	41.440
-0.378	-4.833	0.117	47.218	48.595	44.809	78.215	-99.000	2.594	41.000	36.000	3.500	39.390	41.440
-0.853	-4.833	0.116	46.881	48.314	44.696	78.694	-99.000	2.406	41.000	36.000	3.250	39.390	40.760
-0.616	-4.833	0.136	46.572	48.061	44.584	79.173	-99.000	2.218	41.000	36.000	3.000	39.390	40.760
-0.378	-4.833	0.139	46.347	47.808	44.472	79.576	-99.000	2.299	40.750	36.250	3.250	39.390	40.760
-0.378	-4.833	0.140	46.206	47.584	44.359	79.979	-99.000	2.380	40.500	36.500	3.500	38.700	40.760
-0.140	-4.833	0.157	46.010	47.359	44.246	80.382	-99.000	2.462	40.250	36.750	3.750	38.700	40.080
-0.140	-4.833	0.136	45.925	47.218	44.134	80.785	-99.000	2.543	40.000	37.000	4.000	38.700	40.080
1.760	-2.879	0.141	45.588	46.965	44.022	81.163	-99.000	2.393	40.250	37.000	4.000	38.000	39.390
6.036	3.632	0.110	45.419	46.768	43.910	81.541	-99.000	2.243	40.500	37.000	4.000	38.000	39.390
14.112	14.050	0.113	45.279	46.628	43.797	81.919	-99.000	2.092	40.750	37.000	4.000	38.000	39.390
25.514	22.515	0.129	45.166	46.516	43.685	82.297	31.554	1.942	41.000	37.000	4.000	38.700	40.080
44.425	32.282	0.125	45.279	46.487	44.516	80.420	80.526	2.105	42.250	37.500	3.000	38.700	40.080
74.448	82.933	0.160	45.447	46.544	45.347	78.544	129.497	2.267	43.500	38.000	2.000	39.390	40.760
147.611	209.392	0.188	45.813	46.712	46.178	76.667	178.469	2.430	44.750	38.500	1.000	40.080	41.440
200.821	331.154	0.147	46.431	47.078	47.009	74.790	227.441	2.593	46.000	39.000	0.000	41.440	42.800
244.054	435.987	0.151	47.190	47.612	48.266	71.704	276.413	2.681	47.500	39.000	1.000	46.800	49.420
278.260	495.241	0.153	48.314	49.017	49.524	68.618	325.384	2.768	49.000	39.000	2.000	55.200	56.470
317.217	558.401	0.180	49.432	51.490	50.782	65.532	374.356	2.856	50.500	39.000	3.000	59.000	59.630
355.224	613.748	0.214	51.771	53.879	52.039	62.446	423.328	2.944	52.000	39.000	4.000	61.520	62.150
387.530	663.234	0.167	53.992	56.296	53.139	60.380	460.504	2.850	53.000	38.750	3.750	64.670	65.300
414.610	708.163	0.200	55.987	58.629	54.240	58.314	497.680	2.756	54.000	38.500	3.500	67.820	67.820
438.839	749.185	0.178	57.898	60.765	55.340	56.249	534.855	2.662	55.000	38.250	3.250	69.070	68.440
460.218	784.346	0.197	59.585	62.789	56.440	54.183	572.031	2.568	56.000	38.000	3.000	70.950	70.950
478.747	815.601	0.121	61.046	64.756	57.495	51.941	593.049	2.180	56.750	37.750	2.250	73.470	73.470
492.999	841.646	0.118	62.283	66.611	58.550	49.699	614.068	1.792	57.500	37.500	1.500	75.390	75.390
497.750	853.366	0.163	64.250	68.354	59.606	47.457	635.086	1.404	58.250	37.250	0.750	75.890	75.890
504.401	829.274	0.212	65.318	69.253	60.661	45.215	656.105	1.016	59.000	37.000	0.000	76.530	76.430
509.627	875.505	0.199	66.162	70.715	60.841	44.069	661.538	1.022	59.250	36.750	0.000	77.120	76.890
511.527	878.761	0.249	67.117	72.176	61.021	42.923	666.972	1.029	59.500	36.500	0.000	77.970	77.320
516.278	887.877	0.254	67.679	72.963	61.200	41.776	672.406	1.035	59.750	36.250	0.000	79.900	79.250
508.677	878.761	0.258	68.091	73.582	61.380	40.630	677.839	1.041	60.000	36.000	0.000	80.540	78.610
498.225	860.529	0.262	69.478	74.650	61.560	40.542	667.258	1.586	60.500	36.250	1.000	83.130	81.190
488.248	841.646	0.263	70.321	75.549	61.739	40.453	656.677	2.130	61.000	36.500	2.000	82.480	80.540
476.846	818.205	0.274	70.378	75.999	61.918	40.365	646.097	2.674	61.500	36.750	3.000	82.480	80.540
455.942	781.741	0.241	70.715	76.336	62.098	40.277	635.516	3.219	62.000	37.000	4.000	82.480	81.190
433.138	742.022	0.142	71.052	77.123	62.123	39.899	606.490	3.294	62.000	37.250	4.000	81.830	80.540
406.058	697.094	0.167	71.277	77.460	62.548	39.521	577.464	3.370	62.000	37.500	4.000	82.480	81.190
382.304	655.421	0.246	71.839	77.404	62.772	39.144	548.439	3.445	62.000	37.750	4.000	81.830	80.540
348.573	602.679	0.280	71.727	77.292	62.997	38.766	519.413	3.520	62.000	38.000	4.000	81.830	79.900
313.892	551.239	0.290	71.783	77.235	63.087	38.804	477.376	3.332	62.250	38.250	4.000	81.190	79.250
276.835	492.636	0.292	71.839	77.123	63.176	38.841	435.339	3.144	62.500	38.500	4.000	81.190	79.250
239.303	430.778	0.288	71.783	76.898	63.266	38.879	393.302	2.956	62.750	38.750	4.000	79.250	77.970
200.346	365.013	0.300	71.502	76.505	63.356	38.917	351.265	2.768	63.000	39.000	4.000	77.970	77.320
159.013	297.946	0.307	71.052	75.943	63.132	39.207	300.792	2.837	62.250	38.750	3.000	76.030	75.390
122.907	238.042	0.294	70.659	75.324	62.907	39.496	250.319	2.906	61.500	38.500	2.000	74.740	74.100
86.325	174.881	0.288	70.040	74.481	62.682	39.786	199.845	2.975	60.750	38.250	1.000	72.200	72.200
52.640	98.698	0.294	69.253	73.357	62.458	40.076	149.372	3.044	60.000	38.000	0.000	69.070	69.700
11.262	40.096	0.297	68.241	72.064	61.740	41.235	110.588	2.694	-99.000	-99.000	-99.000	64.670	65.300
2.472	6.888	0.302	66.892	70.434	61.021	42.394	71.803	2.343	-99.000	-99.000	-99.000	60.890	62.780
-3.466	-2.228	0.294	65.487	68.747	60.302	43.552	33.019	1.992	-99.000	-99.000	-99.000	59.000	60.890
-4.654	-6.135	0.295	64.250	67.286	59.584	44.711	-5.765	1.642	-99.000	-99.000	-99.000	57.740	59.630
-4.179	-6.135	0.295	63.070	66.105	59.300	45.958	-99.000	1.573	-99.000	-99.000	-99.000	56.470	59.000
-3.466	-6.135	0.295	62.339	65.150	58.416	47.205	-99.000	1.504	-99.000	-99.000	-99.000	55.840	57.740
-3.229	-6.135	0.289	62.171	64.250	57.832	48.452	-99.000	1.435	-99.000	-99.000	-99.000	55.200	57.100
-2.991	-6.135	0.288	61.552	63.463	57.248	49.699	-99.000	1.166	45.000	42.000	0.000	54.560	56.470
-2.753	-6.135	0.301	60.597	62.629	56.731	51.021	-99.000	1.094	44.500	41.750	0.000	53.290	55.840
-2.753	-6.135	0.301	59.810	62.452	56.215	52.344	-99.000	0.822	44.000	41.500	0.000	52.650	55.200
-3.466	-6.135	0.286	59.360	61.440	55.699	53.667	-99.000	0.549	43.500	41.250	0.000	52.650	54.560
-1.803	-6.135	0.295	59.023	60.934	55.182	54.989	-99.000	0.277	43.000	41.000	0.000	52.000	53.930
0.097	-6.135	0.289	58.517	60.372	54.958	54.876	-99.000	0.831	42.750	40.750	0.000	51.360	53.290
0.335	-5.484	0.303	57.955	59.753	54.733	54.762	-99.000	1.385	42.500	40.500	0.000	50.710	52.650
0.572	-5.484	0.307	57.477	59.191	54.508	54.649	-99.000	1.939	42.250	40.250	0.000	50.070	52.000
0.572	-5.484	0.300	56.999	58.685	54.284	54.536	-99.000	2.493	42.000	40.000	0.000	50.070	51.360
0.097	-5.484	0.209	56.521	58.292	54.037	54.599	-99.000	2.662	41.750	40.000	0.000	50.070	51.360
-0.378	-5.484	0.299	56.353	57.898	53.790	54.662	-99.000	2.831	41.500	40.000	0.000	49.420	51.360
-0.140	-5.484	0.318	56.156	57.561	53.543	54.725	-99.000	3.000	41.250	40.000	0.000	49.420	51.360
-0.616	-5.484	0.313	56.015	57.280	53.296	54.788	-99.000	3.169	41.000	40.000	0.000	49.420	50.710
-0.853	-5.484	0.305	55.819	57.027	53.161	54.523	-99.000	3.181	40.500	39.500	0.000	48.770	50.710
-1.091	-5.484	0.275	55.453	56.746	53.027	54.259	-99.000	3.194	40.000	39.000	0.000	48.770	50.070
-1.091	-5.484	0.317	55.285	56.437	52.892	53.994	-99.000	3.207	39.500	38.500	0.000	48.110	50.070
-1.091	-5.484	0.316	55.172	56.240	52.757	53.730	-99.000	3.219	39.000	38.000	0.000	48.110	50.070
-1.328	-5.484	0.309	55.144	56.100	52.555	54.208	-99.000	2.837	38.750	37.500	0.000	48.110	50.070
-0.616	-5.484	0.320	55.060	55.959	52.353	54.687	-99.000	2.456	38.500	37.000	0.000	48.110	50.070
-0.140	-5.484	0.319	54.722	55.734	52.151	55.166	-99.000	2.074	38.250	36.500	0.000	47.460	48.770

Figure B.30. Measured Data from the Solar Test Bench (Case 6, 12/15/98, Overhang Shade; Part 2).

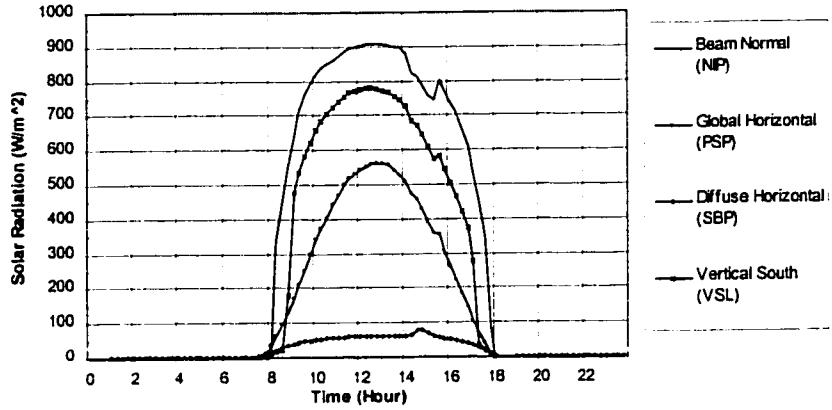

Figure B.31. Measured Beam Normal, Global Horizontal, Diffuse Horizontal and Vertical South Solar Radiation (Case 7, 01/18/99, Right-fin Shade).

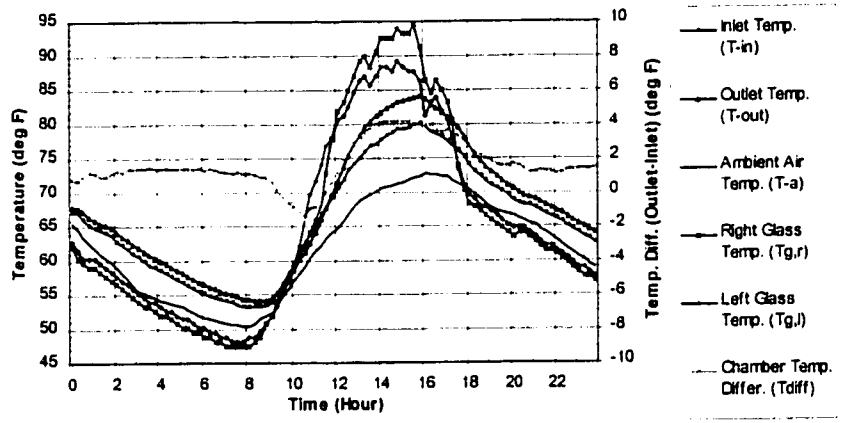

Figure B.32. Measured Chamber Inlet and Outlet Temperature and Outside Air Temperature (Case 7, 01/18/99, Right-fin Shade).

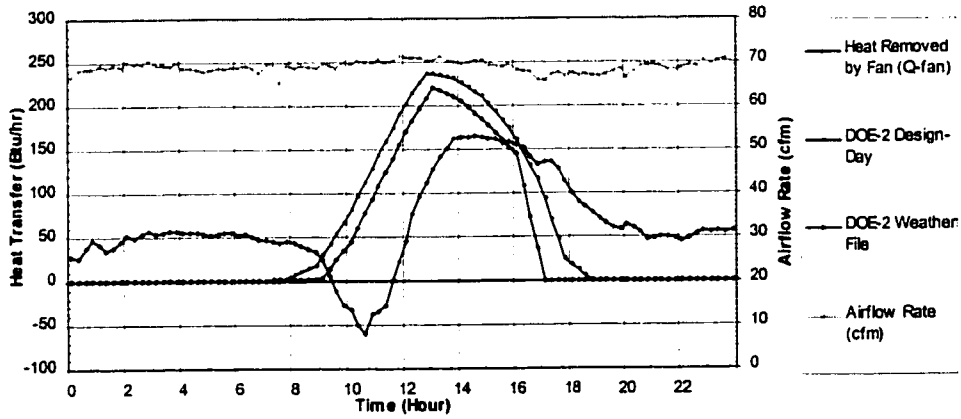

Figure B.33. Heat Transfer of the Experimental Box and Calculated Airflow Rate (Case 7, 01/18/99, Right-fin Shade).

1	2	3	4	5	6	7	8	9	10	11	12	13	14
Site	Month	Day	Year	Julian	Decimal	Hour	ELI	SLI	WLI	LIH	NIP	PSP	BBP
0	1	18	99	99018	6957.000	0	1.953	-1.890	1.812	-1.240	-8.180	-2.890	-5.262
0	1	18	99	99018	6957.010	15	1.824	-1.575	1.812	-1.576	-7.958	-3.099	-4.897
0	1	18	99	99018	6957.021	30	1.696	-1.101	2.107	-1.745	-8.623	-3.099	-5.262
0	1	18	99	99018	6957.031	45	1.696	-1.101	2.107	-1.576	-8.401	-2.472	-5.444
0	1	18	99	99018	6957.042	100	1.696	-1.101	2.107	-1.745	-8.180	-1.427	-5.079
0	1	18	99	99018	6957.052	115	1.696	-1.101	2.107	-1.576	-8.180	-1.218	-5.262
0	1	18	99	99018	6957.063	130	1.824	-1.101	2.255	-1.576	-8.180	-1.427	-5.262
0	1	18	99	99018	6957.073	145	1.696	-1.101	2.107	-1.745	-8.401	-1.427	-5.262
0	1	18	99	99018	6957.083	200	1.824	-1.101	2.107	-1.576	-8.401	-1.218	-5.262
0	1	18	99	99018	6957.094	215	1.824	-1.101	2.255	-1.576	-8.180	-0.591	-5.262
0	1	18	99	99018	6957.104	230	1.824	-1.101	2.255	-1.576	-8.180	-0.800	-5.262
0	1	18	99	99018	6957.115	245	1.824	-1.101	2.255	-1.576	-8.180	-0.382	-5.079
0	1	18	99	99018	6957.125	300	1.824	-1.101	2.107	-1.576	-8.180	-0.382	-5.079
0	1	18	99	99018	6957.135	315	1.824	-1.101	2.107	-1.576	-8.180	-0.591	-5.079
0	1	18	99	99018	6957.146	330	1.824	-1.259	2.107	-1.576	-7.958	-0.382	-4.897
0	1	18	99	99018	6957.156	345	1.824	-1.101	2.255	-1.408	-7.958	-0.173	-4.715
0	1	18	99	99018	6957.167	400	1.824	-1.101	2.107	-1.408	-7.958	-0.591	-4.715
0	1	18	99	99018	6957.177	415	1.824	-1.101	2.107	-1.408	-7.958	-0.800	-4.715
0	1	18	99	99018	6957.188	430	1.824	-1.101	2.107	-1.408	-7.958	-0.800	-4.715
0	1	18	99	99018	6957.198	445	1.824	-1.101	2.107	-1.240	-7.958	-0.591	-4.715
0	1	18	99	99018	6957.208	500	1.824	-1.101	2.107	-1.240	-7.958	-0.382	-4.715
0	1	18	99	99018	6957.219	515	1.824	-1.101	2.107	-1.240	-7.958	-0.382	-4.715
0	1	18	99	99018	6957.229	530	1.824	-1.101	2.107	-1.240	-7.958	-0.800	-4.533
0	1	18	99	99018	6957.240	545	1.824	-1.101	2.107	-1.408	-7.958	-0.591	-4.533
0	1	18	99	99018	6957.250	600	1.953	-1.101	2.107	-1.408	-7.958	-0.591	-4.533
0	1	18	99	99018	6957.260	615	1.824	-1.417	1.812	-1.576	-7.958	-0.800	-4.715
0	1	18	99	99018	6957.271	630	1.824	-1.417	1.959	-1.576	-7.958	-0.591	-4.533
0	1	18	99	99018	6957.281	645	1.953	-1.417	1.959	-1.576	-7.958	-1.009	-4.533
0	1	18	99	99018	6957.292	700	2.209	-1.890	1.664	-0.903	-8.180	0.454	-4.351
0	1	18	99	99018	6957.302	715	2.593	-1.575	1.959	-0.566	-8.180	0.454	-4.169
0	1	18	99	99018	6957.313	730	6.439	1.741	5.058	1.455	-8.180	2.544	-1.983
0	1	18	99	99018	6957.323	745	16.052	10.110	11.255	9.698	-8.180	11.533	6.214
0	1	18	99	99018	6957.333	800	28.869	20.848	20.403	14.593	20.643	33.271	14.775
0	1	18	99	99018	6957.344	815	171.089	209.699	29.666	73.209	131.487	62.535	23.882
0	1	18	99	99018	6957.354	830	532.586	320.863	34.863	121.044	451.430	95.561	30.440
0	1	18	99	99018	6957.365	845	614.103	397.604	39.585	161.469	555.862	130.678	35.904
0	1	18	99	99018	6957.375	900	679.215	468.344	42.536	202.230	640.113	172.483	40.276
0	1	18	99	99018	6957.385	915	733.560	535.295	44.306	243.328	708.401	211.780	43.919
0	1	18	99	99018	6957.396	930	775.600	597.193	64.364	283.753	757.178	251.913	46.833
0	1	18	99	99018	6957.406	945	808.413	655.301	123.984	322.156	795.313	287.481	49.383
0	1	18	99	99018	6957.417	1000	835.072	708.356	192.742	358.538	819.259	340.540	51.931
0	1	18	99	99018	6957.427	1015	854.555	756.990	244.975	392.225	836.109	372.313	53.755
0	1	18	99	99018	6957.438	1030	868.910	803.729	298.979	423.217	849.412	404.921	54.847
0	1	18	99	99018	6957.448	1045	878.138	845.416	354.163	450.840	861.828	442.127	56.669
0	1	18	99	99018	6957.458	1100	881.214	883.944	409.642	476.443	873.357	471.191	57.762
0	1	18	99	99018	6957.469	1115	880.189	917.419	463.940	498.676	883.999	498.147	58.855
0	1	18	99	99018	6957.479	1130	874.037	945.842	517.058	517.541	892.868	518.213	59.583
0	1	18	99	99018	6957.490	1145	860.707	967.348	567.226	532.363	898.189	532.427	60.312
0	1	18	99	99018	6957.500	1200	844.301	985.002	615.622	544.490	903.510	545.805	60.676
0	1	18	99	99018	6957.510	1215	821.742	998.897	660.479	552.575	907.944	553.330	61.405
0	1	18	99	99018	6957.521	1230	795.383	1007.740	701.792	557.292	908.831	560.018	62.133
0	1	18	99	99018	6957.531	1245	764.321	1011.529	739.565	558.639	908.831	563.163	62.133
0	1	18	99	99018	6957.542	1300	729.458	1010.266	773.796	556.618	908.831	561.691	61.405
0	1	18	99	99018	6957.552	1315	690.494	1005.213	803.897	550.554	905.284	555.838	61.769
0	1	18	99	99018	6957.563	1330	647.428	992.581	826.914	539.100	898.189	539.952	62.133
0	1	18	99	99018	6957.573	1345	604.875	982.475	852.883	527.647	898.189	526.574	61.405
0	1	18	99	99018	6957.583	1400	554.119	960.369	868.229	509.456	881.339	509.016	62.862
0	1	18	99	99018	6957.594	1415	486.956	903.524	849.932	471.726	822.806	472.227	67.234
0	1	18	99	99018	6957.604	1430	445.941	888.365	869.999	462.294	811.277	458.013	70.891
0	1	18	99	99018	6957.615	1445	393.134	849.205	862.327	433.323	788.219	429.586	77.434
0	1	18	99	99018	6957.625	1500	333.150	796.782	841.079	394.920	758.065	391.961	71.605
0	1	18	99	99018	6957.635	1515	274.191	739.937	815.701	356.140	744.762	354.353	61.405
0	1	18	99	99018	6957.646	1530	238.046	742.463	855.244	346.747	801.521	353.082	55.212
0	1	18	99	99018	6957.656	1545	185.495	684.355	825.144	308.344	771.368	306.260	54.119
0	1	18	99	99018	6957.667	1600	125.767	625.615	789.732	269.267	736.781	262.365	52.662
0	1	18	99	99018	6957.677	1615	68.859	569.402	753.729	230.864	707.514	223.904	48.290
0	1	18	99	99018	6957.688	1630	41.173	504.346	704.152	191.450	659.624	184.607	42.826
0	1	18	99	99018	6957.698	1645	38.610	441.185	651.034	154.731	609.073	144.055	39.183
0	1	18	99	99018	6957.708	1700	35.277	366.023	573.718	115.654	531.917	103.922	33.718
0	1	18	99	99018	6957.719	1715	32.970	288.966	485.187	70.514	449.882	69.224	26.797
0	1	18	99	99018	6957.729	1730	26.818	204.962	371.869	34.469	346.120	37.870	19.146
0	1	18	99	99018	6957.740	1745	16.821	58.744	107.753	12.572	83.610	10.278	9.128
0	1	18	99	99018	6957.750	1800	7.336	6.321	12.436	3.813	-9.510	-0.382	-0.161
0	1	18	99	99018	6957.760	1815	2.722	-0.469	1.287	-0.566	-9.510	-3.726	-4.897
0	1	18	99	99018	6957.771	1830	1.824	-1.890	1.664	-1.240	-9.288	-4.353	-5.444
0	1	18	99	99018	6957.781	1845	1.824	-2.048	1.517	-1.240	-8.623	-3.099	-5.444
0	1	18	99	99018	6957.792	1900	1.824	-2.048	1.517	-1.408	-8.401	-1.845	-5.262
0	1	18	99	99018	6957.802	1915	1.824	-2.048	1.517	-1.408	-8.623	-2.054	-5.262
0	1	18	99	99018	6957.813	1930	1.953	-2.048	1.517	-1.240	-8.623	-1.845	-5.262
0	1	18	99	99018	6957.823	1945	1.953	-2.048	1.517	-1.240	-8.623	-1.845	-5.262
0	1	18	99	99018	6957.833	2000	1.953	-2.048	1.517	-1.240	-8.623	-2.054	-5.079
0	1	18	99	99018	6957.844	2015	1.953	-2.048	1.517	-1.071	-8.623	-1.636	-5.262
0	1	18	99	99018	6957.854	2030	1.953	-2.048	1.517	-1.240	-8.180	-1.009	-5.079
0	1	18	99	99018	6957.865	2045	1.953	-1.890	1.517	-1.240	-8.401	-0.800	-5.079
0	1	18	99	99018	6957.875	2100	1.953	-1.890	1.517	-1.240	-8.401	-0.800	-5.079
0	1	18	99	99018	6957.885	2115	1.953	-2.048	1.517	-1.240	-8.623	-0.591	-5.079
0	1	18	99	99018	6957.896	2130	1.953	-2.048	1.517	-1.240	-8.623	-1.009	-5.079
0	1	18	99	99018	6957.906	2145	1.953	-2.048	1.664	-1.071	-8.401	-0.800	-5.079
0	1	18	99	99018	6957.917	2200	1.953	-2.048	1.664	-0.903	-8.401	-1.009	-5.079
0	1	18	99	99018	6957.927	2215	2.081	-1.890	1.664	-1.071	-8.401	-0.800	-5.079
0	1	18	99	99019	6957.938	2230	1.953	-2.048	1.664	-1.071	-8.623	-0.591	-5.262
0	1	18	99	99018	6957.948	2245	2.081	-2.206	1.664	-1.071	-8.623	-0.382	-5.262
0	1	18	99	99018	6957.958	2300	2.209	-2.048	1.812	-0.734	-8.401	-0.173	-5.079
0	1	18	99	99018	6957.969	2315	2.209	-2.048	1.812	-0.903	-8.401	0.036	-5.079
0	1	18	99	99018	6957.979	2330	2.209	-2.048	1.664	-0.903	-8.401	-0.382	-5.262
0	1	18	99	99018	6957.990	2345	2.209	-2.048	1.664	-0.734	-8.401	0.036	-5.079

Figure B.34. Measured Data from the Solar Test Bench (Case 7, 01/18/99, Right-fin Shade; Part 1).

15	16	17	18	19	20	21	22	23	24	25	26	27	28
TSP	SVL	APD	TI	TO	Tdb	RH	GHR	Wind	Tdb2	Tdew	Wind2	Tg,r	Tg,l
-4.416	-3.609	0.263	67.230	67.960	65.422	27.581	-99.000	2.668	46.000	41.000	0.000	62.150	62.780
-4.891	-3.609	0.277	66.949	67.623	64.479	28.954	-99.000	3.576	48.000	39.750	1.250	60.260	61.520
-4.654	-3.992	0.281	66.219	67.173	63.536	30.327	-99.000	4.484	50.000	38.500	2.500	59.630	60.260
-5.366	-3.992	0.281	65.206	66.386	62.592	31.700	-99.000	5.391	52.000	37.250	3.750	59.000	60.260
-4.891	-3.992	0.286	64.756	65.824	61.649	33.073	-99.000	6.299	54.000	36.000	5.000	59.000	60.260
-3.941	-3.992	0.282	64.644	65.543	60.998	34.383	-99.000	6.337	53.750	36.250	6.000	58.370	59.630
-4.654	-3.609	0.286	64.194	65.150	60.347	35.693	-99.000	6.374	53.500	36.500	7.000	57.740	59.000
-4.416	-3.992	0.284	63.576	64.700	59.696	37.003	-99.000	6.412	53.250	36.750	8.000	57.100	58.370
-4.416	-3.992	0.291	62.845	64.138	59.045	38.313	-99.000	6.449	53.000	37.000	9.000	56.470	57.740
-3.941	-3.992	0.288	62.283	63.520	58.169	41.223	-99.000	6.988	53.250	37.250	9.500	55.840	57.100
-4.179	-3.609	0.289	61.665	63.014	57.294	44.132	-99.000	7.526	53.500	37.500	10.000	55.200	56.470
-3.941	-3.609	0.295	60.990	62.395	56.418	47.042	-99.000	8.065	53.750	37.750	10.500	54.560	55.840
-3.466	-3.609	0.287	60.484	61.833	55.542	49.951	-99.000	8.603	54.000	38.000	11.000	53.930	55.200
-3.704	-3.609	0.287	59.866	61.271	55.205	50.518	-99.000	8.659	54.000	37.000	10.750	53.290	54.560
-3.466	-3.609	0.282	59.248	60.709	54.868	51.085	-99.000	8.716	54.000	36.000	10.500	53.290	53.930
-2.991	-3.609	0.292	58.910	60.316	54.531	51.651	-99.000	8.772	54.000	35.000	10.250	52.650	53.930
-3.229	-3.609	0.280	58.517	59.922	54.194	52.218	-99.000	8.828	54.000	34.000	10.000	52.000	53.290
-3.466	-3.609	0.280	58.067	59.472	53.925	51.891	-99.000	8.540	53.750	34.000	10.250	52.000	52.650
-3.466	-3.609	0.277	57.617	59.023	53.655	51.563	-99.000	8.252	53.500	34.000	10.500	51.360	52.650
-3.229	-3.609	0.275	57.252	58.629	53.386	51.236	-99.000	7.964	53.250	34.000	10.750	50.710	52.000
-3.466	-3.609	0.277	56.830	58.180	53.116	50.908	-99.000	7.676	53.000	34.000	11.000	50.070	51.360
-3.466	-3.609	0.281	56.353	57.730	52.735	51.525	-99.000	7.507	52.500	33.750	10.250	50.070	51.360
-3.704	-3.609	0.281	55.903	57.308	52.353	52.143	-99.000	7.338	52.000	33.500	9.500	49.420	50.710
-3.466	-3.609	0.282	55.481	56.887	51.972	52.760	-99.000	7.169	51.500	33.250	8.750	49.420	50.070
-3.466	-3.609	0.284	55.200	56.521	51.590	53.377	-99.000	7.000	51.000	33.000	8.000	48.770	50.070
-3.941	-3.226	0.286	54.807	56.156	51.365	53.566	-99.000	6.462	49.750	33.500	8.750	48.770	49.420
-3.941	-3.226	0.281	54.554	55.919	51.141	53.755	-99.000	5.924	48.500	34.000	9.500	48.110	49.420
-4.179	-3.226	0.273	54.301	55.509	50.916	53.944	-99.000	5.385	47.250	34.500	4.250	48.110	48.770
-3.466	-2.843	0.285	54.076	55.256	50.691	54.133	-99.000	4.847	46.000	35.000	3.000	47.460	48.770
-3.704	-2.843	0.288	53.795	54.947	50.601	54.284	-99.000	4.396	45.500	35.000	3.000	47.460	48.110
-1.803	-0.928	0.253	53.514	54.694	50.512	54.435	-99.000	3.946	45.000	35.000	3.000	47.460	48.110
5.323	5.201	0.287	53.317	54.441	50.422	54.586	-99.000	3.495	44.500	35.000	3.000	47.460	48.110
17.200	11.712	0.280	53.149	54.245	50.332	54.737	13.538	3.044	44.000	35.000	3.000	47.460	48.770
48.793	18.224	0.286	53.149	54.160	50.849	53.830	61.938	3.176	46.750	34.500	3.750	48.110	48.770
101.053	23.586	0.284	53.205	54.132	51.365	52.924	110.338	3.307	49.500	34.000	4.500	48.770	49.420
143.336	181.008	0.281	53.401	54.217	51.982	52.017	158.737	3.439	52.250	33.500	5.250	50.710	50.710
186.568	477.467	0.290	53.936	54.526	52.598	51.110	207.137	3.570	55.000	33.000	6.000	52.000	52.000
227.901	536.835	0.286	55.116	55.256	53.543	48.729	259.326	4.058	56.000	32.750	6.500	53.930	53.290
267.133	585.479	0.280	56.606	56.296	54.689	46.349	311.515	4.547	57.000	32.500	7.000	55.840	55.200
307.715	624.930	0.291	58.067	57.393	55.834	43.968	361.704	5.035	58.000	32.250	7.500	57.100	57.100
347.623	655.955	0.290	59.472	58.629	56.979	41.587	415.893	5.523	59.000	32.000	8.000	59.000	59.000
384.679	683.150	0.294	61.271	60.035	58.079	39.471	457.072	5.999	59.750	32.250	8.000	60.890	62.150
415.560	705.748	0.291	62.845	61.327	59.180	37.355	498.252	6.475	60.500	32.500	8.000	62.150	60.560
444.065	724.133	0.291	63.576	62.620	60.280	35.239	539.431	6.950	61.250	32.750	8.000	64.040	64.700
472.095	741.369	0.297	65.037	64.194	61.180	33.123	580.610	7.426	62.000	33.000	8.000	65.930	71.570
495.850	754.775	0.291	66.780	66.105	62.256	31.851	607.062	7.332	62.750	32.750	7.000	68.440	74.100
515.328	765.882	0.295	67.623	67.679	63.132	30.579	633.514	7.238	63.500	32.500	6.000	72.810	76.660
531.481	772.777	0.302	69.141	69.703	64.007	29.306	659.966	7.144	64.250	32.250	5.000	77.470	77.470
540.983	777.756	0.301	70.602	71.727	64.883	28.034	686.418	7.050	65.000	32.000	4.000	81.830	80.540
549.534	779.288	0.300	71.839	73.694	65.849	27.077	695.569	6.811	66.000	32.000	4.250	83.130	81.190
555.235	779.288	0.301	73.132	75.493	66.914	26.120	704.720	6.573	67.000	32.000	4.500	85.100	82.480
558.086	776.990	0.295	74.144	76.954	67.780	25.162	713.871	6.834	68.000	32.000	4.750	87.100	84.450
555.235	772.777	0.294	75.099	78.303	68.745	24.205	723.022	6.095	69.000	32.000	5.000	89.120	86.410
548.584	766.648	0.304	75.943	79.428	69.194	23.525	714.157	6.158	69.250	32.000	5.000	89.790	87.100
537.182	754.775	0.295	76.673	80.440	69.644	22.845	705.292	6.221	69.500	32.000	5.000	88.440	85.770
523.880	744.433	0.291	77.067	81.114	70.093	22.165	696.427	6.283	69.750	32.000	5.000	90.470	87.100
505.826	726.814	0.290	77.629	81.732	70.542	21.485	687.562	6.346	-99.000	-99.000	-99.000	92.530	88.440
488.295	683.533	0.291	78.247	82.351	70.789	21.397	657.679	6.240	-99.000	-99.000	-99.000	92.530	88.440
456.117	668.978	0.295	78.753	82.857	71.036	21.309	627.795	6.133	-99.000	-99.000	-99.000	92.530	87.770
427.437	643.315	0.294	79.147	83.250	71.283	21.220	597.912	6.027	-99.000	-99.000	-99.000	93.920	89.120
389.905	608.843	0.285	79.315	83.419	71.530	21.132	568.028	5.920	-99.000	-99.000	-99.000	93.220	88.440
352.849	574.371	0.285	79.540	83.644	71.822	21.397	531.424	5.282	-99.000	-99.000	-99.000	93.220	87.770
340.496	581.649	0.282	79.877	83.868	72.114	21.661	494.821	4.643	-99.000	-99.000	-99.000	94.610	87.770
300.114	541.815	0.288	80.046	84.037	72.405	21.926	458.217	4.005	-99.000	-99.000	-99.000	91.160	86.430
260.682	502.746	0.278	79.709	83.700	72.697	22.190	421.613	3.366	72.000	34.000	4.000	86.430	83.130
224.100	464.444	0.275	78.866	82.800	72.585	22.732	373.285	3.673	71.500	34.250	4.000	84.450	83.130
184.668	419.631	0.276	78.585	82.238	72.473	23.274	324.956	3.980	71.000	34.500	4.000	86.430	83.790
145.711	374.817	0.260	78.135	81.676	72.360	23.815	276.628	2.286	70.500	34.750	4.000	85.100	83.130
106.279	277.146	0.258	77.404	81.058	72.248	24.357	228.299	2.593	70.000	35.000	4.000	83.130	80.540
66.372	35.076	0.270	76.786	80.327	71.777	25.113	180.042	2.512	68.250	35.750	3.750	80.540	77.970
16.250	22.020	0.271	76.055	79.371	71.305	25.868	131.785	2.431	66.500	36.500	3.500	73.470	74.100
6.036	10.180	0.268	75.156	78.135	70.834	26.624	83.528	2.349	64.750	37.250	3.250	70.320	70.950
-2.278	0.988	0.271	74.088	76.673	70.362	27.379	-99.000	2.268	63.000	38.000	3.000	68.440	69.700
-6.792	-3.226	0.268	73.076	75.437	69.666	28.299	-99.000	2.043	60.500	39.750	2.250	67.820	69.070
-7.504	-3.609	0.270	72.289	74.481	68.970	29.218	-99.000	1.817	58.000	41.500	1.500	67.190	67.820
-6.792	-3.609	0.266	71.558	73.582	68.274	30.138	-99.000	1.592	55.500	43.250	0.750	66.560	67.820
-4.654	-3.609	0.267	71.052	72.907	67.578	31.057	-99.000	1.366	53.000	45.000	0.000	65.930	67.190
-4.654	-3.609	0.270	70.602	72.289	67.309	31.624	-99.000	2.042	52.500	44.250	0.000	65.300	66.560
-4.416	-3.609	0.274	70.096	71.670	67.039	32.191	-99.000	2.718	52.000	43.500	0.000	64.670	65.930
-4.179	-3.609	0.280	69.591	71.108	66.770	32.758	-99.000	3.394	51.500	42.750	0.000	64.040	65.300
-4.416	-3.609	0.265	68.804	70.490	66.500	33.325	-99.000	4.070	51.000	42.000	0.000	63.410	64.670
-4.416	-3.609	0.274	68.354	69.928	66.163	34.408	-99.000	4.177	50.500	42.000	0.000	64.040	64.670
-3.466	-3.609	0.285	68.073	69.478	65.826	35.492	-99.000	4.283	50.000	42.000	0.000	64.040	64.670
-2.991	-3.609	0.286	68.017	69.197	65.489	36.575	-99.000	4.390	49.500	42.000	0.000	63.410	64.040
-3.229	-3.609	0.285	67.679	68.916	65.152	37.658	-99.000	4.496	49.000	42.000	0.000	62.780	63.410
-3.229	-3.609	0.283	67.230	68.523	64.591	39.774	-99.000	5.191	49.000	42.750	0.000	62.150	62.780
-3.941	-3.609	0.278	66.780	68.073	64.030	41.890	-99.000	5.886	49.000	43.500	0.000	61.520	62.150
-3.704	-3.609	0.277	66.386	67.623	63.468	44.006	-99.000	6.580	49.000	44.250	0.000	61.520	62.150
-3.229	-3.609	0.281	66.162	67.286	62.907	46.122	-99.000	7.275	49.000	45.000	0.000	60.890	61.520
-3.229	-3.609	0.286	65.712	66.949	62.323	48.414	-99.000	6.943	50.500	44.250	0.000	60.260	60.890
-3.466	-3.609	0.284	65.037	66.386	61.740	50.707	-99.000	6.612	52.000	43.500	0.000	59.630	60.260
-3.466	-3.609	0.295	64.475	65.881	61.156	52.999	-99.000	6.280	53.500	42.750	0.000	59.000	59.630
-3.229	-3.226	0.288	64.026	65.431	60.572	55.291	-99.000	5.948	55.000	42.000	0.000	58.370	59.000
-2.991	-3.226	0.294	63.520	64.925	60.033	56.009	-99.000	5.879	54.500	42.250	1.000	57.740	59.000
-2.991	-3.609	0.297	63.126	64.475	59.494	56.727	-99.000	5.811	54.000	42.500	2.000	57.740	58.370
-2.516	-3.609	0.286	62.620	64.082	58.955	57.445	-99.000	5.742	53.500	42.750	3.000	57.100	57.740

Figure B.35. Measured Data from the Solar Test Bench (Case 7, 01/18/99, Right-fin Shade; Part 2).

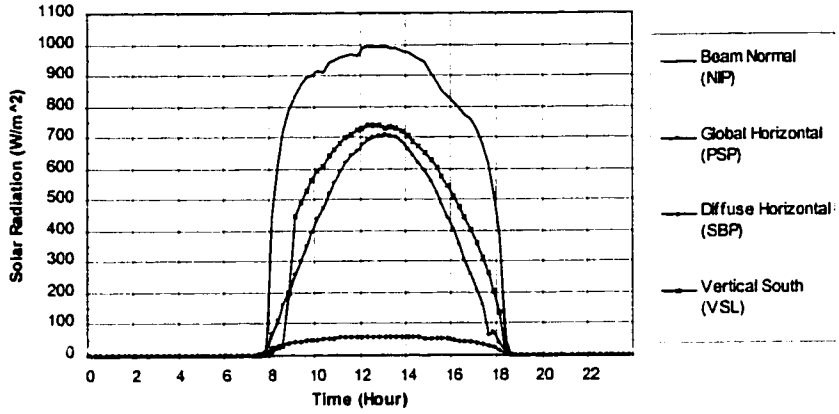

Figure B.36. Measured Beam Normal, Global Horizontal, Diffuse Horizontal and Vertical South Solar Radiation (Case 8, 02/12/99, Overhang and Side Fin Shades).

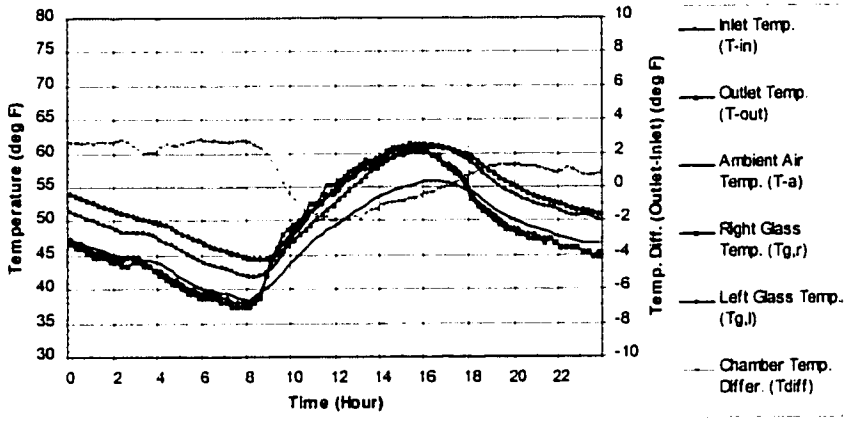

Figure B.37. Measured Chamber Inlet and Outlet Temperature and Outside Air Temperature (Case 8, 02/12/99, Overhang and Side Fin Shades).

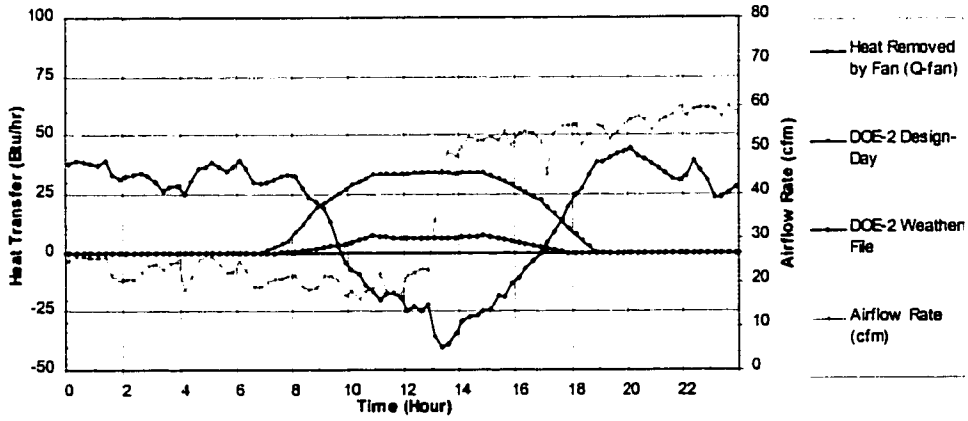

Figure B.38. Heat Transfer of the Experimental Box and Calculated Airflow Rate (Case 8, 02/12/99, Overhang and Side Fin Shades).

1	2	3	4	5	6	7	8	9	10	11	12	13	14
Site	Month	Day	Year	Julian	Decimal	Hour	ELI	SLI	WLI	LIH	NIP	PSP	SBP
0	2	12	99	99043	6982.000	0	2.593	-2.364	1.369	-1.071	-8.180	0.245	-4.533
0	2	12	99	99043	6982.010	15	2.337	-1.732	1.517	-1.240	-7.958	0.245	-4.533
0	2	12	99	99043	6982.021	30	2.081	-0.943	2.107	-1.408	-7.958	0.036	-4.533
0	2	12	99	99043	6982.031	45	2.081	-0.785	2.107	-1.408	-7.958	-0.173	-4.533
0	2	12	99	99043	6982.042	100	2.081	-0.785	2.107	-1.408	-7.736	-0.382	-4.533
0	2	12	99	99043	6982.052	115	2.081	-0.785	2.107	-1.408	-7.736	-0.591	-4.533
0	2	12	99	99043	6982.063	130	2.081	-0.785	2.107	-1.408	-7.736	0.036	-4.533
0	2	12	99	99043	6982.073	145	2.081	-0.943	2.107	-1.408	-7.736	0.036	-4.533
0	2	12	99	99043	6982.083	200	2.081	-0.785	2.107	-1.408	-7.736	-0.382	-4.533
0	2	12	99	99043	6982.094	215	2.081	-0.943	1.959	-1.408	-7.736	-0.382	-4.533
0	2	12	99	99043	6982.104	230	2.081	-0.943	2.107	-1.408	-7.515	-0.173	-4.351
0	2	12	99	99043	6982.115	245	2.081	-0.943	1.959	-1.408	-7.515	0.245	-4.351
0	2	12	99	99043	6982.125	300	2.081	-0.943	1.959	-1.408	-7.515	0.454	-4.351
0	2	12	99	99043	6982.135	315	2.081	-0.943	1.959	-1.408	-7.736	0.663	-4.533
0	2	12	99	99043	6982.146	330	2.081	-0.943	1.959	-1.408	-7.736	0.036	-4.533
0	2	12	99	99043	6982.156	345	2.081	-0.943	1.959	-1.408	-7.736	0.036	-4.533
0	2	12	99	99043	6982.167	400	2.081	-0.943	1.959	-1.408	-7.958	-0.173	-4.533
0	2	12	99	99043	6982.177	415	2.081	-0.943	1.959	-1.408	-7.736	-0.173	-4.351
0	2	12	99	99043	6982.188	430	2.209	-0.943	1.959	-1.408	-7.736	-0.173	-4.533
0	2	12	99	99043	6982.198	445	2.209	-0.943	1.959	-1.408	-7.736	-0.382	-4.351
0	2	12	99	99043	6982.208	500	2.209	-1.101	1.959	-1.408	-7.736	-0.173	-4.351
0	2	12	99	99043	6982.219	515	2.209	-0.943	1.959	-1.408	-7.736	-0.173	-4.351
0	2	12	99	99043	6982.229	530	2.209	-1.101	1.959	-1.408	-7.736	-0.173	-4.351
0	2	12	99	99043	6982.240	545	2.209	-1.101	1.959	-1.408	-7.515	-0.382	-4.533
0	2	12	99	99043	6982.250	600	2.209	-1.101	1.959	-1.408	-7.736	-0.173	-4.533
0	2	12	99	99043	6982.260	615	2.081	-1.890	1.222	-1.576	-7.515	-0.382	-4.533
0	2	12	99	99043	6982.271	630	2.081	-1.890	1.222	-1.576	-7.515	-0.173	-4.533
0	2	12	99	99043	6982.281	645	2.081	-1.732	1.222	-1.408	-7.515	-0.173	-4.533
0	2	12	99	99043	6982.292	700	2.337	-1.890	1.222	-1.240	-7.736	0.036	-4.351
0	2	12	99	99043	6982.302	715	4.003	-1.101	1.812	-0.061	-8.180	1.290	-3.440
0	2	12	99	99043	6982.313	730	8.874	2.531	4.910	2.971	-8.180	5.680	0.567
0	2	12	99	99043	6982.323	745	28.869	15.479	13.321	12.235	33.059	19.058	9.310
0	2	12	99	99043	6982.333	800	481.830	211.910	29.846	90.389	448.995	69.224	23.882
0	2	12	99	99043	6982.344	815	642.814	310.441	36.929	145.973	616.168	114.374	30.440
0	2	12	99	99043	6982.354	830	736.636	388.129	40.470	193.135	715.496	158.269	35.175
0	2	12	99	99043	6982.365	845	809.438	460.765	42.831	240.633	786.445	206.763	39.183
0	2	12	99	99043	6982.375	900	868.910	529.610	44.011	287.795	837.883	257.348	42.097
0	2	12	99	99043	6982.385	915	910.950	592.771	45.192	332.936	869.809	301.662	45.011
0	2	12	99	99043	6982.396	930	944.788	652.143	44.668	376.729	893.755	350.574	47.197
0	2	12	99	99043	6982.406	945	964.270	708.988	130.476	419.175	902.623	394.469	49.181
0	2	12	99	99043	6982.417	1000	987.854	762.675	207.202	458.252	916.813	438.783	50.840
0	2	12	99	99043	6982.427	1015	983.752	798.677	260.320	486.549	907.344	473.899	52.297
0	2	12	99	99043	6982.438	1030	1014.514	862.469	324.062	530.342	944.305	522.394	53.026
0	2	12	99	99043	6982.448	1045	1012.463	902.892	383.671	559.113	950.513	555.002	54.847
0	2	12	99	99043	6982.458	1100	1009.387	940.789	443.281	586.262	956.721	587.610	57.033
0	2	12	99	99043	6982.469	1115	1007.336	976.159	502.894	611.865	965.590	619.382	58.855
0	2	12	99	99043	6982.479	1130	998.107	1003.950	558.963	631.403	968.251	641.121	59.219
0	2	12	99	99043	6982.490	1145	979.651	1027.951	614.442	648.920	962.930	657.843	59.219
0	2	12	99	99043	6982.500	1200	963.245	1048.163	668.150	664.416	986.875	675.401	59.219
0	2	12	99	99043	6982.510	1215	939.661	1062.058	717.727	675.196	992.196	692.123	60.312
0	2	12	99	99043	6982.521	1230	907.874	1068.374	762.582	680.586	991.309	701.320	60.676
0	2	12	99	99043	6982.531	1245	876.087	1073.427	806.257	682.607	993.083	708.009	60.676
0	2	12	99	99043	6982.542	1300	836.098	1074.690	845.211	681.934	992.196	710.518	60.676
0	2	12	99	99043	6982.552	1315	792.519	1070.901	880.033	675.196	986.875	707.173	59.948
0	2	12	99	99043	6982.563	1330	749.453	1069.638	915.445	669.132	988.648	702.993	59.219
0	2	12	99	99043	6982.573	1345	700.235	1055.742	940.233	654.984	978.893	685.414	58.490
0	2	12	99	99043	6982.583	1400	649.479	1039.320	961.481	638.140	972.685	662.859	57.762
0	2	12	99	99043	6982.594	1415	594.109	1016.582	976.826	617.928	962.930	640.285	57.033
0	2	12	99	99043	6982.604	1430	537.200	988.791	987.450	593.673	952.287	619.382	56.669
0	2	12	99	99043	6982.615	1445	478.753	958.474	995.712	568.071	943.419	594.299	54.847
0	2	12	99	99043	6982.625	1500	418.769	920.577	994.532	537.079	907.057	560.018	54.847
0	2	12	99	99043	6982.635	1515	356.733	877.628	989.810	503.392	876.017	523.230	54.119
0	2	12	99	99043	6982.646	1530	294.698	827.731	976.826	467.010	853.846	485.605	54.119
0	2	12	99	99043	6982.656	1545	235.995	774.675	959.120	427.260	829.001	444.636	51.933
0	2	12	99	99043	6982.667	1600	176.780	720.357	935.512	386.161	814.424	405.757	49.747
0	2	12	99	99043	6982.677	1615	102.952	662.249	904.821	342.368	794.427	356.008	46.104
0	2	12	99	99043	6982.688	1630	50.402	602.245	869.999	297.901	774.916	307.514	44.647
0	2	12	99	99043	6982.698	1645	41.173	539.084	825.734	253.098	757.178	258.184	41.733
0	2	12	99	99043	6982.708	1700	40.148	471.502	771.435	207.293	723.478	208.018	38.818
0	2	12	99	99043	6982.719	1715	38.866	398.867	702.382	162.816	676.474	158.269	33.719
0	2	12	99	99043	6982.729	1730	36.815	322.126	617.983	117.339	611.734	61.291	28.982
0	2	12	99	99043	6982.740	1745	34.765	242.543	513.517	64.450	523.935	71.314	23.518
0	2	12	99	99043	6982.750	1800	29.381	155.065	367.737	26.384	389.133	36.616	16.232
0	2	12	99	99043	6982.760	1815	12.206	22.111	50.208	6.845	41.928	7.979	4.192
0	2	12	99	99043	6982.771	1830	4.388	0.794	5.206	0.782	-8.180	0.036	-2.711
0	2	12	99	99043	6982.781	1845	2.593	-1.575	2.107	-0.903	-8.180	-1.636	-4.533
0	2	12	99	99043	6982.792	1900	2.465	-1.732	1.812	-0.903	-8.180	-1.636	-4.715
0	2	12	99	99043	6982.802	1915	2.465	-1.890	1.812	-0.734	-7.958	-2.054	-4.533
0	2	12	99	99043	6982.813	1930	2.465	-1.890	1.812	-0.903	-7.958	-1.845	-4.533
0	2	12	99	99043	6982.823	1945	2.465	-1.890	1.812	-0.903	-7.736	-1.427	-4.533
0	2	12	99	99043	6982.833	2000	2.593	-1.732	1.959	-0.734	-7.736	-1.845	-4.351
0	2	12	99	99043	6982.844	2015	2.593	-1.890	1.812	-0.903	-7.736	-1.636	-4.533
0	2	12	99	99043	6982.854	2030	2.593	-1.890	1.812	-0.566	-7.736	-1.845	-4.533
0	2	12	99	99043	6982.865	2045	2.593	-1.890	1.812	-0.734	-7.515	-1.636	-4.533
0	2	12	99	99043	6982.875	2100	2.593	-1.890	1.812	-0.734	-7.736	-2.681	-4.533
0	2	12	99	99043	6982.885	2115	2.593	-1.890	1.812	-0.566	-7.515	-2.263	-4.351
0	2	12	99	99043	6982.896	2130	2.593	-1.732	1.812	-0.734	-7.515	-1.845	-4.351
0	2	12	99	99043	6982.906	2145	2.593	-1.890	1.812	-0.734	-7.071	-1.636	-4.533
0	2	12	99	99043	6982.917	2200	2.722	-1.890	1.812	-0.566	-7.293	-1.636	-4.533
0	2	12	99	99043	6982.927	2215	2.593	-1.732	1.812	-0.734	-7.293	-1.845	-4.715
0	2	12	99	99043	6982.938	2230	2.593	-1.732	1.812	-0.734	-7.293	-1.845	-4.715
0	2	12	99	99043	6982.948	2245	2.465	-1.732	1.664	-0.903	-7.071	-1.218	-4.533
0	2	12	99	99043	6982.958	2300	2.593	-1.575	1.812	-0.903	-7.071	-1.427	-4.351
0	2	12	99	99043	6982.969	2315	2.593	-1.575	1.812	-0.903	-7.293	-1.009	-4.169
0	2	12	99	99043	6982.979	2330	2.593	-1.732	1.812	-0.903	-7.293	-1.009	-4.169
0	2	12	99	99043	6982.990	2345	2.593	-1.732	1.812	-0.903	-7.293	-1.427	-4.169

Figure B.39. Measured Data from the Solar Test Bench (Case 8, 02/12/99, Overhang and Side Fin Shades; Part 1).

15	16	17	18	19	20	21	22	23	24	25	26	27	28
TSP	SVL	APD	TI	TO	Tdb	RH	GHR	Wind	Tdb2	Tdew	Wind2	Tg,r	Tg,l
-0.378	-2.843	0.038	51.406	54.104	47.278	48.238	-99.000	12.509	47.000	29.000	12.000	46.800	47.460
-0.853	-3.226	0.041	51.069	53.739	46.986	48.956	-99.000	11.676	46.500	29.000	11.250	46.140	46.800
-1.091	-3.226	0.042	50.760	53.373	46.694	49.674	-99.000	10.844	46.000	29.000	10.500	46.140	46.800
-1.328	-3.226	0.040	50.422	53.064	46.402	50.392	-99.000	10.011	45.500	29.000	9.750	45.480	46.140
-1.328	-3.226	0.040	50.141	52.727	46.110	51.110	-99.000	9.178	45.000	29.000	9.000	44.810	45.480
-1.566	-3.226	0.041	49.720	52.390	45.818	51.815	-99.000	9.272	44.750	29.000	9.000	44.810	45.480
-1.328	-3.226	0.029	49.354	52.052	45.527	52.521	-99.000	9.366	44.500	29.000	9.000	44.810	45.480
-1.091	-3.226	0.026	49.129	51.828	45.235	53.226	-99.000	9.460	44.250	29.000	9.000	44.140	44.810
-1.328	-3.226	0.027	48.736	51.518	44.943	53.931	-99.000	9.554	-99.000	-99.000	-99.000	44.140	44.810
-1.566	-3.226	0.027	48.371	51.209	44.831	53.150	-99.000	9.961	-99.000	-99.000	-99.000	43.470	44.140
-1.328	-3.226	0.031	48.202	50.900	44.719	52.369	-99.000	10.368	-99.000	-99.000	-99.000	43.470	44.810
-0.853	-3.226	0.035	48.258	50.703	44.606	51.588	-99.000	10.775	-99.000	-99.000	-99.000	44.140	44.810
-0.378	-3.226	0.036	48.314	50.507	44.494	50.807	-99.000	11.182	-99.000	-99.000	-99.000	44.140	44.810
-0.140	-3.226	0.032	48.314	50.338	44.337	50.681	-99.000	11.007	-99.000	-99.000	-99.000	43.470	44.140
-0.616	-3.226	0.036	48.089	50.169	44.180	50.556	-99.000	10.831	-99.000	-99.000	-99.000	43.470	43.470
-1.091	-3.226	0.038	47.836	49.888	44.022	50.430	-99.000	10.656	-99.000	-99.000	-99.000	42.800	42.800
-1.566	-3.226	0.021	47.246	49.663	43.865	50.304	-99.000	10.480	-99.000	-99.000	-99.000	42.120	42.800
-1.803	-3.226	0.028	46.797	49.354	43.281	52.307	-99.000	10.117	-99.000	-99.000	-99.000	41.440	42.120
-1.803	-3.226	0.039	46.431	48.933	42.698	54.309	-99.000	9.754	-99.000	-99.000	-99.000	40.760	41.440
-2.041	-2.843	0.041	46.010	48.511	42.114	56.312	-99.000	9.391	-99.000	-99.000	-99.000	40.760	41.440
-2.041	-2.843	0.041	45.560	48.174	41.530	58.314	-99.000	9.028	-99.000	-99.000	-99.000	40.080	40.760
-2.041	-2.843	0.036	45.110	47.780	41.126	59.612	-99.000	8.690	-99.000	-99.000	-99.000	39.390	40.080
-2.041	-2.843	0.030	44.689	47.443	40.722	60.909	-99.000	8.352	-99.000	-99.000	-99.000	39.390	40.080
-2.278	-2.843	0.031	44.239	47.106	40.317	62.207	-99.000	8.014	-99.000	-99.000	-99.000	38.700	39.390
-2.041	-2.843	0.037	43.930	46.740	39.913	63.504	-99.000	7.676	-99.000	-99.000	-99.000	38.700	39.390
-2.041	-2.843	0.032	43.592	46.375	39.756	62.433	-99.000	8.052	-99.000	-99.000	-99.000	38.700	39.390
-1.566	-2.843	0.023	43.368	46.150	39.599	61.363	-99.000	8.427	-99.000	-99.000	-99.000	38.700	39.390
-1.328	-2.843	0.023	43.227	45.925	39.441	60.292	-99.000	8.803	-99.000	-99.000	-99.000	38.000	38.700
-1.091	-2.843	0.025	43.058	45.729	39.284	59.221	-99.000	9.178	-99.000	-99.000	-99.000	38.000	38.700
-0.140	-2.077	0.027	42.777	45.419	39.048	59.511	-99.000	8.559	-99.000	-99.000	-99.000	37.300	38.000
3.185	0.604	0.027	42.384	45.138	38.813	59.801	-99.000	7.939	-99.000	-99.000	-99.000	37.300	38.000
9.836	5.967	0.029	42.075	44.801	38.577	60.090	-99.000	7.320	-99.000	-99.000	-99.000	37.300	38.000
20.763	16.691	0.029	41.878	44.548	38.341	60.380	16.129	6.700	-99.000	-99.000	-99.000	37.300	38.000
50.694	22.054	0.023	41.934	44.436	38.947	58.214	100.043	6.919	-99.000	-99.000	-99.000	38.000	38.700
93.452	29.331	0.021	42.131	44.436	39.554	56.047	163.957	7.138	-99.000	-99.000	-99.000	38.700	39.390
133.359	200.159	0.022	42.466	44.492	40.160	53.881	227.870	7.357	-99.000	-99.000	-99.000	42.120	42.120
176.117	449.123	0.029	43.087	44.661	40.766	51.714	291.784	7.576	-99.000	-99.000	-99.000	44.810	44.140
219.824	493.554	0.029	43.986	45.382	41.653	48.868	347.405	7.964	-99.000	-99.000	-99.000	46.140	45.480
266.383	532.239	0.026	45.191	45.700	42.540	46.021	403.025	8.352	-99.000	-99.000	-99.000	48.110	46.900
310.566	565.945	0.018	46.937	46.544	43.427	43.175	458.646	8.740	-99.000	-99.000	-99.000	48.770	47.460
351.898	594.672	0.020	48.005	47.274	44.314	40.328	514.266	9.128	-99.000	-99.000	-99.000	49.420	48.770
379.453	609.609	0.017	48.989	48.005	45.145	37.759	557.733	9.404	-99.000	-99.000	-99.000	50.070	49.420
421.261	644.847	0.020	50.113	48.736	45.976	35.189	601.200	9.679	-99.000	-99.000	-99.000	51.360	50.710
454.642	663.616	0.021	51.069	49.523	46.806	32.620	644.667	9.955	-99.000	-99.000	-99.000	52.650	51.360
478.747	680.469	0.030	51.996	50.366	47.637	30.050	688.134	10.230	-99.000	-99.000	-99.000	52.650	52.000
505.826	698.471	0.020	52.811	51.069	48.154	28.879	717.589	10.368	-99.000	-99.000	-99.000	53.930	52.650
524.830	711.493	0.019	53.345	51.631	48.670	27.707	747.043	10.506	-99.000	-99.000	-99.000	55.200	53.930
549.534	722.984	0.019	54.357	52.390	49.187	26.536	776.498	10.643	-99.000	-99.000	-99.000	55.200	53.930
563.787	732.177	0.029	55.116	53.120	49.703	25.364	805.952	10.781	52.000	18.000	13.000	55.840	54.560
577.089	737.539	0.030	55.622	53.795	50.242	24.766	817.391	10.612	52.250	18.250	12.000	56.470	55.840
580.890	739.454	0.033	56.181	54.498	50.781	24.168	828.830	10.443	52.500	18.500	11.000	57.210	56.950
582.790	740.603	0.032	56.859	55.144	51.320	23.569	840.268	10.274	52.750	18.750	10.000	57.740	56.470
573.289	729.112	0.071	57.674	55.819	51.859	22.971	851.707	10.105	53.000	19.000	9.000	58.370	57.740
574.239	735.241	0.127	58.180	56.634	52.376	21.749	844.844	10.268	53.500	18.500	9.500	59.000	57.740
567.588	731.027	0.148	58.798	57.421	52.892	20.528	837.981	10.431	54.000	18.000	10.000	58.370	57.740
553.335	718.771	0.143	59.248	58.011	53.409	19.306	831.117	10.593	54.500	17.500	10.500	59.000	58.370
538.132	705.365	0.154	59.472	58.461	53.925	18.084	824.254	10.756	55.000	17.000	11.000	59.000	59.000
521.979	688.512	0.169	59.810	58.910	54.217	17.568	799.089	10.719	55.500	16.500	11.250	60.260	59.630
495.850	670.127	0.164	60.259	59.360	54.509	17.051	773.924	10.681	56.000	16.000	11.500	60.890	60.260
473.996	650.976	0.164	60.653	59.810	54.800	16.535	748.758	10.644	56.500	15.500	11.750	60.890	60.260
445.015	626.462	0.170	60.990	60.203	55.092	16.018	723.593	10.606	57.000	15.000	12.000	60.260	59.630
396.557	601.566	0.163	61.046	60.428	55.317	15.710	682.128	10.581	57.000	15.000	12.500	61.520	60.890
368.051	573.222	0.176	61.327	60.709	55.542	15.401	640.663	10.556	57.000	15.000	13.000	60.260	60.260
338.121	542.964	0.157	61.327	60.878	55.766	15.093	599.198	10.530	57.000	15.000	13.500	60.260	60.260
298.214	510.790	0.175	61.327	60.990	55.991	14.784	557.733	10.505	57.000	15.000	14.000	60.260	60.260
253.081	476.318	0.176	61.271	61.046	55.901	15.049	504.543	10.524	56.750	15.000	12.500	59.630	59.630
211.273	440.697	0.174	61.103	60.990	55.811	15.313	451.353	10.543	56.500	15.000	11.000	59.000	59.630
168.990	402.012	0.163	60.878	60.878	55.721	15.578	398.163	10.562	56.250	15.000	9.500	58.370	58.370
125.757	359.113	0.120	60.540	60.709	55.631	15.842	344.973	10.581	56.000	15.000	8.000	57.740	58.370
88.701	310.086	0.174	60.147	60.428	55.294	16.944	296.993	10.349	55.250	15.750	7.750	57.100	57.740
39.292	262.209	0.184	59.697	60.147	54.958	18.046	229.014	10.118	54.500	16.500	7.500	56.470	57.100
16.963	206.287	0.185	59.191	59.810	54.621	19.148	171.034	9.886	53.750	17.250	7.250	55.200	55.840
10.311	135.811	0.187	58.573	59.360	54.284	20.250	-99.000	9.654	53.000	18.000	7.000	53.290	53.930
1.997	11.712	0.156	57.842	58.798	53.633	21.541	-99.000	8.890	51.750	18.500	6.250	52.000	52.650
-2.991	-2.077	0.171	57.027	58.123	52.982	22.833	-99.000	8.127	50.500	19.000	5.500	51.360	52.000
-3.941	-3.609	0.186	56.353	57.561	52.330	24.124	-99.000	7.363	49.250	19.500	4.750	50.710	51.360
-3.466	-3.609	0.182	55.706	56.943	51.679	25.415	-99.000	6.599	48.000	20.000	4.000	50.070	50.710
-3.229	-3.609	0.165	55.088	56.437	51.208	26.120	-99.000	5.942	46.750	21.750	3.000	49.420	50.070
-2.753	-3.609	0.177	54.498	55.875	50.736	26.826	-99.000	5.285	45.500	23.500	2.000	48.770	49.420
-2.278	-3.609	0.188	54.020	55.369	50.265	27.531	-99.000	4.627	44.250	25.250	1.000	48.770	48.770
-1.803	-3.226	0.194	53.570	54.947	49.793	28.236	-99.000	3.970	43.000	27.000	0.000	48.110	48.770
-1.566	-3.226	0.198	53.233	54.498	49.546	28.438	-99.000	3.920	41.500	27.250	0.000	48.110	48.110
-1.091	-3.226	0.194	52.896	54.132	49.299	28.639	-99.000	3.870	40.000	27.500	0.000	47.460	48.110
-1.091	-3.226	0.179	52.530	53.739	49.052	28.841	-99.000	3.820	38.500	27.750	0.000	47.460	48.110
-1.091	-3.226	0.191	52.277	53.401	48.805	29.042	-99.000	3.770	37.000	28.000	0.000	47.460	47.460
-1.566	-3.226	0.197	52.109	53.149	48.513	29.647	-99.000	3.902	36.750	28.750	0.000	46.800	47.460
-1.091	-3.226	0.201	51.996	52.952	48.221	30.251	-99.000	4.033	36.500	29.500	0.000	47.460	47.460
-1.091	-3.226	0.213	51.856	52.755	47.929	30.856	-99.000	4.165	36.250	30.250	0.000	46.800	46.800
-0.140	-2.843	0.202	51.490	52.474	47.637	31.460	-99.000	4.296	36.000	31.000	0.000	46.140	46.140
-0.378	-2.843	0.210	50.928	52.081	47.435	32.027	-99.000	4.396	35.750	30.750	0.000	46.140	46.140
-0.616	-2.843	0.214	50.760	51.799	47.233	32.594	-99.000	4.496	35.500	30.500	0.000	46.140	46.140
-0.616	-3.226	0.214	50.675	51.575	47.031	33.161	-99.000	4.596	35.250	30.250	0.000	46.140	46.140
-0.140	-3.226	0.211	50.872	51.575	46.829	33.728	-99.000	4.696	35.000	30.000	0.000	45.480	45.480
-0.140	-3.226	0.198	50.731	51.462	46.784	33.237	-99.000	4.308	34.500	30.250	0.000	45.480	45.480
0.572	-2.843	0.215	50.507	51.265	46.739	32.746	-99.000	3.920	34.000	30.500	0.000	44.810	44.810
0.572	-3.226	0.206	50.141	50.984	46.694	32.254	-99.000	3.532	33.500	30.750	0.000	44.810	45.480

Figure B.40. Measured Data from the Solar Test Bench (Case 8, 02/12/99, Overhang and Side Fin Shades; Part 2).

APPENDIX C

DOE-2 SIMULATION

Total of 16 DOE-2 simulations (i.e., 8 simulations using a packed weather file and 8 simulations using the DESIGN-DAY instructions) were conducted for the comparative validation of the proposed computer model. Section 4.5 describes the comparative validation using the DOE-2 program. The Appendix C.1 shows an example of the DOE-2 input file for a simulation using the DESIGN-DAY instructions. Appendix C.2 shows DOE-2 hourly-reports that were created by the DOE-2 simulation. Five different levels of hourly-reports were created for each siumlation including two reports for global variables, a report for the heat transfer of the main room, for variables of the front wall, and for variables of the main window.

C.1 DOE-2 Input File

```
$ ***************************************************************************
$       INPUT FILE FOR THE DOE-2 SIMULATION TO COMPARE WITH THE PROGRAM 'S.F.D.'
$ ***************************************************************************
$                                                                BY JOHN KIE-WHAN OH
$ ***************************************************************************
TITLE LINE-1 'DOE2 SIMULATION FOR S.F.D.'
        LINE-2 'BY JOHN KIE-WHAN OH'
        LINE-3 'INPUT UPDATE: 09/01/99'  ..

ABORT WARNINGS  ..
DIAGNOSTIC COMMENTS, NARROW, NO-ECHO  ..
RUN-PERIOD  MAR 22 1999  THRU  MAR 22 1999  ..


$ ***************************************************************************
$       LOADS INPUT INSTRUCTIONS
$ ***************************************************************************
INPUT LOADS  ..

$ ***************************************************************************
$       DESIGN DAYS
$ ***************************************************************************
        CASE2-DAY = DESIGN-DAY
                DRYBULB-HI = 55.991
                DRYBULB-LO = 38.341
                HOUR-HI = 16
                HOUR-LO = 8
                DEWPT-HI = 31.
                DEWPT-LO = 15.
                DHOUR-HI = 22
                DHOUR-LO = 16
                WIND-SPEED = 6.74
                WIND-DIR = 15
                CLOUD-AMOUNT = 0          $ *** 0 TO 10 (0:CLEAR DAY)
                CLEARNESS = 1.
                GROUND-T = 50.
                CLOUD-TYPE = 2  ..        $ *** 0 TO 2
                                          $(0:SUMMER, 1:WINTER, 2:FALL & SPRING)


$ ***************************************************************************
$       BUILDING DESCRIPTION
$ ***************************************************************************
        BUILDING-LOCATION
                LATITUDE = 30.6
                LONGITUDE = 96.4
                ALTITUDE = 0     $ *** NOT TO ADJUST 'AIR FLOW RATES' FOR ALTITUDE
                TIME-ZONE = 6
                DAYLIGHT-SAVINGS = YES
```

```
                AZIMUTH = 0  ..

$ ***************************************************************************
$       BUILDING SHADE
$ ***************************************************************************
        EX-WALL1 = BUILDING-SHADE
                HEIGHT = 15.3
                WIDTH = 20.3
                TRANSMITTANCE = 0.0
                X = 41.2
                Y = 2.9
                Z = 0.0
                AZIMUTH = -37.13
                TILT = 90  ..

        EX-WALL2 = BUILDING-SHADE
                HEIGHT = 15.3
                WIDTH = 41.3
                TRANSMITTANCE = 0.0
                X = 24.9
                Y = -9.3
                Z = 0.0
                AZIMUTH = -127.13
                TILT = 90  ..

        EX-WALL3 = BUILDING-SHADE
                HEIGHT = 121.0
                WIDTH = 150.0
                TRANSMITTANCE = 0.0
                X = 115.2
                Y = -302.8
                Z = 0.0
                AZIMUTH = -37.13
                TILT = 90  ..


$ ***************************************************************************
$       SCHEDULES
$ ***************************************************************************
        DS1 = DAY-SCHEDULE  HOURS = (1,24)  VALUES = (1.)  ..
        WS1 = WEEK-SCHEDULE  DAYS = (ALL)  DAY-SCHEDULE = DS1  ..
        S_ON = SCHEDULE  THRU DEC 31,  WEEK-SCHEDULE = WS1  ..

        DS2 = DAY-SCHEDULE  HOURS = (1,24)  VALUES = (0.)  ..
        WS2 = WEEK-SCHEDULE  DAYS = (ALL)  DAY-SCHEDULE = DS2  ..
        S_OFF = SCHEDULE  THRU DEC 31,  WEEK-SCHEDULE = WS2  ..


$ ***************************************************************************
$       GLASS-TYPE
$ ***************************************************************************
$ GLASS TYPE (TYPE=3, TRANSMITTANCE=79%, REFLECTANCE=7%, CONDUCTANCE=1.47)
        GLASS-TYPE1 = GLASS-TYPE
                GLASS-TYPE-CODE = 3
                PANES = 1  ..



$ ***************************************************************************
$       MATERIALS & LAYERS (USER DEFINED)
$ ***************************************************************************
$ EXTERIOR WALL LAYER
        EX-LAYER = MATERIAL
                TH = 0.5, COND = 0.029, DENS = 18.0, S-H = 0.31  ..
                        $ (RESISTANCE = 35.0)

$ INTERIOR WALL LAYER
        IN-LAYER = MATERIAL
                TH = 0.5, COND = 0.04, DENS = 18.0, S-H = 0.31  ..
                        $ (RESISTANCE = 25.0)

$ ROOF LAYER
        RF-LAYER = MATERIAL
                TH = 0.5, COND = 0.014, DENS = 18.0, S-H = 0.31  ..
                        $ (RESISTANCE = 71.4)

$ FLOOR LAYER
        FL-LAYER = MATERIAL
```

```
                TH = 0.5, COND = 0.025, DENS = 18.0, S-H = 0.31  ..
                        $ (RESISTANCE = 40.2)

$ EXPER ROOM WALL LAYER
        EXPER-LAYER = MATERIAL
                TH = 0.5, COND = 0.029, DENS = 18.0, S-H = 0.31  ..
                        $ (RESISTANCE = 35.0)


$ ***************************************************************************
$       WALL (ROOF, & FLOOR) CONSTRUCTION DESCRIPTION
$ ***************************************************************************

$ ---------------------------------------------------------------------------
$       FRONT WALL
$ ---------------------------------------------------------------------------
        F-WALL-LAYER1 = LAYERS
                INSIDE-FILM-RES = 0.68
                MATERIAL = (EX-LAYER) ..
        F-WALL1 = CONSTRUCTION
                LAYERS = F-WALL-LAYER1  ..

$ ---------------------------------------------------------------------------
$       RIGHT WALL
$ ---------------------------------------------------------------------------
        R-WALL-LAYER1 = LAYERS
                INSIDE-FILM-RES = 0.68
                MATERIAL = (IN-LAYER) ..
        R-WALL1 = CONSTRUCTION
                LAYERS = R-WALL-LAYER1  ..

$ ---------------------------------------------------------------------------
$       LEFT WALL
$ ---------------------------------------------------------------------------
        L-WALL-LAYER1 = LAYERS
                INSIDE-FILM-RES = 0.68
                MATERIAL = (EX-LAYER) ..
        L-WALL1 = CONSTRUCTION
                LAYERS = L-WALL-LAYER1  ..

$ ---------------------------------------------------------------------------
$       BACK WALL
$ ---------------------------------------------------------------------------
        B-WALL-LAYER1 = LAYERS
                INSIDE-FILM-RES = 0.68
                MATERIAL = (EX-LAYER) ..
        B-WALL1 = CONSTRUCTION
                LAYERS = B-WALL-LAYER1  ..

$ ---------------------------------------------------------------------------
$       ROOF
$ ---------------------------------------------------------------------------
        ROOF-LAYER1 = LAYERS
                INSIDE-FILM-RES = 0.68
                MATERIAL = (RF-LAYER) ..
        ROOF1 = CONSTRUCTION
                LAYERS = ROOF-LAYER1  ..

$ ---------------------------------------------------------------------------
$       FLOOR
$ ---------------------------------------------------------------------------
        FLOOR-LAYER1 = LAYERS
                INSIDE-FILM-RES = 0.68
                MATERIAL = (FL-LAYER) ..
        FLOOR1 = CONSTRUCTION
                LAYERS = FLOOR-LAYER1  ..


$ ---------------------------------------------------------------------------
$       EXPER ROOM WALL
$ ---------------------------------------------------------------------------
        EXPER-LAYER1 = LAYERS
                INSIDE-FILM-RES = 0.68
                MATERIAL = (EXPER-LAYER) ..
        EXPER-WALL1 = CONSTRUCTION
                LAYERS = EXPER-LAYER1  ..


$ ***************************************************************************
```

```
$       SPACE CONDITIONS DESCRIPTION
$ ************************************************************************
        MAIN-RM-COND = SPACE-CONDITIONS
                TEMPERATURE = (80)                  $ *** UNCONDITIONED ZONE, AVERAGE TEMP
                PEOPLE-SCHEDULE = S_OFF
                NUMBER-OF-PEOPLE = 0
                PEOPLE-HEAT-GAIN = 600              $ *** NO PEOPLE HEAT GAIN
                LIGHTING-SCHEDULE = S_OFF
                LIGHTING-W/SQFT = 0                 $ *** NO LIGHTING HEAT GAIN
                TASK-LIGHT-SCH = S_OFF
                TASK-LT-W/SQFT = 0                  $ *** NO TASK LIGHTING HEAT GAIN
                EQUIP-SCHEDULE = S_OFF
                EQUIPMENT-W/SQFT = 0                $ *** NO EQUIPMENT HEAT GAIN
                SOURCE-SCHEDULE = S_OFF
                SOURCE-BTU/HR = 0                   $ *** NO EQUIPMENT HEAT GAIN
                INF-SCHEDULE = S_ON
                INF-METHOD = AIR-CHANGE
                INF-CFM/SQFT = 15                   $ *** TOTAL 30 CFM FOR MAIN ROOM
                FLOOR-WEIGHT = 70
                ZONE-TYPE = UNCONDITIONED  ..

        EXPER-RM-COND = SPACE-CONDITIONS  LIKE  MAIN-RM-COND  EXCEPT
                INF-CFM/SQFT = 20                   $ *** 40 CFM FOR ROOM
                ZONE-TYPE = CONDITIONED  ..


$ ************************************************************************
$       SPACE DESCRIPTION
$ ************************************************************************
$ ------------------------------------------------------------------------
$       MAIN ROOM
$ ------------------------------------------------------------------------
        MAIN-RM = SPACE
                SPACE-CONDITIONS = MAIN-RM-COND
                X = 0
                Y = 0
                Z = 4.0
                AZIMUTH = 0
                AREA = 2.0
                VOLUME = 4.0  ..

        MAIN-F-WALL = EXTERIOR-WALL
                CONSTRUCTION = F-WALL1
                HEIGHT = 2.0
                WIDTH = 2.0
                X = 0
                Y = 0
                Z = 0
                AZIMUTH = 180
                TILT = 90  ..

        MAIN-WINDOW = WINDOW
                GLASS-TYPE = GLASS-TYPE1
                X = 0.5
                Y = 0.5
                WIDTH = 1
                HEIGHT = 1  ..

        MAIN-B-WALL = EXTERIOR-WALL
                CONSTRUCTION = B-WALL1
                HEIGHT = 2.0
                WIDTH = 2.0
                X = 2.0
                Y = 1.0
                Z = 0
                AZIMUTH = 0
                TILT = 90  ..

        MAIN-L-WALL = EXTERIOR-WALL
                CONSTRUCTION = L-WALL1
                HEIGHT = 2.0
                WIDTH = 1.0
                X = 0
                Y = 1
                Z = 0
                AZIMUTH = 270
                TILT = 90  ..

        MAIN-R-WALL = INTERIOR-WALL  NEXT-TO EXPER-RM
```

```
                CONSTRUCTION = R-WALL1
                HEIGHT = 2.0
                WIDTH = 1.0
                X = 2.0
                Y = 0
                Z = 0
                AZIMUTH = 90
                TILT = 90  ..

        MAIN-ROOF = ROOF
                CONSTRUCTION = ROOF1
                HEIGHT = 1.0
                WIDTH = 2.0
                X = 0
                Y = 0
                Z = 2.0
                AZIMUTH = 180
                TILT = 0  ..

        MAIN-FLOOR = EXTERIOR-WALL
                CONSTRUCTION = FLOOR1
                HEIGHT = 2.0
                WIDTH = 1.0
                X = 0
                Y = 0
                Z = 0
                AZIMUTH = 90
                TILT = 180  ..

$ ------------------------------------------------------------------------------
$       EXPERIMENT ROOM
$ ------------------------------------------------------------------------------
        EXPER-RM = SPACE
                SPACE-CONDITIONS = EXPER-RM-COND
                X = 2.0
                Y = 0
                Z = 4.0
                AZIMUTH = 0
                AREA = 2.0
                VOLUME = 4.0  ..

        EXPER-F-WALL = EXTERIOR-WALL  LIKE  MAIN-F-WALL  EXCEPT
                CONSTRUCTION = EXPER-WALL1  ..

        EXPER-B-WALL = EXTERIOR-WALL  LIKE  MAIN-B-WALL  EXCEPT
                CONSTRUCTION = EXPER-WALL1  ..

        EXPER-R-WALL = EXTERIOR-WALL
                CONSTRUCTION = EXPER-WALL1
                HEIGHT = 2.0
                WIDTH = 1.0
                X = 2.0
                Y = 0
                Z = 0
                AZIMUTH = 90
                TILT = 90  ..

        EXPER-ROOF = ROOF  LIKE  MAIN-ROOF  ..

        EXPER-FLOOR = EXTERIOR-WALL  LIKE  MAIN-FLOOR  ..


$ ******************************************************************************
$       LOADS REPORT
$ ******************************************************************************
        LOADS-REPORT
                SUMMARY =(ALL-SUMMARY)
                VERIFICATION = (ALL-VERIFICATION)  ..


$ ******************************************************************************
$       HOURLY REPORT
$ ******************************************************************************
        RB-G1 = REPORT-BLOCK
                VARIABLE-TYPE = GLOBAL
                VARIABLE-LIST = (1, 3, 4, 9, 16, 18)  ..
                        $ 1. CLEARNESS NUMBER
                        $ 3. WET-BULB TEMP.
                        $ 4. DRY-BULB TEMP.
```

```
                $ 9. WIND DIRECTION (0-15)
                $ 16. WIND SPEED (KNOTS)
                $ 18. DEW-POINT TEMP.
HR-G1 = HOURLY-REPORT
        REPORT-SCHEDULE = S_ON
        REPORT-BLOCK = (RB-G1)  ..

RB-G2 = REPORT-BLOCK
        VARIABLE-TYPE = GLOBAL
        VARIABLE-LIST = (36, 37, 15)  ..
                $ 13. DIFFUSE HORIZONTAL SOLAR RADIATION FROM WEATHER FILE
                $ 14. TOTAL DIRECT NORMAL SOLAR RADIATION FROM WEATHER FILE
                $ 15. TOTAL HORIZONTAL SOLAR RADIATION FROM WEATHER FILE

                $ 36. DIRECT NORMAL SOLAR RADIATION INTENSITY ON A CLEAR DAY
                $ 37. DIFFUSE SOLAR INTENSITY ON A HORIZONTAL SURFACE ON A
                $       CLEAR DAY

                $ 26. HOUR ANGLE OF SUNRISE FOR THE DAY (RADIANS)
                $ 27. CURRENT HOUR ANGLE (RADIANS)
                $ 28. TANGENT OF SOLAR DECLINATION ANGLE
                $ 35. SOLAR DIRECTION (ZENITH) COSINE
HR-G2 = HOURLY-REPORT
        REPORT-SCHEDULE = S_ON
        REPORT-BLOCK = (RB-G2)  ..

RB-S1 = REPORT-BLOCK
        VARIABLE-TYPE = MAIN-RM
        VARIABLE-LIST = (18,19,20,21,31,37,39)  ..
                $ 18. WINDOW CONDUCTION LOAD, WEIGHTED
                $ 19. DELAYED WALL LOAD, WEIGHTED
                $ 20. DELAYED ROOF LOAD, WEIGHTED
                $ 21. INTERIOR WALL LOAD, WEIGHTED
                $ 31. INFILTRATION LOAD, LATENT, UNWEIGHTED
                $ 37. INFILTRATION LOAD, SENSIBLE, UNWEIGHTED
                $ 39. INFILTRATION (FT^3/MIN.)
HR-S1 = HOURLY-REPORT
        REPORT-SCHEDULE = S_ON
        REPORT-BLOCK = (RB-S1)  ..

RB-FW1 = REPORT-BLOCK
        VARIABLE-TYPE = MAIN-F-WALL
        VARIABLE-LIST = (1,2,5,15,16,17,18,19)  ..
                $ 1. SOLAR RADIATION ON WALL AFTER SHADING (BTU/HR)
                $ 2. FRACTION OF THE WALL THAT IS SHADED
                $ 5. HEAT TRANSFER FROM THE WALL TO THE ZONE (BTU/HR)
                $ 15. COSINE OF THE ANGLE BETWEEN THE DIRECTION OF THE SUN AND
                $       THE SURFACE OUTWARD NORMAL
                $ 16. SOLAR RADIATION ON THE WALL REFLECTED FROM THE GROUND
                $       (BTU/HR-FT^2)
                $ 17. INTENSITY OF DIRECT SOLAR RADIATION ON THE SURFACE,
                $       SHADING NEGLECTED (BTU/HR-FT^2)
                $ 18. INTENSITY OF DIFFUSE SOLAR RADIATION ON THE SURFACE
                $       (BTU/HR-FT^2)
                $ 19. TOTAL SOLAR RADIATION ON THE SURFACE, SHADING NEGLECTED
                $       (BTU/HR-FT^2)
HR-FW1 = HOURLY-REPORT
        REPORT-SCHEDULE = S_ON
        REPORT-BLOCK = (RB-FW1)  ..

RB-WD1 = REPORT-BLOCK
        VARIABLE-TYPE = MAIN-WINDOW
        VARIABLE-LIST = (10,11,12,13,14,15,16,17)  ..
                $ 10. FRACTION OF WINDOW AREA THAT IS SHADED
                $ 11. DIRECT SOLAR RADIATION INCIDENT ON UNSHADED PART OF
                $       WINDOW, DIVIDED BY TOTAL WINDOW AREA (BTU/HR-FT^2)
                $ 12. DIFFUSE SOLAR RADIATION INCIDENT ON WINDOW,
                $       DIVIDED BY TOTAL WINDOW AREA (BTU/HR-FT^2)
                $ 13. SOLAR ENERGY TRANSMITTED THROUGH GLASS DIVIDED BY TOTAL
                $       WINDOW AREA, BEFORE MULTIPLICATION BY SHADING
                $       COEFFICIENT (BTU/HR-FT^2)
                $ 14. SOLAR ENERGY ABSORBED BY GLASS AND CONDUCTED INTO THE
                $       SPACE DIVIDED BY TOTAL WINDOW AREA, BEFORE MULTIPLICATION
                $       BY SHADING COEFFICIENT
                $ 15. HEAT GAIN THROUGH WINDOW BY SOLAR RADIATION (BTU/HR)
                $       (13:QTRANS)*(WINDOW AREA)*(SHADING COEFFICIENT)
                $ 16. SHADING COEFFICIENT
                $ 17. HEAT GAIN THROUGH WINDOW BY CONDUCTION (BTU/HR)
                $       (WINDOW U-VALUE)*(WINDOW AREA)*(OUTSIDE DBT-ZONE TEMP)
```

```
                        $       +(14:QABS)*(WINDOW AREA)
        HR-WD1 = HOURLY-REPORT
                 REPORT-SCHEDULE = S_ON
                 REPORT-BLOCK = (RB-WD1)  ..

$ ***************************************************************************
$       END LOADS INSTRUCTIONS
$ ***************************************************************************
END  ..

$ ***************************************************************************
$       COMPUTE LOADS
$ ***************************************************************************
COMPUTE LOADS  ..

$ ***************************************************************************
$       END PROGRAM
$ ***************************************************************************
STOP  ..
```

C.2 DOE-2 Hourly Report

_DOE2 SIMULATION FOR S.F.D. BY JOHN KIE-WHAN OH DOE-2.1E-058

HR-G1 = HOURLY-REPORT

MMDDHH	GLOBAL CLEARNES NUMBER	GLOBAL WET BULB TEMP F	GLOBAL DRY BULB TEMP F	GLOBAL WIND DIR 360/16	GLOBAL CLOUD TYPE	GLOBAL DEW POINT F
	----(1)	----(3)	----(4)	----(9)	----(16)	----(18)
322 1	1.00	51.9	61.6	15.	2.	44.0
322 2	1.00	48.5	59.7	15.	2.	37.5
322 3	1.00	46.1	58.1	15.	2.	32.7
322 4	1.00	44.8	56.8	15.	2.	31.0
322 5	1.00	44.4	55.8	15.	2.	31.2
322 6	1.00	44.4	55.2	15.	2.	31.8
322 7	1.00	44.6	55.0	15.	2.	32.7
322 8	1.00	45.3	55.6	15.	2.	34.0
322 9	1.00	46.7	57.2	15.	2.	35.6
32210	1.00	48.5	59.7	15.	2.	37.5
32211	1.00	50.7	62.8	15.	2.	39.6
32212	1.00	52.9	66.1	15.	2.	41.7
32213	1.00	55.1	69.2	15.	2.	44.0
32214	1.00	57.0	71.7	15.	2.	46.3
32215	1.00	58.6	73.4	15.	2.	48.4
32216	1.00	59.7	74.0	15.	2.	50.5
32217	1.00	60.5	73.7	15.	2.	52.4
32218	1.00	61.1	73.1	15.	2.	54.0
32219	1.00	61.4	72.1	15.	2.	55.3
32220	1.00	61.5	70.8	15.	2.	56.2
32221	1.00	61.3	69.2	15.	2.	56.8
32222	1.00	60.8	67.4	15.	2.	57.0
32223	1.00	59.1	65.5	15.	2.	55.3
32224	1.00	55.8	63.5	15.	2.	50.5
DAILY SUMMARY (MAR 22)						
MN	1.00	44.4	55.0	15.	2.	31.0
MX	1.00	61.5	74.0	15.	2.	57.0
SM	24.00	1280.7	1547.5	360.	48.	1056.0
AV	1.00	53.4	64.5	15.	2.	44.0
MONTHLY SUMMARY (MAR)						
MN	1.00	44.4	55.0	15.	2.	31.0
MX	1.00	61.5	74.0	15.	2.	57.0
SM	24.00	1280.7	1547.5	360.	48.	1056.0
AV	1.00	53.4	64.5	15.	2.	44.0
YEARLY SUMMARY						
MN	1.00	44.4	55.0	15.	2.	31.0
MX	1.00	61.5	74.0	15.	2.	57.0
SM	24.00	1280.7	1547.5	360.	48.	1056.0
AV	1.00	53.4	64.5	15.	2.	44.0

ESL-TH-00/05-01 Development and validation of a computer model for energy - efficient shaded f

_DOE2 SIMULATION FOR S.F.D. BY JOHN KIE-WHAN OH DOE-2.1E-058

HR-G2 = HOURLY-REPORT

MMDDHH	GLOBAL DIFFUSE SOLAR BTU/HR-SQFT	GLOBAL DIRECT NORM SOL BTU/HR-SQFT	GLOBAL GLOBAL SOLAR BTU/HR-SQFT	GLOBAL NORMAL SOL INT BTU/HR-SQFT	GLOBAL DIFF SOL HORIZNTL BTU/HR-SQFT
	----(13)	----(14)	----(15)	----(36)	----(37)
322 1	0.0	0.0	0.0	0.0	0.0
322 2	0.0	0.0	0.0	0.0	0.0
322 3	0.0	0.0	0.0	0.0	0.0
322 4	0.0	0.0	0.0	0.0	0.0
322 5	0.0	0.0	0.0	0.0	0.0
322 6	0.0	0.0	0.0	0.0	0.0
322 7	0.0	0.0	2.1	34.7	2.5
322 8	0.0	0.0	53.2	183.5	13.4
322 9	0.0	0.0	128.8	258.5	18.9
32210	0.0	0.0	195.7	288.6	21.1
32211	0.0	0.0	247.5	303.0	22.1
32212	0.0	0.0	280.6	309.9	22.6
32213	0.0	0.0	292.5	312.1	22.8
32214	0.0	0.0	282.5	310.3	22.6
32215	0.0	0.0	251.2	303.8	22.2
32216	0.0	0.0	200.9	290.3	21.2
32217	0.0	0.0	135.1	262.2	19.1
32218	0.0	0.0	59.9	194.0	14.2
32219	0.0	0.0	3.5	45.7	3.3
32220	0.0	0.0	0.0	0.0	0.0
32221	0.0	0.0	0.0	0.0	0.0
32222	0.0	0.0	0.0	0.0	0.0
32223	0.0	0.0	0.0	0.0	0.0
32224	0.0	0.0	0.0	0.0	0.0
DAILY SUMMARY (MAR 22)					
MN	0.0	0.0	0.0	0.0	0.0
MX	0.0	0.0	292.5	312.1	22.8
SM	0.0	0.0	2133.5	3096.6	226.0
AV	0.0	0.0	88.9	129.0	9.4
MONTHLY SUMMARY (MAR)					
MN	0.0	0.0	0.0	0.0	0.0
MX	0.0	0.0	292.5	312.1	22.8
SM	0.0	0.0	2133.5	3096.6	226.0
AV	0.0	0.0	88.9	129.0	9.4
YEARLY SUMMARY					
MN	0.0	0.0	0.0	0.0	0.0
MX	0.0	0.0	292.5	312.1	22.8
SM	0.0	0.0	2133.5	3096.6	226.0
AV	0.0	0.0	88.9	129.0	9.4

_DOE2 SIMULATION FOR S.F.D. BY JOHN KIE-WHAN OH DOE-2.1E-058

HR-S1 = HOURLY-REPORT

MMDDHH	MAIN-RM GLS COND LOAD BTU/HR	MAIN-RM DELAY WL LOAD BTU/HR	MAIN-RM DELAY RF LOAD BTU/HR	MAIN-RM INT WALL LOAD BTU/HR	MAIN-RM INFILTRN LATENT BTU/HR	MAIN-RM INFILTRN SENS GN BTU/HR
	----(18)	----(19)	----(20)	----(21)	----(31)	----(37)
322 1	-14.24	-0.68	0.42	0.00	0.00	-584.24
322 2	-15.65	-1.54	0.40	0.00	0.00	-641.55
322 3	-16.90	-2.47	0.36	0.00	0.00	-692.90
322 4	-18.05	-3.45	0.31	0.00	0.00	-734.28
322 5	-18.93	-4.46	0.24	0.00	0.00	-765.64
322 6	-19.60	-5.47	0.16	0.00	0.00	-785.03
322 7	-19.94	-6.49	0.07	0.00	0.00	-791.59
322 8	-19.15	-7.48	-0.03	0.00	0.00	-773.49
322 9	-14.81	-8.41	-0.13	0.00	0.00	-721.38
32210	-11.24	-9.22	-0.23	0.00	0.00	-641.55
32211	-7.78	-9.75	-0.33	0.00	0.00	-543.62
32212	-4.77	-9.85	-0.42	0.00	0.00	-439.40
32213	-2.49	-9.49	-0.49	0.00	0.00	-341.47
32214	-1.40	-8.70	-0.53	0.00	0.00	-261.63
32215	-0.74	-7.59	-0.53	0.00	0.00	-209.53
32216	-1.21	-6.22	-0.47	0.00	0.00	-191.43
32217	-2.65	-4.65	-0.38	0.00	0.00	-197.99
32218	-4.72	-2.99	-0.26	0.00	60.17	-217.37
32219	-6.31	-1.39	-0.12	0.00	125.36	-249.74
32220	-6.45	-0.06	0.03	0.00	177.98	-290.72
32221	-8.71	0.76	0.17	0.00	214.76	-341.47
32222	-9.97	0.97	0.28	0.00	233.44	-398.78
32223	-11.34	0.68	0.36	0.00	157.74	-460.14
32224	-12.78	0.09	0.41	0.00	0.00	-522.87
DAILY SUMMARY (MAR 22)						
MN	-19.94	-9.85	-0.53	0.00	0.00	-791.59
MX	-0.74	0.97	0.42	0.00	233.44	-191.43
SM	-249.85	-107.84	-0.71	0.00	969.45	-11796.20
AV	-10.41	-4.49	-0.03	0.00	40.39	-491.51
MONTHLY SUMMARY (MAR)						
MN	-19.94	-9.85	-0.53	0.00	0.00	-791.59
MX	-0.74	0.97	0.42	0.00	233.44	-191.43
SM	-249.85	-107.84	-0.71	0.00	969.45	-11796.20
AV	-10.41	-4.49	-0.03	0.00	40.39	-491.51
YEARLY SUMMARY						
MN	-19.94	-9.85	-0.53	0.00	0.00	-791.59
MX	-0.74	0.97	0.42	0.00	233.44	-191.43
SM	-249.85	-107.84	-0.71	0.00	969.45	-11796.20
AV	-10.41	-4.49	-0.03	0.00	40.39	-491.51

_DOE2 SIMULATION FOR S.F.D. BY JOHN KIE-WHAN OH DOE-2.1E-058

HR-FW1 = HOURLY-REPORT

MMDDHH	MAIN-F-W ALL SOL RAD ON WALL BTU/HR-SQFT ----(1)	MAIN-F-W ALL SHADED FRACTION FRAC.OR MULT. ----(2)	MAIN-F-W ALL OUT SURF HEAT FLO BTU/HR ----(5)	MAIN-F-W ALL SOLAR COSINE ----(15)	MAIN-F-W ALL GRND REF SOL INT BTU/HR-SQFT ----(16)	MAIN-F-W ALL DIR SOL INTENSTY BTU/HR-SQFT ----(17)	MAIN-F-W ALL DIF SOL INTENSTY BTU/HR-SQFT ----(18)
322 1	0.00	0.000	1.02	0.00000	0.0	0.0	0.0
322 2	0.00	0.000	0.44	0.00000	0.0	0.0	0.0
322 3	0.00	0.000	-0.11	0.00000	0.0	0.0	0.0
322 4	0.00	0.000	-0.63	0.00000	0.0	0.0	0.0
322 5	0.00	0.000	-1.12	0.00000	0.0	0.0	0.0
322 6	0.00	0.000	-1.57	0.00000	0.0	0.0	0.0
322 7	1.65	1.000	-2.00	0.02335	0.4	0.4	1.6
322 8	18.00	1.000	-2.39	0.12011	10.6	22.0	18.0
322 9	93.91	0.000	-2.73	0.24345	25.8	62.9	31.0
32210	139.40	0.000	-3.00	0.34080	39.1	101.0	38.5
32211	174.10	0.000	-3.07	0.43190	49.5	130.9	43.2
32212	195.82	0.000	-2.81	0.48416	56.1	150.0	45.8
32213	203.55	0.000	-2.22	0.50301	58.5	157.0	46.6
32214	197.07	0.000	-1.36	0.48718	56.5	151.2	45.9
32215	176.55	0.000	-0.34	0.43774	50.2	133.0	43.5
32216	142.92	0.000	0.72	0.35806	40.2	103.9	39.0
32217	98.26	0.000	1.70	0.25357	27.0	66.5	31.8
32218	44.92	0.000	2.51	0.13140	12.0	25.5	19.4
32219	3.27	0.000	3.07	0.02918	0.7	0.7	2.5
32220	0.00	0.000	3.29	0.00000	0.0	0.0	0.0
32221	0.00	0.000	3.18	0.00000	0.0	0.0	0.0
32222	0.00	0.000	2.78	0.00000	0.0	0.0	0.0
32223	0.00	0.000	2.23	0.00000	0.0	0.0	0.0
32224	0.00	0.000	1.62	0.00000	0.0	0.0	0.0
DAILY SUMMARY (MAR 22)							
MN	0.00	0.000	-3.07	0.00000	0.0	0.0	0.0
MX	203.55	1.000	3.29	0.50301	58.5	157.0	46.6
SM	1489.42	2.000	-0.79	3.85290	426.7	1105.0	406.8
AV	62.06	0.083	-0.03	0.16054	17.8	46.0	17.0
MONTHLY SUMMARY (MAR)							
MN	0.00	0.000	-3.07	0.00000	0.0	0.0	0.0
MX	203.55	1.000	3.29	0.50301	58.5	157.0	46.6
SM	1489.42	2.000	-0.79	3.85290	426.7	1105.0	406.8
AV	62.06	0.083	-0.03	0.16054	17.8	46.0	17.0
YEARLY SUMMARY							
MN	0.00	0.000	-3.07	0.00000	0.0	0.0	0.0
MX	203.55	1.000	3.29	0.50301	58.5	157.0	46.6
SM	1489.42	2.000	-0.79	3.85290	426.7	1105.0	406.8
AV	62.06	0.083	-0.03	0.16054	17.8	46.0	17.0

_DOE2 SIMULATION FOR S.F.D. BY JOHN KIE-WHAN OH DOE-2.1E-058

HR-WD1 = HOURLY-REPORT

MMDDHH	MAIN-WIN DOW SHADED FRACTION FRAC.OR MULT. ----(10)	MAIN-WIN DOW DIRECT SOLAR BTU/HR-SQFT ----(11)	MAIN-WIN DOW DIFFUSE SOLAR BTU/HR-SQFT ----(12)	MAIN-WIN DOW SOL TRAN THRU GLS BTU/HR-SQFT ----(13)	MAIN-WIN DOW SOL ABS BY GLS BTU/HR-SQFT ----(14)	MAIN-WIN DOW SOL GAIN GLAS+FRM BTU/HR ----(15)	MAIN-WIN DOW SHADING COEFF ----(16)	MAIN-WIN DOW CONDUCTN GLAS+FRM BTU/HR ----(17)
322 1	0.000	0.0	0.0	0.0	0.0	0.0	1.000	-16.82
322 2	0.000	0.0	0.0	0.0	0.0	0.0	1.000	-18.40
322 3	0.000	0.0	0.0	0.0	0.0	0.0	1.000	-19.79
322 4	0.000	0.0	0.0	0.0	0.0	0.0	1.000	-20.85
322 5	0.000	0.0	0.0	0.0	0.0	0.0	1.000	-21.62
322 6	0.000	0.0	0.0	0.0	0.0	0.0	1.000	-22.08
322 7	1.000	0.0	1.6	1.2	0.1	1.3	1.000	-22.21
322 8	1.000	0.0	18.0	12.8	1.2	14.0	1.000	-21.72
322 9	0.000	62.9	31.0	51.5	6.5	58.0	1.000	-20.41
32210	0.000	101.0	38.5	87.2	9.6	96.8	1.000	-18.46
32211	0.000	130.9	43.2	117.2	11.8	129.0	1.000	-15.98
32212	0.000	150.0	45.8	136.6	12.8	149.4	1.000	-13.25
32213	0.000	157.0	46.6	143.5	12.6	156.1	1.000	-10.50
32214	0.000	151.2	45.9	137.7	10.0	147.7	1.000	-7.18
32215	0.000	133.0	43.5	119.4	9.7	129.1	1.000	-6.73
32216	0.000	103.9	39.0	90.2	8.0	98.2	1.000	-6.46
32217	0.000	66.5	31.8	54.6	5.4	60.0	1.000	-6.51
32218	0.000	25.5	19.4	21.0	2.3	23.3	1.000	-6.71
32219	0.000	0.7	2.5	1.8	0.1	2.0	1.000	-6.95
32220	0.000	0.0	0.0	0.0	0.0	0.0	1.000	-6.93
32221	0.000	0.0	0.0	0.0	0.0	0.0	1.000	-10.15
32222	0.000	0.0	0.0	0.0	0.0	0.0	1.000	-11.72
32223	0.000	0.0	0.0	0.0	0.0	0.0	1.000	-13.40
32224	0.000	0.0	0.0	0.0	0.0	0.0	1.000	-15.12
DAILY SUMMARY (MAR 22)								
MN	0.000	0.0	0.0	0.0	0.0	0.0	1.000	-22.21
MX	1.000	157.0	46.6	143.5	12.8	156.1	1.000	-6.46
SM	2.000	1082.6	406.8	974.7	90.1	1064.9	24.000	-339.96
AV	0.083	45.1	17.0	40.6	3.8	44.4	1.000	-14.16
MONTHLY SUMMARY (MAR)								
MN	0.000	0.0	0.0	0.0	0.0	0.0	1.000	-22.21
MX	1.000	157.0	46.6	143.5	12.8	156.1	1.000	-6.46
SM	2.000	1082.6	406.8	974.7	90.1	1064.9	24.000	-339.96
AV	0.083	45.1	17.0	40.6	3.8	44.4	1.000	-14.16
YEARLY SUMMARY								
MN	0.000	0.0	0.0	0.0	0.0	0.0	1.000	-22.21
MX	1.000	157.0	46.6	143.5	12.8	156.1	1.000	-6.46
SM	2.000	1082.6	406.8	974.7	90.1	1064.9	24.000	-339.96
AV	0.083	45.1	17.0	40.6	3.8	44.4	1.000	-14.16

APPENDIX D

SELECTED VISUAL BASIC SOURCE CODE OF SFD

This appendix contains selected visual basic source code for the functions and subroutines that were used for the calculation of the various kinds of solar radiation and solar angles. The functions to calculate the solar and local times are also included.

```
Function GetLeapYear(GivenYear As Integer) As Boolean
    Dim TempLeapYear As Boolean

    TempLeapYear = False
    If (GivenYear Mod 4) = 0 Then
        If (GivenYear Mod 100) <> 0 Then
            TempLeapYear = True
        Else
            If (GivenYear Mod 400) = 0 Then TempLeapYear = True
        End If
    End If

    GetLeapYear = TempLeapYear
End Function


Function GetDOY(GivenYear As Integer, GivenMonth As Integer, GivenDate As _
    Integer) As Integer

    Dim TempDOY As Integer, M As Integer, Days As Integer

    TempDOY = 0
    For M = 1 To (GivenMonth - 1)
        Select Case M
        Case 1, 3, 5, 7, 8, 10, 12: Days = 31
        Case 2: Days = 28
            If (GetLeapYear(GivenYear)) Then Days = 29 'Leap year?
        Case Else: Days = 30
        End Select

        TempDOY = TempDOY + Days
    Next
    TempDOY = TempDOY + GivenDate

    GetDOY = TempDOY
End Function


Function GetDecimalDate(GivenYear As Integer, GivenMonth As Integer, _
    GivenDate As Integer) As Long

    Dim GivenDOY As Integer

    ' Day of Year Calculation
    GivenDOY = GetDOY(GivenYear, GivenMonth, GivenDate)

    ' Timeline Calculation
    GetDecimalDate = Int((GivenYear - 1900) * 365.25 + GivenDOY + 0.75)
End Function
```

```
Function GetDOW(GivenYear As Integer, GivenMonth As Integer, GivenDate As _
    Integer) As Integer

    ' 1 for Sunday through 7 for Saturday

    Dim GivenDecimalDate As Long

    ' Decimal Date Calculation
    GivenDecimalDate = GetDecimalDate(GivenYear, GivenMonth, GivenDate)

    ' Day of Week Calculation
    GetDOW = ((GivenDecimalDate - 1) Mod 7) + 1
End Function


Function GetDOWText(GivenDOW As Integer) As String
    Select Case GivenDOW
    Case 1: GetDOWText = "Sunday"
    Case 2: GetDOWText = "Monday"
    Case 3: GetDOWText = "Tuesday"
    Case 4: GetDOWText = "Wednesday"
    Case 5: GetDOWText = "Thursday"
    Case 6: GetDOWText = "Friday"
    Case 7: GetDOWText = "Saturday"
    End Select
End Function


Function GetDST(GivenYear As Integer, GivenMonth As Integer, GivenDate As _
    Integer, GivenTime As Single) As Boolean

    Dim FirstSunday As Integer, LastSunday As Integer
    Dim TempDOW As Integer

    ' Dalylight Saving Time (DST):
    ' DST begins at 2am on the first Sunday in April
    ' DST ends at 2am on the last Sunday in October

    GetDST = False

    If (DSTMode = 0) Then Exit Function

    Select Case GivenMonth
    Case 4:
        TempDOW = GetDOW(GivenYear, 4, 1)  'April 1st
        FirstSunday = 9 - TempDOW
        If (FirstSunday > 7) Then FirstSunday = 1

        If (GivenDate > FirstSunday) Then GetDST = True
        If ((GivenDate = FirstSunday) And (GivenTime >= 2)) Then GetDST = True
    Case 5 To 9: GetDST = True
    Case 10:
        TempDOW = GetDOW(GivenYear, 10, 31)  ' October 31st
        LastSunday = 31 - TempDOW + 1

        If (GivenDate < LastSunday) Then GetDST = True
        If ((GivenDate = LastSunday) And (GivenTime <= 2)) Then GetDST = True
    End Select
End Function
```

```
Function GetSolarTimeDiff(CurrentDOY As Integer, Longitude As Single, _
    TimeZone As Integer, DST As Boolean, SolarModel As Integer) As Single

    'Declare variable
    Dim B As Double
    Dim ET As Double

    If (SolarModel = 2) Then
        'Kreider & Rabl(1994)'s Model
        B = (CurrentDOY - 81) / 364 * 360
        ET = 9.87 * DSin(2 * B) - 7.53 * DCos(B) - 1.5 * DSin(B)
    Else
        'Spencer(1971)'s Model (Duffie & Beckman, 1991)
        B = (CurrentDOY - 1) / 365 * 360
        ET = 229.2 * (0.000075 + 0.001868 * DCos(B) - 0.032077 * DSin(B) _
            - 0.014615 * DCos(2 * B) - 0.04089 * DSin(2 * B))
    End If

    GetSolarTimeDiff = (TimeZone - (Longitude / 15)) + (ET / 60)

    'If it is daylight saving time
    If (DST = True) Then GetSolarTimeDiff = GetSolarTimeDiff - 1
End Function


Function GetDeclination(CurrentDOY As Integer, SolarModel As Integer) As Single
    If (SolarModel = 2) Then    ' Kreider & Rabl(1994)'s Model
        GetDeclination = ArcSin(-DSin(23.45) * DCos(360 / 365.25 * _
            (CurrentDOY + 10)))
    Else    ' Cooper(1969)'s Model (Duffie & Beckman, 1991)
        GetDeclination = 23.45 * DSin(360 / 365 * (284 + CurrentDOY))
    End If
End Function


Function GetSunsetHourAngle(Latitude As Single, Declination As Single, _
    SolarModel As Integer) As Single

    'Kreider & Rabl(1994)'s Model
    GetSunsetHourAngle = ArcCos(-DTan(Latitude) * DTan(Declination))
End Function


Function GetSolarHourAngle(SolarTime As Single) As Single
    GetSolarHourAngle = (SolarTime - 12) * 15
End Function


Function GetZenith(Latitude As Single, Declination As Single, _
    SolarHourAngle As Single, SolarModel As Integer) As Single

    'Kreider & Rabl(1994)'s Model
    GetZenith = ArcCos(DCos(Latitude) * DCos(Declination) * _
        DCos(SolarHourAngle) + DSin(Latitude) * DSin(Declination))
End Function


Function GetSolarAzimuth(Latitude As Single, Declination As Single, _
    Zenith As Single, SolarHourAngle As Single, SolarModel As Integer) _
    As Single

    Dim PseudoSolarAzimuth As Single
```

```
    Dim EWHourAngle As Single
    Dim C1 As Single, C2 As Single, C3 As Single

    If (SolarModel = 0) Then     ' ASHRAE Handbook
        GetSolarAzimuth = ArcCos((DSin(90 - Zenith) * DSin(Latitude) _
            - DSin(Declination)) / (DCos(90 - Zenith) * DCos(Latitude)))
        If (SolarHourAngle < 12 * 15) Then GetSolarAzimuth = -GetSolarAzimuth

    ElseIf (SolarModel = 1) Then     'Braun && Mitchell's Model (1983)
        PseudoSolarAzimuth = ArcSin(DSin(SolarHourAngle) * DCos(Declination) _
            / DSin(Zenith))
        EWHourAngle = ArcCos(DTan(Declination) / DTan(Latitude))

        If (Abs(SolarHourAngle) < EWHourAngle) Then
            C1 = 1
        Else
            C1 = -1
        End If
        If (Latitude * (Latitude - Declination) >= 0) Then
            C2 = 1
        Else
            C2 = -1
        End If
        If (SolarHourAngle >= 0) Then
            C3 = 1
        Else
            C3 = -1
        End If

        GetSolarAzimuth = C1 * C2 * PseudoSolarAzimuth + C3 * (1 - C1 * C2)*90

    Else     ' Kreider & Rabl(1994)'s Model
        GetSolarAzimuth = ArcSin(DCos(Declination) * DSin(SolarHourAngle) / _
            DSin(Zenith))
    End If
End Function


Function GetIncidenceAngle(Zenith As Single, SolarAzimuth As Single, _
    SurfaceTilt As Single, SurfaceAzimuth As Single, SolarModel As Integer) _
    As Single

    SurfaceSolarAzimuth = SolarAzimuth - SurfaceAzimuth

    If (SolarModel = 2) Then     ' Kreider & Rabl(1994)'s Model
        GetIncidenceAngle = ArcCos(DSin(Zenith) * DSin(SurfaceTilt) * _
            DCos(SurfaceSolarAzimuth) + DCos(Zenith) * DCos(SurfaceTilt))
    End If
End Function


Function GetSolarConstant(SolarModel As Integer) As Single
    ' Solar Constant Calculation
    Select Case SolarModel
    Case 0: 'ASHRAE Handbook (1993)'s Model
        GetSolarConstant = 1367
    Case 1: 'Duffie & Beckman (1991)'s Model
        GetSolarConstant = 1367
    Case 2: 'Kreider & Rabl (1994)'s Model
        GetSolarConstant = 1373
    End Select
End Function
```

```
Function GetExTer(SolarConstant As Single, CurrentDOY As Integer, _
    SolarModel As Integer) As Single

    Dim PreDate As Integer, PostDate As Integer
    Dim PreRad As Single, PostRad As Single

    ' Extraterrestrial Calculation

    If (SolarModel = 0) Then        'ASHRAE Handbook (1993)'s Model
        Select Case (CurrentDOY)
        Case 1 To 21:
            PreDate = -9:       PostDate = 21
            PreRad = 1416.91:   PostRad = 1415.96
        Case 22 To 52:
            PreDate = 21:       PostDate = 52
            PreRad = 1415.96:   PostRad = 1401.45
        Case 53 To 80:
            PreDate = 52:       PostDate = 80
            PreRad = 1401.45:   PostRad = 1380.94
        Case 81 To 111:
            PreDate = 80:       PostDate = 111
            PreRad = 1380.94:   PostRad = 1356.33
        Case 112 To 141:
            PreDate = 111:      PostDate = 141
            PreRad = 1356.33:   PostRad = 1336.46
        Case 142 To 172:
            PreDate = 141:      PostDate = 171
            PreRad = 1336.46:   PostRad = 1325.73
        Case 173 To 202:
            PreDate = 172:      PostDate = 202
            PreRad = 1325.73:   PostRad = 1326.05
        Case 203 To 233:
            PreDate = 202:      PostDate = 233
            PreRad = 1326.05:   PostRad = 1338.04
        Case 234 To 264:
            PreDate = 233:      PostDate = 264
            PreRad = 1338.04:   PostRad = 1358.86
        Case 265 To 294:
            PreDate = 264:      PostDate = 294
            PreRad = 1358.86:   PostRad = 1379.68
        Case 295 To 325:
            PreDate = 294:      PostDate = 325
            PreRad = 1379.68:   PostRad = 1404.92
        Case 326 To 355:
            PreDate = 325:      PostDate = 355
            PreRad = 1404.92:   PostRad = 1416.91
        Case 355 To 366:
            PreDate = 355:      PostDate = 365 + 21
            PreRad = 1416.91:   PostRad = 1415.96
        End Select

        GetExTer = ((PostDate - CurrentDOY) * PreRad + (CurrentDOY - PreDate) _
            * PostRad) / (PostDate - PreDate)
    ElseIf (SolarModel = 1) Then    'Duffie & Beckman(1991)'s Model
        GetExTer = (1 + 0.033 * DCos(360 / 365 * CurrentDOY)) * SolarConstant
    ElseIf (SolarModel = 2) Then    'Kreider & Rabl(1994)'s Model
        GetExTer = (1 + 0.033 * DCos(360 / 365.25 * CurrentDOY))* SolarConstant
    End If
End Function
```

```
Function GetAtmTrans(Zenith As Single, Altitude As Single, ClimateType _
    As Integer, Visibility As Integer, SolarModel As Integer) As Single

    'Atmospheric Transmittance Calculation

    Dim R0 As Single, R1 As Single, RK As Single
    Dim A0 As Single, A1 As Single, K As Single
    Dim TempA As Single
    Dim GetAtmTrans1 As Single, GetAtmTrans2 As Single

    If (Zenith > 90) Then
        GetAtmTrans = 0
        Exit Function
    End If

    TempA = Altitude / 3281      ' Altitude from feet to KM
    If TempA > 2.5 Then TempA = 2.5

    Select Case ClimateType
    Case 0: 'Tropical
        Select Case Visibility
        Case 0: R0 = 0.95
        Case 1: R0 = 0.92
        End Select

        R1 = 0.98
        RK = 1.02
    Case 1: 'Midlatitude Summer
        Select Case Visibility
        Case 0: R0 = 0.97
        Case 1: R0 = 0.96
        End Select

        R1 = 0.99
        RK = 1.02
    Case 2: 'Subartic Summer
        Select Case Visibility
        Case 0: R0 = 0.99
        Case 1: R0 = 0.98
        End Select

        R1 = 0.99
        RK = 1.01
    Case 3: 'Midlatitude Winter
        Select Case Visibility
        Case 0: R0 = 1.03
        Case 1: R0 = 1.04
        End Select

        R1 = 1.01
        RK = 1#
    Case 4: 'Midlatitude Average
        Select Case Visibility
        Case 0: R0 = 1#
        Case 1: R0 = 1#
        End Select

        R1 = 1#
        RK = 1.01
    End Select
```

```
Select Case Visibility
Case 0:
    A0 = R0 * (0.4237 - 0.00821 * (6 - TempA) ^ 2)
    A1 = R1 * (0.5055 + 0.00595 * (6.5 - TempA) ^ 2)
    K = RK * (0.2711 + 0.01858 * (2.5 - TempA) ^ 2)
Case 1:
    A0 = R0 * (0.2538 - 0.0063 * (6 - TempA) ^ 2)
    A1 = R1 * (0.7678 + 0.001 * (6.5 - TempA) ^ 2)
    K = RK * (0.249 + 0.081 * (2.5 - TempA) ^ 2)
End Select

GetAtmTrans = (A0 + A1 * Exp(-K / DCos(Zenith)))

If (Visibility = 1) Then
    Select Case ClimateType
    Case 0: 'Tropical
        R0 = 0.95
        R1 = 0.98
        RK = 1.02
    Case 1: 'Midlatitude Summer
        R0 = 0.97
        R1 = 0.99
        RK = 1.02
    Case 2: 'Subartic Summer
        R0 = 0.99
        R1 = 0.99
        RK = 1.01
    Case 3: 'Midlatitude Winter
        R0 = 1.03
        R1 = 1.01
        RK = 1#
    Case 4: 'Midlatitude Average
        R0 = 1#
        R1 = 1#
        RK = 1.01
    End Select

    A0 = R0 * (0.4237 - 0.00821 * (6 - TempA) ^ 2)
    A1 = R1 * (0.5055 + 0.00595 * (6.5 - TempA) ^ 2)
    K = RK * (0.2711 + 0.01858 * (2.5 - TempA) ^ 2)

    GetAtmTrans1 = (A0 + A1 * Exp(-K / DCos(Zenith)))

    Select Case ClimateType
    Case 0: 'Tropical
        R0 = 0.92
        R1 = 0.98
        RK = 1.02
    Case 1: 'Midlatitude Summer
        R0 = 0.96
        R1 = 0.99
        RK = 1.02
    Case 2: 'Subartic Summer
        R0 = 0.98
        R1 = 0.99
        RK = 1.01
    Case 3: 'Midlatitude Winter
        R0 = 1.04
        R1 = 1.01
        RK = 1#
    Case 4: 'Midlatitude Average
        R0 = 1#
```

```
            R1 = 1#
            RK = 1.01
        End Select

        A0 = R0 * (0.2538 - 0.0063 * (6 - TempA) ^ 2)
        A1 = R1 * (0.7678 + 0.001 * (6.5 - TempA) ^ 2)
        K = RK * (0.249 + 0.081 * (2.5 - TempA) ^ 2)

        GetAtmTrans2 = (A0 + A1 * Exp(-K / DCos(Zenith)))

        GetAtmTrans = (GetAtmTrans1 + GetAtmTrans2) / 2
    End If
End Function


Function GetBeamNormal(Extraterrestrial As Single, AtmTrans As Single, _
    Zenith As Single, SolarModel As Integer) As Single

    Dim A As Single, B As Single
    Dim PreDate As Integer, PostDate As Integer
    Dim PreA As Single, PostA As Single
    Dim PreB As Single, PostB As Single

    If ((Zenith < 0) Or (Zenith >= 90)) Or (AtmTrans < 0) Then
        GetBeamNormal = 0
        Exit Function
    End If

    If (SolarModel = 0) Then    ' ASHRAE Handbook(1993)'s Model
        Select Case (CurrentDOY)
        Case 1 To 21:
            PreDate = -9:       PostDate = 21
            PreA = 1233.61:     PostA = 1230.45
            PreB = 0.142:       PostB = 0.142
        Case 22 To 52:
            PreDate = 21:       PostDate = 52
            PreA = 1230.45:     PostA = 1214.68
            PreB = 0.142:       PostB = 0.144
        Case 53 To 80:
            PreDate = 52:       PostDate = 80
            PreA = 1214.68:     PostA = 1186.28
            PreB = 0.144:       PostB = 0.156
        Case 81 To 111:
            PreDate = 80:       PostDate = 111
            PreA = 1186.28:     PostA = 1135.8
            PreB = 0.156:       PostB = 0.18
        Case 112 To 141:
            PreDate = 111:      PostDate = 141
            PreA = 1135.8:      PostA = 1104.25
            PreB = 0.18:        PostB = 0.196
        Case 142 To 172:
            PreDate = 141:      PostDate = 171
            PreA = 1104.25:     PostA = 1088.48
            PreB = 0.196:       PostB = 0.205
        Case 173 To 202:
            PreDate = 172:      PostDate = 202
            PreA = 1088.48:     PostA = 1085.32
            PreB = 0.205:       PostB = 0.207
        Case 203 To 233:
            PreDate = 202:      PostDate = 233
            PreA = 1085.32:     PostA = 1107.41
            PreB = 0.207:       PostB = 0.201
```

```
        Case 234 To 264:
            PreDate = 233:      PostDate = 264
            PreA = 1107.41:     PostA = 1151.58
            PreB = 0.201:       PostB = 0.177
        Case 265 To 294:
            PreDate = 264:      PostDate = 294
            PreA = 1151.58:     PostA = 1192.59
            PreB = 0.177:       PostB = 0.16
        Case 295 To 325:
            PreDate = 294:      PostDate = 325
            PreA = 1192.59:     PostA = 1220.99
            PreB = 0.16:        PostB = 0.149
        Case 326 To 355:
            PreDate = 325:      PostDate = 355
            PreA = 1220.99:     PostA = 1233.61
            PreB = 0.149:       PostB = 0.142
        Case 355 To 366:
            PreDate = 355:      PostDate = 365 + 21
            PreA = 1233.61:     PostA = 1230.45
            PreB = 0.142:       PostB = 0.142
        End Select

        A = ((PostDate - CurrentDOY) * PreA + (CurrentDOY - PreDate) _
            * PostA) / (PostDate - PreDate)
        B = ((PostDate - CurrentDOY) * PreB + (CurrentDOY - PreDate) _
            * PostB) / (PostDate - PreDate)

        GetBeamNormal = A / (Exp(B / DSin(SolarAltitude)))
    ElseIf (SolarModel = 1) Then    ' Duffie & Beckman(1991)'s Model
        GetBeamNormal = Extraterrestrial * AtmTrans
    Else    'Kreider & Rabl(1994)'s Model
        GetBeamNormal = Extraterrestrial * AtmTrans
    End If

    If (GetBeamNormal < 0) Then GetBeamNormal = 0
End Function


Function GetDirectHorizon(BeamNormal As Single, Zenith As Single, _
    SolarModel As Integer) As Single

    If ((Zenith < 0) Or (Zenith >= 90)) Or (AtmTrans < 0) Then
        GetDirectHorizon = 0
        Exit Function
    End If

    GetDirectHorizon = BeamNormal * DCos(Zenith)

    If (GetDirectHorizon < 0) Then GetDirectHorizon = 0
End Function


Function GetDiffuseHorizon(Extraterrestrial As Single, AtmTrans As Single, _
    Zenith As Single, SolarModel As Integer) As Single

    If ((Zenith < 0) Or (Zenith >= 90)) Or (AtmTrans < 0) Then
        GetDiffuseHorizon = 0
        Exit Function
    End If

    GetDiffuseHorizon = (0.271 * Extraterrestrial - 0.2939 * BeamNormal) _
        * DCos(Zenith)
```

```
    If (GetDiffuseHorizon < 0) Then GetDiffuseHorizon = 0
End Function


Function GetDirectTilted(BeamNormal As Single, IncidenceAngle As Single, _
    Zenith As Single, SolarModel As Integer) As Single

    If ((Zenith < 0) Or (Zenith >= 90)) Or (AtmTrans < 0) Then
        GetDirectTilted = 0
        Exit Function
    End If

    GetDirectTilted = BeamNormal * DCos(IncidenceAngle)

    If (GetDirectTilted < 0) Then GetDirectTilted = 0
End Function


Function GetDiffuseTilted(DiffuseHorizon As Single, SurfaceTilt As Single, _
    Zenith As Single, SolarModel As Integer) As Single

    If ((Zenith < 0) Or (Zenith >= 90)) Or (AtmTrans < 0) Then
        GetDiffuseTilted = 0
        Exit Function
    End If

    GetDiffuseTilted = DiffuseHorizon * (1 + DCos(SurfaceTilt)) / 2

    If (GetDiffuseTilted < 0) Then GetDiffuseTilted = 0
End Function


Function GetGrndReflTilted(GlobalHorizon As Single, AtmTrans As Single, _
    GrndReflTilted As Single, Zenith As Single, SolarModel As Integer) _
    As Single

    If ((Zenith < 0) Or (Zenith >= 90)) Or (AtmTrans < 0) Then
        GetGrndReflTilted = 0
        Exit Function
    End If

    GetGrndReflTilted = GlobalHorizon* GrndReflTilted * (1-DCos(SurfaceTilt))/2

    If (GetGrndReflTilted < 0) Then GetGrndReflTilted = 0
End Function


Function GetTrans(IncidenceAngle As Single, Zenith As Single) As Single

    Dim N2 As Single, KL As Single, Theta2 As Single
    Dim ThetaA As Single, AbsorPerp As Single, AbsorPar As Single
    Dim Perp As Single, Par As Single

    N2 = 1.526
    KL = 0.1016 '(0.125in = 3.2mm & 0.812802/in)

    If ((Zenith < 0) Or (Zenith >= 90)) Then
        GetTrans = 0
        Exit Function
    End If
```

```
    Theta2 = ArcSin(DSin(IncidenceAngle) / N2)
    ThetaA = Exp(-KL / DCos(Theta2))

    AbsorPerp = (DSin(Theta2 - IncidenceAngle)) ^ 2 / _
        (DSin(Theta2 + IncidenceAngle)) ^ 2
    AbsorPar = (DTan(Theta2 - IncidenceAngle)) ^ 2 / _
        (DTan(Theta2 + IncidenceAngle)) ^ 2

    Perp = ((1 - AbsorPerp) * (1 - AbsorPerp ^ 2)) / _
        ((1 + AbsorPerp) * (1 + AbsorPerp ^ 2))
    Par = ((1 - AbsorPar) * (1 - AbsorPar ^ 2)) / _
        ((1 + AbsorPar) * (1 + AbsorPar ^ 2))

    GetTrans = 0.5 * ThetaA * (Perp + Par)
End Function


Sub SolarCalc(CurrentDOY As Integer, SolarTime As Single, SolarModel _
    As Integer)

    Dim TempInciAngle As Single

    '-------------------------------------
    ' Solar Time Calculation
    '-------------------------------------

    ' Daylight saving time set
    DST = GetDST(CurrentYear, CurrentMonth, CurrentDate, CurrentTime)

    ' Day of year calculation
    CurrentDOY = GetDOY(CurrentYear, CurrentMonth, CurrentDate)

    ' Solar Time Calculation
    SolarTimeDiff = GetSolarTimeDiff(CurrentDOY, Longitude, TimeZone, DST, _
        SolarModel)
    SolarTime = CurrentTime + SolarTimeDiff

    '-------------------------------------
    ' Solar Angle Calculation
    '-------------------------------------

    ' Declination Calculation
    Declination = GetDeclination(CurrentDOY, SolarModel)

    ' Sunset/Sunrise Hour Angle Calculation
    SunsetHourAngle = GetSunsetHourAngle(Latitude, Declination, SolarModel)

    ' Solar Hour Angle Calculation
    SolarHourAngle = GetSolarHourAngle(SolarTime)

    ' Zenith Angle Calculation
    Zenith = GetZenith(Latitude, Declination, SolarHourAngle, SolarModel)

    ' Solar Altitude Angle Calculation
    SolarAltitude = 90 - Zenith

    ' Solar Azimuth Angle Calculation
    SolarAzimuth = GetSolarAzimuth(Latitude, Declination, Zenith, _
        SolarHourAngle, SolarModel)

    ' Solar Incidence Angle Calculation
    IncidenceAngle = GetIncidenceAngle(Zenith, SolarAzimuth, SurfaceTilt, _
```

```
        SurfaceAzimuth, SolarModel)

    '-------------------------------------
    ' Solar Radiation Calculation (W/m^2)
    '-------------------------------------

    ' Solar Constant Calculation
    SolarConstant = GetSolarConstant(SolarModel)

    ' Extraterrestrial Calculation
    Extraterrestrial = GetExTer(SolarConstant, CurrentDOY, SolarModel)

    ' Atmospheric Transmittance Calculation
    AtmTrans = GetAtmTrans(Zenith, Altitude, ClimateType, Visibility, _
        SolarModel)

    ' Beam Normal Radiation
    BeamNormal = GetBeamNormal(Extraterrestrial, AtmTrans, Zenith, SolarModel)

    ' Direct Solar Radiation on the Horizon
    DirectHorizon = GetDirectHorizon(BeamNormal, Zenith, SolarModel)

    ' Diffuse Solar Radiation on the Horizon
    DiffuseHorizon = GetDiffuseHorizon(Extraterrestrial, AtmTrans, Zenith, _
        SolarModel)

    ' Global Solar Radiation on the Horizon
    GlobalHorizon = DirectHorizon + DiffuseHorizon


    ' Direct Solar Radiation on a Tilted Surface
    DirectTilted = GetDirectTilted(BeamNormal, IncidenceAngle, Zenith, _
        SolarModel)

    ' Diffuse Solar Radiation on a Tilted Surface
    DiffuseTilted = GetDiffuseTilted(DiffuseHorizon, SurfaceTilt, Zenith, _
        SolarModel)

    ' Ground Refelcted Solar Radiation on a Tilted Surface
    GrndReflTilted = GetGrndReflTilted(GlobalHorizon, AtmTrans, GrndRefl, _
        Zenith, SolarModel)

    ' Global Solar Radiation on a Tilted Surface
    GlobalTilted = DirectTilted + DiffuseTilted + GrndReflTilted
End Sub
```

VITA

■ NAME & ADDRESS

Name: Kie Whan Oh
Address: Sooyoung-Gu Mangmi-Dong 884-21, Pusan, South Korea, 613-131

■ EDUCATION

1994-1999 Ph.D. in Architecture, Department of Architecture, Texas A&M University, Co-Advisors: Larry O. Degelman & Jeff S. Haberl.

1991-1994 Master of Architecture, Department of Architecture, University of California, Los Angles, Thesis Title: The CAD Program for the Element-Standardized House Design, Advisor: Robin S. Liggett.

1987-1989 Master of Engineering in Architecture, Department of Architectural Engineering, Pusan National University, Korea, Thesis Title: A Study on the Expression of Abstract Form in the Contemporary Architecture, Advisor: Soonil Kim.

1981-1985 Bachelor of Engineering in Architecture, Department of Architectural Engineering, Pusan National University, Korea.

■ PUBLICATIONS

1997 Oh, J. and Haberl, J. "New Educational Software for Teaching the Sunpath Diagram and Shading Mask Protractor", Building Simulation '97: Fifth International IBPSA Conference, Prague, Czech Public, (September), Vol. I, pp. 307-312.

1996 Oh, J. and Haberl, J. "A New MS-Windows-based Educational Software for Teaching the Sunpath Diagram and Shading Mask Protractor", Proceedings of the 10th Symposium on Improving Building System in Hot and Humid Climates, published by the Texas Building Energy Institute, Austin, Texas, (May), pp. 262-268.

1994 Oh, K. W. "The CAD Program for the Element-Standardized House Design", A Thesis for Master of Architecture, UCLA.

1989 Oh, K. W. and Kim, S. "A Study on the Expression of Abstract Form in the Contemporary Architecture", Korean Academy of Architecture, Seoul, Korea.

1989 Oh, K. W. "A Study on the Expression of Abstract Form in the Contemporary Architecture", A Thesis for Master of Engineering in Architecture, Pusan National University, Pusan, Korea.

■ WORK EXPERIENCE

1995 - 1999 Graduate Research Assistant, Energy Systems Laboratory, Texas A&M University, involves computer programming & data analysis for the LoanSTAR project, and ASHRAE research project 1050 RP.

1997 - 1999 Graduate Teaching Assistant, Department of Architecture, Texas A&M University, for ARCH 633, ARCH 615, & ARCH 334.

1990 - 1991 Lecturer, Doneui Junior College, Pusan, Korea, taught architectural structure.

1991 Instructor, Norano Design Academy, Pusan, Korea, taught computer graphics, CAD, and computer programming in Macintosh and in PC with the MS-Windows environment.

1989 - 1990 Full-time Teaching Assistant, Department of Architectural Engineering, Pusan National University, Korea.

1986 - 1987, 1990 Architectural Designer, Samhyung General Architect Office, Pusan, Korea.